CRYOCHEMISTRY

G. B. SERGEEV
V. A. BATYUK

MIR PUBLISHERS
MOSCOW

Professor GLEB B. SERGEEV, D.Sc., a leading Soviet authority on chemical kinetics, is a disciple and follower of N. N. Semenov, a Nobel Prize Laureate. His scientific interests lie basically in the field of chemical kinetics and low-temperature chemistry. Has penned over 200 publications on chemical kinetics and physical chemistry. At present, he is deputy dean of the Chemical Department at Moscow University.

In 1976, he was awarded the Lomonosov Prize for his work in cryochemistry.

VLADIMIR A. BATYUK, Cand.Sc., is a senior research worker at the Chemical Department, Moscow University. He is mainly interested in chemical and biochemical reactions at low temperatures. Has published over 80 papers on the subject. In 1978-79 he worked at the Massachusetts Institute of Technology within the framework of a USSR-US Scientific Exchange Program.

This is the first Soviet monograph on the cryochemistry and related subjects. Written by leading Soviet authorities in the field, it covers low-temperature homogeneous and heterogeneous reactions involving gases and liquids, experimental apparatus and techniques, radical and ion reactions in frozen solid, low-temperature polymerization, chain reactions, spontaneous low-temperature reactions, kinetic models for cryogenic chemical reactions in the solid phase, reactions in multicomponent frozen systems, biochemical reactions at subzero and low temperatures, and applications of low temperatures in science technology. The book will be of interest to those concerned with cryochemistry and cryogenics of all levels of sophistications.

TO THE READER

Mir Publishers welcome your comments on the content, translation and design of this book.

We would also be pleased to receive any proposals you care to make about our future publications.

Our address is:
Mir Publishers
2 Pervy Rizhsky Pereulok,
I-110, GSP, Moscow, 129820
USSR

Printed in the Socialist Republic of Romania

CRYOCHEMISTRY

G. B. SERGEEV, V. A. BATYUK

Translated from the Russian
by B. V. Kuznetsov

Mir Publishers Moscow

First published 1981
Revised from the 1978 Russian edition

На английском языке

© Издательство «Химия», 1978
© English translation, Mir Publishers, 1981

Г.Б. СЕРГЕЕВ, В.А. БАТЮК

КРИОХИМИЯ

Издательство «Химия»
Москва

ИЗДАТЕЛЬСТВО · МИР ·

FOREWORD TO THE RUSSIAN EDITION

The current trend in chemical kinetics today is the growing shift of emphasis from studies on reactions in the gas and liquid phases to those in solids and at low temperatures. Low temperatures open up unique potentialities for the researcher to learn more about the kinetics and mechanism of reactions involving unstable reactive species and the tunnelling of electrons and protons.

In recent years, a large number of publications dealing with chemical reactions at low temperatures have appeared both in and outside the Soviet Union. The present monograph is the first attempt by Soviet authors to examine systematically the kinetics of various low-temperature reactions. This approach to the subject lays a theoretical foundation for an important scientific discipline which will, in all probability, extend into the engineering field before long. A sizeable contribution to the emergence and establishment of this division of chemistry in the USSR has come from the present authors and their associates in research on low-temperature chemical synthesis carried out at the Moscow State University.

The Russian manuscript had already gone to press when a collected volume on cryochemistry (*Cryochemistry*, M. Moskovits and G.A. Ozin (Eds), John Wiley and Sons, New York, 1976) appeared in the United States. Taken together, the two books give an all-around picture of cryochemistry — a new division of chemistry.

June 1977

Academician N. N. Semenov,
Nobel Prize Laureate

PREFACE

Cryochemistry (from the Greek *kruos* for cold) is a new field of chemistry concerned with the behaviour of reactive substances at low temperatures and with phenomena which set apart low-temperature chemical reactions from those taking place at higher temperatures.

Obviously, the term "low temperatures" is a relative one, and its definition has been varying with advances in science and engineering. In physics, this term applies to temperatures around the boiling point of helium, that is, 4.2 K (—269°C). In chemistry, it goes for temperatures between 223 and 70 K, whereas the term "extremely low" applies to temperatures below 70 K.

Systematic studies on low-temperature chemical reactions began in the late 1950s when it was found that reactive atoms and radicals could be trapped at the boiling point of liquid helium. Trapping studies gave an impetus to further investigations in the field of cryochemistry. Sizeable contributions to cryochemistry on the world scale have been made by the Soviet scientists Semenov, Kargin, Voyevodsky, their disciples and followers.

This book is the first Soviet monograph on the subject, pooling together a wealth of data in the rapidly developing field of chemical reactions at low temperatures. A large variety of low-temperature reactions have been investigated in both the Soviet Union and other countries in the past 20 years. Unfortunately, the space available in a single volume is not sufficient for an appropriate coverage of all experimental data and all theoretical aspects of cryochemistry closely related to other divisions of chemistry and cryogenic engineering. Cryochemistry is drawing heavily on advances in solid-state physics and chemistry, polymer chemistry, photochemistry, radiation chemistry, cryophysics, and biochemistry. In turn, advances in cryochemistry stimulate work on many problems in the associated divisions of chemistry and physics.

Ample space in the monograph is devoted to studies by Soviet scientists who have actively contributed to advances in the most important divisions of cryochemistry. The literature has been covered mainly up to 1975, although some references published in 1976 are also included.

The subject-matter presented in the book deals with reactions in gases and liquids, production and transformations of ions in frozen solids, and some kinetic models proposed to explain processes involving reactive species. The very fact that no generally accepted model for cryogenic reactions in solids has been developed yet is an indication of the complexity of the problems raised.

Ample space is given to the use of low temperatures in various fields of science and engineering, notably low-temperature polymerization, chain reactions, reactions involving molecular complexes, chemical and biochemical reactions in frozen multicomponent solutions. Naturally, the book also covers these authors' studies on the stimulation of chemical reactions by low temperatures, reactions with a negative temperature coefficient, and the effect of phase and structural inhomogeneity of the system on chemical processes at low temperatures.

We sincerely hope that this monograph will win more workers for this new and challenging field of chemistry.

G.B. Sergeev
V.A. Batyuk

CONTENTS

Foreword to the Russian Edition 5

Preface 6

Introduction 13

Chapter One 15

HOMOGENEOUS AND HETEROGENEOUS LOW-TEMPERATURE REACTIONS INVOLVING GASES AND LIQUIDS 15

1.1. Noninitiated Spontaneous Reactions 15
1.2. Reactions Involving Reactive Species 16
  1.2.1. Activation by an Electric Discharge and an Explosion 17
  1.2.2. Activation by Pyrolysis 19
  1.2.3. Activation by Irradiation 21
1.3. Reactions Involving Oxygen and Fluorine Compounds 23
  1.3.1. Oxygen-Containing Compounds 23
  1.3.2. Fluorine-Containing Compounds 26
1.4. Heterogeneous Reactions 27
  1.4.1. Contact Reactions of Hydrogen Atoms 27
  1.4.2. Contact Reactions of Other Atoms 32

Chapter Two

APPARATUS AND TECHNIQUES FOR CRYOGENIC RESEARCH 35

2.1. Cryostats 35
2.2. Practical Aspects of Low-Temperature Experiments 43
  2.2.1. Gases and Liquids 43
  2.2.2. Solids 44
2.3. Experimental Techniques for Low-Temperature Processes 46
  2.3.1. UV-Visible Spectroscopy 47
  2.3.2. Circular Dichroism and Dispersion of Optical Rotation 48
  2.3.3. Infrared and Raman Spectroscopy 49
  2.3.4. Calorimetric Methods 49
  2.3.5. Diffraction Methods, ESR and NMR 52

Chapter Three

REACTIONS OF RADICALS AND IONS IN FROZEN SOLIDS 55

3.1. Radical Stabilization and Kinetics of Accumulation 55
3.2. Kinetics of Radical Loss. Stepwise Recombination 58

3.3. Photochemical Reactions. The Cage Effect 61
3.4. Spatial Distribution of Radicals 63
3.5. Reactions of Charged Species. Trapped Electrons 68
3.6. The Effect of Impurities and Radiation Type on Stability of Reactive Species 70
3.7. Kinetics of Radiophotoluminescence and Radiothermoluminescence at Low Temperatures 76

Chapter Four
LOW-TEMPERATURE POLYMERIZATION 81

4.1. Radiation- and Photo-Induced Polymerization 82
4.2. Polymerization in Molecular-Beam Cocondensates 90
4.3. Effects of Phase Changes and Lattice Structure on Solid-Phase Polymerization 95

Chapter Five
CHAIN REACTIONS 104

5.1. Photochemical Hydrobromination of Olefins 105
5.2. Photochemical Hydrobromination of Some Olefin Halides 116

Chapter Six
SPONTANEOUS REACTIONS 126

6.1. Halogenation and Hydrohalogenation of Olefins in the Absence of Solvents 126
  6.1.1. Basic Pattern of Reactions in Layered Samples of the Starting Materials 126
  6.1.2. Reactions in Cocondensates 129
  6.1.3. Thermographic and Spectroscopic Investigation of the Propylene-Bromine System 132
  6.1.4. The Mechanism of the Low-Temperature Reaction 135
6.2. Reactions of Addition to Olefins in Solvents 138
  6.2.1. Chlorination 138
  6.2.2. Bromination 139
  6.2.3. Nitration and Nitrosyl-Chlorination 140
6.3. Role of Molecular Complexes in the Halogenation of Olefins 143
6.4. Molecular Complexes in Conversions of α-Oxides 150
6.5. Reactions in Frozen Solutions 154
  6.5.1. Addition to Double Bonds and the Menshutkin Reaction 155
  6.5.2. Solvolysis Reactions 157

Chapter Seven
KINETIC MODELS OF CHEMICAL REACTIONS IN THE SOLID PHASE 166

7.1. The Relaxation Mechanism of the Loss of Radiolyzed Reactive Products 166
7.2. The Effect of Matrix Structure on the Loss of Radicals 172
7.3. A Model for Diffusion-Controlled Reactions in the Condensed Phase 175

7.4. The Cage Model for Reactions in the Solid Phase 177
7.5. The Tunnel Mechanism of Reactions 180

Chapter Eight

REACTIONS IN MULTICOMPONENT FROZEN SYSTEMS 186

8.1. The Structure of Frozen Solutions According to ESR Data 186
8.2. The Phase State of Frozen Solutions According to NMR Data 193
8.3. Kinetics of Reactions in Frozen Solutions 198
8.4. A Structural-Kinetic Model of Chemical Reactions in Frozen Solutions 205
8.4.1. Experimental Data 209
8.4.2. Effect of the Solvent 221
8.4.3. Correspondence Between Experiment and the Model 225

Chapter Nine

BIOCHEMICAL REACTIONS AT REDUCED AND LOW TEMPERATURES 241

9.1. Physico-Chemical Properties of Organo-Aqueous Solvents at Low Temperatures 242
9.2. Enzyme Activity at Reduced Temperatures 245
9.3. Frozen Solutions and Hydration of Macromolecules 252
9.4. Photochemical Processes in Frozen Biopolymer Solutions 253
9.5. Biochemical Processes and Stabilization of Dynamic Biopolymer Conformations in Frozen Solutions 255

Chapter Ten

APPLICATIONS OF LOW TEMPERATURES IN SCIENCE AND ENGINEERING 262

References 278
Index 295

INTRODUCTION

Temperature is a decisive factor controlling chemical reactions. As a rule, the temperature dependence of the reaction rate is described by the Arrhenius equation which states that for most reactions the rate increases with rising temperature exponentially. This appears to have been the main reason why chemical reactions at low temperatures interested investigators so little until quite recently.

On the other hand, it has been found that some chemical reactions, contrary to traditional thought, would proceed at rates which increase with decreasing temperature. Indeed, some processes have been noted to change their path drastically if the reacting system was cooled to cryogenic temperatures. More and more of such low-temperature reactions are being discovered all the time. It has also been found that some reactions that would not proceed at room temperature will do so at low temperatures. Analysis and understanding of these seemingly anomalous events are important for both theory and practice.

As the reactive systems change from the gaseous to the liquid and finally the solid state, weak intermolecular interactions play an increasingly important role. Owing to them, investigators have been able to isolate and analyze the otherwise unstable molecular complexes at cryogenic temperatures. Various physical effects can be utilized to process frozen substances so as to generate and trap radicals and ions. At low temperatures or during the subsequent warm-up, the reactive intermediates may enter into various reactions. Chemical transformations taking place in the solid phase at low temperatures markedly widen our knowledge of elementary chemical events and open up a road towards the synthesis of chemical species unattainable by alternate routes.

Thus, cooling the reactive species to cryogenic temperatures stimulates interactions which are responsible for the formation of complexes, brings about changes in the phase and structure of the system, and enables chemical processes to be conducted under unorthodox extremal conditions.

Cryogenic temperatures affect chemical processes differing in activation energy likewise differently. The probability of occurrence in the circumstances is the highest for a reaction having the lowest activation energy. Thus, cryogenic temperatures put to work a kind of selection in terms of energy, promoting a particular reaction from among the several reactions proceeding in parallel, which may well serve as the basis for a novel chemical technology. In particular, cryogenic temperatures make it possible to isolate extremely pure substances free from any impurities or by-products.

Of late, interest in cryochemistry has been growing not only among chemists. To them may be added, and in an ever growing number at that, biologists, medical research workers, food specialists, geologists, and people in many other fields of science and industry. This interest is stimulated by development work in permafrost localities, the use of low temperatures for the preservation of food, blood, medicines and biological preparations, etc.

Cryogenic temperatures, however, have another facet as regards their effect on chemical reactions. By promoting some reactions and inhibiting others, they may lead to the formation of an unwanted end product. To avoid this and to exercise proper control over such processes in general, it is essential to have a working knowledge of their nature, notably kinetic characteristics, and the effects that cooling may have on the structure and phase of the systems involved.

For many substances, chemical reactions at low temperatures usually entail a change from the gaseous or liquid state to the solid state. This is accompanied by radical changes in the physico-chemical properties and reactivity of the species. As often as not, such changes cannot be predicted or extrapolated from the macroscopic characteristics of the reactive systems at room temperature — what is needed is a detailed study into the properties of the reactive species at cryogenic temperatures, and this calls in turn for the development and use of appropriate techniques and procedures.

Knowledge of the behaviour of structured systems at cryogenic temperatures is a goal of paramount importance to present-day chemical kinetics. This knowledge will permit deeper insight into the mechanisms of reactions in solids and into general matters of reactivity.

For proper control over the behaviour of chemical species at low temperatures, it is essential to know their physico-chemical properties and understand the factors governing their reactivity. It is these matters, along with studies into the specific aspects of reactions at cryogenic temperatures, that constitute the subject of cryochemistry — a new division of chemistry.

CHAPTER ONE

HOMOGENEOUS AND HETEROGENEOUS LOW-TEMPERATURE REACTIONS INVOLVING GASES AND LIQUIDS

Early attempts to investigate the chemical reactions that take place at low temperatures date back to the 19th century. They were made by Dewar who was looking for ways and means to liquefy air and other gases. Dewar and his co-workers observed the interactions of alkali metals, hydrogen sulphide, hydrogen iodide, and some others with liquid oxygen. Their studies were not carried to completion, and today they are of purely historical interest.

A systematic effort as regards low-temperature chemical reactions began in the late 1950s. The publications that have appeared since then are reviewed in detail in [1], [2], and [3]. We shall dwell in brief only on the most important work carried out by the mid-1950s, placing emphasis on the studies that, in our opinion, have contributed most to establishing cryochemistry as a new division of chemical physics.

1.1. NONINITIATED SPONTANEOUS REACTIONS

A relatively small number of chemical reactions are known to be capable of proceeding at cryogenic temperatures as the reactive species are simply mixed together. For the first time, reactions occurring in the absence of any initiating agent were observed at the beginning of this century. Those were reactions between liquid hydrogen and fluorine. At normal temperature, mixtures of hydrogen and fluorine were observed to self-ignite and remain stable only at 90 K [4]. Experiments with the low-temperature reactions of hydrogen and fluorine in the gaseous phase had led to the discovery of a new class of ramified chain processes [5, 6].

Experiments at the beginning of this century also included reactions involving liquid fluorine. It was found that fluorine can react with many substances, including metals [3].

A distinction of a spontaneous reaction between oxygen and nitric oxide is that the reaction rate markedly rises as the temperature is brought down. This has been observed by many investigators. The most detailed description was given by Hiraki and reviewed in [3]. According to him, a mixture of NO and O_2 when held under a pressure of 1.3 Pa would not react at 195 K or 161 K, but would readily do so at 88 K. In the temperature interval 83-90 K, the reaction showed a negative activation energy and was heterogeneous. Hiraki proposed the following mechanism for this reaction:

$$2NO \underset{k_2}{\overset{k_1}{\rightleftarrows}} N_2O_2 \tag{1.1}$$

$$N_2O_2 + O_2 \xrightarrow{k_3} N_2O_4$$

The limiting factor was the second stage of the process. The surface of the reaction vessel strongly affected the rate of the reaction, too.

Several explanations can be offered for the negative temperature coefficient. For one, it may be traced to the fact that one of the reactions (1.1) is exothermal and reversible. As the temperature is brought down, the concentration of dimers builds up, and this leads to an increase in the observed reaction rate. The experimental rate constant is a complex combination of the constants for the various elementary stages. The temperature dependence of each of these constants is described by the Arrhenius equation to have a positive activation energy. In reality, however, a situation may arise in a certain temperature interval where the overall rate constant leads to a negative temperature coefficient — thus, at least formally, the reaction has a negative activation energy. Another explanation is based on the temperature dependence of the pre-exponential factor [7].

1.2. REACTIONS INVOLVING REACTIVE SPECIES

These reactions may be divided into three basic groups as follows. Those in the first group are reactions of synthesis involving species activated by an electric discharge or an explosion. They basically produce inorganic compounds containing halides and oxygen. Those in the second group are reactions of synthesis producing organic compounds and hydrazine derivatives, which proceed by condensation of substances raised to elevated temperatures on a cooled surface (temperature activation). Those in the third group are reactions in which species are activated by penetrating radiations.

1.2.1. Activation by an Electric Discharge and an Explosion

Basically, activation consists in that an electric discharge or an explosion causes the molecules of a reacting species to dissociate into active atoms, radicals and ions which can in some cases be trapped at low temperatures. Precisely in this way, a number of bromine, nitrogen and oxygen compounds are reported to have been obtained at low temperatures from discharge-activated gaseous mixtures of N_2, O_2 and Br_2 [8]. The walls of the discharge tube immersed in liquid air were found to be coated by $BrO_2 \cdot 3NO_2$, BrO_2, N_2O_3, and Br_2. Near 233 K, the compound $BrO_2 \cdot 3NO_2$ decomposed according to the reaction

$$BrO_2 \cdot 3NO_2 \longrightarrow BrO_2 + 3NO_2 \qquad (1.2)$$

The compound BrO_2 decomposed into the constituent elements at room temperature, but proved sufficiently stable at 233 K. The decomposition was accompanied by the evolution of 52 ± 3 kJ $mole^{-1}$ of heat [9].

Reacting with oxygen atoms at 83 K, nearly all of the bromine turned into BrO_2. Given the same conditions, a similar reaction with chlorine would all but fail, leaving only insignificant amounts of Cl_2O and ClO_2. When allowed to react with oxygen atoms at low temperature, hydrogen chloride would oxidize to Cl_2, H_2O, ClO_2, and traces of HClO.

In a reaction chamber held at the temperature of liquid air (83 K), oxygen atoms would oxidize hydrogen sulphide to sulphuric acid with a yield of 70%, whereas their reaction with nitrogen dioxide would produce a blue compound recognized as N_2O_3, when analyzed at room temperature.

At low temperature (90 K), oxygen atoms were found to react with ammonia, methyl amine, and $HC(NH_2)_3$.

Early studies into reactions between atoms and molecules at cryogenic temperatures were conducted by Geib and Harteck [10]. They showed that passing a gaseous stream of explosion-produced hydrogen atoms and molecular oxygen through a cooled trap would produce hydrogen peroxide. The concentration of peroxide was noted to rise with a fall in temperature to below 166 K, with the yield of peroxide rising to 82% at 20 K. It was also found that at low temperatures hydrogen atoms would react with HCN, SO_2, C_2H_2, C_2H_4, and C_3H_6, but would not with NH_3 and NO_2.

Of all cryogenic reactions involving oxygen atoms, the most detailed studies have been concerned with the synthesis of ozone [11]. Ozone was obtained in a discharge tube immersed in liquid nitrogen or oxygen. It was found that the maximum yield was 300 g of ozone per kilowatt of power input, which works out to 26% of electricity being converted to chemical energy. Ozone was also obtained by the deep cooling of the dissociation products of oxygen subjected to an electrodeless discharge [12]. Using calorimetric techniques, the investigators measured the percentage of oxygen atoms in the mixture and studied their reaction with oxygen molecules in the course of heating [13, 14]. In further experiments with the synthesis of ozone from precipitates condensed at 4.2 K, the yield of ozone was 78% [15].

The reactive species produced by reactions in the gaseous phase can be isolated and trapped on a cooled surface for the purpose of accumulation and detailed investigation of their ESR spectra. In this way, it was possible to obtain the phenyl radical [16] by reacting discharge-produced hydrogen atoms with benzene

$$H + C_6H_6 \longrightarrow H_2 + \dot{C}_6H_5 \qquad (1.3)$$

This method is valuable in that the chemical structure of the resultant radicals is exactly known, and their ESR spectra can be utilized to identify them in other systems.

Bennet and Thomas [17] obtained a number of radicals, namely, propyl, butyl, heptyl, allyl, and phenyl among others. They employed a rotating cryostat in which the reacting surface was given a coat of the substance that was to react with a beam of sodium atoms. The radicals were obtained by the following reaction:

$$Na + RHal \longrightarrow NaHal + R \qquad (1.4)$$

Using the same experimental setup and a third beam (in addition to the RHal and Na beams), it was possible to trace further reactions of the radical R, for example

$$\begin{aligned} R + O_2 &\longrightarrow R\dot{O}_2 \\ R + C_2H_4 &\longrightarrow RCH_2\dot{C}H_2 \end{aligned} \qquad (1.5)$$

Oxygen was found to react already at 77 K, whereas ethylene had to be heated to 90-500 K. In Bennet's and Thomas's opinion, the true reaction rate constant and the activation energy could be found on a computer from the degree of conversion of R to $\cdot CH_2CH_2R$, with proper allowance for the gradual cooling of the ethylene. For example, computations for the reaction $\cdot C_6H_5 + C_2H_4$ yielded $E_{act} = 628\ J\ mole^{-1}$. Unfortunately, the accuracy with which the reaction parameters could be deduced from a comparison of the cumbersome computations with experiment was low.

In the forties and fifties, detailed studies were conducted on the cryogenic isolation of combustion products in flames and explosions. Early work by M.V. Polyakov and co-workers [18] showed that if a mixture of hydrogen and oxygen under a pressure of about 1×10^3 Pa was placed in liquid air and ignited, the cryogenically isolated products would carry as much as 13% hydrogen peroxide. A decrease in pressure would lead to an increase in the yield of hydrogen peroxide. Polyakov's work was carried on by British investigators [19] who found that the peroxide yield could further be raised to 30% by bringing the pressure down to 5×10^2 Pa. The formation of hydrogen peroxide was attributed to the reactions of the excited $\mathrm{H\dot{O}_2}$ radical

$$\mathrm{H\dot{O}_2 + H_2 \longrightarrow H_2O_2 + H} \tag{1.6}$$

Minkoff and co-workers [20] investigated in detail the effect of various factors on the yield of hydrogen peroxide. It is interesting to note that, whatever the temperature of the trap, the yield of hydrogen peroxide at temperatures below 190 K was the same for a discharge in water vapour and for a discharge in hydrogen subsequently mixed with molecular oxygen. At 190 K, however, there was a difference: a discharge in water vapour would additionally produce H_2 and O_2, and a discharge in a mixture of H and O_2 would additionally produce H_2O [21].

In the late 50s, attempts were made to obtain argon-fluorine and crypton-fluorine compounds by activating the molecules of the reacting species in a gaseous discharge [3]. It is only recently that compounds of inert gases were synthesized. Work in this field has advanced to a point where we may speak of the chemistry of inert-gas compounds as a division of chemistry in its own right.

1.2.2. Activation by Pyrolysis

One of the most challenging and, at the same time, most controversial subjects in cryochemistry is the production of solid and liquid CCl_2 [22]. The substance was synthesized by isolating at the temperature of liquid air the products of CCl_4 pyrolysis conducted in the presence of carbon at 1300°C. The product was a yellow solid melting at 159 K and boiling at 253 K. In the two experiments, the carbon-to-chlorine ratio was 1 to 1.92 and 1 to 1.88, and the molecular mass of the product under a pressure of 14.4 kPa and 11.7 kPa was 84.62 and 84.70, respectively, which is close to the theoretical value of 82.92 for the CCl_2 compound. When the reaction was carried out in the presence of atmospheric oxygen, the products were found to include carbon oxychloride which had apparently been formed according to the reaction

$$\mathrm{2CCl_2 + O_2 \longrightarrow 2COCl_2} \tag{1.7}$$

Rice and co-workers [8, 9, 23-25] carried out detailed studies on chemical compounds produced by the low-temperature condensation of the products of the decomposition of substances on warming. Rice's work is reviewed in [1, 2], so we shall only recapitulate its highlights. According to [23], sulphur vapours raised to 773 K were condensed at 77 K to form a purple solid, presumably with an S_2

structure. The effects of temperature, jet velocity, and trap temperature are described in [26]. The investigators obtained P_2 by analogy with S_2 [8].

To a considerable extent, the early interest in cryochemical studies and the trapping of free radicals was stimulated by Rice's and Freamo's work [9]. The two investigators discovered the existence, at 77 K, of a blue paramagnetic solid condensed from vapours of hydrazoic acid, heated to 1273 K at a pressure of 13 Pa. They found that every 6 moles of HN_3 would yield 1 mole of H_2 and 7 moles of N_2 [27]. Proceeding from stoichiometric considerations, they suggested the following path for the reaction

$$6HN_3 \longrightarrow 7N_2 + H_2 + 4\ddot{N}H \qquad (1.8)$$

The existence of the $\ddot{N}H$ radical was not proved beyond doubt. Using ESR data, Rice and co-workers suggested [28] that the condensate might basically consist of NH_4N_3. At low temperatures, it was believed [29] that the $\ddot{N}H$ radical could be attached to a nondissociated molecule of hydrazoic acid with the formation of diiminohydrazine

$$\ddot{N}H \quad N_3H \longrightarrow HN_4H \qquad (1.9)$$

It was also hypothesized that diiminohydrazine could dissociate with the formation of an HN_2 radical and that it was that radical that gave the precipitate blue colour and paramagnetic properties. On the other hand, mass-spectral analysis of the glow discharge in hydrazoic acid and hydrazine pointed to the presence of $\ddot{N}H$ radicals [30].

Studies similar to those concerned with hydrazoic acid were conducted on hydrazine. At 77 K, the products of the reaction revealed the presence of a bright-yellow solid [24]. The solid was proved to be nonparamagnetic, which fact prompted the investigators to conclude that the respective radicals were first dimerized into NH_2—NH—NH—NH_2 which then decomposed at 95 K according to the reaction

$$NH_2\text{—}NH\text{—}NH\text{—}NH_2 \longrightarrow 2NH_3 + N_2 \qquad (1.10)$$

This reaction would explain the evolution of nitrogen at 95 K.

Bombardment of solid hydrazine at 77 K by Tesla-discharge species was found to bring about chemical changes. Heating led to the evolution of nitrogen, hydrogen, and ammonia [22]. This was explained by the formation of triazene at low temperatures.

Cooling the pyrolytic products of tetramethyltetrazene, $(CH_3)_2N$—N_2—$N(CH_3)_2$, to 77 K was found to lead to the formation of a violet paramagnetic solid [25]. This solid was presumed to be the frozen dimethylamino radical; when heated to 113 K, it would dimerize according to the reaction

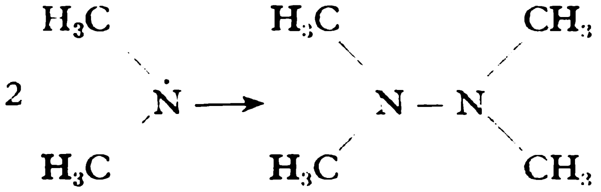

$$2\,(H_3C)_2\dot{N} \longrightarrow (H_3C)_2N-N(CH_3)_2 \qquad (1.11)$$

As is seen, low temperatures can be utilized to synthesize new stable nitrogen compounds.

1.2.3. Activation by Irradiation

Exposure of a substance to ionizing radiations produces in that substance electrons, other charged species, and excited molecules usually possessing an appreciable excess energy. As a result of secondary processes in which the above species take part, there appear other active species, including radicals. Many of these active species can be trapped in a solid phase, especially at low temperatures, and their chemical transformations studied. A large body of literature, including monographs [31-35] has been devoted to the effects of radiations on materials and studies into radiation-induced chemical transformations. We shall not dwell in detail on the production and trapping of reactive species in solids at cryogenic temperatures. For one thing, these matters have been taken up in the above references. For another, the yield of the end products under the circumstances except chain reactions is low. We shall only discuss in brief the key investigations and the matters relating to the specific action of various radiations and the behaviour of active species in solid matrices.

The earliest example of radiation-induced chemical synthesis, it appears, was the production of ozone from oxygen under the action of ultraviolet radiation early in this century [3]. Since then, ozone synthesis has been the subject of many studies, a review of photochemical data can be found in [36]. It has been found that photochemical activity is displayed only by light at $\lambda < 210$ nm. Exposure to light at $\lambda \leqslant 175$ nm would initiate the photodissociation of an oxygen molecule into atoms each of which, on reacting with an oxygen molecule, would form ozone with a quantum yield of two. Exposure to light at $\lambda > 210$ nm would cause the process to involve oxygen dimers

$$\begin{aligned} (O_2)_2 &\longrightarrow O_3 + O \\ O + O_2 &\longrightarrow O_3 \end{aligned} \qquad (1.12)$$

Studies have also been conducted into the photochemistry of diluted solutions (0.1 molar per cent) of O_2 in liquid N_2 and liquid CO [37]. It was found that exposure to light at $\lambda = 185$ nm would cause up to 10% of the oxygen in liquid nitrogen to transform into ozone and nitrous oxide, N_2O. If the solvent was CO, the main product would be CO_2, and the ozone would only account for 0.1%.

For the first time, ozone was obtained by a radiolysis at low temperatures in the Soviet Union [38]. Exposure of liquid oxygen and its mixtures with nitrogen to bombardment by electrons with an energy of 240 keV would lead to the formation of 15 molecules of ozone and 15 molecules of nitric oxide for every 100 eV of absorbed energy. Irradiation of liquid oxygen with gamma-rays from a Co-60 source at 77 K would produce 6 molecules of O_3 for every 100 eV absorbed [39].

Recently, penetrating radiations have come to be used in cryochemistry not only for chemical reactions in gases and liquids. They are also used, and on a large scale, to produce reactive species and radicals directly in solid matrices.

Among those who were the first to investigate photochemical reactions in rigid glassy matrices at cryogenic temperatures were Lewis and Lipkin [40]. At present, this is a well-developed division of cryochemistry. The requirements for a matrix capable of trapping free radicals are formulated in [1] and [2]. Firstly, a matrix must be sufficiently rigid to prevent the diffusion of the trapped species, secondly, a matrix must be inert, thirdly, a matrix must comply with some specific requirements, depending on the manner in which the free radicals have been produced.

Free radicals can be obtained by photolysis, radiolysis, bombardment by electrons, beta-particles, ions, neutral atoms and molecules, neutrons, etc. Most commonly, free radicals are produced by photolysis and radiolysis. Among the advantages of photolysis is the fact that it can be conducted under conditions controlled by the experimentor. Light used for excitation is allowed to fall on a solution of the desired material in a matrix, with the energy of excitation known in advance and amenable to adjustment at will, say, by means of filters. The photolytically produced free radicals and other species can be given desired spatial orientation, which fact opens up new possibilities for studying their behaviour. A more recent addition to this technique is the use of polarized light and the highly monochromatic laser beam. These advantages are unfortunately nonexistent in radiolysis.

Photolysis, however, suffers from several disadvantages. Above all, free radicals can only be produced by systems of substances capable of photodissociation. Also, existing sources usually emit light of low intensity, light is heavily scattered in solids, and the quantum yield is low, therefore one has to resort to long exposure times in order to attain a sufficient degree of dissociation.

Among the advantages of radiolysis are its versatility and high penetrability owing to which active species are produced throughout the bulk of specimens widely differing in nature.

In conclusion, it is to be noted that there is a good deal of difference between systems where free radicals are produced by condensation from the gaseous phase, and systems where they are produced by irradiation. In the former case, free radicals of a desired structure are more readily obtained and it is easier to say what happens upon isolation and trapping. In this case, chemical transformations do take place in the gaseous phase and at the time of condensation, but do not in the solid phase, because the temperature of the matrix can be sufficiently low. In the latter case, free radicals are produced as a result of secondary chemical processes and possess appreciable excess energy so that they can take part in further transformations at low temperatures in the solid phase. In the circumstances, it is extremely difficult to keep under control the processes in the system that lead to the formation of isolated and trapped radicals.

1.3. REACTIONS INVOLVING OXYGEN AND FLUORINE COMPOUNDS

Substances thermodynamically unstable at room temperature can well exist at low temperatures. This is true, for example, of oxygen-fluorine and oxygen-hydrogen compounds which have figured so prominently in many cryochemical studies as substances capable of acting as strong oxidants.

1.3.1. Oxygen-Containing Compounds

Quite a number of oxygen-containing compounds have been produced at low temperatures and a good deal of effort has been put into studies concerned with low-temperature hydrogen-oxygen systems and hydrogen-oxygen derivatives. Of special interest is the use oj cryogenic temperatures in the synthesis of H_2O_4. For some time past, many investigators have been occupied with this superoxide of hydrogen H_2O_4. A valuable contribution in this field has come from Soviet scientists, notably L.I. Nekrasov and his co-workers who have undertaken a detailed study into the conditions required for the synthesis of H_2O_4 and its properties. Nekrasov's papers also contain a review of the work done by other investigators. What follows is a brief overview of the results obtained by Nekrasov and his co-workers [41-47].

For the first time, he produced H_2O_4 by reacting atomic hydrogen with liquefied ozone. This technique gave more reliable evidence on the existence of H_2O_4. The yield of H_2O_4 was 20% (mole). The ratio of the liberated oxygen to the hydrogen peroxide forming upon the subsequent dissociation of peroxide condensates was equal to unity, which answers the reaction

$$H_2O_4 \longrightarrow H_2O_2 + O_2 \tag{1.13}$$

Initially, no hydrogen peroxide was seen to form in the low-temperature reaction of atomic hydrogen and ozone. Using a thermographic technique, Nekrasov *et al.* found that the decomposition of hydroxide-radical condensates would begin in the temperature interval from 158 to 163 K and would proceed in three stages. The first two took place in the solid phase, and the last upon the melting of the condensate. The three stages were accompanied by the evolution of 4, 16, and 80% of oxygen, respectively.

From studies into the magnetic susceptibility of frozen condensates and model systems of the H_2O_2-O_2 type and a series of specific experiments, the investigators concluded that the frozen systems contained no oxygen and that this would only be produced upon the decomposition of H_2O_4. Unfortunately, the possibility of oxygen formation according to the reaction was not investigated in detail

$$H\dot{O}_2 + H\dot{O}_2 \longrightarrow H_2O_2 + O_2 \tag{1.14}$$

This reaction was apparently dismissed in the light of ESR data which suggested that the concentration of trapped $H\dot{O}_2$ radicals in the condensate did not exceed 0.4%. According to present evidence (see Chap. 3), however, a large proportion of radicals may be lost rather than trapped in the course of condensation and radical formation, so ESR data do not provide a sufficient ground for dismissing the reaction between the hydroperoxide radicals.

Thermochemical studies of frozen condensates made it possible to determine the heat effect of condensate decomposition (it was found to be equal to 163 ± 17 kJ mole^{-1}) and to evaluate the thermodynamic properties of H_2O_2, H_2O_3, and H_2O_4.

The structure of frozen hydrogen-oxygen systems was investigated by low-temperature IR spectroscopy and electron diffraction analysis. Using IR spectra of various condensates and model experiments, the investigators were able to detect and assign some vibrations to the O_4 fragment which is the core of the H_2O_4 structure. According to calculations, the best agreement with experiment was shown by the O_4 configuration in which the planes of the two outer oxygen atoms make angles of $119°$ and $90°$. Raman spectroscopy data could substantially expand our knowledge of the structure.

Electron diffraction analysis revealed that the frozen condensates were H_2O_4 molecules held together by water molecules. This brought the investigators to assume that the H_2O_4 molecules did not form a separate phase in the condensates.

The data gathered in kinetic, thermographic, calorimetric, magnetochemical, electron-diffraction, spectral, and X-ray studies of frozen hydrogen-oxygen systems had led Nekrasov and his co-workers to believe in the existence of H_2O_4.

In 1975, a new technique [48] was proposed for the synthesis of H_2O_4 condensates. It consisted in depositing the products of reaction between hydrogen and oxygen in a glow discharge upon the walls of a gas-discharge tube at 77 K. The activation energies required for the decomposition of H_2O_4 in various temperature intervals were determined by methods of nonisothermal kinetics. From studies into the transformations of $H\dot{O}_2$ radicals it was shown that their recombination could lead to the formation of H_2O_4 molecules in the temperature range from 90 K to 153 K.

In addition to the formation of H_2O_4, it was proved that there existed oxygen-hydrogen compounds of the form H_2O_3 which could, among other things, be produced as a result of radiation-induced chemical transformations in solutions of sulphuric and perchloric acids. Thus, low-temperature studies seem to have proved the existence of a new series of oxygen-hydrogen compounds traceable to hydrogen peroxide, namely, H_2O_2, H_2O_3, and H_2O_4.

When ozone was reacted with liquid and solid ammonia and with a solution of NH_3 in a mixture of $CHCl_3$ and C_2H_5Cl at 173 K, the formation of NH_4O_3 with yields up to 5% was observed [49]. The low yield can be explained by the fact that NH_4O_3 is only stable at temperatures below 147 K, whereas at 178 K as much as 17% of it would decompose in a matter of 2 to 10 min. The compounds containing the O_3 group were found to be paramagnetic and to have absorption bands in the visible spectrum.

Low temperature has been found to promote stabilization of exoteric reactive species. To initiate a chemical transformation at cryogenic temperatures, especially in the solid phase, it is customary to use physical agents. Typically, the transformation products of systems close in composition but activated differently would often contain similar compounds. A pertinent example is offered by the formation of CO_3 [50, 51]. CO_3 molecules, detected using IR spectra and isotope labels, are reported to have been produced by vacuum-UV photolysis ($\lambda = 147$ nm) of solid carbon dioxide at 77 K, mercury-lamp photolysis ($\lambda = 253.7$ nm) of O_3 in a CO_2 matrix at 50-60 K, photolysis of an O_3-CO_2 mixture in an argon matrix [51], and also by the cocondensation (at 50-70 K) of the products of an r.f. discharge in CO_2 [50]. Photolysis of CO_2 in an argon matrix was not found to produce CO_3. With the temperature of the argon matrix containing CO_3 and O_2 raised to as high as 38 K, the reaction

$$CO_3 + O_2 \longrightarrow CO_2 + O_3 \qquad (1.15)$$

was observed to proceed at a high rate.

1.3.2. Fluorine-Containing Compounds

Low temperatures have more than once been employed to produce various fluorine-containing compounds. Of special interest in this respect are various oxygen fluorides. These compounds show a high reactivity and will remain in a liquid state to nearly the temperature of liquid nitrogen. This enables them to be used as both reactants and solvents.

A large variety of oxygen fluorides have been produced and investigated to date: OF_2 [52], O_2F_2 [53], O_3F_2 [54], O_4F_2 [55], O_5F_2, and O_6F_2 [56]. As NMR studies on the nuclei of ^{19}F [57, 58] and ^{17}O [57] have shown, O_3F_2 does not exist as an entity. On the strength of experimental data, it is concluded by Solomon *et al.* [57] that O_3F_2 appears to be a mixture of O_2F_2 and, probably, O_4F_2 in equilibrium with $\dot{O}_2F$. The existence of $\dot{O}OF$ radicals was, for example, detected by Arkel [59] in the photolysis of OF_2-O_2 and F_2-O_2 mixtures in oxygen, nitrogen, and argon matrices at 40 K [59].

Solomon *et al.* come out in support of their view-point in a later work [60] by pointing out that O_3F_2 was noted to react with BF_3 with the formation of the same products as were produced by the reaction of O_2F_2 with BF_3 [61]:

$$3O_3F_2 + 6BF_3 \longrightarrow 6O_2BF_4 + F_2 \qquad (1.16)$$

$$2O_2F_2 + 2BF_3 \longrightarrow 2O_2BF_4 + F_2 \qquad (1.17)$$

There also exists a different point of view. It is suggested [58] that O_3F_2 is a stable compound $2O_2F_2 \cdot O_2$ $(2O_3F_2)$ of complex type. If it were so, then it would be legitimate to expect that O_2BF_4 should be formed and oxygen liberated in addition to the formation of BF_3.

According to [61], there is another reaction taking place at 147 K and involving phosphorus pentafluoride:

$$O_2F_2 + PF_5 \longrightarrow O_2PF_6 + \frac{1}{2} F_2 \qquad (1.18)$$

The compounds O_2BF_4 and O_2PF_6 remain rather stable up to 273 K. At room temperature, they rapidly dissociate:

$$O_2BF_4 \longrightarrow O_2 + \frac{1}{2} F_2 + BF_3 \qquad (1.19)$$

On hydrolyzing they give up a large amount of ozone.

When CF_3OOH reacts with F_2 in the presence of CsF, it produces CF_3OOF with a yield of up to 35%. This compound possesses interesting properties: it boils at 203.8 K and melts at below 77 K. Depending on the reaction temperature (77-258 K) and the relative amounts of reactants the yield of CF_3OOF also varies and other compounds are formed. The scheme written below depicts the reactions that take place when CF_3OOH is reacted with F_2 in the presence of CsF at cryogenic temperatures [62]:

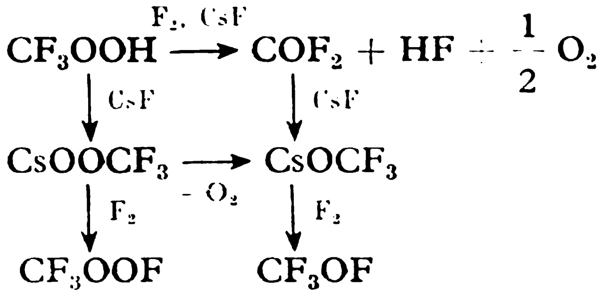

CF_3OOF is sufficiently stable at room temperature.

Reactions between fluorine, nitrogen oxides (NO, NO_2), nitrogen-fluorine compounds such as N_2F_4 or NF_3, ozone, and oxygen derivatives of fluorine like OF_2 in the gaseous phase, accompanied by the cocondensation of the products at 77 K, produce various mixed nitrogen-oxygen-fluorine-containing compounds. They are all strong oxidants [63]. Using mass spectrometry, the investigators have determined energy characteristics and heats of formation for the compounds ONF, NO_2F, NO_3F, ONF_3 and the unstable compounds ON_2F_2 and $O_2N_2F_2$ [64].

1.4. HETEROGENEOUS REACTIONS

Many cryogenic reactions proceed with the participation of a solid phase and may in a sense be treated as heterogeneous. This section will, however, be concerned only with processes in which the atoms or molecules produced in a gaseous phase usually react with solids at low temperatures. In this respect, the most detailed studies have been carried out on contact reactions with the participation of hydrogen atoms.

1.4.1. Contact Reactions of Hydrogen Atoms

Reactions of hydrogen atoms obtained in a gaseous phase with solid oxygen have been investigated by Klein and Scheer [65]. It appears that the first to take place as a result of the diffusion of hydrogen atoms was the following reaction:

$$H + O_2 \longrightarrow H\dot{O}_2 \qquad (1.20)$$

The reaction typical of the gaseous phase

$$H + O_2 \longrightarrow \dot{O}H + O \qquad (1.21)$$

does not seem likely at cryogenic temperatures from energy considerations. The reaction (1.20) seems to be followed then by the reactions involving hydrogen atoms:

$$\begin{aligned} &H + H\dot{O}_2 \longrightarrow H_2O_2 \\ &H + H_2O_2 \longrightarrow H_2O + \dot{O}H \\ &H + \dot{O}H \longrightarrow H_2O \\ &2H\dot{O}_2 \longrightarrow H_2O_2 + O_2 \end{aligned} \tag{1.22}$$

The investigators hypothesized the above reactions because, on warming up, they detected water and hydrogen peroxide, their yields were not determined, however.

Klein and Scheer have also investigated the reactions of hydrogen atoms with several unsaturated hydrocarbons [66-70]. The attachment of hydrogen atoms to solid olefins was observed when the latter were uniformly condensed on the inner surface of a sphere immersed in liquid nitrogen. Hydrogen atoms were obtained by hydrogen dissociation over a tungsten filament heated to 1500 K. Hydrogen was admitted via a palladium capillary tube.

Olefins were found to react at various rates. According to the reactivity in the above reaction, they may be arranged in the following series:

propylene >	1-butene >	3-methyl 1-butene >	isobutene >	1-pentene >	1-hexene
10.0	8.0	4.0	1.0	0.1	0.0

According to mass spectrometric data, the reaction of hydrogen with, say, propylene would produce 37% propane and 5% 2,3-dimethyl butene, the remainder being the unreacted propylene. The reaction of hydrogen with 1-butene was found to yield 56% *n*-butane, 40% 2-butene, and 4% 3,4-dimethyl hexane.

The above data suggest that hydrogen atoms add first to the double-bond carbon atom of on olefin molecule with the formation of a secondary alkyl radical

$$H + -CH_2-CH=CH_2 \longrightarrow -CH_2-\dot{C}H-CH_3 \tag{1.23}$$

The propane and butane detected upon hydrogenation can be formed as a result of addition of a second hydrogen atom to the alkyl radical.

Cryogenic studies have brought out the difference in reactivity between various olefins, because even the minutest differences in activation energy are strongly felt under such conditions. In the case of propylene and 1-butene, the recombination of secondary alkyl radicals yields 2,3-dimethyl butane and 3,4-dimethyl hexane. In the case of butene-1, it is not unlikely that a reaction of disproportionation takes place, leading to butene-2:

$$2(-CH_2-\dot{C}H-CH_3) \longrightarrow -CH=CH-CH_3 + -CH_2-CH_2-CH_3 \quad (1.24)$$

Experiments with deuterium [68] have shown that the isomerization of butene-1 into butene-2 can alternatively be brought about because a deuterium atom detaches a hydrogen atom from a secondary butyl radical. This can proceed as follows:

$$CH_3-CH_2-\dot{C}H-CH_2D + D \longrightarrow CH_3-CH=CH-CH_2D + HD \quad (1.25)$$

No HD is produced by the reaction involving propylene. In the case of 3-methyl butene-1, HD is formed at a higher rate than in the case of butene-1. According to the rate at which the hydrogen atom in the α-position relative to free valency breaks off, the radicals may be arranged in the following sequence:

$$\text{tertiary} > \text{secondary} > \text{primary}$$

Thus, at 77 K a deuterium atom attacks only tertiary and secondary carbon atoms, leading to the appearance of secondary olefins which are no longer capable of reacting with hydrogen atoms at cryogenic temperatures.

Activation energies for the addition of hydrogen atoms to various olefins have been determined by experiments at various temperatures. In the temperature interval from 77 to 86 K for propylene $E_{act} = 6.3$ kJ mole^{-1} and for butene-1 it is 4.2 kJ mole^{-1}. For isobutene $E_{act} =$ $= 12.6$ kJ mole^{-1} in the temperature interval from 91 to 113 K, and for hexene-1 $E_{act} = 17.2$ kJ mole^{-1} in the temperature interval from 117 to 130 K. In the gaseous phase, the activation energies for these reactions are the same and equal to 10.5 kJ mole^{-1} [71].

The cryogenic hydrogenation technique has markedly been improved by V.L. Talrose and A.N. Ponomarev [71-73].

A good deal of effort is being put into studies concerned with the reactions of hydrogen atoms with olefins and other hydrocarbons, which exemplify cryogenic reactions between a solid surface at a low temperature and a reactant in the gaseous phase.

For example, reactions of tritium atoms with frozen hydrocarbons and the subsequent changes of the radicals are described in [74-76]. Using the Klein-Scheer technique, the investigators have studied the reactions of tritium atoms with frozen cyclohexane [74], cyclohexene [76], cyclohexyl-1-cyclohexene and cyclohexyl-2-cyclohexene [75] and also the reactions of disproportionation and recombination of the resultant radicals. The products detected and their yields for cyclohexyl cyclohexene isomers in various matrices at 77 K are given in Table 1.1.

TABLE 1.1

Composition and Yield of Products of the Reactions of Tritium Atoms with Cyclohexyl-1-Cyclohexene (I) and Cyclohexyl-2-Cyclohexene (II) in Various Matrices at 77 K

Target	Yield, % of total tritium activity in liquid products (±0.3%)					k_d/k_r[1]
	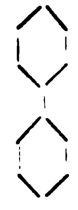	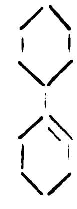	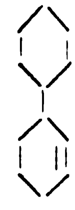	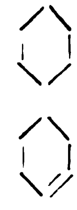	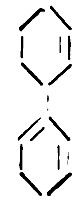	
3% I in cyclohexane	65.8	32.1[2]	1.3	0.8	–	0.5
3% II in cyclohexane	56.7	12.8	22.6	4.2	3.7	0.7
3% II in n-pentane	37.2	19.0	23.2	13.3	7.3	1.5

---

[1] The computed ratio of reaction rate constants for disproportionation, k_d, and for recombination, k_r, of labelled bicyclohexyl radicals with tritium atoms.

[2] Including 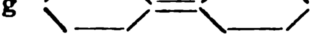.

As is seen, in addition to hydrogenation products, there are isomeric products. In simplified form, the formation of reaction products in the case of cyclohexyl cyclohexene may be depicted thus:

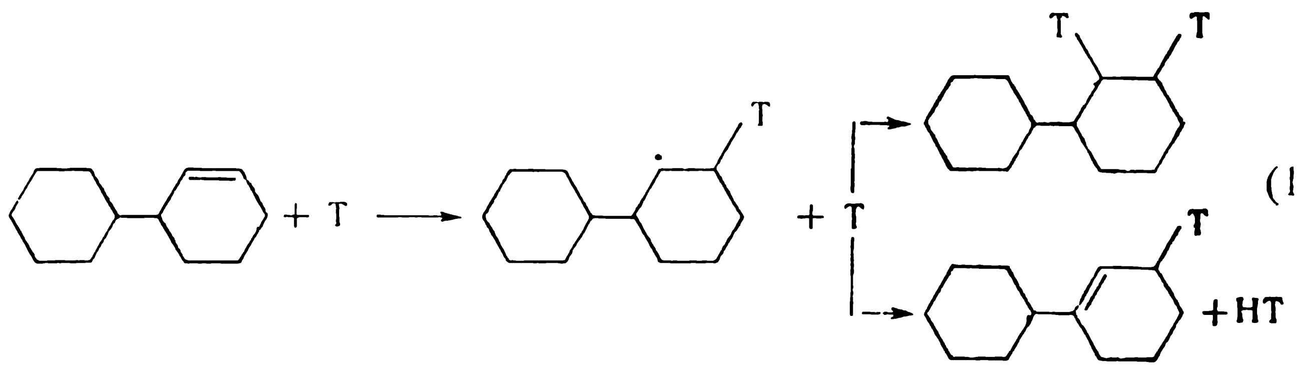

(1.26)

In the case of cyclohexyl cyclohexene, reactions like (1.26) convert over 90% radicals, or, which is the same, less than 10% radicals take part in the reactions of recombination. It is seen from Table 1.1 that the relative yield of the reaction products varies with the type of matrix used. It has been suggested that this is related to the degree of rigidity of the matrix [74]. The ratio k_d/k_r varies with the character of the matrix, also, it appears that the rates of disproportionation and recombination are determined by the aggregate state of the system (that is, whether the system is solid, liquid or gaseous), and temperature.

The results of a study into the reactions of disproportionation and recombination involving cyclohexyl radicals at 77-145 K are presented in Table 1.2. The yield of bicyclohexyl (III), which is the product of recombination, is seen to increase with temperature, the rate of increase being especially high at temperatures above that of phase transition for cyclohexene (138.8 K) [77]. In contrast, the ratio of yields for cyclohexene and bicyclohexyl, which is indicative of the ratio of rates for the reactions of disproportionation and recombination, decreases with rising temperature. According to [78], the ratio k_d/k_r increases with the transition from the gaseous to liquid and from liquid to solid phase, varies from solvent to solvent, and decreases with rising temperature within a particular phase. For example, the ratio k_d/k_r for ethyl radicals depends on the phase state of the system and can, within a particular phase, be approximated by a relation of the form

TABLE 1.2

Composition and Yield of Products of the Reaction between Tritium and Cyclohexene at Different Temperatures

T_M, K	Yield, % of total activity of tritium in liquid products			Ratio of product yields		k_d/k_r
	$C_6H_{11}T$ (I)	C_6H_9T (II)	$C_{12}H_{21}T$ (III)	[II]/[I]	[II]/[III]	
77	87.5	12.2	0.3	0.14	40.8	49±2
90	83.2	15.0	1.5	0.18	10.0	—
112	76.3	16.1	6.7	0.21	2.4	4.5±0.5
145	43.3	22.5	30.4	0.52	0.7	—

$$k_d/k_r \sim T^{-n}$$

where $n = 0.7$ for the gaseous phase, 0.86 for the liquid phase in isooctane, and 0.33 for the solid phase in isooctane. Formally, this form of relation can be ascribed to the difference $E_r - E_d$ respectively equal to 1135, 1758, and 335 J mole^{-1}.

A similar processing of the results for cyclohexyl radicals in the temperature range 77-145 K leads to a relation of the form

$$k_d/k_r \sim T^{-5.1}$$

or to

$$E_r - E_d = -5.0 \text{ to } 5.4 \text{ kJ mole}^{-1}$$

In the light of experimental data, it is suggested in [79] that the unfreezing of molecular motion taking place during a phase transition is especially strongly felt in the recombination of radicals.

1.4.2. Contact Reactions of Other Atoms

There is a group of reactions that stand close to the contact reactions of hydrogen and tritium with olefins discussed in the previous section. These are reactions of gaseous fluorine with various organic solids, which apparently involve an adsorption stage.

At temperatures close to 77 K, oxygen-containing gaseous fluorine can react with solid organic compounds, such as ethylene and its chlorine derivatives, divinyl, butene-1, toluene, cyclohexane, benzene, and aniline, with the formation of peroxide radicals [80, 81]. The reaction of F_2 with H_2S and D_2S in the presence of O_2 has also been noted to lead to the formation of radicals. A study into the kinetics of the reaction involving F_2 and ethylene or its chlorine derivatives has revealed that, on the basis of conversion rates, the compounds involved can be arranged in a reactivity series as follows:

$$C_2H_4 > C_2H_3Cl > C_2H_2Cl_2 > C_2HCl_3 > C_2Cl_4$$

As more hydrogen atoms are replaced by chlorine, the rate of fluorination decreases. Benzene rapidly fluorinates at 77 K, whereas cyclohexane, difluoromethane and dichloromethane do not react with fluorine. In the case of ethylene, the products of reaction are mainly C_2H_5F, C_2H_3F, 1,4-difluorobutane, and 1,2-difluoroethane. A plausible explanation for this composition of reaction products seems to be that radicals begin to form via a reaction between valence-saturated molecules

$$F_2 + C_2H_4 \longrightarrow C_2H_4F + F \qquad (1.27)$$

It is suggested in [80] and [81] that the reaction (1.27) proceeds by way of a collision between fluorine molecules from the gaseous phase and the solid surface of the organic compound. On the basis of kinetic data, the reaction probability per collision for fluorine and trichloroethylene (with allowance for the magnitude of surface area) has been found to be 3×10^{-9} and 5×10^{-9} at 77 K and 110 K, respectively, which corresponds to an activation energy of less than 2 kJ mole^{-1}. Accordingly, it has been suggested that the fluorination of olefins and hydrocarbons proceeds by a radical mechanism.

In [81], attention is drawn to the intriguing decrease in activation energy for the reaction between fluorine and ethylene as the system changes from the gaseous to the solid phase. In the gaseous phase, it is over 10 kJ mole^{-1} (for example, for ethylene $E_{act} = 18.8$ kJ mole^{-1}) [82], whereas for the solid phase the activation energy in the same reaction has been found to be around 2 kJ mole^{-1}. In the opinion of [81], the lower activation energy in cryogenic fluorination may be explained by the fact that the direct chemical interaction is preceded by the adsorption of fluorine on the surface of trichloroethylene.

Brief mention should be made of other heterogeneous cryogenic processes. Upon UV-irradiation at 77 K, silicagel with adsorbed oxygen has been found to give ESR signals, which is an indication of the presence of paramagnetic centres [83]. The signals are assigned to O_3^- anion radicals which are stable at 77 K, but begin to break up reversibly with increasing temperature according to the reaction

$$O_3^- \rightleftarrows O^- + O_2 \qquad (1.28)$$

At 173 K, they disappear completely.

In the system $SiO_2 + (O_2)_{ads}$ exposed to light in the presence of hydrogen and carbon monoxide at 77 K, the following reactions have been noted to take place with the participation of hole centres [84-87]:

$$\begin{gathered} O^- + H_2 \longrightarrow OH^- + H \\ O^- + CO \longrightarrow CO_2^- \qquad (1.29) \\ CO_2^- + M^{n+} \longrightarrow CO_2 + M^{(n-1)+} \end{gathered}$$

It has been established that upon exposure to light at 77 K silicagel with adsorbed oxygen becomes a catalyst for the isotopic exchange of oxygen, for which the following scheme has been suggested, involving O_3^- anion radicals:

$${}^{16}O^-_{ads} + {}^{18}O^{18}O \rightleftarrows [{}^{16}O^{18}O^{18}O]_{ads} \rightleftarrows {}^{18}O^-_{ads} + {}^{16}O^{18}O \qquad (1.30)$$

At 173 K, the rate of exchange reaction has been found to remain practically unchanged for a half-hour at 10^{11} molecules/cm^2 s.

Low-temperature reactions between H_2, CO and ethylene, on the one hand, and the trapped radiation defects produced in silicagel by gamma irradiation, on the other, are examined in [88]. The mechanism involved in the homo- and heteromolecular low-temperature isotopic exchange between oxygen on silicagel and vanadium pentoxide applied to it is examined in [89]. The experimental results seem to suggest that on newly reduced samples the low-temperature exchange proceeds without the participation of the ion-radical reactive forms of the adsorbed oxygen. In the investigators' opinion, such forms may well be atomic and molecular oxygen adsorbed without transfer of an electron on a metal ion.

The adsorption of oxygen on a gamma-irradiated silicagel sample at 77 K produces an O_2^- ion radical [90].

Using the ESR technique, the authors of [91] have investigated the properties and interaction of O_2^- with olefins and hydrogen on a gamma-irradiated silicagel sample. According to ESR spectra, upon adsorption on the surface of olefins and hydrogen they react with O_2^- ion radicals. The reaction of O_2^- with hydrocarbons and olefins can produce radicals by at least two mechanisms.

Firstly, this may happen via a direct reaction with an olefin molecule. In such a case, the double bond is ruptured and a compound of the form $^{-}CH_2—CH_2—O—\dot{O}$ is produced. The electron localized on the first carbon atom contributes to the chemical bond with the sorbent atoms; in other words, chemisorption takes place. Thereafter, a chain reaction may take place:

$$^{-}R-O-\dot{O} + O_2 \longrightarrow RO_2 + O_2^{-} \qquad O_2 + C_2H_4 \longrightarrow C_2H_4O-\dot{O}$$

The chain is broken off upon interaction with a hole.

Secondly, this may happen via a reaction of O with a positive ion derived from an olefin molecule. Positive ions can be derived from an olefin molecule in any one of two ways: either when an olefin molecule captures a hole centre on the surface of the irradiated silicagel

$$C_2H_4^{+} + O_2^{-} \longrightarrow C_2H_4-O-\dot{O} \text{ (chemisorption)}$$

or when an olefin molecule interacts with an acid centre on the surface of the silicagel.

From the material presented in this chapter, it is seen that isolated studies into individual low-temperature chemical processes have gradually grown into a ramified and multifaceted research area in its own right.

CHAPTER TWO

APPARATUS AND TECHNIQUES FOR CRYOGENIC RESEARCH

This chapter will offer only a brief outline of the apparatus and the basic physical methods used for cryochemical research. For a more detailed exposition, the reader is to refer to monographs and handbooks [92-98].

2.1. CRYOSTATS

As a rule, low-temperature investigations are carried out in devices known as cryostats. The specific design of a cryostat depends, above all, on the experimental techniques adopted, the refrigerant used, and the experimental temperature to be maintained. Few cryostats are available commercially, so experimentors ordinarily build whatever apparatus they need in their laboratories.

According to the purpose served, cryostats may be classed into two groups. The first group, more numerous, encompasses cryostats intended to measure physical and physico-chemical properties. In such cases, the samples are usually solid individual compounds which are loaded in a disassembled cryostat at room temperature. Then the cryostat is assembled, and the sample is cooled, which requires an appreciable interval of time in some cases.

The second group covers cryostats intended to study chemical reactions. The construction of such cryostats poses a formidable engineering problem because it is not an easy matter to carry out and investigate a chemical reaction involving several components directly at low temperature.

What follows is a brief outline of cryostats widely used by chemical laboratories. Emphasis is placed on cryostats of more simple designs which can readily be built in the laboratory. The first to be described are simple cryostats for spectral and magnetic resonance spectroscopy experiments, operating at a constant temperature. In such devices, the samples are enclosed in tubes or spectral cells immersed directly in a refrigerant, usually liquid nitrogen or helium. Where appro-

*

priate, the design of cells, which are important components of a cryostat, is described. Then come cryostats capable of operating at a variable temperature. In such devices, the refrigerant is ordinarily a cooled gas. The chapter is concluded by a description of cryostats used in the investigation of low-temperature chemical reactions.

According to the source of cryogenic temperature, cryostats may arbitrarily be classed into several groups as follows: cryostats in which the refrigerant is a liquefied gas; cryostats in which the refrigerant is a cooled gas; thermoelectric coolers; and cryostats built around various refrigerating machines. This classification seems convenient in examining the specific features of cryostat designs.

The most commonly used and convenient sources of cryogenic temperature are liquid refrigerants, especially liquefied gases. The physical properties of the most commonly used liquefied gases [1, 99] are given below.

Refrigerant	^4He	$H_2$1)	N_2	O_2	Ar	NH_3
T_{boil}, K	4.215	20.27	77.34	90.190	87.4	239.8
Triple point, K	—	13.8	63.24	54.36	—	—
Heat of vaporization						
J g^{-1}	20.7	442.7	200.8	213.4	158.6	1368
J cm^{-3}	2.59	31.3	161.9	243		
ρ, g cm^{-3}	0.125	0.0707	0.807	1.14		
C_P, kJ $kg^{-1}K^1$						
for liquid at T_{boil}	4.52	9.50				
for gas at 273 K and $P = 0.1$ MPa	5.19	14.2	1.042	0.916		

---

1) 99.97% parahydrogen.

A very popular refrigerant, especially in the food industry, is solid carbon dioxide ('dry ice'). Under normal pressure, it sublimes at 194.6 K, and its heat of vaporization is 573.6 J g^{-1}. The refrigerants used in industrial applications are examined in detail in [100].

Cryostats maintaining a constant temperature are the simplest and, therefore, the most commonly used units. In such a cryostat, the desired experimental temperature is produced owing to the fact that the refrigerant (a liquefied gas or a solid) boils or melts at a constant temperature. The substances and mixtures suitable as refrigerants for fixed temperature cryostats are described in [101]. The compositions of cryogenic baths securing a fixed temperature in the range from 273 K to 113 K are given in [102]. The desired experimental temperature is produced by pouring liquid nitrogen into a suitable solvent to obtain a pasty mass. Temperatures above 195 K can be obtained by using solid carbon dioxide instead of liquid nitrogen.

As a rule, the refrigerant in a fixed-temperature cryostat is contained in a glass or a metal Dewar vessel fitted with optical windows.

Figure 2.1 shows in sketch form a quartz Dewar vessel widely used in ESR work at the boiling point of liquid nitrogen, a quartz cell for optical measurements, and a cell for studies involving the absorption and ESR spectra of the same sample at 77 K [103-105]. In such a cryostat, the experimental temperature can be maintained at below 77 K by evacuating nitrogen vapour at a high rate. In helium cryostats, this technique ensures temperatures down to 1.2 K. As a rule, however, refrigerant vapour is pumped out not for cooling, but for improving the conditions under which ESR spectra are measured, because this reduces the formation of bubbles by the nitrogen as it boils.

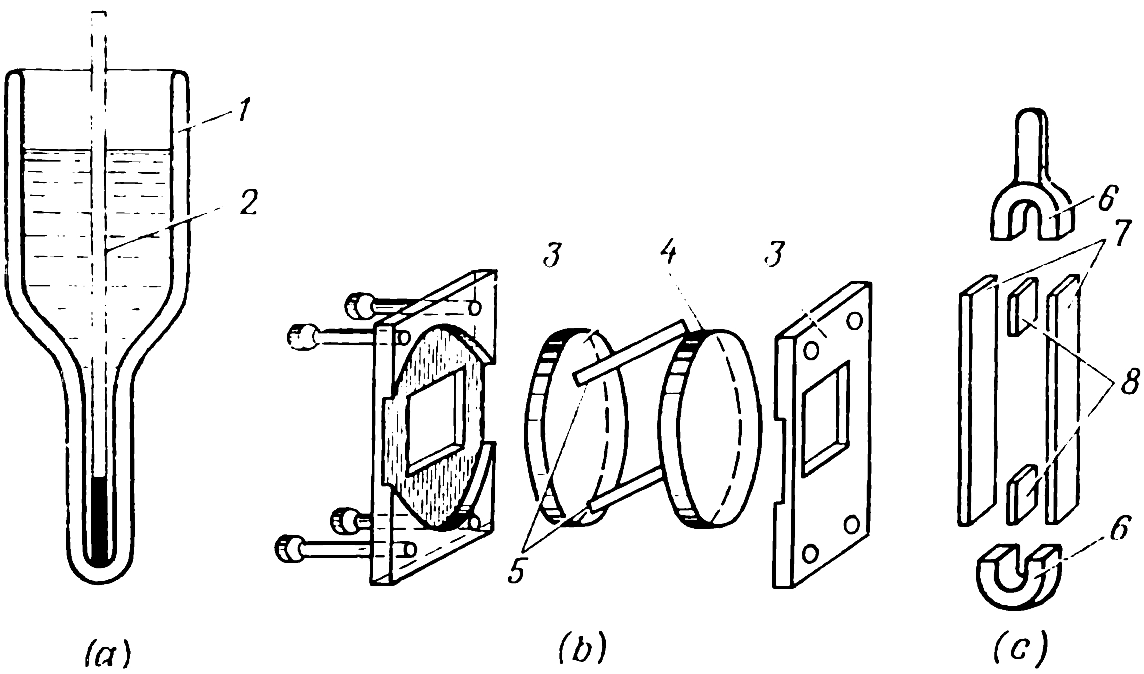

Fig. 2.1. (a) A quartz Dewar flask, (b) quartz cells for optical measurements, with stratum depth from 1 mm to 10 μm, (c) quartz cells for joint spectrophotometric and ESR measurements on a single sample at 77 K [103, 105]:

(1) Dewar flask; (2) ESR sample tube; (3) metal mount; (4) quartz plates; (5) spacers; (6) clamps; (7) quartz plates; (8) spacers

A more elaborate cryostat for optical measurements is described in [106]. It uses a metal Dewar vessel in which the sample is immersed in liquid nitrogen or liquid helium, and absorption or fluorescence spectra are observed through optical windows.

A still more elaborate design is used in cases where the sample ought not to be immersed in the refrigerant for some reason or other. An example is the cryostat shown in Fig. 2.2. It is used for spectrophotometric investigations of samples in tubes used in ESR work [107].

One of the early designs of glass cryostats which may be used for work at the temperature of liquid helium is described in [108]. Similar cryostats are described in [1] and [2]. Their basic design has changed but little in the meantime. In most cases, thermal insulation is provided by a vacuum shroud. Since this calls for a deep vacuum, the cryostat is equipped with suitable vacuum facilities. In many of the cryostats described in the literature, the experimental space is likewise evacuated [108]. An example is the metal cryostat for optical measurements described in [109].

Cryostats with an evacuated experimental space are difficult to handle and cannot take liquid samples. They are widely used in the physical studies of semiconductor materials and in solid-state physics. In such cryostats samples are prepared under normal conditions. A simple and reliable cryostat intended for the visible-UV measurement of absorption spectra of samples in evacuated experimental space is described in [110]. Despite its simplicity, the cryostat suffers from obvious drawbacks. Among other things, each time the sample is changed, the cryostat must be taken apart, re-assembled, and evacuated. Measurements can be made only on solid or pre-frozen samples, the cryostat having only one working temperature of liquid nitrogen. The cryostat is unsuitable for kinetic studies on systems where two components must be brought in contact.

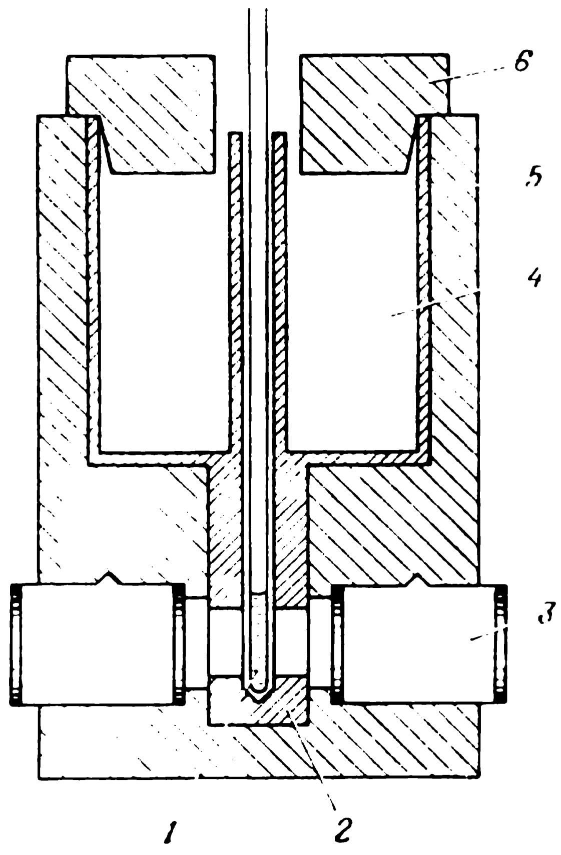

Fig. 2.2. Sketch of a cryostat for UV spectrum work [107]:

(1) sample tube; (2) copper block; (3) quartz vacuum shrouds with optical windows; (4) refrigerant reservoir; (5) foamed-plastic insulation; (6) lid

A relatively simple glass cryostat with a metal sample holder and an evacuated experimental space is described in [111]. Owing to the heater and three quartz windows, the cryostat can be used for spectrophotometric measurements and photochemical investigations in the temperature range 77-450 K.

Spectral experiments in the visible and UV regions widely use cryostats in which the experimental space is not evacuated. In sketch form, such a cryostat is shown in Fig. 2.3. The cell is set up on a holder of brass, copper, aluminium or some other metal. The lower elongated part of the holder is always immersed in a liquid refrigerant poured in a glass or quartz Dewar vessel. This cryostat can be used together with any stock-produced spectrophotometer. The path of the optical beam is intercepted only by refrigerant vapours, so the bubbles forming as it boils do not interfere with measurements. The sample in such a cryostat can be maintained at only one temperature close to that of the liquid refrigerant. Such cryostats are described, for example, in [112-114], where they were used to obtain the absorption spectra of biological objects in the visible spectrum.

In designing a cryostat, one runs into difficulties because the cell material must satisfy conflicting requirements: on the one hand, it must be a good thermal conductor; on the other, it must be chemically inert and not react with the sample. A problem common to all cryostat designs is the maintenance of a good thermal contact with the sample.

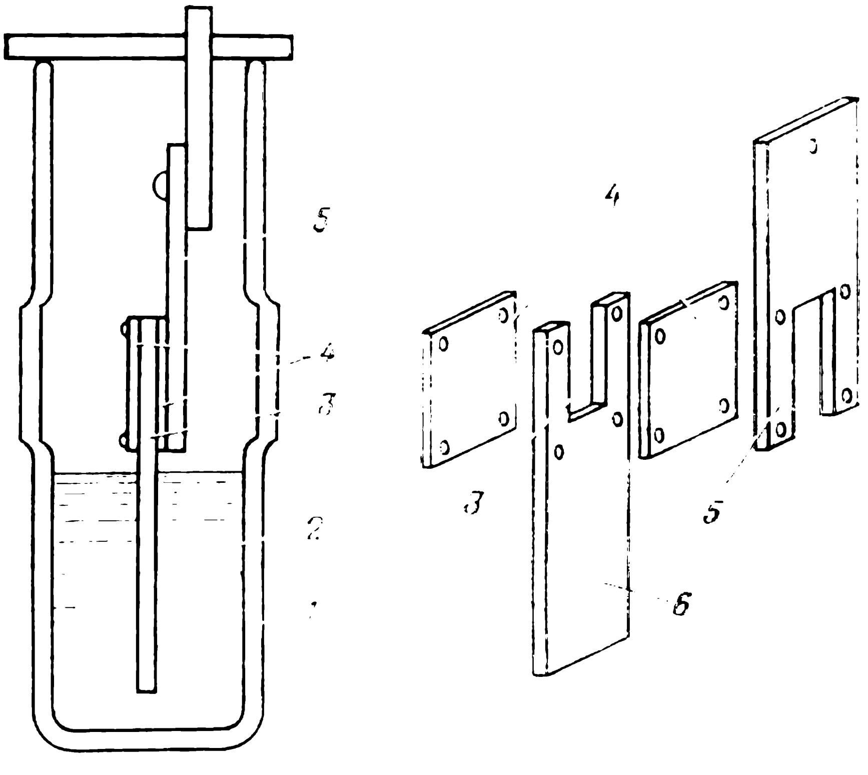

Fig. 2.3. Sketch of a cryostat for optical studies:

(1) Dewar flask with optical windows; (2) liquid refrigerant; (3) sample space; (4) quartz optical plates; (5) holder; (6) metal shank

As already noted, in liquid-gas cryostats the sample can be thermostatted at only one temperature, which is usually sufficient for spectral studies. The resolution of spectra depends on the sample temperature and improves as the temperature is brought down. In the study of chemical reactions, however, it is often necessary to investigate a process at several temperatures, and this calls for the possibility of changing the experimental temperature to the required value.

Figure 2.4 shows a cryostat incorporating an electrical heater with which the experimental temperature can be raised as may be required, notably in the range 250-77 K when using liquid nitrogen as refrigerant. This type of cryostat has been used to maintain samples at a predetermined temperature. Inclusion of a heater controlled by an automatic system and placed next to the sample turns the cryostat of Fig. 2.3 into a variable-temperature cryostat. This apparatus can give considerably lower temperatures than cryostats using a stream of gas for the refrigerant [115]. The efficiency is improved by a better utilization of the heat of vaporization of the liquid refrigerant. Because the cooled part of the sample is usually held in the vapour phase of the liquid refrigerant, the condensation of water vapours on the cell windows is avoided. A further advantage is that the experimental space need not be evacuated, which fact simplifies the design and improves thermal contact with the sample. Such cryostats can also take liquid samples. On the demerit side of this design is the larger size of the experimental space, since the sample must be placed as close as possible to the refrigerant bottle. Because of this, experimentors often turn down this type of apparatus, especially where it must be part of an experimental setup.

Wide use is made of cryostats in which the refrigerant is a stream of gas. The basic arrangement of such a cryostat for spectrophotometric experiments is shown in Fig. 2.5. It suffers from a number of drawbacks, namely: the heat of vaporization of liquid nitrogen is utilized incompletely; the lowest temperature attainable in this arrangement is seldom below 153 K because the lines carrying nitrogen vapour from the Dewar vessel to the sample space are long whereas the heat capacity of nitrogen vapour is low; the consumption of nitrogen is prohibitively large. A simple cryostat of this design, intended for maintaining small samples in the temperature interval from 100 to 400 K, is described in [116]. More elaborate designs are described in [117-123].

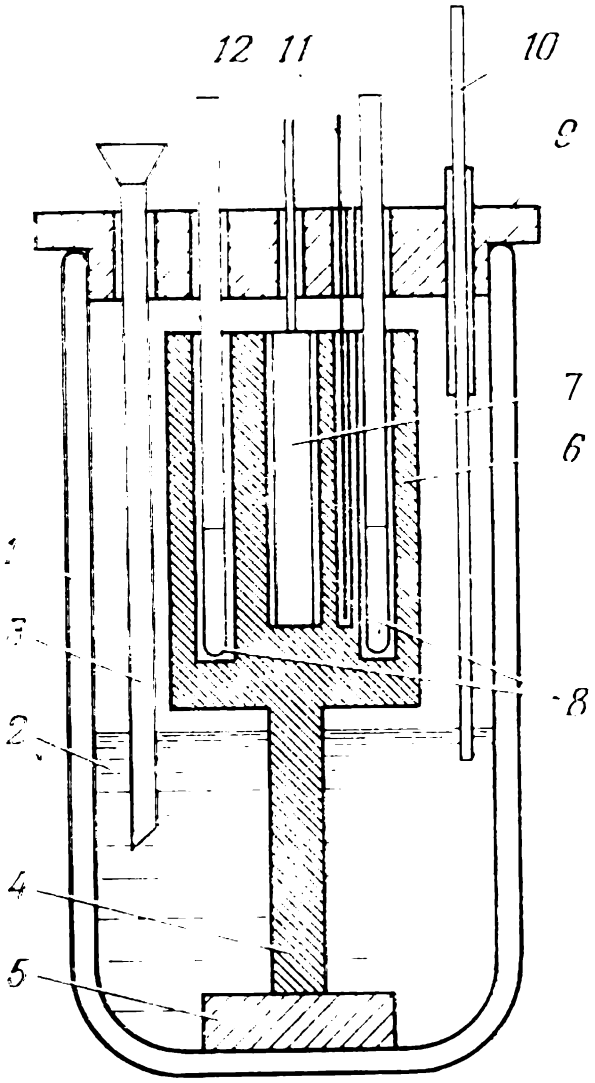

Fig. 2.4. Multi-temperature cryostat [97]: (1) Dewar flask; (2) refrigerant; (3) refrigerant filling tube; (4) metal shank; (5) support; (6) metal block; (7) heater; (8) sample tubes; (9) lid; (10) refrigerant level indicator; (11) thermocouple; (12) power for heater

In [124] and [125], a description is given of a low-temperature setup which combines a helium cryostat and a high-vacuum photochemical reactor utilizing photolysis of cocondensation products and matrix isolation.

In the cryostat sketched in Fig. 2.6, the heat of vaporization of liquid nitrogen is effectively utilized owing to the fact that the refrigerant is gaseous nitrogen drawn from a storage bottle and cooled on passing through a Dewar vessel containing liquid nitrogen. The nitrogen gas can be passed through a metal coil immersed in the Dewar vessel or bubbled through the liquid nitrogen directly. Either method has merits and demerits of its own. The former arrangement can use any Dewar vessel, including a glass one, provided it has a sufficiently wide neck. In the latter arrangement, the Dewar vessel must be hermetically sealed and be capable of standing up to a positive pressure differential of 0.2 MPa.

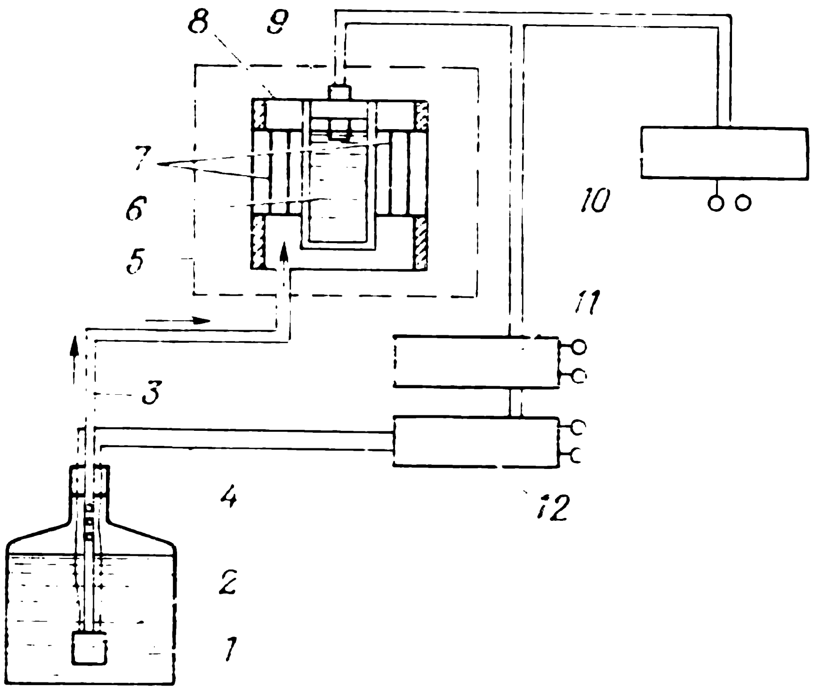

Fig. 2.5. Arrangement of a cryostat using nitrogen vapours as refrigerant:

(1) liquid-nitrogen Dewar flask; (2) heater-evaporator; (3) tube to carry liquid-nitrogen vapours; (4) power to heater-evaporator; (5) cell space of spectrophotometer; (6) sample cell; (7) quartz windows of thermally insulated cell holder; (8) cell stopper; (9) thermocouple; (10) reference-junction thermostat; (11) voltmeter; (12) discriminator

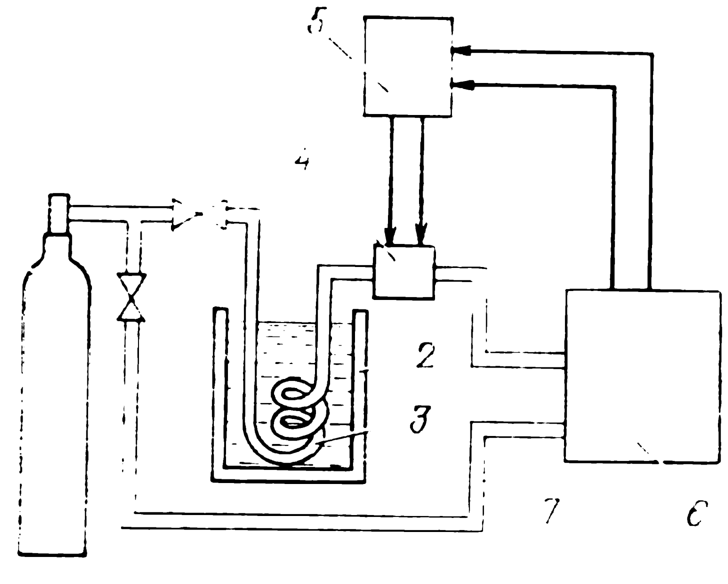

Fig. 2.6. Cryostat using nitrogen vapours as refrigerant [126]:

(1) gas cylinder; (2) liquid-nitrogen Dewar flask; (3) coil; (4) heater; (5) temperature measurement and control unit; (6) optical section of cryostat; (7) anti-fog blow system

Reference [126] describes a continuous-flow cryostat adapted to spectrophotometric work by stock-produced spectrophotometers. The cryostat can operate in the temperature range from 153 to 273 K. The temperature is maintained accurate to within ± 0.1 K, and the time required for the system to be cooled from 278 K to 223 K at a nitrogen flow rate of 5×10^{-4} m^3 s^{-1} is 720 s.

Recent years have seen a growing use of thermoelectric cooling apparatus [127, 128]. A thermoelectrically cooled chamber for laboratory work and thermoelectric coolers for spectroscopic cells are described in [129-131]. Thermoelectrically cooled cryostats are simple in design and operation and require no refrigerants such as liquid nitrogen or helium. They are especially advantageous in prolonged experiments and in cooling electronic devices. A major limitation with them is that the existing thermoelectric coolers cannot give sufficiently low temperatures. The lowest limit for two-stage thermoelectric batteries is 223 K. With all other conditions being equal, the size of a thermoelectric cooler increases as the desired temperature is decreased.

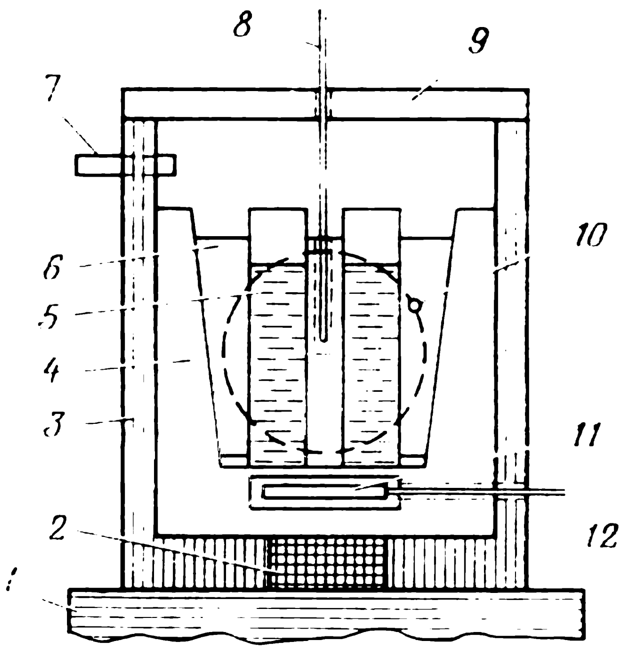

Fig. 2.7. Refrigerator-based cryostat for optical studies [97]:

(1) refrigerator housing; (2) cold head; (3) optical section; (4) brass cell holder; (5) samples; (6) brass wedges; (7) purge-gas pipe union; (8) thermocouple; (9) lid; (10) optical quartz windows positioned on front and rear walls of cryostat in the beam path; (11) electric heater; (12) power to heater

Reference [132] describes a four-stage microcooler operating over a temperature range from 130 to 350 K. Undoubtedly, further improvements in thermoelectric batteries will be accompanied by a decrease in their size (for the same power) and in their cost. It may therefore be expected that thermoelectric coolers will find wide use in cryochemical studies at temperatures down to about 173 K before long.

At present, by far the most convenient cryostats are those based on refrigerating machines. In sketch form, this type of cryostat used by these authors in spectrophotometric experiments is shown in Fig. 2.7. A small closed-cycle helium refrigerator produces a temperature of about 20 K in the cold head in a vacuum shroud. The cell compartment adapted to take both solid and liquid samples can give temperatures down to about 123 K. Only sealed quartz cylinders with round optical-quartz windows are evacuated for good thermal insulation. To avoid fogging and condensation of moisture, the outer windows are blown over and a positive pressure of gaseous nitrogen is built up in the inside. The desired constant temperature is maintained by means of an electric heater located in the cell housing and connected in an automatic thermostatic control circuit.

The advantages offered by cryostats based on refrigerating machines are obvious. They are indispensable in experiments going on for days and can give temperatures down to the boiling point of liquid helium. Among their drawbacks are the vibration generated by the refrigerating machine and the stringent requirements for the design of the experimental section of the cryostat, arising from the design of the machine itself and from the need to locate the sample as close to the cold head as possible.

2.2. PRACTICAL ASPECTS OF LOW-TEMPERATURE EXPERIMENTS

Chemical processes at low temperatures pose a number of problems before the experimentor, especially in the preparation of samples. No difficulties usually arise in cases involving a single substance or a system in which no irreversible changes take place in the course of sample preparation. In the circumstances, the experimentor can prepare the samples and load them into the cryostat at room temperature, then cool the cryostat and carry out whatever experiments there may be. To reach thermal equilibrium, the sample should be maintained in the cryostat for the required interval of time. Cryostats intended for such applications are appreciably simpler in design than those used in the study of chemical processes.

Difficulties usually arise when the experimentor is to investigate chemical reactions at low temperatures, because the reactions already begin while the sample is still being prepared, that is, at higher temperatures. Because of this, samples must be prepared in a minimum interval of time, and this is sometimes unfeasible, especially where solid reactants have to be handled. The experimentor often fails to ensure a truly homogeneous distribution of solid components.

2.2.1. Gases and Liquids

In the case of low-temperature chemical processes taking place in gases and liquids, the problem of reactant mixing inevitably arising in the study of chemical reactions in multicomponent systems is relatively simple to solve. Most frequently, the reactants are mixed by the partition method. With this method, the starting gaseous or liquid materials are separated by a partition which is quickly removed after they have been cooled to the temperature of the experiment. The mixing time by this method is about 2×10^{-2} s as against about 4×10^{-2} s required for mixing by injecting one of the reactants into the other by a syringe.

A description of low-temperature reaction cells for liquid solutions, with the reactants being first thermostatted and then mechanically mixed, can be found in [133-135].

As the temperature is brought down, the number of substances that can reside in the gaseous or liquid state progressively decreases. This calls for the use of solvents that will not freeze at low temperature, and their number is very limited.

In experiments involving solutions, the lower temperature limit is set, as a rule, by that of reactant solubility and by the increase in solvent viscosity. A solution in which the solvent is isopentane will not freeze down to 133 K.

One solvent widely used in low-temperature experiments consists of 5 parts of ether, 5 parts of isopentane, and 2 parts of ethanol, and another is made up of 3 parts of isopentane and 1 part of methylcyclohexane. These solvents remain liquid down to very low temperatures and form glassy samples upon freezing. Also, they are efficient solvents. The freezing points of other low-freezing solvents can be found in [102]. When using them, care must be taken to remove water, since otherwise it will crystallize at low temperatures and make the samples foggy.

As the temperature of a sample is brought down, its viscosity increases, and this in turn interferes with stirring and sets a limit to the lower temperature of the range. Because of the considerable increase in viscosity, on one hand, and the slow-down in the reaction rate with decreasing temperature, on the other, the kinetic mode of the reaction gives way to the diffusion mode, and this is undesirable in most cases. This point must always be borne in mind in low-temperature experiments.

Another important factor is that a decrease in temperature entails a decrease in the solubility of many substances. Because of this the experimentor has to use techniques of an increasingly higher sensitivity.

2.2.2. Solids

Most systems of practical interest are solids at low temperatures. As already noted, experiments with reactions in solids run into considerable difficulties. One way to circumvent them is to prepare samples by freezing the liquid mixtures pre-prepared at elevated temperatures. With this method, the components can intimately be mixed prior to freezing, but there is quite a number of snags that are difficult to avoid. For one thing, because the components are mixed together in the liquid phase and at a temperature higher than the experimental one, unwanted reactions take place in most cases. For another, it is likely that freezing may cause a multicomponent mixture to separate. Also, multicomponent solid samples obtained by this method must carefully be inspected for structure and phase, because they may depend, among other things, on the rate at which the sample has been frozen. In most investigations known to these authors, such inspection has not been even attempted because of the difficulties, both basic and procedural. Classical methods like X-ray diffraction would practically be of no avail when the solution contains minute amounts of components. Therefore, it is customary to assume that fast freezing (for example, in liquid nitrogen) produces uniform samples, which is not, however, always true.

Samples of a sufficiently homogeneous composition can be produced by condensing the components of the gaseous phase onto a cooled surface. This method has found wide use in studying the intermediate products of reactions in the gaseous phase, and also for detecting radicals and the reactions in which they participate. The condensation of reactive species from a gaseous phase along with chemically inert molecules has come to be known as the matrix isolation technique.

The reactive species in such a case are trapped or immobilized in a matrix of a chemically inert material. At a sufficiently low temperature, the matrix is fairly rigid and inhibits the diffusion of reactive species. For the first time, the matrix isolation technique was proposed by Whittle, Dows and Pimentel [136] and, independently, by Norman and Porter [137].

A better way to obtain homogeneous condensates is the cocondensation technique [138]. For the first time, this technique was proposed for the preparation of samples and the study of chemical reactions at low temperatures by Semenov and Shalnikov [139]. Subsequently, it was successfully used for experiments with low-temperature polymerization [140, 141]. The method consists in cocondensing the molecular beams of two or more substances onto a cooled surface, on the condition that the average spacing between the individual molecules in the beams does not exceed the mean free path in the collision zone.

Figure 2.8 shows in sketch form a setup for experiments in the low-temperature halogenation of unsaturated compounds prepared by the cocondensation method [142]. The starting materials, which are in the gaseous state, are admitted by capillaries into the experimental space continually pumped to a vacuum of about 1×10^{-2} Pa and are cocondensed on a thin glass membrane cooled by liquid nitrogen. The rate of freezing is found by trial and error for each particular case, according to the system under study. Despite the complexity of experimental arrangement the cocondensation method is preferable in the preparation of solid samples. It must, however, be noted that not all substances can be handled with the cocondensation technique. Notably, high-molecular-weight substances and biological macromolecules cannot practically be converted to the gaseous state without decomposition, and recourse has to be had to quick freezing.

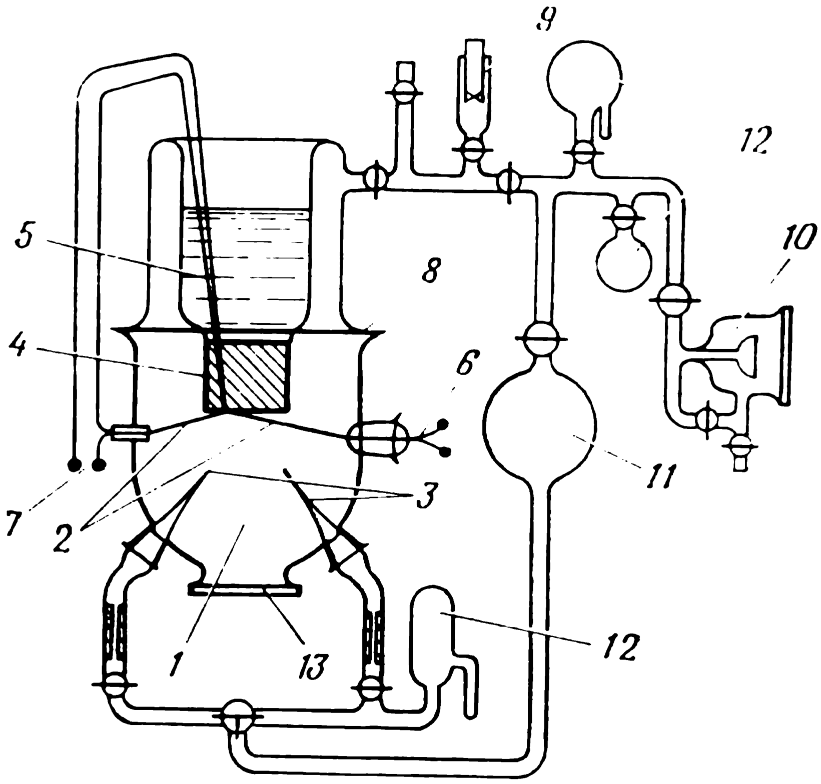

Fig. 2.8. Flow circuit and reaction vessel for studies on reactions in molecular-beam cocondensates [142]:

(1) glass substrate for deposition of starting substances; (2) thermocouples; (3) capillaries; (4) iron filings to improve thermal contact; (5) liquid nitrogen; (6) simple thermocouple lead-in; (7) differential thermocouple lead-in; (8) ground seal; (9) vacuum-meter lamp; (10) diaphragm pressure gauge; (11) bypass flask; (12) flasks to store gases and liquids; (13) quartz window for photolysis

2.3. EXPERIMENTAL TECHNIQUES FOR LOW-TEMPERATURE PROCESSES

Basically, low-temperature processes can be investigated in one of two ways. The simpler of the two consists in that the system in question is cooled to the experimental temperature, maintained at that temperature for some time, then warmed up, and analyzed under normal conditions (warm-up experiments). In the other, the process of interest is watched *in situ*, that is, directly at cryogenic temperatures. Accordingly, all experimental techniques may arbitrarily be classed into two groups. One group, adapted to warm-up experiments, encompasses practically all known physical and chemical methods known today. They need not be listed or, the less so, described here. We shall only touch upon the most important of them, especially those not practically employed in *in-situ* experiments. Among them are chemical methods used for the composition analysis and separation of reaction products, chromatography, and mass spectroscopy. The other group includes techniques applicable to *in-situ* experiments directly at low temperatures. We shall dwell on the most important of them.

Low temperatures combined with physico-chemical techniques offer a convenient tool with which to trace reactions proceeding too fast at ordinary temperatures. For chemical reactions with an activation energy of 40 kJ mole^{-1}, a decrease of 125°C in temperature will slow down the reaction rate by a factor of more than 10^6.

2.3.1. UV-Visible Spectroscopy

Of all forms of spectrophotometry, that in the UV and visible spectrum has gained the widest use. When investigated by this technique, the system under study experiences no perturbation.

The technique in itself is extremely versatile. On their part, cryogenic temperatures go a long way towards disclosing the spectral properties of molecules and, especially, highly reactive ions, immobilized electrons, ion radicals, and radicals. As the temperature of the sample is brought down, the lines in the optical spectra grow progressively narrower, and the spectra display fine structure. This enhances sensitivity in the detection of various species and facilitates their identification. A discussion of the optical properties of molecules in matrices, mixed crystals, and frozen solutions can be found in reference [143], which also contains an extensive bibliography (about 2000 references).

The key advantages of the method, as already noted, are sensitivity and versatility. The spectral data thus obtained make it possible to identify both intermediate and end products of reactions.

Among its disadvantages is the fact that it imposes stringent requirements as regards the design of the cryostat. Because of appreciable light scatter, it often happens that no absorption spectra can be obtained for polycrystalline and turbid samples. In such cases, it may prove advantageous to use two-wave spectroscopy which has especially advanced in recent years, and integrating spheres. A description of an integrating sphere designed for measurements at low temperature will be found in [144].

To avoid light scatter, every effort is made to use transparent, uncracked samples obtained by cooling vitrifying mixtures. However, it is not always possible to prepare glassy samples. For example, on freezing, water expands and causes glass tubes and ordinary quartz cells to burst. This limitation can be avoided by using knock-down cells with elastic spacers. In addition to the instruments covered above, cryostats for optical measurements at low temperatures are described in [145-151]. Reference [152] describes a cell for liquid solutions used in UV spectroscopy; the cell permits two components to be mixed.

Reference [153] briefly describes a setup for fluorescent studies into the solid-phase polymerization of paradiethynyl benzene at low temperatures under the action of light. The experiments were carried out in the temperature range from 4.2 K to 373 K. A brief description of an experimental setup for radiophotoluminescence studies is given in [154], and reference [155] describes the cryostat used for the purpose.

A very promising approach to experiments with extremely rapid reactions in solutions appears to be the concurrent use of low temperatures and fast-process methods [156]. Reference [157] describes an early stop flow setup, still one of the few, in which fast reactions can be investigated by a spectrophotometric method down to 153 K. All-Pyrex stop flow apparatus can operate down to 233 K [158]. An apparatus for the same application but built from other materials and adapted to work at temperatures down to 228 K is described in [159]. Other techniques intended for fast reactions in solutions, such as the temperature-jump method, may likewise be adapted to low temperatures.

2.3.2. Circular Dichroism and Dispersion of Optical Rotation

Circular dichroism and dispersion of optical rotation are widely used in low-temperature experiments involving optically active substances. Optical activity is a property of biologically important compounds, so it is no coincidence that most low-temperature experiments have been concerned with such compounds [160-162].

The experimental technique is about the same as in conventional spectrophotometry, except that the requirements are more stringent. Among other things, it is required that the cryostat parts and cells must be fabricated from optically inactive materials. However, thermal and mechanical stresses cause the otherwise optically inactive quartz of the cell windows to become optically active. This is also true of some other materials and gives rise to special requirements for the design of cryostats intended for work with optically active compounds. For example, reference [163] describes several alternative designs of seals for the optical windows of metal cryostats, including those free from birefringence. A simple and reliable cryostat is used in the instruments by a French firm. This cryostat can take both solid and liquid samples, needs no vacuum-producing or maintaining equipment, uses liquid nitrogen as refrigerant, and has a simple refrigerant feed system.

2.3.3. Infrared and Raman Spectroscopy

Infrared and Raman spectroscopy can yield extensive information about chemical reactions because it is capable of detecting the formation of new chemical bonds and the rupture of the old ones [164]. Low-temperature IR spectra are simpler and better defined because the number of configurations that a complex molecule can take on is reduced. However, the interpretation of spectra is often impeded by the disturbing effect of the matrix.

Unfortunately, IR and Raman spectroscopy has been used on a limited scale in low-temperature experiments. It is interesting to note that a good deal of important findings were obtained by IR spectroscopy in early studies on trapped radicals. Later, IR spectroscopy was practically ousted by the ESR technique. Whereas this may be justified in experiments with free radicals (where IR spectroscopy can hardly vie with ESR technique), IR spectroscopy is still second to none as far as nonradical products are concerned.

Several factors seem to be responsible for the limited use of IR and Raman spectroscopy in the study of low-temperature reactions. Above all, these are the engineering difficulties posed by the design of cryostats. By far the most formidable problem is the brittleness of the materials that go to make optical windows. A glass cryostat for IR spectroscopy is described in [108], and a metal cryostat for the matrix isolation technique in [165]. The use of AgCl and AgBr optical windows for cryostats is proposed in [166]. Such windows are very convenient, do not crack, and can be sealed into the housing by a simple technique described in the same reference. With such windows, IR spectra can be recorded down to 23 μm and 35 μm, respectively.

An interesting cryostat is described in [167]. Its distinction is that vacuum is applied only to the optical windows which are round, hollow, steel lenses with the outer walls made of NaCl and the inner walls of germanium. As a precaution against fogging, the outer windows are heated and blown over with warm dry nitrogen. The cryostat is fitted with PTFE-sealed mechanical manipulators to carry out all the necessary handling inside the cell down to about 85 K without having to break its vacuum. Unfortunately, no means are provided for temperature control inside the cell. An optical cryostat with controlled cooling in the range 5-260 K is described in [168]. A cryostat for magneto-optical studies is described in [169].

2.3.4. Calorimetric Methods

Calorimetric methods occupy a special place in the study of chemical reactions at low temperatures. They are most versatile because the system under study has in effect to meet only one requirement—the process must evolve or absorb heat.

Calorimetric methods provide insight into the thermodynamics and kinetics of the process under study. Unfortunately, they cannot establish the chemistry of the process and identify the intermediate and end products, unless some other methods are used to supplement them. So, in practice, calorimetric findings must always be supplemented by data found by other methods. Most often, such supplementary methods are chromatography, mass spectroscopy, IR spectroscopy, and, more recently, NMR spectroscopy.

Calorimetric methods were widely used in the early studies of chemical reactions at low temperatures. In sketch form, one of the earliest differential thermal analysis (DTA) setups for fast reactions near the temperature of liquid nitrogen is shown in Fig. 2.9 [170]. The use of DTA in kinetic experiments is outlined in [171] which also describes a partition-type cell with which the liquid reactants

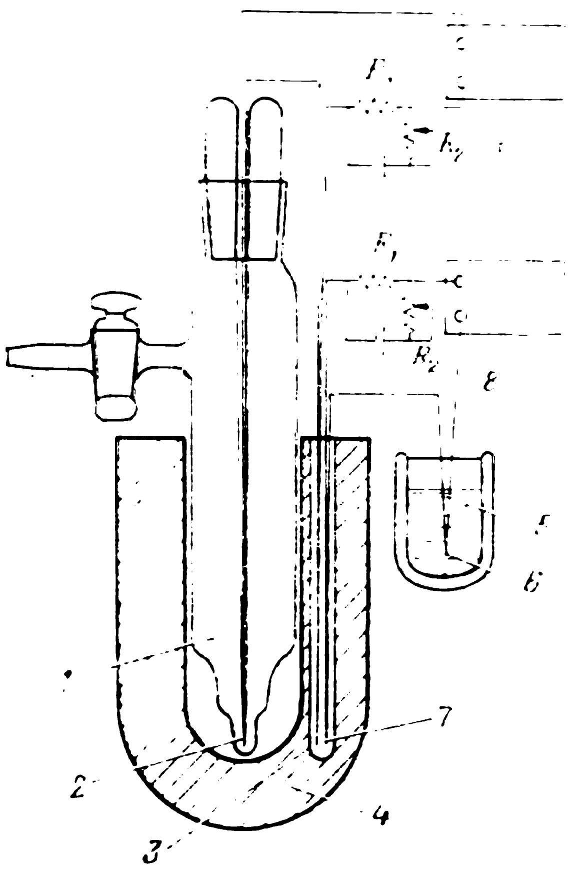

Fig. 2.9. Experimental setup for studies on chemical reactions at low temperatures by the differential thermal analysis (DTA) method:

(1) glass or quartz vessel; (2) capillary junction of a differential thermocouple; (3) reference junction of a differential thermocouple; (4) metal block or liquid-refrigerant Dewar flask; (5) liquid-nitrogen Dewar flask; (6) reference junction of a simple thermocouple; (7) measuring junction of a simple thermocouple; (8) temperature measurement potentiometers

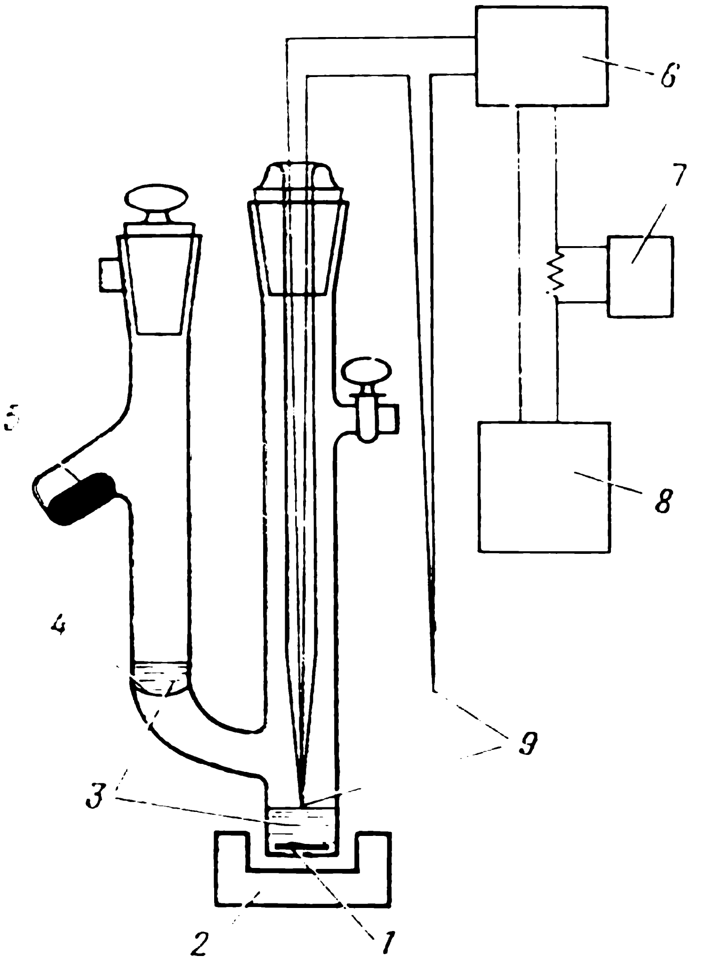

Fig. 2.10. Cell and measuring circuit for thermographical investigation of reactions in solutions:

(1) magnetic stirrer; (2) motor-drive magnet; (3) solutions being mixed; (4) glass membrane; (5) membrane breaker; (6) current amplifier; (7) stylus-positioning d.c. potentiometer; (8) electronic potentiometer; (9) measuring junction of a differential thermocouple

can conveniently be brought in contact and mixed (Fig. 2.10). DTA can be used in cases where the heat evolved is proportional to the number of reacted moles of the substance. This condition holds for single-stage reactions. In multistage reactions, on the other hand, the DTA method will mainly respond to the stage associated with the largest heat output.

Calorimetric methods offer many more advantages in addition to versatility. Most important, the cryostats are simple in design and samples can be made very small. Improvements in experimental techniques and advances in the theory of calorimetric methods have expanded their capabilities to a point where the experimentor can determine kinetic parameters quantitatively from calorimetric data. Sensitive low-temperature calorimeters are described in [172-74]. In sketch form, an adiabatic and a non-adiabatic calorimeter successfully used in experiments with low-temperature polymerization are shown in Figs. 2.11 and 2.12 [173]. Undoubtedly, the progress achieved in the field of calorimetric methods will, when backed by stock-produced sensitive microcalorimeters, lead to their wider use in low-temperature experiments in the future.

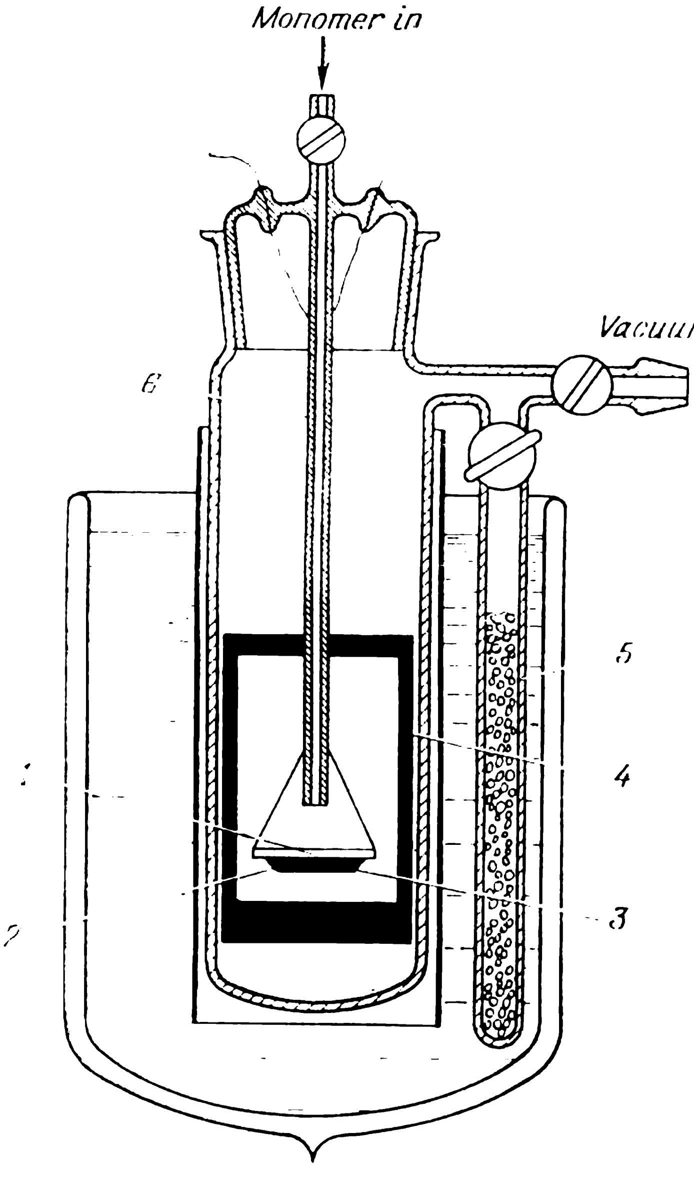

Fig. 2.11. Sketch of a low-thermal-lag adiabatic film calorimeter [173]:

(1) aluminium disc; (2) resistance thermometer; (3) calibration heater; (4) copper heat shield; (5) carbon adsorption pump; (6) Kovar capillary

Calorimetric methods require an accurate measurement of low temperatures. This is a specialized field, so we shall limit ourselves to references to the literature on the subject and some remarks. The measurement of low temperatures is given a fairly detailed coverage in [175-177]. Low temperatures can be measured by thermocouples and resistance thermometers [177, 178]. The most commonly used thermocouples are of the copper-constantan type. Their thermo-emf-vs-temperature characteristic is given in [177]. According to [179], the best method for forming the hot junction of a copper-constantan thermocouple is by tin soldering. Four methods were tried: silver soldering, gas-torch welding, electric welding, and tin soldering. A tin-soldered thermocouple showed that the maximum deviation from the calibration curves was more than by an order of magnitude smaller in comparison with the remaining three methods.

Another important problem in low-temperature experiments is temperature control. In a general form, this problem is examined in [180, 181]. References [182-190] describe a variety of temperature controllers for low-temperature cryostats. Devices used to measure and automatically control the level of liquefied gases in cryostats, low-temperature cells, seals for optical windows and other useful accessories are described in [189-199].

2.3.5. Diffraction Methods, ESR and NMR

Valuable information about the phase state of a cryogenic system can be obtained by X-ray diffraction, electron-diffraction and electron-microscopy techniques. As regards the mechanism of chemical reactions at low temperatures, important data can be gathered by means of nuclear gamma resonance [200]. This method and the cryostats adapted to NGR work are described in [201]. A cryostat complete with temperature control features is described in [202].

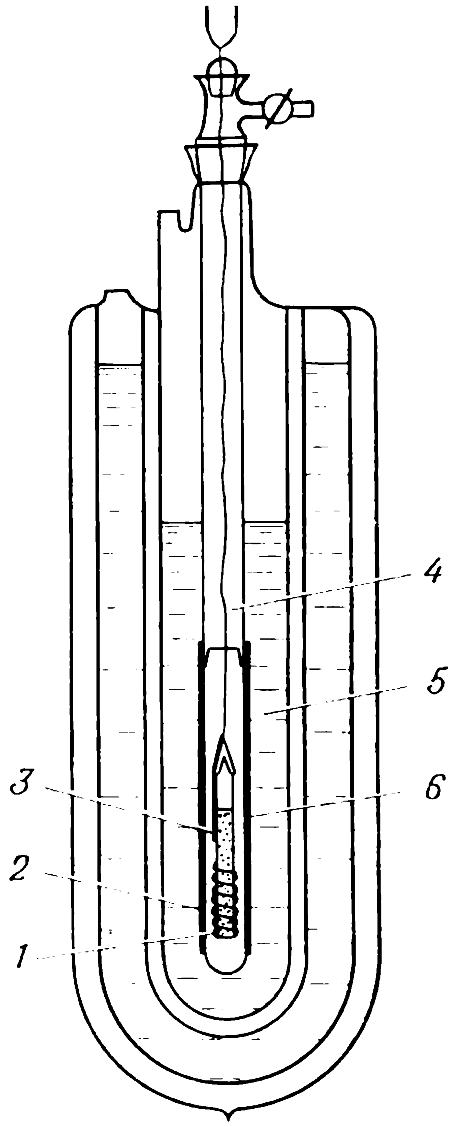

Fig. 2.12. Sketch of a diathermal calorimeter [173]: (1) Kovar capillary; (2) calibration heater; (3) thermocouple; (4) glass vacuum shroud; (5) glass helium cryostat; (6) copper shield

Many studies at cryogenic temperatures are based on the ESR technique [203]. At present, it is basic in the study of processes involving paramagnetic species at low temperatures. Like optical methods, ESR and NMR are physical techniques with which the processes taking place in solids can be observed *in situ*. They are also widely used in the study of reactions in the liquid and gaseous phases.

The ESR technique yields information about the nature of radicals, ion radicals, and molecules in triplet states. Because the spectral characteristics of paramagnetic species are substantially dependent on their surroundings, ESR spectra can tell much about the character and strength of intermolecular interactions, and the structure and properties of the medium. Of special value in this respect are pulse techniques. In ESR spectroscopy, the more recent addition is the electron spin echo (ESE) technique. It is effective in determining the spatial distribution of the radicals that form upon irradiation of solids, the structure of the radicals themselves and of their nearest surroundings [204].

Several cryostats used for ESR work are described in [205]. A cryostat with the temperature controlled in the range 2-300 K is outlined in [206]. Figure 2.13 shows, in sketch form, the reactor used in ESR studies on low-temperature polymerization in the system acrylonitrile-magnesium, using cocondensation technique [207]. An experimental setup incorporating an ESR spectrometer and a 1.6-MeV linear electron accelerator, used in studies of low-temperature processes involving radicals, is described in [208].

Recently, there has been a growing interest in the kinetics of processes taking place in solids. Such studies give insight into diffusion in solids, the mechanisms of various relaxation processes, and the relationship between the structure of solids and the chemical reactions occurring inside them.

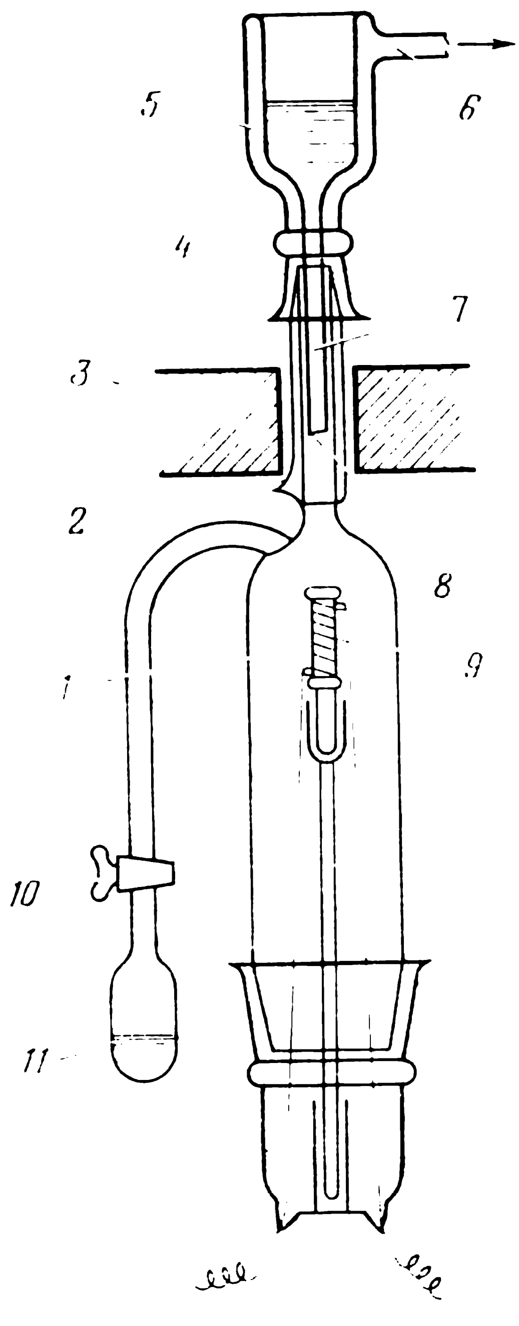

Fig. 2.13. Sketch of a reaction vessel for ESR studies on polymerization in molecular-beam cocondensation samples [207]:

(1) quartz vessel; (2) Dewar tube; (3) ESR spectrometer resonator; (4) ground seal; (5) trap; (6) evacuating tubulation; (7) thin-walled finger; (8) depression in finger; (9) electric oven; (10) cock; (11) reactant tube

In conclusion, it is to be noted that most spectral and magnetic resonance instruments are equipped with low-temperature units adapted to work at the liquid nitrogen temperature (77 K) only.

Because of this, stock-produced instruments have often to be supplemented by "home-made" special-purpose cryostats.

In making cells and sample holders, account must be taken of the effect that temperature gradients may have on their materials. Because most substances are in the solid state at low temperature, spectrophotometric experiments may be handicapped by the scatter of light, as this would corrupt the spectra; for magnetic resonance studies this may cause substantial signal broadening with the accompanying loss of information.

The use of solid samples also requires that the effects of anisotropy should be taken into account.

Furthermore, as already noted, it is important to remove any traces of water from the reactants and apparatus used in cryochemical work. This also goes for the windows of optical cells and the cavities of ESR spectrometers. These difficulties, however, are more than offset by the value of the information obtained.

CHAPTER THREE

REACTIONS OF RADICALS AND IONS IN FROZEN SOLIDS

The behaviour of reactive species at low temperatures occupies a prominent place in cryogenic experiments. In fact, it was such experiments that gave birth to cryochemistry. Since reactions leading to the generation and loss of radicals and ions in frozen solids are the subject of many reviews [1, 31-35, 209-212], no detailed analysis of available data will be attempted in this book. We shall only dwell on some experimental results that we regard as interesting, and on the basic patterns in the behaviour of reactive species in solids. Proper attention will be paid to findings which point to the important role of the matrix structure in the behaviour of reactive species.

A radical immobilized in a solid is a kind of label which can conveniently be traced by the ESR technique. The ESR spectra yield valuable information about the radicals proper and the sample as a whole, and help understand the specific features of low-temperature chemical reactions. One of the simplest reactions involving radicals is their recombination. Analysis of recombination is essential for an understanding of the mechanisms involved in other, more elaborate low-temperature processes. In the context of radical loss experimentors were able for the first time to show the role of phase transitions, to detect stepwise recombinations and to trace the effect of radical distribution on radical transformations in solids. These aspects are of interest to cryochemistry, and they will be taken up in this chapter.

3.1. RADICAL STABILIZATION AND KINETICS OF ACCUMULATION

The behaviour of reactive systems in the solid phase at low temperatures is basically approached from two angles. One is concerned with the nature and properties of reactive species in a matrix, including, for example, the effect of the matrix on the behaviour of the radicals. Such experiments are mainly based on spectroscopic data. The other refers to the kinetics of accumulation and loss of reactive species.

The kinetics of radical accumulation in frozen solids has been investigated by many authors [1, 31-35, 209-212]. At first, statistical position models of radical stabilization were proposed [1, 213, 214]. These models were essentially based on the following premises: (1) the radicals are trapped in a perfect lattice and surrounded by inert species; (2) there is a complete freezing which implies that the radicals and molecules can take up any positions with equal probability. However, calculations based on such models give an exaggerated number of immobilized radicals.

An important step forward as regards understanding the accumulation and stabilization of radicals and determining the critical conditions under which a rapid recombination would take place was made on the basis of a dynamic statistical model [215-217]. A detailed theoretical examination of the kinetics involved in the accumulation of frozen radicals in solids is given in [217]. It discusses the mechanisms of radical accumulation associated with charge transfer, migration of mobile atoms, excitation transfer, and propagation of a thermal wave, derives expressions giving the concentrations of immobilized radicals for all the mechanisms, and compares theory with experiment. A satisfactory agreement of theory with experiment is, however, noted only for the recombination of nitrogen atoms at helium temperatures.

At present, studies into the kinetics of radical accumulation continue, with emphasis on the effect of the nature of irradiated substances. Such experiments are important because they lay the foundation for a theory of light and radiation stability of materials, including polymers and biopolymers. It is especially important to establish the mechanisms that lead to the relative change in the rates of generation and loss of radicals. According to [34], the loss of radicals and the associated reduction in the maximum attainable concentrations of stabilized radicals appears to involve several mechanisms, namely: (1) radical recombination whose probability increases with the accumulation of radicals and which can proceed, upon reaching a certain moment, by a chain mechanism with a "thermal" branching, (2) loss of radicals upon interaction with ions and electrons, and as a result of charge recombination; (3) loss of radicals due to transfer of excitation energy from the matrix to the radicals; (4) loss of radicals caused by direct exposure to radiation, including light.

It is to be stressed that, when taken within the framework of existing models, the above mechanisms fail to explain all aspects of the kinetics of accumulation. It seems important to formulate a better theory that would explain such experimental facts as the linear temperature dependence of $[R]_{lim}$ [218, 219] and the exceptionally high probability of radical loss per unit of absorbed energy. For example, in isopropyl alcohol as many as 240 stable 2,2,6,6-tetramethyl-4-oxyl-1-piperidinyloxy radicals are lost per 100 eV of absorbed energy [220]. This fact cannot be explained solely by direct exposure of the radicals to radiation.

Of the other experimental facts awaiting a quantitative explanation, we can point to the strong dependence of the rate of radical accumulation on the manner in which the sample has been prepared and on whether it has been irradiated prior to experiment. According to [221], the rate of the subsequent radical accumulation in aniline samples exposed to 30 Mrad of gamma radiation from a Co-60 source and stored in liquid nitrogen for two months prior to experiments differed materially from that of samples not irradiated prior to experiments. It is interesting that the rate of accumulation was higher in the former case, although the concentration of pre-stabilized radicals remained unchanged during the prolonged storage in liquid nitrogen. It is inferred that radiolysis products might influence the accumulation of radicals and that some of the radiolysis products might diffuse during storage. Apparently, this is a general occurrence and must be taken into account in radiolysis experiments.

Exposure to radiation can result in local heating, the actual temperature being dependent above all on the kind of radiation, sample geometry, conditions of heat exchange, and secondary chemical reactions, if any. Conditions of freezing, degree of crystallinity and dispersion may also affect the extent of heating and the nature of thermal relaxation.

In the opinion of these authors, the heating and the changes in the conditions of thermal relaxation in evacuated samples upon liberation of gaseous products (say, hydrogen) when exposed to radiation can materially affect the kinetics and mechanism of both the accumulation and the subsequent loss of reactive species. This important matter is still insufficiently explored. It is generally believed that all processes taking place in such samples proceed under isothermal conditions. Contrary to this belief, reference [222] reports the heating of an entire sample.

In multicomponent systems, radical accumulation follows a more complex pattern than in single-component samples. Of special interest is the increased yield of products, including radicals, occurring in binary mixtures in comparison with the yield that ought to be expected on the strength of radiation-chemical additivity. It may be caused by various factors, such as transfer of electron excitation energy, reactions of flow electrons, charge transfer, reactions of atoms and radicals, localization of excitation on one of the components, and intermolecular interactions in the system [34]. The last mentioned factor manifests itself in the increased radical yield (in comparison with the additive yield) upon gamma-irradiation of frozen mixtures of water and hydrogen peroxide. The radical yield is a maximum in the case of the mixture answering the composition of an intermolecular compound [223].

It is to be stressed that the mechanisms and patterns of behaviour are of common nature and can be observed in the most diverse systems.

3.2. KINETICS OF RADICAL LOSS. STEPWISE RECOMBINATION

Recombination of immobilized radicals is examined in detail in [34] which also compares the theoretical models proposed by many investigators to explain the kinetics of recombination. In quite a number of systems, radicals undergo stepwise recombination. It consists in that an increase in temperature causes the rapid loss of some fraction of radicals, following which their concentration remains unchanged at a given temperature. The fraction of radicals stable at a certain temperature has been found to be independent of their original concentration and to be solely decided by the sample temperature. Thus, only a part, rather than all of the radicals are lost at a given temperature, and the kinetic "annealing" curve shows a step. No plausible explanation of the phenomenon has been proposed yet.

For the first time, stepwise recombination was observed in experiments concerned with the loss of peroxide radicals photolyzed in the system H_2O-H_2O_2 [224, 225]. In connection with the thermal transformations of silver atoms in gamma-irradiated (Co-60) frozen aqueous solutions of silver nitrate (0.05-0.35*M*) in the temperature range 77-150 K [226], stepwise recombination is explained in the light of the concepts advanced in [227, 228], including the formation of silver atoms by reactions involving electrons. This form of recombination is characterized by two features. Firstly, the fraction of radicals remains stable at a given temperature and independent of the manner in which the sample is warmed up to this temperature. Secondly, the fraction of stabilized radicals is a linear function of temperature.

In the opinion of these authors, several other aspects must be pointed out. The rate at which the radicals are lost immediately after the sample is warmed up is ordinarily high. A formal kinetic description leads to radical reactions with an order of over ten, the order increasing with rising difference in temperature. The rapidly disappearing radicals account for 70% or even more of the total number of radicals lost at a given "step". The temperature interval within which the loss of radicals occurs depends on the manner in which the sample has been prepared (rate of freezing, annealing, etc.) and the manner in which the radicals have been produced (kind and dose of radiation, etc.). The kinetics of radical loss is in some way related to the spatial arrangement of radicals.

We shall now examine some interesting experimental data. It has been found that the low-temperature gamma-radiolysis of single crystals and polycrystalline samples of diketopiperazine-d_2 produces two types of radical pairs differing in their position within the lattice, the spacing between the unpaired electrons being 4.9 Å and 6.3 Å, respectively [229]. Isolated radicals are also formed, and their yield is substantially higher. At a dose of about 150 Mrad the concentration of isolated radicals has been found to be 7×10^{17} per gram, whereas for the pairs of types I and II the figure has been found to be by two orders of magnitude lower.

It has also been found that radical pairs of types I and II markedly differ in thermal stability. Type I radical pairs are lost at a marked rate already at —10°C, whereas for type II radical pairs the loss begins at over 110°C. In either case, the loss of radical pairs within a narrow temperature interval is described by a kinetic equation of order one. The following expressions have been deduced for rate constants: $k_{\mathrm{I}} = 2.6 \times 10^{13} \exp [-(21\,000 \pm 900)/RT]\ \mathrm{s}^{-1}$; and $k_{\mathrm{II}} = 4.0 \times 10^{14} \times \times \exp[-(30\,000 \pm 1\,500)/RT]\ \mathrm{s}^{-1}$ in the temperature intervals extending from 265 K to 279 K and from 378 K to 398 K, respectively. For the loss of type I and II radicals, the activation energies are about proportional to the spacing between the unpaired electrons in the radical pairs. Precisely this relation was postulated in the past to explain stepwise recombination [228].

It is reported in [229] that isolated radicals show high thermal stability, that their loss does not begin until 170°C, and that this loss is obviously stepwise. Therefore, it may be inferred that the presence of radical pairs is not mandatory for stepwise recombination to take place.

Stepwise recombination of radicals is typical of many reactions in the solid phase and at room temperature. This form of recombination has been observed in experiments concerned with the loss of phenoxyl radicals upon interaction with the hydroperoxide of isotactic polypropylene in the temperature interval from 297 K to 326 K [230]. It is important to note that the kinetic curves obtained at one temperature may appear superimposed on that obtained for another. It is only within the initial portions of the curves that no superimposition can be secured. The effective activation energy found from the initial rates of loss has been found to be $98.4 \pm 8.4 \times 10^3$ J mole^{-1} which is more than twice as high as the activation energy for this reaction in the liquid phase.

In the presence of plasticizers, such as chlorobenzene and benzene, the pattern of loss for phenoxyl radicals becomes appreciably simpler, and the rate of radical loss is described by a kinetic equation of order one:

$$dR/dt = k_{\mathrm{exp}}\ [\mathrm{R}] \tag{3.1}$$

The constant k_{exp} is proportional to the concentration of hydroperoxide and increases with increasing ratio $m_{\mathrm{p}}/m_{\mathrm{s}}$ (where m_{p} is the mass of the amorphous part of polypropylene and m_{s} is the mass of the solvent).

The rate constant for the reaction of a phenoxyl radical with hydroperoxide of plasticized polypropylene

$$\mathrm{Ph\dot{O}} + \mathrm{ROOH} \xrightarrow{k_1} \mathrm{PhOH} + \mathrm{RO\dot{O}}$$

is found from the equation

$$1/k_{\mathrm{exp}} = (1/2k_1\,[\mathrm{ROOH}])\left(1 + \frac{1}{\alpha}\,\frac{m_{\mathrm{s}}}{m_{\mathrm{p}}}\right) \qquad (3.2)$$

where α is a dimensionless factor.

Hence,

$$2k_1 = (5.2 \pm 0.9) \times 10^4 \exp\left[-(9\,500 \pm 800)/RT\right]\ \mathrm{kg\ mole^{-1}\ s^{-1}}.$$

The values of k_1 found for 298 K and the activation energies are in good agreement with data for this reaction in liquid benzene as the solvent.

Equation (3.2) has been derived on the assumption that the reaction is not diffusion-limited. This assumption is corroborated by the fact that the concentration of $\mathrm{Ph\dot{O}}$ decreases owing to its diffusion from the pellet immersed in chlorobenzene at a faster rate than it would due to a chemical reaction. The high mobility of radicals in plasticized polypropylene is also corroborated by the ESR spectra of the radicals, which become practically identical with such spectra of radicals in liquid chlorobenzene. In the reference quoted, these experimental findings are explained by the difference in the degree of molecular mobility in "dry" and plasticized samples.

In reference [231] dealing with the loss of $\cdot\mathrm{CH(COOH)\,(CH_2)_3COOH}$ radicals in gamma-irradiated adipic-acid single crystals, it is pointed out that an increase in pressure markedly raises the thermal stability of the radicals and affects the appearance of the annealing curves — the practically linear temperature dependence of the concentration of radicals stable under a pressure of about 0.1 MPa becomes curvilinear under pressures of 280 MPa and 415 MPa. These findings appear to bear out the view-point shared by most investigators that molecular mobility is one of the factors limiting radical loss, because an increase in pressure leads to a slow-down in diffusion [232].

Interesting results have been obtained in studies concerned with the effects of mechanical factors on radical reactions in solids [233]. It is shown that a marked change in the structure of a solid as a result of a mechanical action directly affects the kinetics of radical transformations. These findings provide better insight into the mechanism of deterioration and help extend the service life of materials, notably polymers.

3.3. PHOTOCHEMICAL REACTIONS. THE CAGE EFFECT

Many aspects in the formation and behaviour of radicals and ions in frozen solids are traceable to what is known as the cage effect discovered for the first time for reactions in the liquid phase. The cage effect is especially pronounced in photochemical reactions. In viscous liquids, the two radicals formed by the photodissociation of a molecule remain at first close to each other, as if confined in a cage, and it is only some time later that they form two independent particles owing to diffusion. The cage effect influences the extent to which light can affect the decomposition of molecules in the solid phase. Unfortunately, quantitative data about the cage effect at low temperatures are not at all easy to obtain.

It appears convenient to discuss photochemical reactions at low temperatures by reference to the formation and behaviour of radicals in frozen aqueous solutions of hydrogen peroxide. It is in one of these systems that investigators first discovered the special role of phase transitions in chemical reactions at low temperatures [224, 234, 235].

The manner in which the photon energy controls the cage effect in the photolysis of frozen glassy solutions of hydrogen peroxide in a water-perchlorate matrix ($8M$ $NaClO_4$) at 77 K is investigated by the ESR technique in [236]. It is interesting that the ESR spectra recorded during the initial period substantially vary according to the original concentration of peroxide in solution. At $[H_2O_2] > 3.6M$, the recorded spectrum is that of the $H\dot{O}_2$ radical, whereas at $[H_2O_2] < 0.05M$ it is that of the $\dot{O}H$ radical. The spectra of $\dot{O}H$ and $H\dot{O}_2$ radicals are noted to superimpose at intermediate concentrations of H_2O_2. Extended photolysis of frozen diluted aqueous solutions of H_2O_2 ($< 10^{-3}M$) is observed to cause the ESR spectra typical of $H\dot{O}_2$ radicals to change into the ESR spectra of $\dot{O}H$ radicals [237, 238].

The following scheme has been proposed for radical formation. A molecule of hydrogen peroxide breaks up into two $\dot{O}H$ radicals which remain in a cage of surrounding molecules. The radicals can either recombine inside the cage or escape from the cage owing to their excess energy and be immobilized. In the solid phase, diffusion is inhibited, so the probability of escape from the cage and the quantum yield of stabilized radicals are low. The radical escaping from the cage reacts with an H_2O_2 molecule to give a stabilized radical, $H\dot{O}_{2\,\mathrm{stab}}$.

The study of this system has yielded an interesting and rather unusual relation between the quantum yield φ and the concentration of H_2O_2 (Fig. 3.1.). At H_2O_2 concentrations up to about $1M$ the quantum yield remains practically unchanged. In the narrow interval of H_2O_2 concentrations between 2.6*M* and 4.7*M* the quantum yield suddenly increases (by more than one order of magnitude). Now the radical yield rises as high as $(6\pm2.4)\times10^{-3}$ per quantum of absorbed radiation and becomes nearly equal to the quantum yield in a concentrated aqueous solution of hydrogen peroxide $[(8.7\pm3.5)\times10^{-3}]$ where the primary $\dot{O}H$ radicals escape from the cage owing to the reaction with neighbouring molecules of H_2O_2 [239]. At low concentrations of hydrogen peroxide, the quantum yield is a function of the photon energy and is equal to $(0.7\pm0.3)\times10^{-4}$ and $(3.9\pm1.6)\times10^{-4}$ at 313 nm and 254 nm, respectively.

The energy of the O—O bond in an H_2O_2 molecule is 2.2 eV. The excess energy per $\dot{O}H$ radical photolyzed at $\lambda = 313$ nm and $\lambda = 254$ nm is 0.9 eV and 1.4 eV, respectively. The increase in excess energy by half as much again causes, as should be expected, the cage effect to decrease in importance appreciably (φ_R increases six-fold).

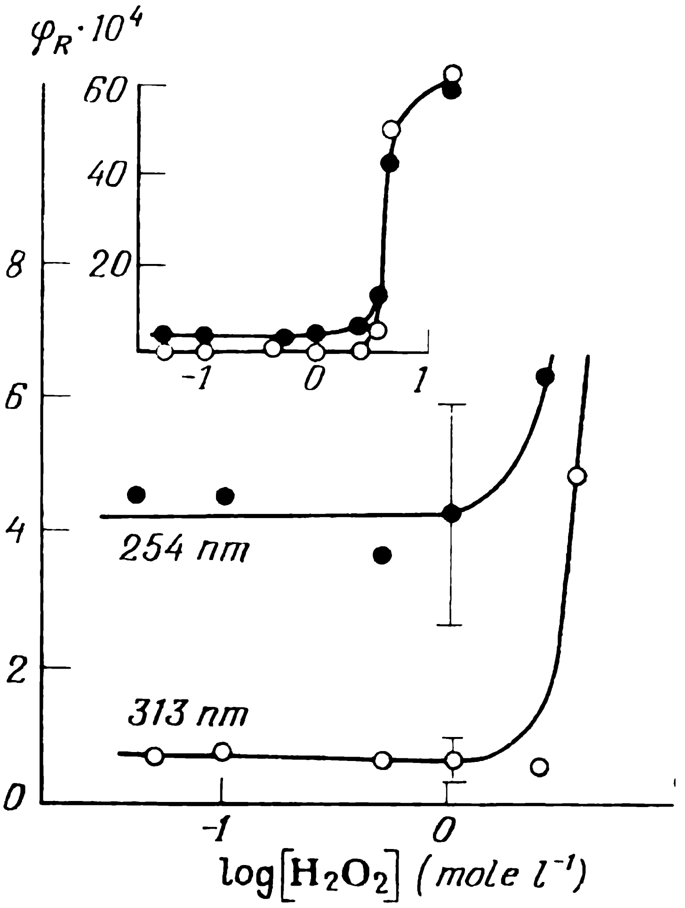

Fig. 3.1. Quantum yields of stabilized radicals as a function of H_2O_2 concentration and photon energy

Assuming that no H_2O_2 association takes place at concentrations of 0.05*M* to 1*M* and that the molecules are uniformly distributed in the frozen solution, and also making other simplifying assumptions, the distance through which the $\dot{O}H$ radicals carrying excess energy move before they are immobilized has been estimated to be about 10 Å in [236].

Among the other features of photochemical reactions, it is to be noted that the quantum yield and nature of the forming radicals may substantially be changed by introducing small amounts of chemically inert substances, including those unsusceptible to photolysis, into the system under study. For example, when small quantities of isopropyl alcohol are added to the frozen aqueous solution of H_2O_2, this leads to the formation of alcohol radicals, and the quantum escape of $\dot{O}H$ radicals from the cage increases by about two orders of magnitude [240]. Photolysis affects solely H_2O_2 molecules, and the formation of alcohol radicals cannot be explained by assuming that the molecules of hydrogen peroxide and alcohol are uniformly distributed throughout the ice matrix. The change in question is associated with the nonuniform distribution of the H_2O_2 and alcohol molecules which form aggregates in the ice matrix.

Changes in the shape of ESR spectra upon illumination of the sample are often ascribed to the secondary photolysis of the radicals. It is to be noted that a similar effect may well be produced by the nonuniform distribution of the substance throughout the sample, because radicals are now formed near those already existing in the sample. This tends to raise the rate of loss of and the average spacing between immobilized radicals with progress in photolysis. As a result, illumination can change the shape of the spectral lines.

The escape of reactive species from the cage may arbitrarily be classed into a physical and a chemical form, each differing in the contribution it makes, according to the chemical properties of the system exposed to radiation, the properties of the matrix, the energy of the quantum, and temperature. In rigid matrices, the escape of radicals is impeded. This above all explains their low quantum yield in photochemical reactions.

If primary radicals are capable of chemical reactions with the surrounding species with the formation of secondary radicals, the probability of radicals escaping from the cage increases. The surroundings may be the molecules of the matrix itself and also those of the dissolved components in the case of frozen solutions.

3.4. SPATIAL DISTRIBUTION OF RADICALS

The rate at which radicals recombine or undergo other changes depends on their spatial distribution in the matrix. As a rule, the kinetics involved in the loss of radiolyzed radicals has been investigated on the assumption that the radicals are distributed throughout the sample uniformly [34]. Actually, however, their distribution is anything but uniform. The size of the areas where the radicals and primary radiolyzed products are localized in solids depends on the manner in which radiant energy is imparted to the material and varies with the mean path of "hot" species, such as secondary electrons or hydrogen atoms, and with the distance over which the excitation is transmitted. Thus, kinetically, the reactions of radicals and other reactive species in solids are closely related to their spatial distribution.

Consider some experimental results confirming the nonuniform spatial distribution of radiolyzed radicals. The local concentrations evaluated from the dipole-dipole broadening of ESR spectra for the $H\dot{O}_2$ and $\dot{O}H$ radicals produced by gamma-irradiation of H_2O_2 solutions in water by UV radiation and by beta particles for which the source was tritium-enriched water, and also in the peroxide-radical condensates produced by condensing the products of a discharge in mixtures of H_2O, H_2O_2, H_2, and O_2 are, as a rule, by several orders of magnitude higher than the average concentrations. As an example, Table 3.1 gives data on the effect of various radiations on the frozen solutions of H_2O_2 in H_2O.

TABLE 3.1

Local and Average Concentrations of Free Radicals Radiolyzed in Frozen Solutions of H_2O_2 in H_2O [241]

Radiation	$[R]_{loc}$, M	$[R]_{loc}$, radicals/cm^3	$[R]_{av}$ radicals/cm^3	$[R]_{loc}/[R]_{av}$
X-rays, 250 keV	0.08	5×10^{19}	3×10^{18}	17
alpha particles, 5.7 MeV	0.22	1.5×10^{20}	3×10^{18}	50
UV, 310-350 nm	0.45	3×10^{20}	3×10^{15}	100
UV, 253.7 nm	0.33	—	—	—
Deuterons, 15 MeV	0.08	—	—	—

The data of Table 3.1 confirm the nonuniform distribution of radicals and show that it substantially depends on the type of radiation. The nonuniformity is especially noticeable in the photochemical production of radicals, which is taken to be related to the generation of radical pairs upon absorption of a quantum of light, the nonuniform distribution of H_2O_2 molecules in the sample, and the nonuniform absorption of light in the sample.

The electron-spin-echo technique has been used to determine the local concentrations of radicals in the tracks of ionizing particles in cyclohexanol, glycerine, isobutanol, allyl alcohol, acetate, lithium glycolate, and sulphuric acid at 77 K for radiations with a linear absorption of energy from 10 to 6 000 eV/nm [242]. Data for methanol are given in Table 3.2. They show that at low doses of radiation the average concentration of radicals is by more than an order of magnitude lower than the local one.

In [245] it is shown that the radiation yields of the end products depend on the kind and energy of the radiation used. Presumably, this is related to the difference in spatial distribution between the radiolyzed intermediates owing to the localization of the absorbed

TABLE 3.2

Radiation Yields G of Free Radicals, Track Radii R_{tr}, and Local Concentrations c_{loc} in Irradiated Glassy Methanol at 77 K [242-244]

Radiation source	Δc_{av} [1], 10^{-18}, cm^{-3}	Linear absorption of energy, eV/Å	Experimental values			Computed values			
			G, p 100 eV	$c_{loc}\times10^{-18}$, cm^{-3}	R_{tr}, Å	G [2] p 100 eV	G [3] p 100 eV	c_{loc} 10^{-18}, cm^{-3}	R_{tr}, Å
β (^3H)	0.2-20	1.1	5.5	2.8	90	—		—	--
$^6Li(n, \alpha)\,^3H$	0.2-8	16	2.6	7.6	130	2.8	2.34	5.1	135
$^{210}Po(\alpha)Pb$	0.2-20	20	3.3	8.8	55	3	2.5	5.7	180
$^{10}B(n, \alpha)\,^7Li$	0.2-3	43	1	8.2	130	1.1	0.75	9.1	120
$^{235}U(n)$	0.2-1.5	540	0.15	8	180	0.4	0.35	9	260
gamma from Co-60 source	0.1-10	1	6	1.7		6.2		1.5	--

[1] Average concentration range in which the measurements were made.
[2] Computed on the basis of the pair model.
[3] Computed on the basis of the diffusion model.

radiant energy in the tracks of the charged particles. Later, Pasalsky *et al.* [246] detected the nonuniform spatial distribution of radicals produced by gamma and alpha radiolysis of polyisobutylene at low temperatures from the consecutive saturation of ESR signals. The local concentration of radicals in the tracks of alpha particles was found to be by nearly an order of magnitude higher (5.1×10^{19} cm^{-3}) than the concentration of the radicals in the spurs (7.4×10^{18} cm^{-3}) produced by the gamma (Co-60) irradiation of polyisobutylene. It is interesting that in the case of alpha irradiation the change from a nonuniform to a uniform radical distribution occurs at higher average concentrations than in the case of gamma radiolysis. It is hypothesized that this is related to the difference in local concentrations [246]. An interesting dependence of the spin-lattice relaxation time T_1 on the absorbed dose for various kinds of radiation is observed in the same reference.

Additional information about the spatial distribution and conformational state of radicals in irradiated samples can be gleaned from the studies of radicals in inclusion compounds. The basic patterns for the distribution of paramagnetic centres in inclusion compounds, the structure of radiolyzed radicals, their conformational state, mobility, and secondary reactions are discussed in [247].

In solid inclusion compounds, the lattice is formed by the host molecules, and the vacant sites are taken up by the guest species. Inclusion compounds are convenient objects in experiments with radical reactions in the solid phase. In contrast to conventional binary or ternary solid solutions, inclusion compounds have a highly organized crystalline structure. This makes them especially attractive in energy-transfer studies of solids and the mechanisms involved in the reactions of radiolyzed reactive species.

With increasing temperature, the ESR spectra of radicals trapped in inclusion compounds experience changes related above all to motions within the radicals. Analysis of these changes has yielded information about the character of the motions and has made it possible to determine their activation energy.

As a rule, radicals in inclusion compounds show a higher thermal stability than they do in the frozen solutions of the included (guest) species. For example, all of the $\underline{CH_2{-}\dot{C}H{-}CH_2}$ radicals in the frozen cyclopropane are lost at 140 K, whereas the loss of radicals produced in irradiated cyclopropane hydrate does not occur until 260 K.

Coupled with a high rotational mobility, the higher thermal stability of radicals in inclusion compounds makes it possible to identify the radicals produced by irradiation and to analyze their reactivity. The difference in solid-phase structure between inclusion compounds and frozen systems leads to different radiolysis mechanisms and different end products. It has been found that the mechanisms of transformations for radicals in cyclopropane and its analogues are different in the individual frozen compounds and in inclusion compounds and depend on the character of the surrounding molecules.

In the solid phase of inclusion compounds, one can observe conformational changes in the cyclic radicals $\underline{CH_2CH_2\dot{C}HCH_2CH_2}$ and $\underline{CH_2O\dot{C}HCH_2CH_2}$. The temperature dependence of transition frequency for both radicals is described by the Arrhenius equation. It is interesting that the activation energy ($E_{act} \approx 10.5$ kJ/mole^{-1}) and the pre-exponential factor are independent of the nature of the matrix. This is an indication that the kinetic characteristics of radicals are above all decided by inner interactions in the radicals themselves.

The nonuniformity in the spatial distribution of radicals affects their thermal stability in inclusion compounds as well.

Experiments with an adduct of the *n*-heptyl ether of valeric acid to carbamide have revealed an interesting relationship between the stability of the primary alkyl radicals, $RCH_2\dot{C}H_2[R_{(1)}]$, and the temperature at which the samples were radiolyzed. The rate of loss for these radicals, which turn into the more stable $R_{(1)}\dot{C}HCOOR_{(2)}[R_{(3)}]$ radicals, has been found to rise with decreasing temperature. In reference [247] the following explanation of the phenomenon is given. Irradiation of carbamide adducts to carbonic acid ethers appears to produce cation radicals M^+ from a carbamide molecule, an alkyl radical, and a nonparamagnetic anion in the inclusion-compound channel. The spacing between the cation radical and the radical-anion pair is decided by the migration of a hole or an electron which in turn depends on the temperature of irradiation. The distance of $R_{(1)}$ radicals from a hole has been noted to increase with increasing temperature of the sample at the time of irradiation. At 77 K, the mobility of the included (guest) molecules and radicals in the channel is too low for any reaction to take place. An increase in temperature leads to an increased mobility along the channel, and the $R_{(1)}$ radicals either react with carbamide molecules with the formation of $R_{(3)}$ radicals (in which case, the anion recombines with the M^+ cation to produce one more $R_{(3)}$ radical), or take part in the reaction

$$M^+ + R_{(1)} + A^- \longrightarrow \text{Products}$$

which brings down the overall concentration of radicals. The probability of the latter reaction increases with decreasing spacing of $R_{(1)}$ relative to A^- and M^+, that is, with decreasing temperature at the time of irradiation. The proposed scheme of radical changes offers a plausible explanation for the manner in which paramagnetic centres are formed and take part in secondary reactions [247].

The behaviour of trapped radicals in a solid sample is markedly affected by various defects in the crystalline matrix and the spatial distribution pattern of such defects. Reference [248] analyzes the loss of free radicals in crystalline phenol, aniline, N-ethylaniline and *o*-nitro-N-methylaniline, and presents annealing curves for the radicals. Stationary concentrations of about 50% of the initial ones have been observed at 200 K in N-ethylaniline and at 260 K in *o*-nitro-N-methylaniline. The loss of up to 80% radicals in aniline has been found to take place in the low-temperature range from 100 to 230 K; in phenol all of the radicals were lost below 260 K. According to [248], the data thus obtained can only be explained by assuming that some of the radicals are trapped near defects and that their loss is promoted by the increase in molecular mobility near the defects upon de-freezing. Qualitatively, this explanation agrees with the estimates given in [249] for the frequencies of molecular mobility near defects.

Experiments with radical stabilization in aniline seem to suggest that the low limiting concentrations of radicals trapped by irradiation of aromatic compounds are due to the nonuniform distribution of radicals [250]. The nonuniformity arises because the radicals are trapped near lattice defects. Presumably, this is promoted by the effective transfer of energy to various lattice defects. At low doses of irradiation, this process leads predominantly to the production of radicals near the defects. At high doses, it results in the loss of radicals and the break-up of the lattice near the defects.

The dielectric properties of crystalline N-ethylaniline, *o*-nitro-N-methylaniline, aniline, and phenol in the frequency range 10^2-10^5 Hz and the temperature interval from 100 to 310 K are examined in [249].

At temperatures substantially below the melting point, an increase is noted in permittivity owing to interlayer polarization which is associated with the mobility of molecules near the lattice defects and the presence of a liquid phase in the sample due to impurities. Interestingly, no phase changes have been observed in the solid phase of the above compounds. According to the estimates made with allowance for the observed variations in permittivity, the proportion (by volume) of molecules whose mobility is characterized by audio and higher frequencies is less than 3 or 4% in phenol and *o*-nitro-N-methylaniline at temperatures up to 260 K. In aniline, the proportion of mobile molecules is slightly higher (6 to 8%) up to 250 K.

Interesting data related to the effect of impurities and, in part, the phase state on the production and recombination of free radicals in solutions of $CoCl_2$ and $MnCl_2 \cdot 2H_2O$ in methanol in the case of gamma radiolysis (a Co-60 source, at 77 K) are presented in [251]. An advantage of this work is that the investigators used both ESR and calorimetric techniques. As should be expected, the effective recombination of the isolated radicals has been found to take place during the transition from the glassy to the liquid state. On the basis of the initial portions in the curves of heat generation due to the recombination of radicals, the activation energy is estimated to be 21 ± 4 kJ mole^{-1}. In all probability, this order of magnitude is decided by the temperature dependence of mobility in the matrix as it changes from the glassy to the liquid state.

In the light of the above brief overview of data about the spatial distribution of radicals in frozen solid samples, it may be argued that the isolation and loss of radicals are substantially affected by a number of difficult-to-control factors, such as the presence of various defects, internal motions, energy transfer, and the likely formation of a liquid phase.

3.5. REACTIONS OF CHARGED SPECIES. TRAPPED ELECTRONS

Processes involving electrons and other charged species have been attracting the attention of many investigators. Of special interest are the chemical reactions in the solid phase that can be explained by the mechanism of tunnel transfer.

References [252] through [254] present data according to which it is highly probable that the tunnel mechanism is responsible for the transfer of electrons over large distances in reactions involving trapped electrons, anion radicals and excited molecules, and in reactions between metallic ions in glassy matrices. The investigators have been concerned with the following redox reactions in glassy water-sulphuric acid samples ($6M$ H_2SO_4) gamma-irradiated (with a dose of about 10^{19} eV/ml) at 77 K and 4.2 K:

$$Cd^{I} + Cr^{VI} \longrightarrow Cd^{II} + Cr^{V} \tag{3.3}$$

$$Cd^{I} + Mn^{VII} \longrightarrow Cd^{II} + Mn^{VI} \tag{3.4}$$

$$Cd^{I} + Ag^{I} \longrightarrow Cd^{II} + Ag^{0} \tag{3.5}$$

The decrease with time and additive concentration in the ESR signal of the Cd^{I} ion produced by radiolysis of Cd^{II} can be described by an equation derived in [255] for the tunnel mechanism of the reaction:

$$n(t, c) / n(t, 0) = \exp\left[-(\pi a^3/6) c \ln^3 (\nu t)\right] \tag{3.6}$$

where $n(t, c)$ is the concentration of Cd^{I} at time t; c is the concentration of the additives (Cr^{VI}, Mn^{VII}); υ and a are the constants in the expression relating the rate constant of the tunnel reaction to the distance R between the reagents, namely

$$k_t = \nu \exp(-2R/a)$$

A point in favour of the tunnel mechanism is the fact that the rate of the reaction (3.3) only slightly depends on temperature, and that of the reaction (3.4) remains unchanged as the temperature is varied from 77 K to 4.2 K. Another point in support of the tunnel concept is that the reactive species are uniformly distributed throughout the bulk of the sample and separated by the host molecules [254]. Presumably, the glassy water solutions of sulphuric acid ($6M$ H_2SO_4) containing 0.05 to $0.16M$ $CdSO_4$ and also additions of $K_2Cr_2O_7$, $KMnO_4$ and $AgNO_3$ in concentrations from zero to $0.06M$ are homogeneous systems in which the components are uniformly distributed. Because this assumption holds out special promise, further evidence is in order. As will be recalled, external physical properties, such as transparency and the lack of a well defined phase change point cannot by themselves guarantee that a given glassy system is homogeneous at the molecular level [256].

Some features in the behaviour of trapped radicals and ions are related to the trapped solvated electrons [32]. As is pointed out in [257], the optical absorption band of trapped electrons, e_t^-, changes in shape with their loss in alkaline glasses ($10M$ NaOH) containing $NaNO_3$ ions (0.01 to $0.075M$ $NaNO_3$) as the acceptor. After the loss of half the trapped electrons in the presence of $0.05M$ $NaNO_3$, the investigators noted that the maximum of the absorption band for the remaining e_t^- had shifted towards the shorter wavelengths. A similar shift in the absorption maximum has been observed in a neat "alkaline" glass irradiated with large doses (10 to 30 Mrad).

According to [257], the loss of trapped electrons in alkaline glasses results from recombination with hole centres. Existing evidence is interpreted in the light of the tunnel mechanism. The rate of spontaneous loss of trapped electrons appears to be related to the depth of intermolecular electron traps. Similar results have been obtained by the same investigators [258] for water-alcohol systems.

The likely tunnelling of electrons from intermolecular traps to acceptor molecules is examined also in [259] through [266].

Kinetic analysis of the accumulation of trapped electrons in low-temperature radiolysis, with allowance for competition between traps (T) and acceptors (A) in capturing thermalized electrons, leads to the following equation relating the yield G of trapped electrons e_t^- in the presence of an acceptor to the latter's concentration:

$$G_0/G = 1 + (k_1[\mathrm{A}]/k_2[\mathrm{T}]) \tag{3.7}$$

where G_0 is the yield of trapped electrons in the absence of the acceptor A; [A] is the concentration of the acceptor; [T] is the concentration of traps; k_1 and k_2 are the rate constants for the reactions of an electron with A and T, respectively.

According to Eq. (3.7), the ratio G_0/G must be a linear function of [A]. In [259] and [262] through [267] it is shown, however, that at higher acceptor concentrations there is a departure from this equation. The causes of, and models for, this departure are examined and proposed in references [263] through [265]. The model proposed in [259] is based on the assumption of far electron transfer by the tunnel mechanism. At low acceptor concentrations (not over $0.2M$), the ratio d_0/d (where d_0 and d are the optical densities of trapped electrons in the absence and presence of the acceptor, respectively, proportional to G_0/G in the case of equal doses) is a linear function of acceptor concentration.

It is shown in [268] that the diffusion-recombination model [269] describing radiation-induced chemical changes in aqueous solutions can successfully be used to explain the mechanism of low-temperature radiolysis in solids from polar solvents. This suggests that the primary processes occurring in tracks at low and high temperatures have much in common.

3.6. THE EFFECT OF IMPURITIES AND RADIATION TYPE ON STABILITY OF REACTIVE SPECIES

As already noted, the production and loss of radicals are substantially affected by various lattice defects, which may be the radicals themselves or the products of their changes. The behaviour of reactive species in frozen solids also depends on the presence of impurities, the type of radiation used, and phase changes. The effect of all of these factors can best be traced in systems favouring the production of solvated electrons.

It is important to note that low irradiation doses, small impurity concentrations, and nonuniform distribution of impurities forming microscopic discontinuities present a serious handicap in evaluating the effect of impurities on the yield of trapped radiolyzed reactive species by experiment. On the one hand, local accumulation of impurities into microscopic discontinuities removes them, as it were, from the sample. On the other, the overall volume of microscopic discontinuities is negligible in comparison with the bulk of the sample and may therefore fail to affect to any noticeable degree the processes proceeding throughout the sample. In the early stages of radiolysis, the overlapping of spurs and the discontinuities already present in the sample may be insignificant to a point where the effect of the impurities may be masked from the observer. In the circumstances, the observer may be tempted into falsely believing that in principle the impurities do not affect the processes taking place. This apparently explains reports to the effect that impurities have not been found to exert any influence even when added deliberately. For example, in reference [270] concerned with the spectral characteristics and radiation yields of hydrated electrons, e_h^-, during flash radiolysis of ice crystals in the temperature interval from 273 to 213 K, it is reported that the small additions of HF ($1.2\times10^{-5}\,M$), $HClO_4$ ($2.0\times10^{-3}\,M$), and KOH ($1.0\times10^{-3}M$) to the ice samples did not change either the position of absorption peaks for e_h or the temperature coefficient of peak shift (equal to -1.0×10^{-3} eV K^{-1}).

It is to be noted that reference [270] is one of the few investigations in which the distribution of additions has been studied experimentally. Experiments with the distribution of impurities in ice have shown that in contrast to hydrofluoric acid, $HClO_4$ and KOH were distributed nonuniformly. Moreover, as is justly pointed out, it is no simple matter to distribute impurities in ice crystals uniformly. The distribution of impurities in ice samples was analyzed by cutting each sample into concentric layers at different distances from the centre. The concentrations of Cl^-, F^-, and K^+ ions were determined by mass spectrometry. The concentrations of $HClO_4$ and KOH were found to increase towards the centre of the sample so that in the operating area they exceeded those of localized electrons produced by irradiation. No anomaly in the distribution of HF was found. This is probably because a fluorine atom can replace an oxygen atom in the ice lattice and HF molecules are present in the dissociated form in the crystal.

It is to be noted that the actual nonuniformity in the distribution of $HClO_4$ and KOH may be still more pronounced. It is hypothesized in [270] that there is a macroscopic gradient of concentration from centre towards the periphery and that this gradient is continuous. The nonuniformity in the distribution of impurities may have an entirely different pattern, namely: when frozen, the impurity molecules may gather into groups which in turn produce microscopic discontinuities [271, 272]. If the nonuniformity in the distribution of such microscopic discontinuities is insignificant, the concentric-ring method of analysis may fail to disclose the presence of such nonuniformities in the distribution of impurities.

Interestingly, the presence of HF, $HClO_4$, and KOH has no effect on the temperature dependence of the yield G of hydrated electrons, e_h^-, in the ice matrix. As the temperature is brought down, the yield of e_h^- drops suddenly. In reference [270], this sudden drop in G is related to the properties of the ice matrix and to the likely re-addition of the ionization-produced electrons back to their parent ions and to their localization with the formation of e_h^-. The equation relating the yield of hydrated electrons to temperature, derived with allowance for the likely competition between recombination and trapping of an electron by the medium (according to the mechanism of radiolysis in polar medium), which leads to the appearance of an optically active species, fairly accurately fits the experimental data:

$$(G_0 - G_{e^-_h})/G_{e^-_h} = \text{Const} \times T^{-5/2} \exp(E_0/kT) \qquad (3.8)$$

where G_0 is the initial ionization yield and E_0 is the threshold energy of electron localization, found to be equal to 0.12 ± 0.02 eV.

Evidence presented in [270] is related to the behaviour of reactive species originating from the host matrix. In our opinion, the impurities may have an appreciable effect in systems where the radicals or other reactive species are produced with the participation of impurity molecules.

Matters related to the photoradiation stability of materials can best be elucidated by experiments involving the use of ionizing radiation and light, simultaneously. Essentially, photoradiation processes consist in that the reactive species produced by ionizing radiation upon absorption of light in the visible and UV regions of the spectrum take part in chemical reactions. Some kinetic aspects of radical accumulation in the case of simultaneous, consecutive and periodic exposure to ionizing radiation and light are examined in [273].

A kinetic analysis of radical accumulation under conditions of simultaneous exposure to gamma radiation and light shows that for weakly absorbing media and thin layers the concentration of radicals reaches its limiting value

$$[\mathrm{R}]_{\mathrm{sim}}^{\infty} = \sqrt{kI/k_1 j}$$

where k and k_1 are the rate constants for the production and photorecombination of radicals, respectively; I and j are the intensities of gamma radiation and light.

In the case of consecutive exposure, the limiting concentration of radicals is

$$[R]^{max}_{con} = 0.5\,[R]^{\infty}_{sim} \tag{3.9}$$

In the case of periodic exposure, the concentration of radicals takes on intermediate values.

According to kinetic considerations, it would seem that simultaneous exposure should result in a lower accumulation of radicals than when the sample is exposed to an ionizing radiation alone. Experiments with radical production at 77 K in a number of polymers (polyacryl amide, poly-ε-caproamide, DNA, etc.) have shown, however, that simultaneous exposure produces either as many radicals or 1.5 to 2 times as many as exposure to gamma radiation alone [274, 275]. In the general case, the increase in radical concentration caused by simultaneous exposure over that due to exposure to one form of radiation may be traced to the action that light has on the reactive species produced by gamma radiation. On absorbing light, these species move into excited electronic states and react with the formation of free radicals. The increase in radical concentration correlates with the number of paramagnetic centres disappearing upon exposure to light. In the case of simultaneous exposure, ions, ion radicals, and other species are continually converted into free radicals. Processes with the participation of short-lived reactive species may likewise contribute to the increased radical concentration in the case of simultaneous exposure.

Light incident on gamma-irradiated samples may initiate a variety of processes. For example, light at $\lambda \geqslant 700$ nm can be responsible for the loss of trapped electrons, the disappearance of primary and secondary cation radicals, and the formation of an additional number of anion radicals. This effect has been observed in experiments on the action of visible light on gamma-irradiated inclusion compounds of methylalkyl ketones and carbamide at 77 K [276]. Under the action of light quanta at $\lambda > 380$ nm, anion radicals undergo a reversible change with the formation of radicals:

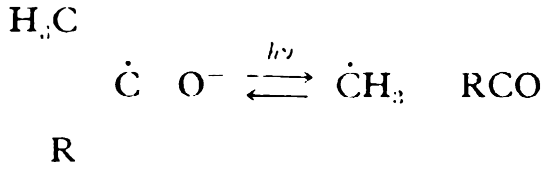

$$\overset{H_3C}{\underset{R}{\dot{C}}}\;O^- \overset{h\nu}{\rightleftarrows} \dot{C}H_3 \quad RCO \tag{3.10}$$

Referring to Table 3.3, the processes taking place in gamma-irradiated methylalkyl ketones under the action of light depend not only on the energy of a quantum, but also on whether they occur in the matrix or in an inclusion compound.

Conflicting views exist in the literature as regards the mechanism by which the primary processes of photolysis proceed in the frozen solutions of amines in alcohols and the formation of $\dot{R}OH$ radicals.

TABLE 3.3

Light-Induced Changes of Species in Gamma-Irradiated Methylalkyl Ketones in Inclusion Carbamide Compounds and the Host Matrix at 77 K

λ, nm	Process in inclusion compound	Process in host matrix
⩾ 700	Trapped electrons, e_t^-, 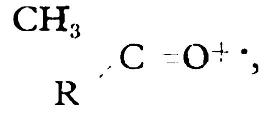 $\mathrm{(CH_3)(R)C{=}O^{+\bullet}}$, and 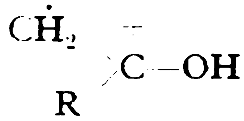 $\mathrm{(\dot{C}H_2)(R)C{-}OH}$ disappear; and 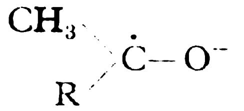 $\mathrm{(CH_3)(R)\dot{C}{-}O^-}$ are formed	Trapped electrons, e_t^-, and 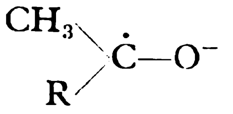 $\mathrm{(CH_3)(R)\dot{C}{-}O^-}$ disappear
⩾ 500	Formation of 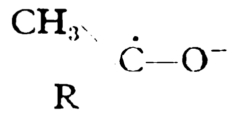 $\mathrm{(CH_3)(R)\dot{C}{-}O^-}$ continues	Disappearance of 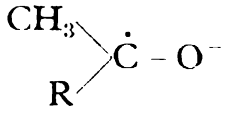 $\mathrm{(CH_3)(R)\dot{C}{-}O^-}$ continues; 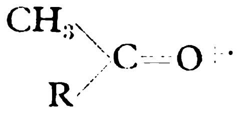 $\mathrm{(CH_3)(R)C{=}O^{+\bullet}}$ disappear
⩾ 380	Reaction (3.10) takes place	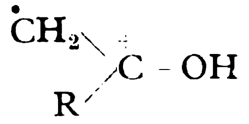 $\mathrm{(\dot{C}H_2)(R)C{-}OH}$ disappear

According to [277] and [278], the formation of $\dot{R}OH$ radicals proceeds concurrently with the photoionization of the amine as a competing process (the sensibilization mechanism). According to other investigators [279], the formation of $\dot{R}OH$ radicals is a secondary process: these radicals are believed to form from photoionization products of amine owing to their subsequent exposure to the luminescence of the amine (the photoionization mechanism followed by the "bleaching" of the photoionization products).

Reference [279] presents evidence based on the kinetic curves for the accumulation of ethanol radicals during the photolysis of the frozen amine-alcohol system for the two mechanisms. It is shown that the experimental data have a better agreement with the amine photoionization mechanism by which cation radicals and solvated electrons are formed first and alcohol radicals afterwards, as the photoionization products are "bleached". These calculations are based on the assumption that the primary photochemical process occurring during the photolysis of frozen ethanol solutions of amines is two-photon ionization and that ethanol radicals, $\dot{C}H(OH)CH_3$, are formed by photoreactions between the solvated electrons and amine cation radicals, on the one hand, and the alcohol molecules, on the other [279].

The outcome of irradiation depends on the structure of the sample and the phase state of the system. Especially strong effects should be expected in the case of exposure to light. Comparison of data on the low-temperature photolysis of several compounds has shown that the quantum yields can vary between broad limits. Unfortunately, the computation of quantum yields for low-temperature photochemical reactions still remains an unresolved problem. Reference [280] sets forth a theoretical approach to the determination of quantum yields for the photochemical reactions occurring in the solid phase exposed to unpolarized and polarized light (that is, with allowance for so-called photoselection) [281, 282]. Photoselection is believed to be related to the difference in spatial orientation of molecules in solids and, as a consequence, to the difference in the probability of absorption of light quanta. In the absence of rotational mobility in a solid, the photochemical process favours above all molecules showing the most favourable spatial arrangement. As a result, the original distribution of molecules in terms of relative orientation is disturbed, causing among other things the optical density of the system to change differently than the concentration. The effect of photoselection on the kinetics of photochemical reactions taking place in rigid matrices is also noted in [282].

The theoretical estimates presented in [280] show that the quantum yield determined for a photochemical reaction in a solid without allowance for the fact that molecules are distributed in a rigid matrix (that is, within the concepts applicable to liquid solutions) differs from the true quantum yield.

As a rule, the quantum yields for photolyzed products in the solid phase are very small. Using low-temperature spectrophotometry, the authors of [283] invesigated the mechanism by which hydrogen atoms are formed during the photolysis of aqueous solutions of Fe^{2+} ions at low temperature. They measured the quantum yield for the photooxidation of Fe^{2+} ions at 77 K in 5.6*M* H_2SO_4 on the basis of Fe^{3+} accumulation by an optical method and on the basis of H formation by ESR. The respective figures are 0.08 ± 0.01 and 0.05 ± 0.02. It is worth while noting the remark made in [283] to the effect that the solution containing 8*M* $HClO_4$ turned to a glassy state sluggishly in deep (1-cm) cells.

The authors of [284] investigated the photolysis of N-bromoethyleneimine in the condensed phase at low temperatures. The end product was hydrocyanic acid. It is hypothesized that hydrocyanic acid is formed via an intermediate cyclic ethyleneimine radical according to the reaction:

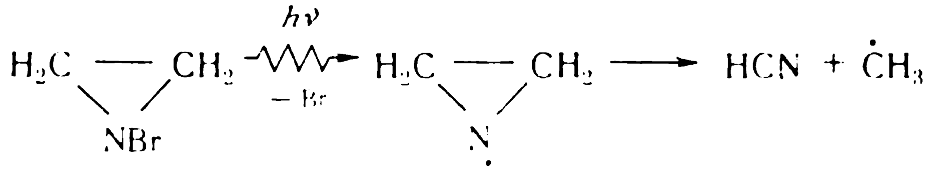

(3.11)

In their experiments, the authors of [284] noted that the yield of HCN in the temperature interval from 77 to 223 K depended only slightly on temperature, but was found to increase suddenly during a phase change and to rise with rising temperature. A similar pattern was observed during the photolysis of 2,2-dimethyl-N-bromoethyleneimine.

3.7. KINETICS OF RADIOPHOTOLUMINESCENCE AND RADIOTHERMOLUMINESCENCE AT LOW TEMPERATURES

When exposed to light or heat, organic samples previously irradiated by gamma-rays or electrons at low temperatures will often display what is respectively known as radiophotoluminescence and radiothermoluminescence. These forms of luminescence are traceable to the recombination of the charges produced and trapped during radiolysis and liberated upon heating and absorption of light quanta [154]. The decay of radiophotoluminescence follows a complex kinetic pattern. Even in the case of a single substance, the kinetic curve may be broken up into portions associated with different life spans. The long-time component of luminescence is usually associated with the formation of molecules due to the recombination of triplet excited states [285] or with the slow diffusion of some charges escaping from traps towards positive ions [154].

The authors of [154] investigated the photoinduced recombination luminescence of gamma- (Co-60)-irradiated samples of methylcyclohexane and cyclohexane at 77 K, using monochromatic radiation at $\lambda = 800$ nm. The radiophotoluminescence time τ was found to be connected to the concentration of trapped radicals [R] by the relation

$$1/\tau \quad 1/\tau_0 \quad k_2\,[R]$$

where τ_0 is the radiophotoluminescence time at zero concentration of radicals. During luminescence, a competition was observed between the secondary trapping of photodetached electrons by radicals and their recombination with positive ions.

According to an existing point of view, electron trapping in hydrocarbon glasses takes place in intermolecular traps known as structural discontinuities [286]. An electron escaping from a trap is either recaptured or recombines with a positive ion, its life time in free state being 10^{-9} s. It is the rapid recombination occurring during this time interval that is responsible for the emission of light.

In interpreting their data, the authors of [286] assumed that the radiolyzed products were uniformly distributed throughout the sample. However, the presence of two persistence intervals in the luminescence curve of the crystalline methylcyclohexane in contrast to a single persistence interval in the case of the amorphous sample brought others to suspect a nonuniformity in the structure and the existence of both a crystalline and an amorphous phase in the former samples [154].

Photoluminescence can be affected by various impurities and defects. The latter may, for example, be trapped radicals. It appears legitimate to expect that impurities possessing electron-acceptor properties should exert influence similar to that of radicals. The influence of such impurities is investigated in [287], using chromatographically pure methylcyclohexane and benzene at 77 K (exposed to gamma and infrared radiation). The authors observed short-lived luminescence excited by infrared light, with a decay period of less than 10^{-3} s, and an extended two-component afterglow. An increase in the benzene content of the sample was accompanied by a gradual reduction in the intensity of the emission and, at the same time, in the duration of both afterglow components. The life time of the first afterglow component was a linear function of the benzene concentration ranging from 10^{-3} to $10^{-2}M$:

$$\tau^{-1} \quad k\,[C_6H_6]$$

where $k = 0.087 \times 10^2$ litres mole^{-1}s^{-1}. The value of k in a similar relationship connecting the period of radiophotoluminescence of methylcyclohexane to the concentration of free radicals was 0.085×10^2 litres mole^{-1}s^{-1} [154]. These results bear out the fact that the duration of radiophotoluminescence is to a considerable degree decided by the concentration of an electron-acceptor impurity in the host substance. A study of the kinetics of radiophotoluminescence can be useful in analyzing the distribution of radicals and impurities in samples [287].

Radiothermoluminescence is markedly affected by various structural changes in frozen solid samples and also by acceptor impurities. The authors of [288] examined the temperature deactivation of electron-excited (gamma-irradiated) UO_2^{2+} ions during radiothermoluminescence in the temperature interval 77-300 K and noticed the effect of structural changes taking place in the acid. The positions of the thermoluminescence maxima are usually correlated with phase changes. A number of phase changes occur in acid solutions of UO_2^{2+} ions in the temperature interval 77-300 K, and therefore changes in τ with temperature are anything but monotone. Referring to Fig. 3.2, there is no portion that might be associated with a purely temperature quenching. The curves display peaks and inflections which are correlated with the temperature intervals of thermoluminescence peaks, that is, structural changes.

In the interval 100-140 K, where the first thermoluminescence peak is observed, the intensity of luminescence passes through a maximum. Within the same temperature interval, gamma-irradiated samples display recombination of hydrogen atoms. Regeneration of hydrogen atoms by warming to 140 K by a method described in [33] does not restore thermoluminescence to its previous maximum. Thus, in the temperature interval 110-140 K, radiothermoluminescence is not related to the loss of hydrogen atoms, but is associated with other radiolyzed products not identified as yet. The loss of such products may well be responsible for the isothermal afterglow which decays in intensity hyperbolically at 77 K.

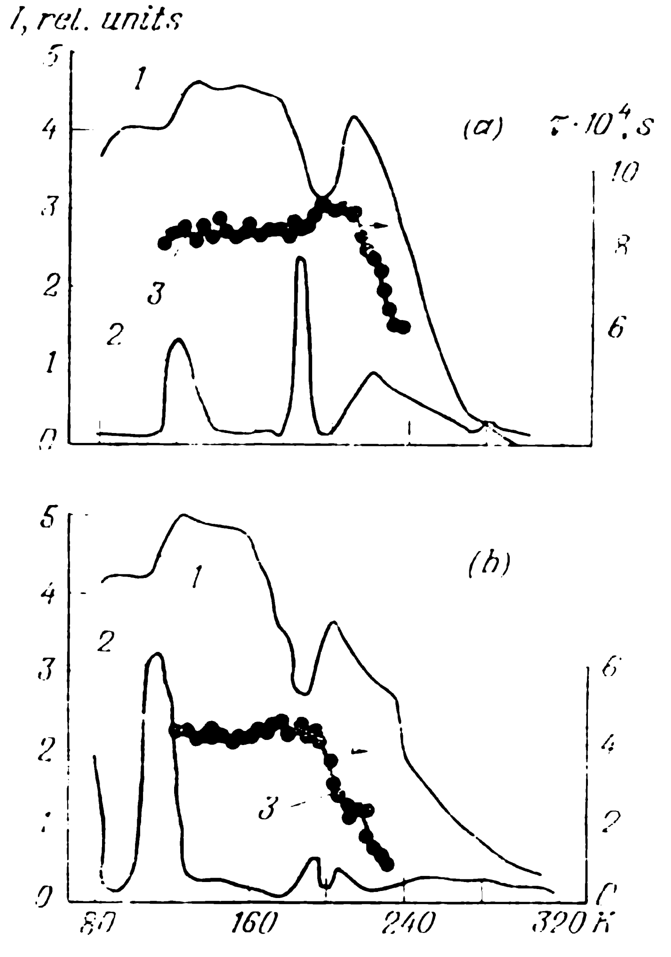

Fig. 3.2. Temperature dependences of (*1*) thermoluminescence intensity after X-ray irradiation ($D = 0.32$ J kg^{-1}) at a heating rate of 5 K min^{-1}; (2) photoluminescence intensity at λ_{excit} 253.7 nm; and (*3*) lifetime of an excited UO_2^{2+} ion for 0.1*M* solution of UO_2^{2+} in (a) 17.5*M* H_2SO_4 and (b) 5 M H_2SO_4

The interval from 140 to 170 K encompasses another, although small peak of thermoluminescence and there is a decrease in both τ and the intensity of fluorescence, I_{fl}. At 183 K, there is a sudden fall in I_{fl}, but τ increases rather than decreases. Here, the rigid glass changes to a viscous glass — a structural change which has also been discovered by other methods. A structural change takes some time to reach completion, so if one holds the temperature fixed at 175 K, that is, at the start of the thermoluminescence peak, one will be able to observe a decrease in I_{fl} for several minutes more. The activation energy for radiothermoluminescence, as determined by a method proposed in [289] appears abnormally high (293 kJ mole^{-1}). A repetition of the warming-cooling cycle in the temperature interval of thermoluminescence brings the activation energy down to 96 kJ mole^{-1}. These are the effective values of activation energy, reflecting the influence of structural changes. An activation energy of 193kJ mole^{-1} obtained in [290] for the loss of $SO_4^{\cdot-}$ radicals in 5-10M H_2SO_4 in the same temperature interval is likewise associated with structural changes and the compensation effect. The value of τ is a maximum near the temperature where I_{fl} is a minimum.

Thus, the quantum yield (according to the values of τ) of photoluminescence within the interval of a structural change increases rather than decreases with rising temperature. As to the fall in I_{fl}, it is decided by the change in the transparency of the acid caused by the loss of optical homogeneity during the structural change. These conclusions have been confirmed by direct measurements of transmittance within the respective temperature interval. The superposition of two processes (an increase in transparency and a decrease in quantum yield) is responsible for the appearance of a peak of I_{fl} at temperatures immediately following the phase change. Past that point both τ and I_{fl} decay monotonically.

To sum up, the temperature dependence of luminescence intensity and, accordingly, the rate of nonradiative deactivation of excited UO_2^{2+} ions cannot be explained by the activation process of temperature quenching alone. A decisive or even predominant role here can be played by the structural changes occurring in the acid within the respective temperature intervals.

At present, the kinetic treatment of radiothermoluminescence is based on one of two simplifying assumptions as regards the distribution of isolated species. Under one assumption (model 1), these species are distributed homogeneously [291]. Under the other (model 2), there exist isolated pairs of charges, and each time a charge escapes from a trap, a recombination event takes place [292].

Recently, an attempt has been made [293] to analyze the kinetics of thermoluminescence by assuming an arbitrary initial charge distribution in the bulk of the sample with allowance for the likely retrapping of the charge escaping from its trap. This consideration is based on a comparison between the kinetics of radiothermoluminescence and that of isothermal radioluminescence. The results of such a consideration were compared with experimental data for polybutadiene gamma-irradiated at 77 K.

The authors of [293] make a number of assumptions. For one thing, they assume that there exists some arbitrary initial distribution of charges in the bulk of the sample in one type of traps having the same probability for electron escape and the same capture cross-section. For another, they assume that the effect of temperature on the migration of an electron towards a positive ion consists solely in cutting down the life time of the electron in the trap τ (T). (Here, τ (T) is a function of temperature, and $T = T(t)$ is an arbitrary law for sample warming). Lastly, the authors assume that the probability that an electron escaping from its trap will be re-trapped is greater than or equal to zero.

On the basis of the above assumptions, the investigators have derived an expression for the intensity of radiothermoluminescence. Proceeding from the kinetic law which defines changes in luminescence under isothermal conditions, it is possible to derive from it an analytical expression describing the kinetics under conditions of varying temperature. A comparison of the above consideration with experimental data for polybutadiene shows that for agreement with experiment on the assumption of traps of one type, allowance must be made for re-trapping and nonuniform spatial distribution of charges.

The kinetics of the thermal loss of charges in butadiene-acrylonitrile copolymer and in *cis*-polybutadiene with and without additions of phenyl-β-naphthylamine and chloranyl irradiated at 77 K is examined in [294]. The thermal loss of charges and radicals is observed to follow a well-defined stepwise pattern and occurs over a wide temperature interval (173-223 K). The additions of electron donors and acceptors have been found to exert a marked and, in our opinion, an interesting influence on recombination. It has also been noticed that the kinetics of charge loss and chemical changes in the irradiated rubber varies with the rate of matrix warming. Curiously, in the presence of an addition of chloranyl the recombination of charges slows down and the annealing curve lies above the curve for the rubber without an addition of chloranyl. The addition of phenyl-β-naphthylamine has been found to produce a slight opposite effect.

The experimental data quoted in this chapter on the production and changes of radicals and ions in frozen solids seem to show that at low temperatures radicals and ions can undergo various changes which in some cases strongly depend on the physical and chemical properties of the sample and which may take a different pathway during the generation and isolation of active centres.

CHAPTER FOUR

LOW-TEMPERATURE POLYMERIZATION

Growing evidence about the formation of appreciable nonequilibrium concentrations of trapped radicals at temperatures close to 77 K and the various reactions with their participation has brought investigators to conclude that low temperatures may also favour chain reactions, notably reactions of polymerization. At present, low-temperature polymerization is a large division of science in its own right. We shall mainly dwell on the specific features of low-temperature polymerization and on the differences between low-temperature polymerization in the solid phase and polymerization in the liquid phase.

At low temperatures, most monomers are crystalline or glassy solids. These states markedly differ in the degree of order with which their molecules are arranged. In crystalline solids, the molecules are arranged in an ordered pattern. In glassy solids, they take up positions at random, so in structure a glassy solid is nearly a liquid. As compared with liquids, however, the degree of molecular mobility in both crystalline and glassy solids is small. The order in the arrangement of the molecular species and their limited mobility in the solid phase must of necessity affect the process of polymerization.

As a rule, cryogenic polymerization takes place at the time of phase changes, when the molecules in the system are arranged in an ordered pattern and show a high mobility typical of the liquid phase. Thus, the chemical reactions occurring in the solid phase at the time of phase changes may be treated as processes in structured, ordered systems.

The polymerization of crystalline trioxane to polyoxymethylene was discovered a relatively long time ago [295]. It has also been observed that acetaldehyde would polymerize on melting [296, 297]. However, large-scale experiments with low-temperature polymerization in structured systems had not begun until the late 50s when high-energy radiation sources were first used to induce the reactions.

Recent studies have shown that many monomers are capable of polymerizing in the solid phase at high rates.

A sizeable contribution to polymerization in the solid phase has been made by Soviet scientists, among them Academicians Kargin, Medvedev, Semenov, and Yenikolopov; the USSR Academy of Sciences' corresponding members Goldansky, Kabanov, Plate, and others. Polymerization in the solid phase, notably at low temperatures, is treated in a number of review articles [173, 298-303].

Studies in the field of low-temperature polymerization have basically been conducted in two directions: firstly, the low-temperature polymerization of solid and liquid monomers under the action of radiation, secondly, the polymerization of monomers (and inducing agents) cocondensed onto a cooled surface.

For the reactions taking place in systems with an ordered structure, the conventional kinetic concepts are often inapplicable. One has also to take into account the effects of the crystal lattice, the presence (or otherwise) of defects, phase changes, and some other factors.

4.1. RADIATION- AND PHOTO-INDUCED POLYMERIZATION

Reactions of solid-state polymerization are most frequently induced by ionizing radiations, because they show high penetration so that the reaction can be induced in practically all of the bulk of a solid monomer without an addition of an initiator. Exposure to radiation produces radicals, ions, and secondary electrons [31], which fact speaks of the versatility of ionizing radiation. Unfortunately, this versatility often handicaps the identification of the mechanism by which a given reaction proceeds. The results are more definite in the case of photo-induced chemical reactions, where use is made of radical photo-inducing agents. But again, one inevitably runs into specific difficulties, because the ionization potential for the solid phase is reduced, and photoionization is likely to occur [304]. Under the action of light the active centres formed are distributed non-uniformly throughout the sample, and this hinders kinetic analysis still more.

A systematic effort in the field of liquid-phase and solid-phase polymerization at low temperatures in the USSR and abroad was started in the early 60s. In the USSR, main emphasis was placed on the specific features of polymerization during changes from the solid to the liquid phase, notably the extent of changes in the reaction mechanism and the applicability of liquid-phase evidence to the solid phase.

At present, a wealth of experimental evidence has been accumulated, but we still know little about the elementary rate constants for the reactions of initiation, chain formation, and chain rupture over a wide temperature interval. Yet, it may be taken as a well-established fact that radiation-induced solid-phase polymerization at low temperatures substantially differs from that in the liquid phase. In the former case, polymerization involves a wider range of reactive species, such as electrons, ion radicals, and excited species. In the solid phase, these species have a longer life time and, as a consequence, a higher concentration. The role of defects gains in significance as well, because the process of polymerization is speeded up near them [305].

In the opinion of some investigators [306, 307], the mechanism of radiation-induced solid-phase polymerization is based on the nonradiative transition of excitons to phonons within extended lattice defects. As this happens, the energy of electron excitation is converted to the energy of motion of the molecules near the dislocations, which fact promotes the initiation of a polymer chain. To some extent, such a mechanism has been corroborated by experiments with the polymerization of metacrylic acid in the crystalline state [308]. Exposure of its crystals to long-wave UV radiation speeded up the reaction of polymerization. This was explained by the formation of phonons from excitons upon the latter's encounter with a lattice defect. The wavelength of light was chosen such that no radicals could be formed.

Polymerization in the solid phase is markedly affected by various phase changes. The rate of polymerization increases in the temperature intervals where the mobility of the reacting molecules increases. Usually, these are areas of various phase changes. Many examples to this effect are quoted in the above review publications.

In experiments with low-temperature polymerization, it is essential to identify the nature of the species taking part in the process. In the gas and liquid phases at room and elevated temperatures, polymerization usually proceeds by the radical mechanism. As the temperature is brought down, the role of radicals is decreased and that of ions increased. The existence of an ion mechanism was, for example, established in the radiation-induced low-temperature polymerization of tetrafluoroethylene [309]. An ion reaction in a crystal involves the expenditure of some energy in order to overcome the crystal field which holds the molecules in the lattice sites. As a rule, this energy is less than the activation energy for the polymer chain propagation involving radicals, so the polymer chain predominantly forms on ion centres as the temperature is brought down. However, solid-phase polymerization proceeding by the radical mechanism has been reported to take place in many instances [303].

As a result of chemical reactions, the bonds are redistributed and the nuclei are shifted. In contrast to the gas and liquid phases, for the nuclei to be shifted in the solid phase the original lattice must be re-arranged. At low temperatures, however, the spatial motions of molecules and their fragments in solids are hindered. This fact explains, above all, why the rate of low-temperature solid-phase polymerization increases in the temperature intervals where the retarding effect is reduced and the molecules gain mobility [302, 310]. For solid-phase polymerization to proceed, it is essential that the monomer molecules should be capable of translational motion and that the extent of such motion should increase as the polymer chain grows. It should be expected, therefore, that solid-phase polymerization will be especially effective where it involves small spatial displacements. Then polymerization will be able to proceed over a wide temperature interval even at low temperatures [298, 302, 311, 312].

Using ESR techniques, the authors of [313] have studied the polymerization taking place in polycrystalline samples of *p*-diethynylbenzene, phenylacetylene, maleinimide, phenylmaleinimide, ethylmaleinimide, and acenaphthylene exposed to various ionizing radiations at 77 K. Gamma radiation was supplied by a Co-60 source, electrons by a type Y-12 accelerator, and UV radiation by a mercury-discharge lamp. The character of the radicals thus formed and the post-polymerization data obtained by the calorimetric, optical spectrometric, and some other methods [311, 313] had brought the investigators to conclude that the reaction taking place at 77 K was one of polymer-chain initiation and monomer addition

$$R_M + M \rightsquigarrow R_g$$

where M is the monomer, R_M is the radical appearing at the initiation of a polymer chain, and R_g is the growing radical.

It is important to note that macroradicals are formed only during exposure to radiation and under photolysis. No changes occur in spectra when irradiated samples are maintained at 77 K. Thus, in the investigated monomers, the initiation of a polymer chain and monomer addition to a free radical, R_g, can effectively proceed at 77 K only under conditions of irradiation.

Solid-phase polymerization strains the crystal lattice of the monomer. The accompanying shifts and re-orientation of molecules begin to change the crystalline structure into an amorphous one. For example, ESR spectra obtained for the postpolymerization in single crystals of acrylic acid lose their anisotropy already at shallow depths of change [310]. On the other hand, the polymerization chain in single crystals of *p*-diethinylbenzene grows along one of the crystallographic axes, without markedly affecting the structure of the monomer matrix [311].

Co-60-induced polymerization of acrylonitrile in dimethylformamide at low temperatures has been investigated by the calorimetric [314] and the gravimetric [315] method. Mixtures containing 25 to

60% of a monomer were found to turn into transparent glasses upon cooling. The samples were irradiated at 77 K, placed in a calorimeter and warmed up. With an absorbed dose of less than 1 Mrad, postpolymerization was observed at the temperature of phase change, T_g, in glass. At doses of 1 to 12 Mrad, postpolymerization proceeded at a temperature several kelvins lower. In the samples given a dose of over 3 Mrad, the polymer was formed in a narrow temperature interval of 0.5 to 1 kelvin. In the authors' opinion, the postpolymerization of acrylonitrile in the above conditions proceeds by the ion mechanism. A point in favour of the ion mechanism, as they believe, is the fact that the addition of 10% acetone, which ordinarily is an inhibitor of ion reactions, would stop postpolymerization.

Radical reactions have activation energies differing only very slightly. Low temperature offers a means for selectively promoting one of several parallel processes even if their activation energies are small and differ little. For example, combining low temperature and protonic acids which are strong complex-forming agents, it is possible to obtain a 100-% yield for gamma-induced polymerization of allylamine ($T_{irr} = 77$ K, a dose of 0.5-30 Mrad). Under such conditions, postpolymerization proceeds practically without any loss of active centres and transmission of the chain [316].

The kinetics of polymerization at various temperatures is analyzed in [311, 312], and the potentialities of the luminescent experimental method are demonstrated in [317]. Owing to its high sensitivity, it is possible to study the initial stages of polymerization where the ratio of polymer-to-monomer concentrations is still very low and one can neglect the processes leading to what is known as the limiting of the polymer chain. The authors of [313] discovered that ionizing radiation can bring about the radical initiation of a polymer chain and addition of monomer molecules at 77 K in a number of crystalline monomers. From our point of view, a piece of especially important experimental evidence is the fact that the polymer chain grows only during exposure to radiation. As we believe, this observation stresses the special role of radiation in processes taking place in solid phases, notably the marked changes in the physico-chemical properties of the medium.

In contrast to liquid-phase polymerization, that induced by radiation in the solid phase is accompanied by changes in the structure of the original sample due to the action of radiation. In crystalline monomers, irradiation leads to the formation of defects in the crystal structure, and these defects play a prominent role in the polymerization. The kinetics of polymerization must depend on the structure and phase state of the sample.

Evidence for the existence of structural inhomogeneity in the investigated systems is presented by the authors of [318] who used the ESR technique to study the radicals produced by the low-temperature Co-60 radiolysis of fluorinated rubber with a grafted oligoesteracrylate. The ESR spectrum of radicals in such a rubber-oligomer system is the superposition of a broad (100 G) and a narrow (10 G) signal. As we believe, these data suggest the existence, in the system, of two phases substantially differing in molecular mobility. This is corroborated by data cited in [319] where the authors discovered the existence of a two-phase system by the paramagnetic-probe method for dicumyl-peroxide-induced polymerization of oligoesteracrylate in nitrile rubbers.

Sometimes, the rate of solid-phase polymerization proves higher than in the liquid phase. To explain the difference, several hypotheses based on the assumption of cooperative interactions have been advanced. Such interactions are likely to take place, if the monomer molecules in the crystal take up a favourable orientation such that a group of pre-oriented molecules rather than one or two molecules can take part in the polymerization. To explain the rapid nonactivated solid-phase polymerization, Semenov [298] hypothesized the existence of energetic chains which develop in a matter of 10^{-13} s. Japanese experimentors [320] proposed an "electron" mechanism for polymerization according to which a strong electron interaction takes place between the monomer molecules in the crystalline state. Direct experimental evidence for the rapid progress of polymerization at low temperatures is presented in [321] where it is found that in the explosive postpolymerization of crystalline acetaldehyde the average time for the addition of a monomer molecule to the growing chain is 10^{-8} to 10^{-9} s. This figure is by several orders of magnitude higher than that for radical polymerization (say, vinyl monomers) in the liquid phase.

Hypotheses about nonactivated solid-phase polymerization are based on the assumption that the crystal as a whole is electron-excited as a result of collective interactions. The explanation seems plausible, but no direct experimental evidence has been obtained yet. Nor has theoretical interpretation of rapid polymerization in the solid phase been carried to completion.

For better insight into low-temperature polymerization, it is essential to know the length of the chain and the mechanism by which the chain grows in the solid phase. It is also important to elucidate whether or not an additional amount of energy is absorbed at the instant when a new link of the chain is formed. Unfortunately, most publications on radiation-induced solid-phase polymerization only note the addition of ions or radicals by a multiple bond.

A detailed and all-round study of solid-phase polymerization is presented in [173] and [322-324] where the investigators are concerned with the radiation-induced polymerization of formaldehyde.

Recently, new evidence has been obtained about solid-phase polymerization with the aid of improved high-sensitivity microcalorimetric techniques. It has been shown, among other things, that the irradiation at 77-80 K brings about the polymerization of solid formaldehyde with a radiation yield of $G \gg 10^5$ molecules per 100 eV [325]. Solid-phase chain polymerization has also been observed at 5 K, with a radiation yield of $G \gg 10^3$ molecules per 100 eV.

The radiation polymerization of formaldehyde at 77 K when the segmental mobility of the forming polymer chains is frozen (the unfreezing of segmental mobility becomes noticeable at above 193 K) leads to a new structural modification of polyoxymethylene which is characterized by monolithic crystalline domains, with the chains hexagonally packed in the polymer lattice. Comparison of its IR-spectra with those of known modifications having the hexagonal and orthorhombic structure shows that the conformation of the $-(CH_2O)_n-$ chains in the polymer produced by solid-phase polymerization at low temperature is unusual and appears to consist of a sequence of *gauche-* and *trans-*conformations of monomer links. The new structural modification of polyoxymethylene is metastable and will change to a hexagonal modification upon re-crystallization or under the action of pressure.

It is hypothesized in [324] that the hexagonal packing of the growing macromolecules is more likely when polymerization proceeds by a mechanism involving the cooperative transition from a monomer crystal to a polymer crystal. This form of transition promotes a concordant growth of each chain with the development of the maximum likely number of adjacent chains, which is six. It may also be hypothesized that the hexagonal packing of polyoxymethylene chains fits the most favourable directions of their growth in the formaldehyde crystal. For the hypothesis to be confirmed we need evidence, which is still lacking, on the crystal lattice of formaldehyde.

In contrast to the process in the solid state, the radiation-induced polymerization of formaldehyde in the liquid state leads to a stable modification of polyoxymethylene. As it appears, the new metastable modification of polyoxymethylene is formed by radiation-induced polymerization of formaldehyde at 77 K as a result of the superposition of two processes, namely the growth of polymer chains in a specific conformation in the crystalline formaldehyde, and the formation of the polymer lattice.

In recent experiments with the low-temperature polymerization of formaldehyde, Goldansky and his associates have observed an unusual and intriguing fact — the existence of a low-temperature quantum limit for the reaction rate [326, 327]. Experimental data and their interpretation can be found in [172, 173, 328, 329]. The above authors studied the kinetics of low-temperature radiation polymerization over a broad range of temperatures (from 180 K to close on 4.2 K, the boiling point of helium) by a calorimetric technique, using the apparatus of their own design [328, 329]. They have established the relationship between the time, τ, of polymer chain growth and temperature, and also between the time required for the addition of a single unit to the polymer chain, τ_0, and temperature, on the assumption that there is no chain transfer and that the radiation yield of chain initiation is equal to unity. In the temperature interval from 80 to 150 K, the time τ_0 (which is the reciprocal of the reaction rate) increases with decreasing temperature, and its temperature dependence is described by Arrhenius' equation in which the activation energy is taken equal to $E_{act} \approx 8$ to 10 kJ mole^{-1}. Below 80 K, however, the temperature dependences of τ and τ_0 do not obey the Arrhenius law, and instead of tending to infinity, τ_0 tends to a constant, relatively small value equal to about 10^{-2} s (at 80 K, $\tau_0 \approx 10^{-5}$ s). (Extrapolation of the Arrhenius equation to 10 K gives $\tau_0 \approx 10^{30}$ years and at 4.2 K, $\tau_0 \approx 10^{100}$ years.) A likely explanation of the low-temperature limit might lie in the hypothesis advanced by Semenov to explain the kinetics of polymerization processes in the solid phase [298]. According to his hypothesis, nonactivated polymerization processes in the solid phase can proceed by the energy-chain mechanism, in the form of motion of an exciton (a quantum of excitation) along the growing chain [298]. In such a case, the chain should propagate at a rate close to the velocity of sound in the solid ($\sim 10^5$ cm s^{-1}) [173]. However, analysis of heat generation and heat transfer rejects such an explanation, because the addition of a next unit to the polymer chain as a result of selective heat concentration 10^{-5} to 10^{-2} s after the previous addition is highly unlikely. In the authors' opinion, the low-temperature limit for the reaction rate observed for the radiation-induced solid-phase polymerization of formaldehyde can only be of quantum chemical origin and will not be observed for endothermal reactions.

A quantum-chemical treatment of the low-temperature limit for the reaction rate is presented in [326]. As a point of departure, it is supposed that the elementary event by which the polymer chain is extended and a chemical bond is formed may be the tunnelling of an electron or a hydrogen atom. The addition of a formaldehyde molecule to the growing chain must be accompanied by the displacement of the monomer molecule from the initial position through a distance $\Delta d = d_0 - d_f$ (where d_f is the spacing between adjacent carbon atoms in the polymer chain, and d_0 is the same spacing in the monomer crystal whose exposure to radiation brings about the reaction). Proceeding from the known values of the bond lengths in polyoxymethylene, valence angles and densities of formaldehyde and the polymer, the value of Δd has been found by extrapolation to be 0.3 to 1.0 Å.

Comparison of the reaction rates for the low-temperature polymerization of formaldehyde and its deuterated analogue, CD_2O, at 5-10 K shows that, within the limits of experimental error, the polymerization of the ordinary and deuterated formaldehyde proceeds at the same rate (for CD_2O at 5-10 K, the radiation yield of polymerization is about 1×10^3 molecules of monomer per 100 eV) [323]. The absence of the kinetic isotope effect is an indication that the low-temperature radiation-induced polymerization of formaldehyde does not proceed by the proton tunnelling mechanism. On this basis, it is presumed that the tunnelling of a proton through the distance d_0 occurs faster than the tunnelling of a formaldehyde molecule through the distance Δd. The tunnelling of an electron must be a still faster event. It has been concluded from the above reasoning that at low temperatures the rate-controlling stage of polymerization is the tunnelling of formaldehyde molecules.

Theoretical consideration of tunnel transitions in simple model systems has shown that as the temperature of the system approaches absolute zero, the reaction rate approaches a constant value which is a function of, firstly, the mass of the species being tunnelled and, secondly, the form of the potential barrier [330, 331]. The probability of a nonradiative transition of the system from the initial state (0) to the final state (f) has been analyzed with special reference to formaldehyde. The expression for the probability $W_{0,f}$ has been derived within the framework of the quantum theory of relaxation processes [332, 333]. The interaction between electron states 0 and f, decided by the nonadiabacity operator $\hat{L}$ brings about a nonradiative transition, $0 \rightarrow f$, to the nearest vibrational energy level of the final state. The probability of transition, $W_{0,f}$, from the initial state, where the system is at a zero vibration level ($v_0 = 0$) and the monomer formaldehyde molecule is at a vibration frequency lower than that of a CH_2—O monomer unit in the polymer chain, to the final state is given [173] by

$$W_{0,f} = (2\pi/h) L_e^2 F_{0,v_f} \rho_f \tag{4.1}$$

where $L_e = \int \Psi_0 \hat{L} \Psi_f d\tau_e$;

Ψ_0 — adiabatic electron wave function for the initial state (without allowance for interaction with the surroundings);

Ψ_f = same for the final state;

F_{0,v_f} = Franck-Condon factor (the squared integral of superposition of the vibrational wave functions in the initial and final states);

ρ_f = vibrational level density in the final state.

The transition probability cannot be computed in a straightforward manner because we do not know the exact values of some variables. On making simplifying assumptions, however, the value of Δd can be determined semi-quantitatively from the expression for the transition probability on the condition that it is about 10^2 s^{-1}. The final result is $\Delta d \approx 0.4$ or 0.5 Å which, in the authors' opinion, does not run counter to experimental evidence and the assumed tunnelling of a —CH_2—O— group as a whole. When more units add to the growing chain in a crystalline formaldehyde matrix, voids are formed, which are likewise filled by the tunnel transition of adjacent formaldehyde molecules. Available evidence is however too scanty in order that a definite answer might be given as to what controls the rate of polymerization — the addition of a new unit or the diffusion of monomer molecules to the growing chain. Since, in the opinion of Goldansky and his co-workers, at low temperature the two processes are quantum-chemical in nature and are due to tunnel transitions from the ground state, it follows then that at $T \to 0$ the quantum-chemical limit for the process rate must be observed in any case.

At higher temperatures, the higher vibrational levels of the system are excited, and Eq. (4.1) is well approximated by an expression leading to the Arrhenius dependence of the process rate on temperature [326]:

$$W_{0,f} = A + B \exp(-E/kT) \tag{4.2}$$

Studies concerned with the low-temperature limit for the reaction rates are of fundamental importance. At temperatures close to absolute zero the entropy factors lose their importance, and exothermal reactions may well take place in highly ordered systems. In this context, it would be interesting to elucidate the role of slow irreversible exothermal chemical reactions in processes of chemical and biological evolution at low and extremely low temperatures [173].

4.2. POLYMERIZATION IN MOLECULAR-BEAM COCONDENSATES

In addition to penetrating radiations, low-temperature polymerization can be induced by introducing appropriate initiators. In the USSR, good results in experiments with low-temperature polymerization have been obtained by cocondensing a monomer and an initiating agent from molecular beams onto a cooled surface. This method has successfully been used by Kargin, Kabanov, Zubov, and their associates.

A few remarks are in order concerning the advantages that the cocondensation method has over radiation-induced reactions. With cocondensation, the experimentor is free to match a specific initiator to the monomer of interest. By varying the temperature of the cooled surface onto which the monomer, additives, and initiator are cocondensed, he is able to produce a glassy or a crystalline sample. Polymerization by cocondensation produces no byproducts which are inevitably present in radiolyzed samples and might affect polymerization.

Work on cocondensation polymerization is overviewed by Kargin and Kabanov [302]. They have mainly been concerned with monomers of the vinyl series. Some of their results are presented in Table 4.1.

TABLE 4.1

Polymerization in Systems Produced by Cocondensation of Molecular Beams

Monomer	Initiator						
	Mg	K, Na	H	NaCl, KCl	$BeCl_2$, $ZnCl_2$	MoO_3	LiCl
α-Methylstyrene	VI	VI		VI	I	I	I
Isoprene	VI	VI		VI	I	I	I
Styrene		V	V		I	I	I
Acrylonitrile	II	II		II			
Methacrylonitrile	II	II					
Methylmethacrylate	II		V	II			
Acrylamide	II						
Methacrylamide	II						
Formaldehyde	II	II					
Acetaldehyde	IV	IV					
Acetone	II						
Diketene	IV						
Ketene	V	V					
Propylene oxide	VI						
Butylester of vinylsulphonic acid	II						
Butylmethacrylate	III						

Note. I — polymerizes rapidly upon melting;
II — polymerizes rapidly upon crystallization of a glassy layer below T_m;
III — polymerizes slowly upon the softening of the glassy layer;
IV — polymerizes differently in crystalline state below T_m and upon melting;
V — starting point of fast polymerization has not been established;
VI — does not polymerize.

As follows from Table 4.1, most varied compounds are capable of polymerization at low temperatures. The initiators may be metal vapours, inorganic oxides, and salts. The best initiator is magnesium. In its presence, acrylonitrile, methylmethacrylate, acrylamide, methacrylamide, and some other monomers polymerize at high rates.

The low-temperature polymerization of acrylonitrile with magnesium has been the first to be investigated [207]. ESR spectra revealed the presence of radicals, so it was hypothesized that the polymerization proceeded by the radical mechanism. Later it was found that the reaction also involves ion radicals [334]. The use of metal salts as initiators would bring about the polymerization of cation-sensitive monomers (α-methylstyrene, styrene, and isoprene). The most active compounds are those capable of forming π-complexes with double bonds. In such cases, polymerization proceeds by the cation mechanism.

As analysis of the experimental conditions shows, the cocondensed mixture of a monomer and the sublimed solid initiator is a non-equilibrium solution. Depending on the conditions, the initiating species may be the individual initiator molecules dispersed in the monomer, the products of the reaction between the initiator and the monomer, complexes, and also the defects produced as the frozen molecular mixtures separate into layers.

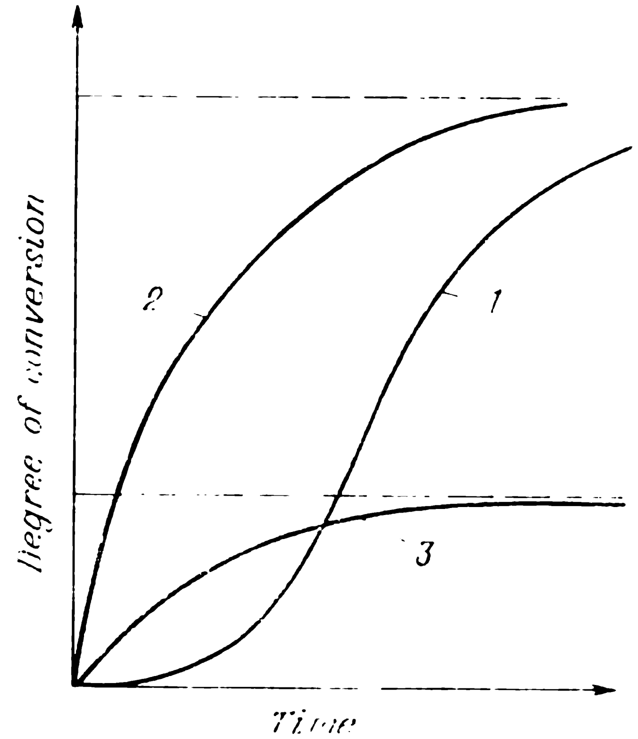

Fig. 4.1. Basic forms of relation between degree of conversion and time for low-temperature solid-phase polymerization

Like many organic and inorganic solid-phase reactions [335], low-temperature polymerization is characterized by two basic types of kinetic curves (curves *1* and *2* in Fig. 4.1). As with other solid-phase reactions, low-temperature polymerization can be interpreted using the concepts of formation and growth of nuclei on the surface and inside the monomer crystals. An autocatalytic curve (curve *1*, Fig. 4.1) will be observed when the initial rate of the reaction is controlled by the rate at which the nucleating centres of a new phase are formed. The other type of curve (curve *2* in Fig. 4.1) will be observed when the free activation energy for the formation of nuclei corresponds to their free energy for growth. Then a large number of nucleating centres will be formed, and the kinetic curve will show no induction period. In some cases where the formation and growth of starting centres are impeded, the reaction may cease at a low degree of conversion, and curves like curve *3* in Fig. 4.1 will be observed. The general pattern of low-temperature polymerization has been analyzed by Kabanov [336].

In structured systems, polymerization proceeds by the chain mechanism. As with any chain process, there must be an initiation step, a propagation step which adds more and more monomer units to the growing chain and builds up the macromolecules, and a termination or cessation step which converts the transient reactive intermediates into stable species. It has been found that the easiest conditions for a chain to be started exist at the interfaces and crystal defects. It should be remembered, however, that, like the wall, a structural defect may play a dual role in chain reaction. An increase in the number of defects by, say, introducing non-cocrystallizing additives may raise the rate of polymerization or it may, as has been established in many cases, slow down the polymerization in poorly shaped monomer crystals. In the latter case, the chain will in all probability be terminated on a defect. In perfect single crystals, too, the polymerization is generally hindered, which is an indication of an important role played by defects.

In solid-phase polymerization, the decisive factor is the compatibility in lattice geometry between the monomer and the polymer. According to this attribute, all monomers may be divided into two broad classes [336]. One class, the more numerous of the two, encompasses those monomers which show no compatibility in terms of lattice structure with the polymer. In such systems, for polymerization to proceed the monomer molecules must be appreciably displaced from their equilibrium sites in the lattice. The second group covers the monomers in which the lattice is geometrically compatible with that of the polymer.

The kinetics of solid-phase polymerization can best be assessed, using induced polymerization as an example [336]. In the general case, the rate of formation for active centres which then change into macromolecules can be written

$$dn/dt = k_1' I y (1 - \eta) \qquad (4.3)$$

where n is the number of active centres, k_1' is the initiation rate constant, I is the intensity of initiation, y is the current concentration of active sites in the sample, and η is the degree of conversion.

An active site is defined as any site in the sample where the initiation and propagation of polymer chains are facilitated. These may be surface irregularities, cracks, interfaces, and the like. In a first approximation, all active sites are rated as equivalent. Equation (4.3) is similar to those describing, for example, absorption of light, when it is assumed that any quantum is expended to produce active centres.

The formation of active centres is accompanied by the cancellation of active sites. As a polymer builds up, there may appear active sites on which new macromolecules can grow. The rate at which active sites disappear can be visualized to be in proportion to $k_2 I y(1 - \eta)$, and the rate at which they are formed, in proportion to $k_3Iy(1 - \eta)$. Then the net rate of change of active site concentration will be given by

$$-dy/dt = (k_2 - k_3)Iy(1 - \eta) \tag{4.4}$$

The time rate of change of the degree of conversion is

$$d\eta/dt = k_1Iy(1 - \eta)\bar{\nu} \tag{4.5}$$

where ν is the mean chain length assumed to be independent of η; $k_1 = k_1'/x_0$, where x_0 is the initial concentration of monomer molecules.

By eliminating time between Eqs. (4.4) and (4.5), we get

$$-dy/d\eta = (k_2 - k_3)/k_1\bar{\nu} \tag{4.6}$$

Integrating Eq. (4.6) gives

$$y = y_0 - [\eta(k_2 - k_3)/k_1\bar{\nu}]\eta \tag{4.7}$$

where y_0 is the original concentration of active sites.

It is obvious from Eq. (4.7) that at $k_2 > k_3$ the number of active sites decreases with increasing η. If, on the other hand, $k_2 < k_3$, the number of active sites will increase.

On substituting for y from Eq. (4.7) into Eq. (4.3), we get

$$d\eta/dt = k_1I\left[y_0 - \frac{k_2 - k_3}{k_1\bar{\nu}}\eta\right]\nu(1 - \eta) \tag{4.8}$$

On designating $k_1y_0\bar{\nu} = \alpha$ and $k_2 - k_3 = \beta$, and integrating Eq. (4.8), we get

$$\eta = \frac{\exp[\alpha(1 - \beta/\alpha)It] - 1}{\exp[\alpha(1 - \beta/\alpha)It] - \beta/\alpha} \tag{4.9}$$

It follows from Eq. (4.9) that two substantially different types of kinetic curves can exist.

If the rate at which active sites are lost exceeds the rate at which they are generated, $\beta > 0$, then for $\beta/\alpha > 1$ the limiting degree of conversion (the limiting yield) will be

$$\eta_\infty = \alpha/\beta = \frac{k_1y_0\bar{\nu}}{k_2 - k_3} < 1 \tag{4.10}$$

In accord with Eq. (4.10), the reaction will be terminated before all of the present monomer has been converted to a polymer. Thus, the result will be curve *3* in Fig. 4.1.

It is obvious from Eq. (4.8) that the initial rate of reaction is

$$(d\eta/dt)_0 = k_1y_0\bar{\nu}I \tag{4.11}$$

If in Eq. (4.11) the mean chain length ν and the value of y_0 are independent of temperature, then in, say, radiation-induced polymerization the chain propagation will be nonactivated. The limiting yield will be decided by the temperature dependence of k_3. If an increase in temperature leads to an increased number of active sites, then, as is seen from Eq. (4.10), the limiting yield will rise. At $\beta/\alpha > 1$, the number of active sites is sufficient for all of the monomer to be converted to a polymer. In such a case, $\gamma_l \rightarrow 1$, and curve *2* of Fig. 4.1 will be observed.

If $\beta < 0$, which means that the rate at which active sites are generated exceeds the rate at which they are lost, the reaction will proceed at a progressively increasing rate, and the observed kinetic curves will look like curve *1* in Fig. 4.1. The increase in the reaction rate may be caused by the generation of new active sites with the formation of the polymer.

Thus, Eq. (4.9) can serve as a basis for a formal kinetic explanation of the typical curves observed in the case of low-temperature polymerization. A large collection of experimental evidence interpreted on the basis of Eq. (4.9) is given in [336]. It is to be noted that Eq. (4.9) has been derived on the basis of several simplifying assumptions, so it cannot cover all the cases likely to be encountered in low-temperature polymerization. It only gives a qualitative picture of the process.

An attempt has also been made to interpret kinetic curves (see curves *1* and *2* in Fig. 4.1) in the light of a model which is based on the hypothesis that irradiation produces 'hot' regions where polymerization can proceed practically instantaneously [337]. The chain forming in such a region is thermodynamically unstable, and a polymerization-depolymerization equilibrium may exist in the system. The existence of such an equilibrium can also explain the incomplete conversion of the monomer in the course of polymerization.

The mechanisms of solid-phase polymerization examined above do not cancel, but rather supplement one another. Cryogenic cooling may stabilize a chain in a 'hot' region, and this stabilized chain may serve as a seed for a polymer chain, that is, an active site in the sample. This may lead to a very complex picture of solid-phase polymerization, notably such that the two types of curves shown in Fig. 4.1 merge into one. In fact, such combined kinetic curves have been observed in the low-temperature polymerization of styrene oxide under the action of fast electrons and also in the polymerization of barium acrylate [320].

4.3. EFFECTS OF PHASE CHANGES AND LATTICE STRUCTURE ON SOLID-PHASE POLYMERIZATION

Referring to Table 4.1, it is seen that the warming of monomers and initiating agents cocondensed onto a cooled surface brings about a fast polymerization. In some cases, the reaction temperature is tens of kelvins below the melting point of the respective monomer. For acrylonitrile ($T_m = 190$ K), the polymerization takes place at 113 K or 143 K, for methylmethacrylate ($T_m = 223$ K) at around 148 K, etc.

Today, it is an established fact that the phase changes taking place in a system consisting of a monomer and an initiator do promote polymerization. Various modifications of differential thermal analysis have been used to investigate the effect. We shall cite some findings from experiments in the polymerization of acrylonitrile with magnesium vapours [340].

The active centres are formed in the course of the reaction in the gaseous phase and are anion radicals. Upon warming and according to the conditions under which the molecular mixture has been obtained, polymerization occurs either at 113 K or around 143 K. The temperature diagrams for a glassy monomer show that two exothermal changes take place at the stated temperatures. The first change associated with the crystallization of the monomer can readily be observed visually. The nature of the second phase change has not yet been elucidated completely. It may be related to the growth of crystals or the change of an unstable crystallographic modification into another. Whatever the nature of the change, however, when it does take place the molecules acquire certain mobility, and it is this mobility that promotes the polymerization.

The rate of polymerization is also affected by the conditions under which the system exchanges heat with the surroundings because the initiation of the reaction depends on the thermal conductivity of the material onto which the mixture is cocondensed. For example, the polymerization of acrylonitrile below its melting point occurs as a thermal explosion and the rate of polymerization is controlled by the rate of phase change [340].

The occurrence of a phase change in the system is a necessary but not sufficient condition for the reaction to proceed in the solid phase. The point is that if a phase change occurs at a relatively low temperature, whereas the activation energy for the chain propagation step is several kilojoules, the trapped reactive species will be unable to bring about the reaction. Thus, the diffusion mobility of monomer molecules alone is not sufficient for the formation of a polymer at low temperatures.

It has also been established that in many cases polymerization is preceded by the formation of a crystalline phase which then takes part in the subsequent reaction [338, 339]. For example, the authors of [340] have observed magnesium-catalyzed copolymerization of acrylonitrile and propionitrile. The phase diagram obtained prior to the experiment is shown in Fig. 4.2. As is seen, an eutectic is formed when acrylonitrile and propionitrile are taken in the proportion 43: 57. This implies that, on de-vitrifying, the mixture of monomers will reject crystals of the pure component present in excess, and an eutectic. According to thermographic evidence, rapid polymerization in the mixture of acrylonitrile and propionitrile commences at 143 K with the crystallization of the original glassy phase. The eutectic is formed at the same temperature. If all the components are cocondensed at 133 K, the subsequent warming will not be accompanied by the generation of heat, nor will there be melting upon warming to the melting point of the eutectic. By that time, a copolymer of acrylonitrile and propionitrile will have formed. The composition of the copolymer is independent of the amount of propionitrile and is solely decided by the composition of the eutectic phase.

This is evidence for the fact that low-temperature polymerization is preceded by the crystallization of the glass, leading to the formation of an eutectic.

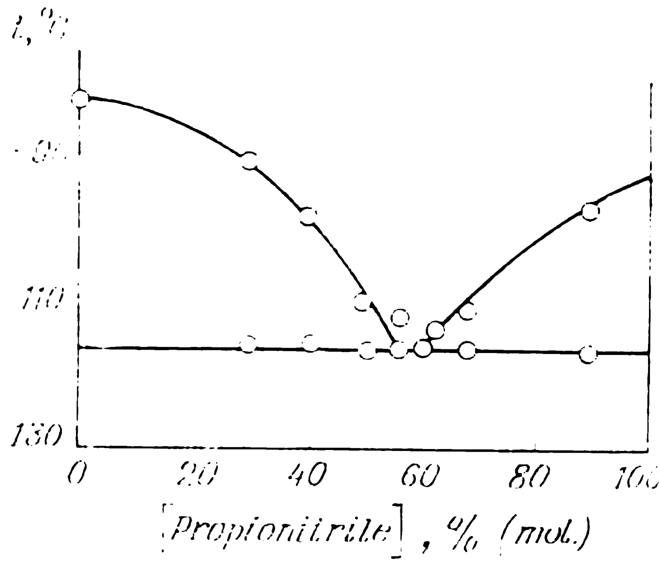

Fig. 4.2. Phase diagram of the system "acrylonitrile-propionitrile"

Thus, no low-temperature polymerization proceeds in a crystal away from a phase change. In solid-phase systems, the most favourable conditions for the formation of macromolecules arise when the structural order characteristic of solids is combined with the molecular mobility associated with liquids. This requirement is met at the instant of a phase change. In order to explain rapid polymerization near a phase change, recourse is had to the concept of "labile blanks", groups of short-lived ordered monomer molecules appearing at the moving boundary of the crystalline phase [336]. The lattice structure may affect the kinetics of polymerization and serve as a stereospecific molecular matrix governing the structure of the forming macromolecules. To get insight into the effect of the lattice, it is convenient to use monomers which can produce macromolecules varying in structure. This, however, is fraught with some difficulty in interpreting the outcome of the experiment. The structure of the resultant polymer may be controlled by the crystal lattice or by the formation of active centres varying in nature.

This difficulty is circumvented in [338], concerned with the polymerization of diketene in the liquid and solid phases with the participation of the same active centres. It has been established that the solid-phase polymerization mainly produces polyester, that is, a structure of the form

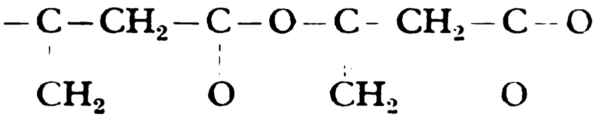

$$-\underset{CH_2}{C}-CH_2-\underset{O}{C}-O-\underset{CH_2}{C}-CH_2-\underset{O}{C}-O^-$$

(In the active centre responsible for the chain propagation, the negative charge is localized on an oxygen atom.) This is because the geometric dimensions of the diketene lattice are close to those of the polyester lattice. The polymerization of diketene in the liquid phase in the presence of magnesium produces practically only poly-β-diketone. For this to happen, there must be an excess of magnesium chelatically bonded to the growing chain. The stereospecific effect of the crystal lattice on polymerization has also been observed in inclusion compounds. For example, the copolymerization of conjugate-bonded dienes in clathrate compounds with carbamide only produces 1,4-*trans* units [341, 342].

Interesting data about the effect of the solid-phase structure on that of the forming polymer have been obtained in experiments with acetaldehyde [339]. The polymerization was brought about by the molecular-beam cocondensation technique, using magnesium and sodium as initiators. In principle, the polymerization of acetaldehyde can produce two polymer structures, namely the polyvinyl alcohol type

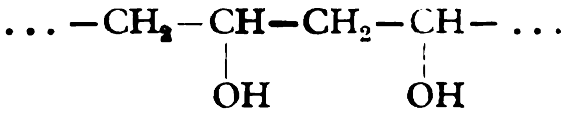

$$\ldots-CH_2-\underset{OH}{CH}-CH_2-\underset{OH}{CH}-\ldots$$

and the polyester type

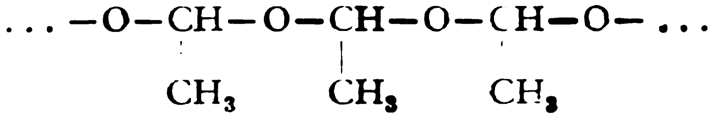

$$\ldots-O-\underset{CH_3}{CH}-O-\underset{CH_3}{CH}-O-\underset{CH_3}{CH}-O-\ldots$$

The presence of pseudo-asymmetrical carbon atoms makes D,L-isomerism very likely. The reaction of magnesium with acetaldehyde produces alkoxides which then induce polymerization. According to spectroscopic data, the reaction in the liquid phase produces vinyl alcohol oligomers at a temperature several kelvins above the melting point of the monomer, whereas in the solid phase at a temperature several kelvins below the melting point the monomer undergoes anionic polymerization leading to a polyester structure with a yield of about 30%. The yield varies with the conditions and temperature of condensation. Thus, in the course of polymerization the crystal lattice promotes the formation of one of the likely structural isomers.

Copolymerization proceeding in the course of devitrification of gamma-irradiated monomers or their solutions may result in copolymers of a composition differing from that produced by copolymerization in the liquid phase. An example is the copolymerization in the system acrylic acid-acetone. In contrast to the liquid phase, the reaction proceeding under conditions of devitrification produces a thermostable copolymer of acetone and acrylic acid [343]. It is possible to obtain copolymers in which for each molecule of acrylic acid there may be two molecules of acetone. The degree of inclusion of acetone depends on the relative concentrations of acetone and acrylic acid. It has been found that the use of deuterated acetone and the addition of water reduces the degree of inclusion for acetone. Presumably, the copolymerization in this case proceeds similarly to the polymerization of acetaldehyde into polyvinyl alcohol [339]:

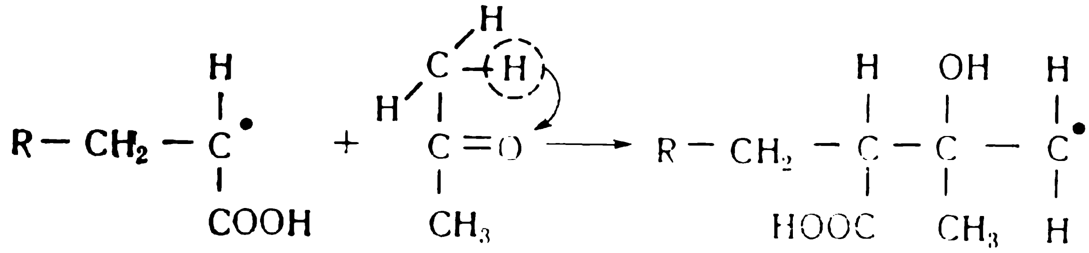

$$R-CH_2-\overset{H}{\underset{COOH}{\dot{C}}} + \underset{CH_3}{\overset{\overset{H}{H-C-H}}{C}}=O \longrightarrow R-CH_2-\overset{H}{\underset{HOOC}{C}}-\overset{OH}{\underset{CH_3}{C}}-\overset{H}{\underset{H}{\dot{C}}}$$

and the rate-controlling stage is the proton transfer which at low temperatures can proceed by the tunnel mechanism [343].

In the authors' opinion, the polymerization begins in the supercooled liquid immediately after the matrix has been devitrified. The reduced mobility of the growing active centres in the supercooled liquid, coupled with a sufficiently high mobility of the monomer molecules, is responsible for the fact that the composition of the copolymer is not decided solely by the relative reactivity of the monomers.

Apart from the lattice structure, solid-phase polymerization is affected by the rate of warming up [344, 345]. It has been found that in the case of acrylonitrile the yield of the polymer falls off with increasing rate of warming up.

In a similar way, the yield of the polymer depends on the rate of warming up in the radiation-induced solid-phase polymerization of amorphous vinylacetate samples. The manner in which the rate of warming, k_w, affects the yield and molecular mass M of a polymer [346] is illustrated in the table that follows [1]:

k_w, °C min^{-1}	180	60	19	6	2
Yield, %	0.7	1.2	2.3	3.0	5.6
M[2]	1.8×10^3	–	–	–	1.1×10^4

As is seen, an increase in the rate of warming up brings about a sudden decrease in the polymer yield. Interestingly, for vinylacetate this is also accompanied by a decrease in the molecular mass of the polymer. The samples were gamma-radiated from a Co-60 source at 77 K. Amorphous samples were produced by quickly freezing liquid monomers to 77 K. The experiments were carried out, using the calorimetric and luminescent techniques [347]. The polymer yield was determined on the basis of heat generation and also by the gravimetric and viscosimetric methods. It is important to note that, according to calorimetric evidence, the polymerization of the monomers did not take place at the time of irradiation at 77 K [345]. A polymer was formed upon warming up the irradiated samples in the softening range of the glass. The warming up of the irradiated monomers was accompanied by radiothermoluminescence with peaks at 131 K and 106 K for vinyl acetate. The intensity of luminescence dropped upon illumination of the samples, and prolonged exposure of the samples to light more than halved the heat generation around 131 K and the polymer yield.

---

[1] The samples were neither vacuum-treated nor bleached.

[2] Accurate to within ± 30%

The radiothermoluminescence accompanying polymerization is presumed to be caused by the recombination of the charged species formed and trapped in the course of low-temperature radiolysis [348-350]. Exposure of irradiated samples to light at low temperatures results in freeing all or some of the immobilized species from their traps and in their recombination, so the intensity of radiothermoluminescence is reduced [348, 350, 351].

Polymerization during warm-up is brought about, above all, by the presence of trapped charged species in the monomer. This is borne out by the effect of exposure to light on the intensity of luminescence and polymer yield.

As the liquid phase changes to the solid phase, the radical mechanism of polymerization is often replaced by the ion mechanism. For monomers like acrylonitrile and methylmethacrylate [352, 353] which polymerize in the liquid phase by the radical mechanism, polymerization in the solid phase proceeds by the ion mechanism.

In [354] the investigators have checked the applicability of the free-volume concept [355] to vitrification in mixtures of incompatible polymers for which there are two glass points. The existence of two glass points is associated with microscopic separation into two phases. Evidence gleaned for amorphous polymers, such as polybutylmethacrylate, polymethylmethacrylate, polystyrene, and polycarbonate, shows that the microscopic phase separation of the system is speeded up near the glass point. At that point, molecular mobility builds up so as to bring about the microscopic separation and compaction of the system. In the authors' opinion, the free volume may well be distributed in a localized manner in microheterogeneous systems. The appearance of a free volume promotes relaxation processes and brings down the activation energy for vitrification.

A number of photochemical cyclic addition and cyclic polymerization reactions have been detected, proceeding in a nonactivated mode in the solid phase at low temperatures [356, 357]. The photodimerization of cinnamic acid in the crystal proceeds quantitatively in the temperature range 4.2-300 K, with the reaction rate being independent of temperature. Characteristically, the reaction rate has been noted to fall with rising temperature to 330 K. It is hypothesized that the reaction mainly proceeds on the defects produced as the nuclei of the new phase (dimer) are formed.

It is to be noted that in contrast to cinnamic acid, ethyl cinnamate dimerizes under the action of light in the glassy state and does not photodimerizes in the crystalline state. The dimer is formed throughout the bulk of the glass, and in the range 4.2-170 K the reaction rate is independent of temperature, whereas at 170 K it rises with increasing temperature, which fact is attributed to the softening of the glass.

Photopolymerization of diethyl *p*-phenylenediacrylate can only proceed [358] in the crystalline state according to the equation

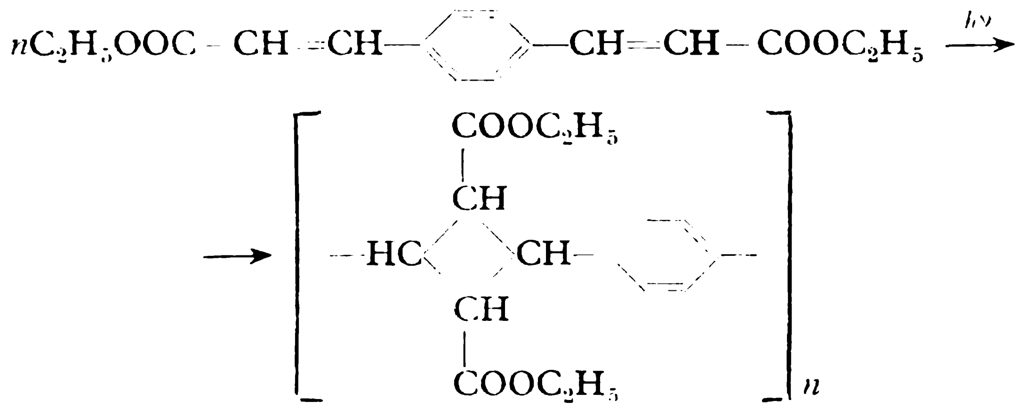

In the range 4.2-90 K, the polymerization proceeds practically in a nonactivated manner, whereas at temperatures above 90 K, the activation energy is $E_{act} \approx 6.7$ kJ mole^{-1}. The reaction proceeds predominantly at the boundary between the polymer phase and the monomer crystal.

According to [357], the addition occurs as some of the radiation energy is converted to that of the motion of molecules of the reacting system. It is also hypothesized that the above reactions go via the formation of an intermediate complex with the formation energy E_f. According to the Franck-Condon principle, the initial excited state of the reacting system of energy E_0 is a nonequilibrium one. If the difference in energy, $E_0 - E_f$, is greater than or equal to the potential barrier on the reaction path, the excited system may pass across the barrier without activation. The probability of such transition near absolute zero depends on the initial arrangement of molecules in the solid. With rising temperature, an increasingly larger part is played by thermal fluctuations, because the life time of fluctuations (about 10^{-12} to 10^{-13} s) is appreciably longer than the time of electron transitions (about 10^{-15} s). According to the opinion advanced in [356, 357], this mechanism fits well experimental evidence.

The fact that the phase state of crystallizable polymers is complex and dependent on a multiplicity of factors is borne out by data describing the dependence of the relative amounts of the crystalline and amorphous phases on the conditions of low-temperature crystallization and the qualitatively different DTA curves for polymer samples produced directly from a melt and after prequenching in liquid nitrogen [359]. Unquenched polyethyleneadipinate crystallizes on a limited number of nuclei in the form of relatively large spherolite structures with alternating layers having a higher and a lower true temperature of crystallization or, which is the same, a higher and a lower melting point. The crystallization of prequenched samples proceeds at low temperatures spontaneously on a very large number of nuclei and produces fine-grained forms [359].

The kinetics of the reactions proceeding in solid polymer matrices is often closely related to the matrix structure. For example, the radiation-induced polymerization of *n*-alkyl-*n*-vinylsulphamides in the solid phase goes on with a higher yield than in the liquid phase. More impressively, irradiation at 198 K induces polymerization in the crystalline state and does not in the vitreous state [360]. For example, the reaction rate in polymers appreciably rises with increasing percentage of low-molecular-weight substances, apparently because the molecular mobility in the sample is then higher. This possibility is pointed out in [361] concerned with the decomposition of benzoyl peroxide in a matrix of amorphous atactic polypropylene.

Kinetic experiments with the decomposition of benzoyl peroxide in a matrix of solid isotactic polypropylene have shown that the reaction rate can be raised by introducing the decomposition product (phenylbenzoate) into the polymer [362]. Interestingly, the decomposition products of benzoyl peroxide have no catalytic effect in liquid low-molecular-weight solvents. This has been explained by the fact that there is a competition between the molecules of two low-molecular-weight substances (A and B) for 'packing defects' in the polymer structure, with the result that one of the substances (in the case on hand, this is phenylbenzoate, B) ousts the other (benzoyl peroxide, A) into the interdefect zone. This will change the rate of the entire process, if the reaction involving substance A proceeds faster in the interdefect than in the defect zone, which is the case with the decomposition of benzoyl peroxide.

Proceeding from the above assumption, the authors of [361] have proposed a qualitative model for the above process called displacement catalysis. In [363], this model is used to describe the kinetics of the reaction between benzoyl peroxide and diphenylamine in a matrix of atactic polypropylene.

As a way of investigating the molecular mobility of rigid and strongly cross-linked polymers, it has been proposed in [364] to use as the probe the NO_2 radical whose molecular dimensions are substantially smaller than those of stable organic nitroxyl radicals. Owing to the high rotational frequency of this probe, it is possible to measure the correlation time for rotational diffusion over a wider range than it is possible with organic radicals. The authors of [364] give a theoretical consideration of ESR spectra of NO_2 for different correlation times τ_c, using the technique proposed in [365]. For the estimation of correlation times, they suggest to use a parameter α defined as

$$\alpha = (I_- / I / I_+) / (I_0 / I_0) \tag{4.12}$$

where $I_\mp$ is the line intensity in the high and the low field, respectively, for the correlation time τ_c, and $I_{0\mp}$ is the same, but for the correlation time $\tau_c = 1 \times 10^{-7}$ s.

The required correlation time τ can be found from the theoretical dependence of α on τ_c given in [364] in graphical form. Using the theoretical dependence of α on correlation time τ_c for the rigid unsaturated polyester resins produced by the polycondensation of ethylene glycol, maleic and chlorendic anhydrides (with a glass temperature of about 353 K) in the temperature range 153-193 K, the following equation has been derived for the temperature dependence:

$$\tau_c = 1.2 \times 10^{-12} \exp(3200/RT)$$

The activation energy for rotational diffusion of NO_2 determined for the polymers in question (13.4 kJ mole^{-1}) is somewhat lower than the activation energy for translational diffusion of small molecules (CO_2, O_2 and N_2) in some polymers (21 to 42 kJ mole^{-1}) [364].

The use of NO_2 as the label is complicated by the fact that NO_2 molecules readily dimerize to produce a nonparamagnetic N_2O_4 molecule which produces no ESR spectra. In frozen aqueous solutions, the ESR spectra of NO_2 can be recorded only after photolysis [366]. On the other hand, the ESR spectra of NO_2 can be recorded at 77 K in polymers (polystyrene, acetic and cellulose esters), probably because some of the NO_2 molecules have no time to dimerize as they are frozen [364].

The material examined in this chapter shows that polymerization at low temperatures has been the subject of many broad and intensive studies. Polymerization has offered a basis on which some concepts of significant importance for proper insight into the aspects common to low-temperature reactions have been formulated.

CHAPTER FIVE

CHAIN REACTIONS

Chain reactions involving free atoms and radicals are a frequent occurrence in gaseous and liquid phases. A theory of such reactions has been formulated by N.N. Semenov and his associates [367-369]. The occurrence of such processes at low temperatures in ordered media is of important theoretical and practical interest. In view of the evidence cited in Chap. 3 for the low-temperature accumulation of substantial nonequilibrium concentrations of radicals and the generation of stable species under the same conditions, it appears legitimate to presume that chain reactions can as well proceed in the solid phase. It is natural to expect that it would be easier for such reactions to occur under conditions of irradiation as it promotes the formation of active centres.

The low-temperature polymerization of monomers examined in Chap. 4 has been the first chain reaction observed in the solid phase at low temperatures. As already noted, a distinction of this process is that only one kind of species contributes to the propagation of the chain. Also, with the most readily polymerized monomers, such as formaldehyde, there is observed a close compatibility between the starting monomer and the resultant polymer in terms of lattice constants. This kind of compatibility reduces the amount of energy required to re-arrange the lattice and promotes polymerization in the solid phase.

In an overwhelming majority of chain reactions, two substances interact, and the propagation step involves these substances in turn. An example is the photochemical hydrobromination of olefins. Studies of this class of reactions once played an important part in advancing the chemistry of free radicals. More recently, these reactions have been applied commercially to the synthesis of ethyl bromide from ethylene and hydrogen bromide, using high-energy radiations [370].

5.1. PHOTOCHEMICAL HYDROBROMINATION OF OLEFINS

The hydrobromination of olefins in the gas and liquid phases readily proceeds under the action of light and is a typical chain reaction producing chains a thousand monomer units long. For this reason, this reaction has been picked as the object of low-temperature experiments. Already the early experiments [371] detected that this reaction could proceed at the boiling point of liquid nitrogen; later, it was analyzed in more detail.

Consider the low-temperature addition of hydrogen bromide to ethylene. Customarily, this kind of experiment is carried out in a reaction vessel in the form of a cylindrical quartz tube into which windows are sealed. The vessel is connected to a vacuum pump, hydrogen bromide and ethylene are mixed in the gas phase and gradually condensed on the bottom of the reaction vessel immersed in liquid nitrogen. The deposited film is usually 10^{-2} to 10^{-3} cm thin. The mixture is exposed to UV light at 77 K for a definite time interval. Gas-chromatographic analysis shows that the following reaction takes place:

$$C_2H_4 + HBr \longrightarrow C_2H_5Br$$

In the absence of irradiation, repeated freezing and warm-up of the starting mixture of hydrogen bromide and ethylene would not induce any reaction. The degree of conversion, η, can conveniently be monitored by measuring variations in pressure:

$$\eta = (\Delta P/P) \times 100\%$$

where ΔP is the change in pressure during the experiment, and P is the total starting pressure of ethylene and hydrogen bromide. The degree of conversion has been found to depend on the exposure time and may be as high as 90%.

Exposure to light of a layer of hydrogen bromide at 77 K, followed by deposition of a layer of ethylene on the cooled HBr substrate, or exposure to light of a mixture of HBr and C_2H_4 brings about the formation of ethyl bromide. Its yield does not vary when ethylene is deposited on the cooled substrate immediately after exposure to light or in, say, two hours thereafter. No reaction is brought about by exposure of the olefin to light and deposition of HBr on the cooled substrate. The photolysis of HBr has been found to result in the evolution of hydrogen in an amount which is a function of exposure time.

Thus, the hydrobromination of olefins appears to involve the bromine atoms produced by the photolysis of hydrogen bromide. In the gas phase, the photolysis of HBr is assumed to proceed [372] as follows:

$$HBr + h\nu \longrightarrow H + Br \tag{5.1}$$

$$H + HBr \longrightarrow H_2 + Br \tag{5.2}$$

$$Br + Br + M \longrightarrow Br_2 + M \tag{5.3}$$

According to NMR data [373] and IR spectra [374], hydrogen halides appear to form dimers or chains at low temperatures. Probably, the emergence of such structures at low temperatures promotes photolysis. The evolution of hydrogen upon the exposure of solid hydrogen bromide is an indication that the reactions described by Eqs. (5.1) and (5.2) seem readily to take place at low temperatures. The activation energy for the reaction of Eq. (5.2) is 5 kJ mole^{-1} [368]. The absence of ESR spectra of hydrogen atoms in photolyzed samples of hydrogen bromide is a further piece of evidence for ease of occurrence of the reaction given by Eq. (5.2) at 77 K. No halogen atoms are detected by the ESR technique in the solid phase. Hydrogen atoms are small and easily diffuse at low temperatures, whereas bromine atoms are large and possess limited mobility. Because of this, recombination is impeded, and bromine atoms in solid hydrogen bromide may be immobilized and grow in number upon exposure to light.

It is interesting to note that in mixtures of hydrogen bromide and ethylene the yield of hydrogen decreases under the action of light. This can be explained if we assume that the reaction given by Eq. (5.2) is accompanied by another reaction:

$$H + C_2H_4 \longrightarrow \dot{C}_2H_5 \qquad (5.4)$$

The activation energy for the reaction of Eq. (5.4) does not exceed 8 kJ mole^{-1} [368], so it can readily compete with the reaction of Eq. (5.2).

The propagation of the chain is effected by bromine atoms. The point is that a chain reaction involving hydrogen atoms and ethyl radicals is very unlikely, because the reaction

$$\dot{C}_2H_5 + HBr \longrightarrow C_2H_5Br + H \qquad (5.5)$$

is endothermic ($\Delta H = 100$ kJ mole^{-1}) and its activation energy is, therefore, high ($E \gg \Delta H$).

In addition to ethyl bromide, gas chromatography detects also traces of 1,2-dibromoethane in the reaction products [375]. The presence of these two products suggests that the chain propagation and the formation of ethyl bromide which is the principal product of the reaction may proceed as follows:

$$Br + C_2H_4 \longrightarrow C_2H_4Br \qquad (5.6)$$

$$C_2H_4Br + HBr \longrightarrow C_2H_5Br + Br \qquad (5.7)$$

To estimate the probability of the above reactions, it is essential to know the amount of heat involved and activation energies. They can be ascertained from data for similar reactions in the gaseous phase.

The activation energy for the addition of atoms to double bonds in the gaseous phase does not usually exceed 4 kJ mole^{-1} [368]. From the photochemical halogenation of olefins [376] it follows that the addition of halogen atoms to olefins requires no activation. For the reactions involving hydrogen atoms and olefins in the temperature interval from 77 to 90 K, the activation energy is 6.3 kJ mole^{-1} [69]. With allowance for the heat of solution of hydrogen atoms in olefin, the activation energy for the reaction $H + C_3H_6 \rightarrow \dot{C}_3H_7$ is 5.9 kJ mole^{-1} [72]. Thus, it may be presumed that the activation energy for reactions of the form given by Eq. (5.6) at low temperatures does not exceed 8 kJ mole^{-1}, which is a small figure.

The activation energy for elementary reactions like that given by Eq. (5.7) can be deduced from the Polanyi-Semenov relation: $E_{act} = A + \alpha \mid q \mid$, where E_{act} is the activation energy for an endothermic reaction, q is its heat, A and α are constants [368]. According to [377], for reactions of the form

$$Hal + RH \longrightarrow HHal + R$$

(where Hal are halogen atoms, and RH stands for hydrocarbons and their derivatives), $A = 4.3$ and $\alpha = 0.91$. Using the equation

$$E_{act} = 4.3 + 0.91\, q$$

for an endothermic reaction, and the equation

$$E_{act} = 4.3 - 0.1\, q$$

for an exothermic reaction involving bromine atoms, and also energies of bond dissociation, it is possible to estimate the activation energy for reactions of the form given by Eqs. (5.6) and (5.7). For a reaction close to that of Eq. (5.7),

$$Br + C_2H_6 \longrightarrow \dot{C}_2H_5 + HBr \qquad (5.8)$$

the heat of the reaction can be found as the difference between the energies for the dissociation of C—H bond and the formation of H—Br bond. Taking $D_{C-H} = 411$ kJ mole^{-1} [378] and $D_{H-Br} = 367$ kJ mole^{-1} [379], we get $q = 44$ kJ mole^{-1}. Attachment of a halogen atom brings down the energy for the dissociation of C—H bonds. Therefore, the heat of the reaction

$$Br + C_2H_5Br \longrightarrow HBr + \dot{C}_2H_4Br \qquad (5.9)$$

must be less than 44 kJ mole^{-1}. The experimentally found heat of hydrobromination for ethylene is 84 kJ mole^{-1} [380]. Thus, it may be deemed that $q_{(5.7)} \approx q_{(5.8)} \approx 40$ kJ mole^{-1} and, according to the Polanyi-Semenov equation, the activation energy for the reaction

$$\dot{C}_2H_4Br + HBr \longrightarrow C_2H_5Br + Br \qquad (5.10)$$

is 12 kJ mole^{-1}.

This is a low figure, so such reactions, it appears, can proceed at low temperatures. The low-temperature hydrobromination of ethylene induced by bromine atoms produced by photolysis of hydrogen bromide proceeds according to the following scheme which checks with experimental data:

$$\begin{aligned} HBr + h\nu &\longrightarrow H + Br \\ H + HBr &\longrightarrow H_2 + Br \\ Br + C_2H_4 &\longrightarrow \dot{C}_2H_4Br \\ \dot{C}_2H_4Br + HBr &\longrightarrow C_2H_5Br + Br \\ Br + \dot{C}_2H_4Br &\longrightarrow C_2H_4Br_2 \end{aligned}$$

Using ferric oxalate for dosimetry, it is possible to determine the lower limit of quantum yield. The exact value is difficult to find because the frozen mixture of HBr and C_2H_4 is polycrystalline, and the resultant reflection and scatter of light are hard to evaluate. In the measurements, the investigators determined the number of quanta per number N of molecules that absorb practically all of incident light. The results are presented in Table 5.1.

TABLE 5.1

Quantum Yield of Photochemical Hydrobromination of Ethylene in an Equimolar Mixture

$N \times 10^{-19}$		Exposure time, t_{exp}, min	γ, %	Intensity of exposure, quanta/min	Quantum yield
starting mixture	C_2H_5Br				
34	3.4	75	20	8×10^{15}	57
36	3.8	106	21	8×10^{15}	45
75	6.7	53	18	2.5×10^{16}	65

The long wavelength boundary for the absorption of light by a solid mixture of hydrogen bromide and ethylene lies around 300 nm. In view of the relative energy distribution in the spectrum of a mercury-discharge lamp used, the value of quantum yield quoted in Table 5.1 must be at least trebled. Thus, the lower limit for chain length in the hydrobromination of ethylene is 150 units.

Chain length in the addition reaction involving HBr and C_2H_4 has also been estimated from chromatographic data [375]. As already noted, in addition to ethyl bromide chromatography detects traces of 1,2-dibromoethane in the reaction products. The two products have been found to be present in the proportion 900: 1. The presence of dibromoethane confirms the radical mechanism of the reaction; in all probability, it is likewise formed owing to the recombination of radicals which are responsible for chain propagation. Chain length can be defined as the number of molecules of the principal product formed by a chain reaction, per active centre. Then, in accordance with the above proportion, the chain length may be estimated to be 450 units. This figure is likewise the lower limit. The actual chain length is apparently much greater. The high values of radiation yield also suggest the chain mechanism for the hydrobromination of ethylene at low temperatures.

In determining the quantum and radiation yields, the quantity of reaction products has been measured after the mixture has been warmed up to room temperature. It is therefore natural to presume that it is only the formation and stabilization of active centres that take place at low temperatures, whereas the chain propagation occurs when the mixture is melted or during any other phase change.

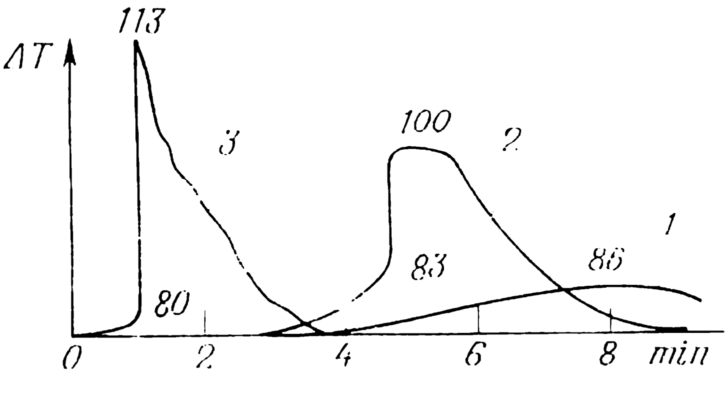

Fig. 5.1. Thermographic curves of equimolar mixtures of hydrogen bromide and ethylene for various absorbed doses of UV radiation at 77 K:
(1) D = 0.6 rel. units, η = 15%; (2) D = 0.9 rel. units, η = 14%; (3) D = 39.5 rel. units, η = 37% (numerals on curves give temperature in kelvins)

To throw light on the conditions in which the reaction proceeds and on the effect of various factors, recourse has been had [381, 382] to differential thermal analysis (DTA). The reaction vessel and the recording setup are similar to those described in Chap. 2 (see Fig. 2.9). DTA has determined the temperatures at which the hydrobromination of olefins takes place and has shown that such reactions can occur at the boiling point of liquid nitrogen (77 K). An indication that the reaction takes place in the solid phase is that the yield of ethyl bromide increases appreciably with increasing time interval during which the irradiated mixture is allowed to stay in darkness. For example, the degree of conversion increases by 25 to 30% when a mixture of HBr and C_2H_4 is maintained in darkness at 77 K for an hour after irradiation with ultraviolet light.

As an example, Fig. 5.1 shows the thermographic curves plotted during the warm-up of HBr and C_2H_4 mixtures pre-irradiated by ultraviolet light of a fixed intensity for various spans of time at 77 K. As is seen, given the same experimental conditions and standard samples, the number of absorbed quanta of light varies with the length of exposure time. In other words, the radiation doses absorbed by the samples are proportional to exposure time. From reference to curve *1* in Fig. 5.1 it is seen that at short exposure times the hydrobromination of ethylene proceeds in the solid phase at a temperature below the melting point of the mixture; for the system HBr-C_2H_4 the melting point is 112 K. With increase in the absorbed radiation dose (curve *2* in Fig. 5.1), the fast reaction takes place at a lower temperature. This is an indication that the hydrobromination of olefins is controlled by the concentration of pre-stabilized active centres — bromine atoms. Thus, at low temperatures two processes concur in the system HBr-C_2H_4, namely the stabilization of bromine atoms and the progress of the reaction. It is these two factors that are responsible for the explosive reaction (curve *3*) that may take place at 77 K after some induction period, τ.

It has been found that the induction period varies with the intensity of illumination, I. It is seen from Table 5.2 that the induction period τ is inversely proportional to I over a wide range of values. An interesting feature of the reaction in liquid nitrogen is that the explosion occurs at one and the same absorbed radiation dose, $D_{expl} = I\tau$ = constant = 4.2 relative units (see Table 5.2).

TABLE 5.2

Induction Period τ as a Function of Light Intensity I for Hydrobromination of Ethylene at 77 K

I/I_0	τ, s	Pre-explosion warm-up, K	Maximum warm-up, K	γ, %	D_{expl}, rel. units 1)
1	4.4	0.9	31	17.1	4.4
0.62	6.5	1.1	30	16.4	4.0
0.51	9.0	1.0	31	16.3	4.6
0.34	11.5	1.0	30	16.0	3.9
0.25	16.3	1.3	31	16.2	4.1
0.10	45.7	1.1	30	15.2	4.6
0.04	No explosion takes place at 77 K				

1) One relative unit is the dose absorbed by a sample per second at standard light intensity I_0.

Thus, for an explosive chain reaction to proceed at low temperatures, it is essential that the concentration of active centres reach a certain level, and this is decided by radiation dose and not radiation intensity. Basing himself on this evidence, N.N. Semenov believes that the fast photochemical hydrobromination of ethylene at 77 K is a kind of chain explosion during which the number of stabilized active centres participating in the reaction increases owing to the heat of the reaction [383].

Further experiments with the photochemical hydrobromination of olefins have disclosed other interesting aspects giving better insight into the mechanism of such reactions. For example, it has been found that at a radiation intensity of 0.04 I_0 and lower (see Table 5.2), the fast exothermic reaction at 77 K ceases to progress despite an increase in exposure time to values corresponding to absorbed radiation doses tens of times exceeding the explosion-inducing dose. In such cases, the fast reaction only occurs upon the subsequent warm-up of the mixture and goes on to a very high degree of conversion.

The hydrobromination of ethylene has also been investigated at 90 K. In contrast to experiments in liquid nitrogen, the rate of the reaction at 90 K increases gradually. The relationship $I\tau$ = constant is followed fairly closely, but the fast exothermic reaction occurs at shorter exposure times (at lower absorbed doses). An interesting aspect of the reaction at 90 K is shown in Fig. 5.2. As is seen, the increase in the reaction rate takes place after radiation is turned off.

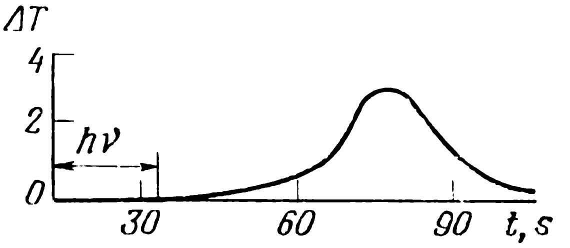

Fig. 5.2. Thermographic curve for hydrobromination of ethylene at 90 K after removal of illumination ([HBr]: $[C_2H_4]$ = 1 : 3, t_{illum} = 19.5 s, $I = 0.27\ I_0$, $\eta = 10\%$)

It has been found that the photochemical hydrobromination of olefins is strongly dependent on the conditions in which heat exchange with the surroundings takes place [381]. At low rates of heat abstraction, the fast reaction takes place at shorter exposure times. Conversely, at high rates of heat abstraction and short exposure times the reaction does not occur at the temperature of liquid nitrogen, but does so at higher temperatures.

At constant heat abstraction, the rate of hydrobromination of ethylene as a function of pre-exposure time has been investigated by noting the pattern of variations in the degree of conversion as a function of holding time at 77 K. It has been found that an increase in exposure time, that is, an increase in the concentration of stabilized active centres, brings about an increase in the rate of the reaction in darkness. Thus, the accumulation of immobilized active centres in solid cryogenic mixtures of HBr and C_2H_4 is accompanied by a slow reaction. If, at the same time, the reaction rate exceeds some critical value, it may so happen that heat input due to the reaction will exceed heat abstraction if the latter is maintained at a constant value. In the circumstances, the reaction rate rises abruptly, and a fast exothermic process occurs. If so, the reaction may be said to proceed by the thermal explosion mechanism [367, 368].

It is to be noted, however, that the fast reaction occurring at low temperatures cannot be interpreted as a purely thermal explosion. In fact, it has been proved by experiment that the explosion can take place at a progressively lower temperature as the exposure time (radiation dose) is increased or, which is the same, the concentration of stabilized active centres is raised. When instead of 90 K, the reaction is conducted at 77 K, the critical rate of reaction falls off to less than one-tenth of its original value. If it were a purely thermal explosion, such a decrease in the reaction rate would have to be associated with a proportionate increase in heat abstraction. Given the same samples, such a change in the condition of heat exchange with the surroundings is very unlikely in the temperature interval 90-77 K. The evidence given in Fig. 5.2 and obtained under isothermal conditions at 90 K also supports the view-point that the fast photochemical hydrobromination of ethylene cannot be explained by the thermal explosion mechanism alone.

In the light of experimental evidence, the photochemical hydrobromination of ethylene may be treated as a chain explosion in which the increase in the number of active centres takes place owing to the stabilization of bromine atoms. The greater proportion of active centres produced by photolysis is immobilized, and it is only very seldom that a chain reaction can take place, accompanied by a strong heat wave. The hydrobromination of olefins is exothermic. Propagating in a system containing immobilized bromine atoms, the heat wave may bring them into the reaction, thereby leading to an explosion. N.N. Semenov has called this reaction mechanism the propagation of a continuous chain which branches off with the aid of elementary heat waves [383]. Obviously, the rate of such heat branchings will depend on the concentration of stabilized atoms and radicals.

Under isothermal conditions, the evolution of heat in the course of a reaction obeys an exponential law. So, in a first approximation, variations in energy among the stabilized bromine atoms and their nonuniform distribution throughout the sample may be neglected. Variations in the concentration R of stabilized radicals due to exposure to light with intensity I may be described by an equation of the form

$$dR/dt = k_0(x_0 - R)I - k_1R - k_2Rn \qquad (5.11)$$

In the above expression, the first term describes the accumulation of radicals in traps, x_0, with a rate constant k_0. It is assumed that, owing to thermal fluctuations, some of the stabilized radicals may turn into reactive ones and take part in a reaction. The rate of this process analogous to the branching reaction, but with rate constant k_1, is described by the second term. The term k_2Rn describes the rate of loss of stabilized radicals as they interact with a number n of reactive species, with constant k_2.

Variations in the concentration of reactive species may be written

$$dn/dt = \alpha I + k_1R - k_2Rn \qquad (5.12)$$

where αI is the rate of formation of active centres under the action of light.

Most of the active centres forming upon absorption of light are immobilized. The time of chain propagation is shorter than the accumulation time for stabilized radicals.

On assuming that $dn/dt \ll \alpha I + k_1 R$, we get

$$dR/dt = (k_0 x_0 - \alpha)I - (k_0 I + 2k_1)R \tag{5.13}$$

On integrating, we get

$$R = \frac{(k_0 x_0 - \alpha)I}{k_0 I + 2k_1}\{1 - \exp[-(k_0 I + 2k_1)t]\} \tag{5.14}$$

From the above equation it is obvious that at low values of t, but high values of I,

$$R \approx (k_0 x_0 - \alpha)It \tag{5.15}$$

That is, the critical concentration R must be achieved under conditions such that It = constant, which under standardized conditions of experiment corresponds to a certain definite absorbed radiation dose. At low values of I, the concentration R may fail altogether to reach the value required for a given temperature, and no explosion will take place. Both results check with experimental evidence.

The validity of the above mechanism is confirmed by Fig. 5.2. At 90 K the reaction is seen to proceed even after radiation has been turned off. This outcome appears natural and provides evidence for the likelihood of thermal branching. From Eq. (5.12) it is also seen that in darkness the chain formation can be initiated only by conversion of trapped into active centres, say $Br_{stab} \rightarrow Br_{act}$. It is interesting to note that no such aftereffect is to be observed at 77 K. This may be related to the fact that the energy of traps is a function of temperature. Also, it may be presumed that exposure to radiation not only produces radicals, but also facilitates the conversion of trapped centres into reactive species. Similar reasoning can be applied to the effect of temperature and variations in heat exchange with the surroundings.

Thus, low-temperature chain reactions reveal an intimate union of a chain and a heat explosion. Evidence in favour of a chain explosion is the increase in the number of free valences; evidence in favour of a thermal explosion is the dependence of the reaction rate on conditions of heat exchange. A distinction of low-temperature chain reactions is that active centres may simultaneously be trapped and take part in a reaction. Exactly this factor leads to the initiation of specific chain processes at low temperatures.

The system HBr-C_2H_4 belongs to the few two-component systems of reactive substances for which low-temperature phase diagrams have been investigated. Maass and Wright [384] have concluded from visual observation that the crystals of hydrogen bromide and ethylene in the system HBr-C_2H_4 form an eutectic with a melting point of 98 K. A detailed thermographic investigation of unilluminated crystal mixtures widely varying in composition carried out by Kovalev [385] has yielded a refined phase diagram for the system HBr-C_2H_4. Mixtures containing an excess of ethylene exhibit an endothermic process at 98 K. No such process occurs in equimolar mixtures; they melt at 113 K. Dilution of the mixtures with hydrogen bromide reduces the height of the peak associated with melting. At the same time, the endothermic processes occurring at 90, 117, and 119 K gain in intensity. When held at the above temperatures, the solid hydrogen bromide experiences phase changes associated with the re-arrangement of the lattice [386].

Available knowledge gives every ground for concluding that mixtures of hydrogen bromide and ethylene form a molecular complex melting at 113 K. The point is that in the case of a simple eutectic the endothermic melting and the phase changes in HBr would be observed with any composition and no process would occur at 113 K. That this process does take place in equimolar mixtures is a sufficient reason to believe that the molecular compound has the composition $HBr \cdot C_2H_4$. The endothermic process at 98 K is in all probability related to the melting of the eutectic formed by the crystals of ethylene and the molecular complex.

The presence of a molecular complex in the system HBr-C_2H_4 provides a clue to understanding the fast hydrobromination of ethylene in the solid state. The $HBr \cdot C_2H_4$ compound forming in the course of condensation turns the two-component system into a one-component system of oriented molecules. The favourable orientation of the HBr and C_2H_4 molecules minimizes the opposition to diffusion typical of solids and facilitates the propagation of hydrobromination chain reaction along the ordered molecules of the $HBr \cdot C_2H_4$ crystal.

The formation of a 1 : 1 molecular complex is also helpful in explaining the effect that the change in the mixture composition has on the progress of the reaction. For mixtures varying in composition, the thermographic curves are analogous in their general aspect to the curves for the complex having a stoichiometric composition. With an increase in the proportion of ethylene in the mixture, however, progressively longer exposure times are required to bring about and sustain the reaction. This is because the ethylene crystals dilute the crystals of the molecular complex, and this naturally impedes the reaction. For a mixture containing an excess of HBr, the dominant feature is endothermic processes associated with phase changes in the solid hydrogen bromide. Apparently, the excess hydrogen bromide crystallizes into a separate phase. The phase change leads to a re-arrangement of the lattice which is accompanied by an increase in the mobility of the molecules, and this in turn favours the diffusion of bromine atoms from the hydrogen bromide crystals into the crystals of the molecular compound, thereby speeding up the reaction.

The aspects of the low-temperature photochemical hydrobromination of ethylene examined above are likewise characteristic of the hydrobromination of other olefins. Detailed studies have been conducted into the hydrobromination of propylene, 1-octene, and cyclohexene. In all of these cases, the respective products of addition contrary to Markovnikov's rule have shown a high yield, which points to the radical mechanism of low-temperature photochemical hydrobromination. At low temperatures, 1-octene and its mixtures with hydrogen bromide can be produced in both the crystalline and the glassy (amorphous) state. The rate of the reaction in the amorphous state is higher than it is in the crystalline state.

The photochemical hydrobromination of cyclohexene evokes special interest. Cyclohexene is one of the few olefins that can exist in various crystalline modifications at low temperatures [387, 388]. According to thermographic evidence, cyclohexene is capable of phase changes at 98 K, 113 K, and, in some cases, 133 K, and 139 K. In mixtures containing hydrogen bromide and an excess of cyclohexene, two endothermic processes have been observed at 147 K and 163 K. The former is apparently related to the melting of the eutectic formed by the $HBr \cdot C_6H_{10}$ molecular complex and C_6H_{10}; the latter to the melting of the $HBr \cdot C_6H_{10}$ compound. The above temperatures are close to the respective figures in the system $HCl\text{-}C_6H_{10}$ [389].

From an analysis of the thermographic curves recorded when warming up various HBr and C_6H_{10} mixtures that have previously been irradiated in liquid nitrogen, it may be concluded that the progress of hydrobromination is retarded by phase changes in cyclohexene [390]. Apparently, this is one of the few cases described in the literature where the phase change does not promote the reaction at low temperatures. The slowdown of the reaction at the phase-change points might be caused by the absorption of heat at the instant of an endothermic transition superimposed on the exothermic reaction. However, a similar slowdown is also observed at 133 K and 139 K, where the heat of phase changes is insignificant. It is hypothesized in [390] that the slowdown is traceable to the behaviour of the active centres.

To conclude this section, we shall stress again that a necessary condition for chain reactions to proceed in two-component systems at low temperatures is the formation of molecular complexes. This requirement is further confirmed by studies of the low-temperature addition of hydrogen sulphide to olefins under the action of light. In the gaseous and liquid phases, exposure to radiation causes hydrogen sulphide to add to a double bond by a chain mechanism analogous to that involved in the photochemical hydrobromination of olefins [391, 392]. In this case, the part of the active centre is played by the $H\dot{S}$ radical.

It has been shown that at 93 K the degree of conversion in the addition of hydrogen sulphide to ethylene, propylene, and other olefins is only by a small factor lower than the degree of the respective hydrobromination [385]. Irradiation of hydrogen sulphide and olefin mixtures at 77 K does not lead to hydrosulphation. It has been found by differential thermal analysis that at low temperatures hydrogen sulphide and olefins form a mixture of crystals that do not form a molecular compound. Obviously, for this reaction to take place at low temperatures and in the solid phase, it is essential that at least some of the mixture should be in a specific homogeneous phase. In the hydrobromination of olefins the likely formation of molecular donor-acceptor complexes at low temperatures leads to the appearance of such a specific homogeneous phase in which the progress of the reaction does not involve appreciable displacements of molecules. Since in the hydrogen sulphide-olefin system molecular complexes are absent, this necessitates substantial displacements of the reacting species, and this is handicapped in a heterogeneous system.

5.2. PHOTOCHEMICAL HYDROBROMINATION OF SOME OLEFIN HALIDES

In the photochemical low-temperature hydrobromination of olefins examined in the previous section, a mixture of an olefin and hydrogen bromide is usually condensed in a polycrystalline state. Coupled with complex formation, this fact may strongly affect the progress of the reaction at low temperature. Therefore, it is interesting to trace photochemical chain hydrobromination in the glassy (amorphous) rather than the crystalline state. As will be recalled [393], a glassy state is a nonequilibrium solution of supercooled structures standing midway between liquids and crystals. The temperature at which a substance passes into its glassy state (the glass point) refers to the temperature at which the equilibrium of the nearest order has not yet been attained and the structure of the system as a whole remains unchanged as the temperature is brought down further. The introduction of a hydroxyl or halogen atoms into an olefin molecule enhances the ability of the compound to condense in the glassy state. Also, the introduction of a halogen atom into olefin, as will be recalled, reduces the reactivity of the double bond, and the polarization of the double bond makes the character of the eventual products unpredictable [394]. In view of this, experiments have been conducted on allyl bromide and allyl chloride which vitrify at low temperatures with particular ease [390, 395].

When cooled rapidly to 77 K, allyl chloride and its liquid mixtures with hydrogen bromide form transparent glasses. Differential thermal analysis (curves *1* and *2* in Fig. 5.3) and visual observations have shown that, when frozen in the glassy state, allyl chloride crystallizes at 110 K and melts at 136 K. It has been established that the temperatures at which glassy mixtures of C_3H_5Cl and HBr varying in composition crystallize or begin to melt differ but little from the respective temperatures stated above for allyl chloride.

The warming up of the glasses previously exposed at 77 K to ultraviolet radiation leads to the reaction of hydrobromination which proceeds in the solid phase at a temperature below the melting point of the C_3H_5Cl-HBr mixture. Gas chromatography has shown that the principal reaction product is 1-chloro-3-bromopropane. This kind of addition points to the free-radical mechanism of the reaction. From a comparison of the degree of conversion and the number of light quanta absorbed by the sample it may be concluded that the low-temperature hydrobromination of allyl chloride proceeds by the chain mechanism.

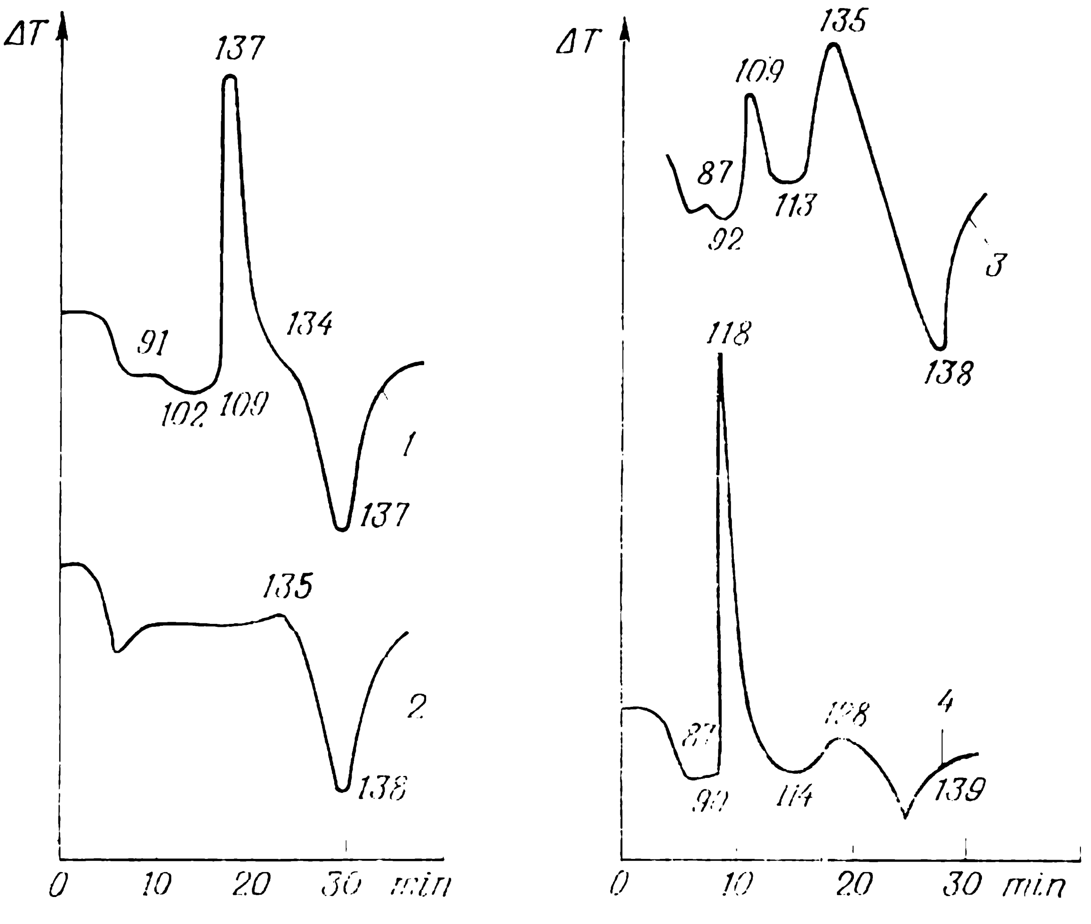

Fig. 5.3. Thermographic curves for equimolar mixtures of hydrogen bromide and allyl chloride (numerals on curves give temperature in kelvins):

(1) heating of a glassy sample; (2) heating of a crystalline sample; (3) illumination of sample prior to heating with UV light at 77 K, $I = I_0$, $t_{illum} = 5$ s, $\eta = 7\%$; (4) $t_{illum} = 3$ min, $I = I_0$, $\eta = 11\%$

When glass samples previously irradiated at 77 K are warmed up, their thermograms (curves *3* and *4* in Fig. 5.3) show that a new exothermic process takes place at around 88 K. As is seen from Table 5.3 and Fig. 5.3, the strength of a DTA signal and the degree of conversion as determined upon warming up increase with increasing exposure time. This points to a connection between the process occurring at 88 K and the hydrobromination of allyl chloride.

TABLE 5.3

Results of Thermographic Investigation of the System C_3H_5Cl-HBr as a Function of Exposure Time at 77 K

t, min	η, %	Initial temp. of reaction, K	Warm-up due to reaction, ΔT, K	Crystallization point, K	Warm-up due to crystallization, K	Melting point, K	Value of ΔT at peak of melting, K
1	5	88	11	110	7	132	7
5	9	90	25.5	110	3.5	130	4.5
15	13	88	28.5	113	2	130	3
45	23	91	33.5	108	5.5	130	3
80	30	88	36	–	0.2	133	2
120	39	88	36	115	2	131	2
240	46	90	39			–	–

It is also seen from Table 5.3 that the temperature at which the exothermic reaction of addition commences is independent of exposure time. This is a most intriguing aspect of chain hydrobromination in the glassy mixtures of allyl chloride and hydrogen bromide. The fact that the temperature of the reaction is independent of exposure time is in no way related to the occurrence of a reaction at 77 K, because no warm-up has been noticed during irradiation. Maintaining the irradiated samples in darkness at 77 K does not lead to appreciable changes in the system and, accordingly, in the general aspect of the thermographic curves. It is also to be noted that the temperature of hydrobromination (85-95 K) only slightly changes as the molar ratio of the mixture, [HBr] : [C_3H_5Cl], varies from 0.5: 1 to 12.0: 1.

The fact that the temperature at which the reaction commences is independent of exposure time and also the fact that it only slightly varies with the composition of the mixture can be explained, if we assume that 85-88 K marks the lower limit of the interval within which the allyl chloride-hydrogen bromide glass softens [395]. In this interval, the system undergoes radical changes in some of its properties (heat capacity, viscosity, thermal and electrical conductivity, specific volume, permittivity, etc.), which fact facilitates the initiation of the reaction by the active centres immobilizied at 77 K [393]. In the case on hand, the principal part seems to be played by the decrease in the viscosity of the system as it leads to an increase in the mobility of the reacting species.

A qualitative indication that the softening of allyl chloride-hydrogen bromide glass occurs in the temperature interval below 85 K is the "healing" at 90 K of the cracks produced in the glass at 77 K. The softening range of the glass can alternatively be found thermographically from the abrupt change in heat capacity [396]. To demonstrate, curve *2* in Fig. 5.3 plotted for nonirradiated mixtures of C_3H_5Cl and HBr points to a weak endothermic process which commences around 87 K. With short pre-exposure times, this endothermic process precedes the endothermic reaction. In the circumstances, the reaction kinetics in the system seems to be mainly controlled by the gradual decrease in the viscosity of the system. As the exposure time is increased, an appreciable rate of the reaction should, it would appear, be expected at higher values of viscosity. Since, however, the viscosity increases at a high rate, the observed shift in the initial reaction point is insignificant.

Some investigators [397, 398] have shown that the softening of glasses takes place at a viscosity of about 10^{12} Pa s, irrespective of their chemical composition and temperature. Hence, it may be deemed that a stabilized active centre initiates the chain hydrobromination of allyl chloride in the narrow temperature interval and at a viscosity of about 10^{12} Pa s. The subsequent abrupt rise in the reaction rate is mainly associated with the decrease in viscosity due to the self-heating of the mixture. As in the low-temperature photochemical hydrobromination of ethylene, an important factor seems to be the relation between the rate of heat input due to the reaction and the rate of heat abstraction through the walls of the reaction vessel.

Depending on the prevailing conditions, mixtures of C_3H_5Cl and HBr can be produced in the crystalline state as well. This enables the experimentor to use the same sample for a comparison of the reactions. Interestingly, the illumination of crystalline mixtures of allyl chloride and hydrogen bromide at 77 K does not lead to any reaction. At a low level of initiation, hydrobromination in crystalline samples is only observed in the temperature interval from 110 to 130 K. As the exposure time is extended, the hydrobromination of allyl chloride in crystalline samples begins at a temperature below 110 K, but its rate does not rise sufficiently high until the sample is brought to 100-110 K. An excess of hydrogen bromide brings down the initial reaction temperature. However, neither very long exposure times nor variations in the composition of the crystalline mixture can bring about an appreciable hydrobromination at below 90 K (which is the lowest initial reaction point for glasses). Thus, chain hydrobromination of the double-bond type in the glassy and the crystalline state show a different pattern of progress. On the other hand, it is obvious that there is a connection between the properties of the glassy mixtures and the reaction that takes place in the crystalline state.

Resort to well-vitrifying mixtures of HBr and C_3H_5Cl has made it easier to use UV spectroscopy in the *in-situ* studies of the changes in a system exposed and not exposed to radiation [400]. In the experiments a cell of the type described in Chap. 2 (see Fig. 2.8) was used. The mixture was deposited onto a cooled quartz plate in a manner close to molecular-beam cocondensation. This produced films about 10^{-4} cm thick which were exposed to UV rays for a predetermined span of time. Then the mixture was warmed up, and the reaction products were analyzed by gas chromatography. The absorption spectra for the nonirradiated equimolar mixtures of HBr and C_3H_5Cl at 79 K are shown in Fig. 5.4. As is seen, there is a broad absorption band with a peak at around 283 nm. This band appears to be caused by the absorption associated with the donor-acceptor type of molecular compound, $HBr \cdot C_3H_5Cl$. Hydrogen bromide is an electron acceptor, and allyl chloride is an electron donor. This guess about the absorption band at around 283 nm is borne out by the fact that the spectra recorded for allyl chloride and its hydrobrominated products under similar conditions show no absorption bands. A further confirmation that HBr and C_3H_5Cl interact as an acceptor and a donor is supplied by experiments in which the starting materials were deposited on a cooled substrate layer by layer. With two layers, the absorption band at 283 nm is poorly resolved; with the increase in the number of layers it gradually approaches in appearance the band displayed by the films produced by molecular-beam cocondensation. It is also interesting to note that absorption at a wavelength of 283 nm is a maximum when the sample is deposited from an equimolar gaseous mixture.

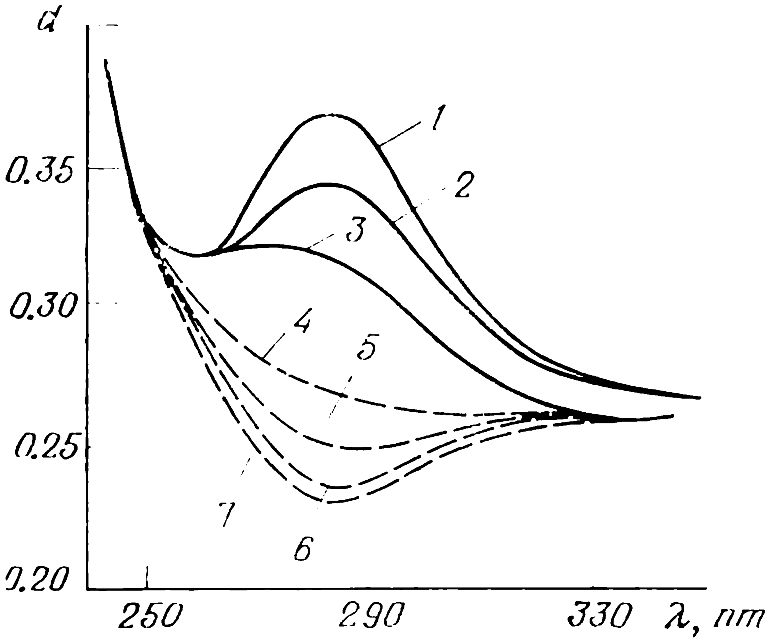

Fig. 5.4. UV absorption spectra at 79 K:

(1) nonilluminated mixture of hydrogen bromide and allyl chloride; (2) same after illumination by filtered light (λ 313 nm) for 26 min; (3) same after illumination for 50 min; (4) after heating to 103 K which destroyed the complex, the spectrum was recorded at 80 K; (5) mixture without complex, after illumination by filtered light for 60 min; (6) illumination for 120 min; (7) illumination for 180 min

Molecular complexes are formed in the course of condensation. Apparently, at that time the molecules are oriented so as to favour donor-acceptor interaction, and the rapid abstraction of the heat generated by the condensation serves to immobilize the otherwise unstable compounds. Molecular complexes such as $HBr \cdot C_3H_5Cl$ are stable only at very low temperatures. When a sample whose spectrum at 79 K shows an absorption band at a wavelength of 283 nm is warmed up to 103 K, the absorption band irreversibly disappears from the spectrum (see curve *4* in Fig. 5.4). The warming up of frozen mixtures of hydrogen bromide and allyl chloride changes the initial pressure. In all probability, in a glassy mixture containing molecular complexes the end products are formed at the lower limit of the softening temperature interval, and this is accompanied by a substantial decrease in viscosity. As determined from the change in pressure, the maximum degree of conversion is 4%.

There exists a certain degree of correlation between the intensity of the absorption band around 283 nm and the degree of convesrion. In the case of multi-layered samples whose spectra do not display a well-defined absorption band at 283 nm, the change in the concentration of the starting components corresponds to a degree of conversion not exceeding 1%. The degree of conversion is a maximum (4%) in the case of samples produced by molecular-beam cocondensation, that is, when the absorption at 283 nm is a maximum.

The above correlation seems to point to the important part played by molecular complexes in the chemical reaction. When held at room temperature in darkness, HBr takes a very long time to add to allyl chloride [399]. This is apparently because the existing thermodynamic conditions do not favour the formation of unstable molecular complexes which are intermediates in the reaction. Such complexes can, however, be formed at low temperatures, so the reaction of hydrobromination proceeds at a high rate. As the gas chromatography of the reaction products shows, the hydrobromination of allyl chloride in darkness produces two chlorobromopropanes, $CH_2ClCH_2CH_2Br$ and $CH_2ClCHBrCH_3$. Apparently, the electron transfer from the double bond to the hydrogen bromide in the molecular complexes not only leads to a strong polarization of the bonds in the starting molecules, but also promotes conformational transformations.

Thus, spectroscopic investigation of thin films of hydrogen bromide and allyl chloride at low temperatures has established the fact of intermolecular interaction involving charge transfer and formation of complexes.

Irradiation of frozen hydrogen bromide-allyl chloride films produces a large amount of 1-chloro-3-bromopropane. The degree of conversion is close to 100%. IR spectroscopy has shown that no hydrobromination takes place at a temperature close to 77 K.

The formation of molecular complexes during the condensation of hydrogen bromide and an olefin may have a decisive effect on the mechanism of hydrobromination, notably, the formation of active centres [400]. When an equimolar mixture of hydrogen bromide and allyl chloride frozen at 81 K is illuminated through a filter whose transmission peak lies at around 313 nm, the absorption band associated with the molecular complex disappears from the spectrum. Complex-containing samples and samples in which the molecular complex has previously been destroyed show different plots of optical density at $\lambda = 283$ nm as a function of exposure time at 81 K (Fig. 5.5). The respective degrees of conversion are plotted in Fig. 5.6, and Table 5.4 gives the quantum yields for several degrees of conversion.

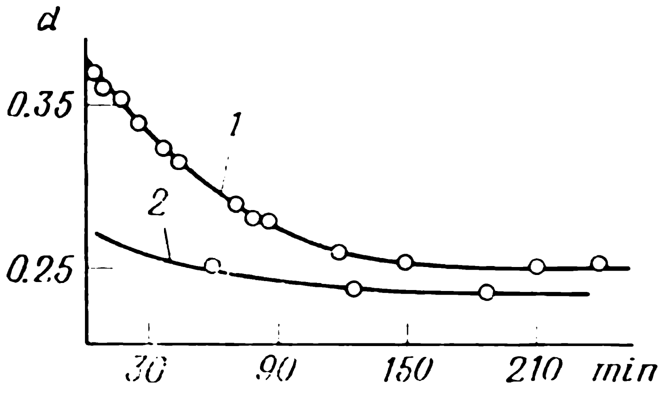

Fig. 5.5. Optical density as a function of time in the system HBr-C_3H_5Cl at 81 K:

(1) mixture with complex; (2) mixture without complex

TABLE 5.4

Degrees of Conversion and Quantum Yields for Hydrobromination of Allyl Chloride at an Initial Pressure of $P = 1.2 \times 10^3$ Pa

η, %	t_{exp}, min	Number of converted molecules 10^{-20}	Quantum yield, φ
34	15	1.04	42
58	30	1.74	35
83	75	2.50	20
84	150	2.53	10
15 ¹)	15	0.3	11
69 ¹)	180	2.20	7

¹) The complex has previously been destroyed by heating.

The evidence cited above makes it possible to note some distinctions in the low-temperature reactions in the solid phase and to evaluate the role played by molecular complexes in the photochemical hydrobromination of allyl chloride. As already noted, illumination at 81 K cannot initiate any reaction. Upon warm-up, however, the degree of conversion in such samples may be close to 100%. Thus, the changes in the UV spectra at 81 K shown in Fig. 5.5 seem to be related to the formation and stabilization of active centres. Obviously, this process involves the participation of molecular complexes, and the probability of photolysis for hydrogen bromide fixed in a complex is increased. The contribution of the various reactions to the formation of active centres can readily be estimated from spectrophotometry of the hydrogen bromide-allyl chloride system.

Comparison of the yields for the initial stage of photolysis (curve *1*) and 1.5 h later when practically all of the complex has been depleted points to the high efficiency of the reaction involving the complex as compared with the reaction in the system without the complex. For example, during the existence of the complex, $\tau = 0.2\ t$ (where t is the exposure time of the mixture corresponding to 85% conversion) the reaction is two-thirds (62%) complete. The formation of active centres at 81 K can be visualized taking place as follows:

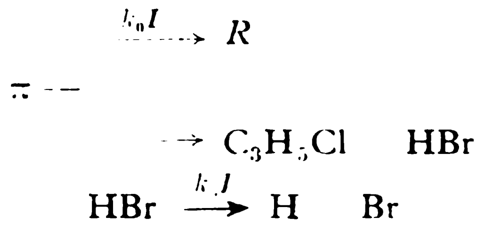

$$\pi \xrightarrow{k_0 I} R$$
$$\pi \rightarrow C_3H_5Cl \quad HBr$$
$$HBr \xrightarrow{kI} H \quad Br$$

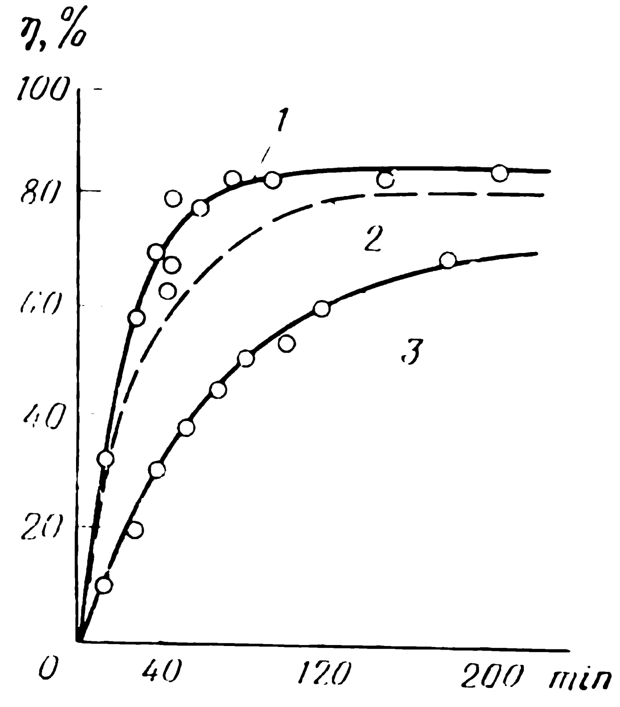

Fig. 5.6. Degree of conversion of starting reactants as a function of illumination time in photochemical hydrobromination of allyl chloride:
(1) system with complex; (2) same without complex; (3) calculated curve

where R is the number of active centres forming from a π-complex.

The above scheme reflects the existence of two competing reactions. In one, active centres are formed by the photolysis of the complex; in the other by photolysis of hydrogen bromide.

The above scheme has been described by a system of differential equations and analyzed on an analog computer for various relative concentrations of the complex and hydrogen bromide. The analysis has shown that initially the formation of reactive species from the complex proceeds many times faster than from the hydrogen bromide, although the concentration of the complex in the system appears to be a small fraction of that of hydrogen bromide. Thus, in contrast to the gaseous and liquid phases, where the chain initiation takes place only as a result of photolysis of hydrogen bromide, in the solid phase at low temperatures active centres are mainly formed from the donor-acceptor type of complexes under the action of light.

Assuming that active centres are produced by the photolysis of molecular complexes, we shall examine the kinetic pattern of the reaction. Let the initial concentration of the complexes leading to the formation of active centres be π_0, and their current concentration be π. Then the rate of depletion for the complex will be

$$-d\pi/dt = k_0 I\pi \qquad (5.16)$$

where I is the light intensity, k_0 is a factor proportional to the probability of light absorption, extinction factor, and quantum yield of the formation of active centres.

Integrating Eq. (5.16) on the assumption that at $t = 0$ $\pi = \pi_0$, we get

$$\pi = \pi_0 \exp(-k_0 It) \qquad (5.17)$$

On the other hand, variations in the concentration of active centres may be presented as

$$dR/dt = k_0 I\pi - k_2 R \qquad (5.18)$$

In this equation the first term describes the rate of formation of active centres and the second term, their rate of loss. The number of active centres available for the subsequent chain propagation is given by

$$R = (k_0 I/k_2)\,\pi \qquad (5.19)$$

The rate of formation of the end product is

$$d\eta/dt = k_1 R \qquad (5.20)$$

where η is the degree of conversion for the starting materials, and k_1 is the rate constant of chain propagation.

Substituting Eqs. (5.17) and (5.19) into Eq. (5.20) gives

$$d\eta/dt = (k_1 k_0/k_2)\, I\pi = (k_1 k_0/k_2)\, I\pi_0 \exp(-k_0 It) \qquad (5.21)$$

Integration of Eq. (5.21) yields

$$\eta = (k_1 \pi_0/k_2)\,[1 - \exp(-k_0 It)] \qquad (5.22)$$

Equation (5.22) describes the degree of conversion as a function of exposure time.

For the low-temperature photochemical hydrobromination of olefins, the degree of conversion vs. exposure time curves usually have the form shown in Fig. 5.6. Eq. (5.22) satisfactorily fits experimental data (see curve *2* in Fig. 5.6).

Thus, in the light of experimental evidence, the mechanism of photochemical chain hydrobromination in the glassy state may be visualized as follows. The reaction of chain initiation at low temperatures involves unstable molecular complexes derived during the preparation of the starting mixture. The chain initiation and the chain propagation are separated in time. The formation of radicals or of non-radicals takes place at 77 K and is not accompanied by any reaction that would result in the end product. A fast chain reaction occurs in the softening interval of the glass and is associated with an abrupt reduction in the viscosity of the material. Donor-acceptor interaction in the hydrogen bromide-allyl chloride system turns the glass into a structure of oriented molecules. The presence of hydrogen bromide and allyl chloride chains containing stabilized active centres coupled with the mobility of molecules in the softening interval promotes the propagation of photochemical chain hydrobromination at temperature lying substantially below the melting point of the mixture.

In conclusion, it may be noted that the photochemical hydrobromination of olefins has expanded the range of low-temperature reactions, and its studies have thrown light on the kinetic pattern typical of induced low-temperature reactions in the solid phase.

CHAPTER SIX

SPONTANEOUS REACTIONS

Experiments with the formation and conversion of free radicals at low temperatures in the solid phase and photochemical chain hydrobromination have shown that for olefins like cyclohexene and isobutylene the reaction can proceed with an appreciable yield already during the condensation of the starting materials even in darkness. Further experiments have discovered a whole range of such fast spontaneous chemical processes at low temperatures [235, 401, 402].

6.1. HALOGENATION AND HYDROHALOGENATION OF OLEFINS IN THE ABSENCE OF SOLVENTS

As will be recalled [368], the halogenation and hydrohalogenation of olefins proceed in the gaseous phase usually at room or elevated temperatures. Using layered samples prepared by depositing the reactants in turn in a reaction vessel cooled to 77 K, it is possible to prevent contact between the reactants at ordinary temperatures and to verify the feasibility of such reactions at low temperatures and to establish their basic pattern.

6.1.1. Basic Pattern of Reactions in Layered Samples of the Starting Materials

Thermographic data for some chemical reactions conducted at low temperature in layered samples of the starting materials [403] are presented in Table 6.1 and Fig. 6.1. The reaction vessel, measurement and analysis techniques are similar to those described in Chap. 2 (see Fig. 2.9).

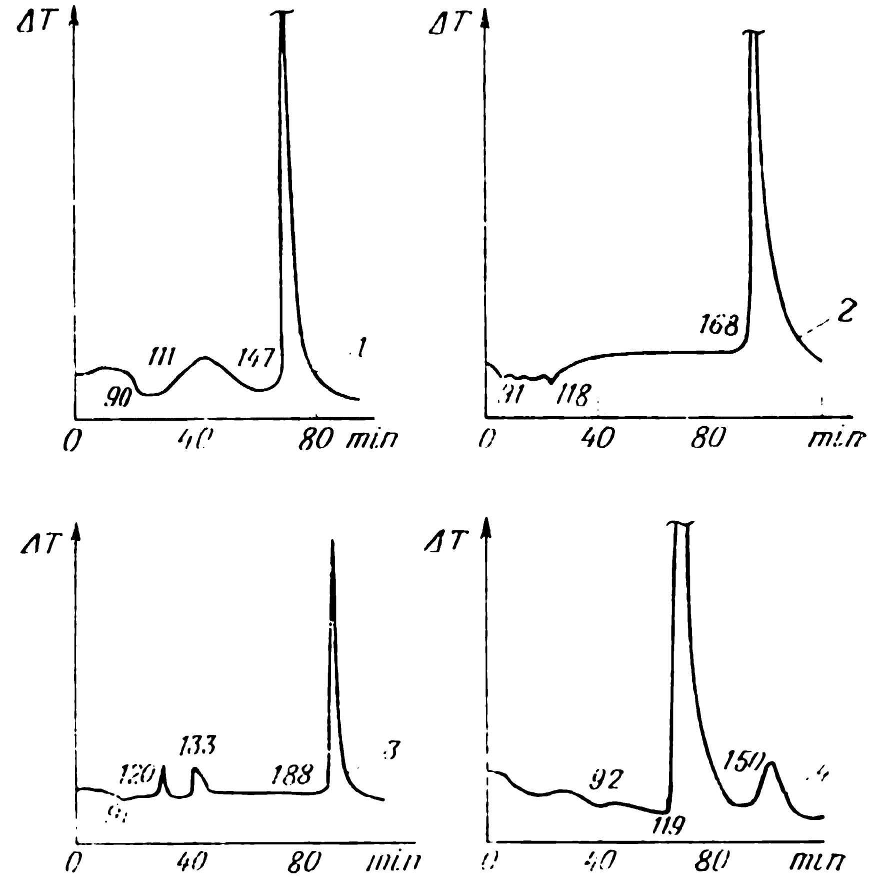

Fig. 6.1. Thermographic curves for reactions in condensates produced by multiple layer deposition of starting reactants (ΔT is the warm-up interval; numerals on curves give temperature in kelvins):
(1) propylene-chlorine; (2) hydrogen bromide-chlorine; (3) isobutylene-bromine; (4) isobutylene-hydrogen bromide

TABLE 6.1

Halogenation and Hydrohalogenation of Olefins at Low Temperatures Using Layered Samples of Starting Materials

System	T_m, K 1st component	T_m, K 2nd component	Temperature of fast reaction, K	Reaction product	Yield, % of theoretical
Ethylene-chlorine	104	172	**106**, 119, 171	1,2-dichloroethane	97
Propylene-chlorine	88	172	**91**, 111, 147	1,2-dichloropropane	92
Isobutylene-chlorine	133	172	112, **130**	1,2-dichloro-2-methylpropane	80
Propylene-bromine	88	266	117, 158, **193**	1,2-dibromopropane	98
Isobutylene-bromine	133	266	120, 133, **188**	1,2-dibromo-2-methylpropane	96
Cyclohexene-bromine	169	266	153, 178, **203**, **228**	1,2-dibromo-cyclohexane	90
Isobutylene-hydrogen bromide	133	186	84, **119**, *150*	2-bromo-2-methyl-propane	98
Isobutylene-hydrogen chloride	133	159	100, 119, 133, **155**	2-chloro-2-methyl-propane	93

Note. The temperature at which the bulk of the starting materials reacts is given in bold type.

It is seen from Table 6.1 that at low temperatures the reactions of double-bond addition involving halogens and hydrogen halides practically proceed to completion. Also, it has been found that several types of reactions will readily proceed in the condensed phase at low temperatures, namely the reaction of olefins with nitrogen tetraoxide and tetranitromethane, inorganic addition reactions, for example,

$$2NO \quad O_2 \longrightarrow 2NO_2$$

$$2NO + Cl_2 \longrightarrow 2NOCl$$

and displacement reactions, such as

$$2HBr \quad Cl_2 \longrightarrow 2HCl \quad Br$$

and some others. According to gas chromatography of the products of low-temperature chlorination of ethylene, bromination and chlorination of propylene, a yield of about 100% is only shown by the addition product.

From Table 6.1, Fig. 6.1, and some other experimental evidence, several common features can be noted in the low-temperature reactions.

1. The reactions proceed spontaneously, in the absence of any initiator. Some of the reactions listed in Table 6.1 occur at very low temperatures. For example, propylene chlorination can take place at 91 K.

2. It is seen from Fig. 6.1 that all the reactions listed in Table 6.1 proceed at high rates at temperatures close to the boiling point of liquid nitrogen, which is an indication of an abnormally high reactivity.

3. The low-temperature addition of halogens to olefins is characterized by high selectivity and a quantitative yield (see Table 6.1). It is to be noted that in the gaseous phase [368] and in the liquid phase [404, 405] the addition products are accompanied by displacement products. Thus, a kind of selection from among the parallel reactions takes place at low temperatures.

4. Chemical reactions at low temperatures are highly selective. For example, it has been found that chlorine will readily add to ethylene but will not do so to acetylene. Hydrogen bromide will add to isobutylene in darkness, and to propylene only when exposed to light.

5. As a rule, reaction temperatures are related to phase changes. Ordinarily, a reaction commences and proceeds at the instant when one of the starting components melts. If the system is capable of allotropic transitions in the solid phase, the reaction may well go on at a temperature below the melting point of the starting components (for example, in the systems hydrogen bromide-isobutylene and hydrogen chloride-isobutylene).

It has been proposed to interpret the above features of chemical reactions at low temperatures on the basis of the formation of intermediate donor-acceptor complexes and their subsequent participation in the reaction [170].

In experiments, low-temperature halogenation and hydrohalogenation usually yield solid products. The product film appearing when the starting materials are frozen layer by layer may interfere with contact between and interaction of the reactants and cause the reaction to occur in several temperature intervals (see Table 6.1).

6.1.2. Reactions in Cocondensates

Selective freezing out of the starting components prevents contact between the substances in the gaseous and liquid phases, but produces heterogeneous mixtures at low temperatures. It is reasonable to assume that in homogeneous mixtures chemical reactions would proceed at still lower temperatures. This assumption has been verified by conducting the bromination and chlorination of unsaturated compounds in the condensates produced by cocondensing the starting materials out of molecular beams [142, 406]. The experimental setup and the reaction vessel used for the purpose are described in Chap. 2 (see Fig. 2.8). The starting materials were deposited onto a liquid-nitrogen-cooled thin glass membrane through capillaries, while the vapours were continually pumped away from the surface of the condensate. The rate of condensation was chosen to suit each system by trial and error and usually ranged between 2×10^{16} and 5×10^{16} molecules s^{-1}. The quantity of each component was about 4×10^{-4} mole. The reaction temperature was measured by a conventional and a differential thermocouple.

Figure 6.2 shows a typical thermographic curve, and Table 6.2 gives some of the results obtained.

As is seen, the halogenation and hydrohalogenation of olefins occurs at very low temperatures almost instantaneously. The bromination of ethylene and propylene is observed at temperatures close to the melting points of the olefins, that is, at the instants of phase changes. In other systems, the reaction temperature lies substantially below the melting points of the starting materials. Experiments with the cocondensation of cyclohexene and cyclopentadiene from molecular beams have shown that, on cooling, they pass into a glassy state. At the temperatures associated with the initiation of the reaction, these substances begin to crystallize, so all of the reactions in question actually occur near phase changes.

A comparison of the reactions in cocondensates and in layered samples graphically illustrates the effect that the degree of homogeneity of the medium has on the reaction temperature. From a comparison of Tables 6.1 and 6.2 and Fig. 6.2, it is an easy matter to see that, given the same system, fast reactions will take place in cocondensates at a lower temperature. Cocondensation disperses the starting materials to a very high degree, thereby enhancing contact between the reactants. The latter factor promotes the formation of complexes in large concentrations, accompanied by the evolution of a large amount of heat raising the system to the temperature of a phase change and leading to a fast reaction. At low beam intensities (10^{16} molecules s^{-1}), no reaction takes place at the time of cocondensation, and heat evolution in the system is nil. It is not unlikely, however, that the mixture can be warmed up by the heat of condensation. For example, in the bromination of ethylene and propylene, thermocouple indications showed that each time the starting components were cocondensed from the molecular beams, a reaction would take place

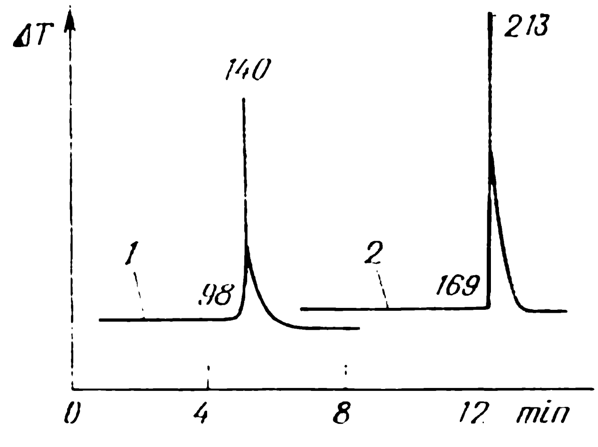

Fig. 6.2. Thermographic curves for cyclohexene-chlorine mixtures (numerals on curves give temperature in kelvins): (1) molecular beam cocondensation; (2) multiple-layer deposition on a cooled substrate

TABLE 6.2

Halogenation and Hydrohalogenation of Olefins in Cocondensates

System	T_m, K 1st component	T_m, K 2nd component	Reaction temperature, K	Warm-up, K	Reaction product	Yield, % of theoretical
Ethylene-bromine	104	266	103	36	dibromoethane	93
Propylene-bromine	88	266	90	30	1,2-dibromopropane	95
Cyclohexene-chlorine	169	172	98	54	dichlorocyclohexane	90
Cyclopentadiene-bromine	188	266	98	51	—	—
Cyclopentadiene-hydrogen bromide	188	185	103	45	—	—

on a liquid-nitrogen-cooled surface. The magnitude of warm-ups and the time intervals between them have been found to vary with the rate of condensation. This observation is similar to that described earlier by N.N. Semenov and A.M. Shalnikov for the cocondensation of cadmium and sulphur [139].

Cocondensation from molecular beams has proved that the low-temperature halogenation of olefins is not related to the warm-up due to heat of condensation. To evaluate the heat input due to the beam, it is necessary to know the heats of condensation for the halogen and olefin involved. Unfortunately, they are unknown, but can be estimated with sufficient accuracy from the heat capacities of the gaseous, liquid and solid states, and the heats of melting and evaporation. For bromine, ethylene and propylene, the heat of condensation can be found by the following equation:

$$Q = C_p^g (T_1 - T_{ev}) + \lambda_l + C_p^l (T_{ev} - T_m) + \lambda_m + C_p^s (T_m - T_l) \qquad (6.1)$$

According to [407], for bromine $C_p^g = 27$ J K^{-1} mole^{-1}, $C_p^l =$ $= 27$ J K^{-1} mole^{-1}, $C_p^s = 24$ J K^{-1} mole^{-1}, the heat of evaporation is $\lambda_l = 30.6$ kJ mole^{-1}, the heat of melting is $\lambda_s = 10.5$ kJ mole^{-1}, $T_{ev} = 298$ K, and $T_m = 266$ K. On substituting these numerical values in Eq. (6.1), we get $Q_{cond,\, Br_2} = 46$ kJ mole^{-1}. Similarly, according to [407], for propylene $Q_{cond,\, C_3H_6} \approx 32$ kJ mole^{-1}. At a condensation rate of 10^{17} molecules s^{-1}, the specific heat inputs due to the bromine and the propylene are $q_{Br_2} \approx 8 \times 10^{-3}$ J s^{-1}, and $q_{C_3H_6} \approx 4 \times 10^{-3}$ J s^{-1}. Hence, the total heat input is $q \approx 12 \times 10^{-3}$ J s^{-1}. The deposited films are $h \approx 1.2 \times 10^{-3}$ cm thick, and heat abstraction through such a film, assuming that its thermal conductivity is $\lambda = 12 \times 10^{-4}$ J s^{-1} cm^{-1} K^{-1} and its temperature gradient is $\Delta T \approx 5°$, will be $q = \lambda S \Delta T/h \approx 8$ J s^{-1} (where S is the surface area of heat abstraction, equal to about 1.5 cm^2). From a comparison of the heat input due to the beam and the heat abstraction through the film, it is seen that the heat evolved in the course of condensation at a rate of 10^{17} molecules s^{-1} cannot play any decisive role in the temperature build-up of the surface layer.

Under conditions of cocondensation from molecular beams, a fast reaction begins during the subsequent warm-up; an explosion takes place in what may be called a forced state [408]. Assuming a high rate of heat abstraction, such a state can, it seems, be attained owing to the temperature gradient across the layer deposited on the cooled surface. This gradient mainly exists in the layer whose thickness is $h \approx 1.2 \times 10^{-3}$ cm. If the thickness of the glass membrane is $h_0 =$ $= 0.1$ mm, the temperature of liquid nitrogen is T_l, the surface temperature of the glass is $T_0 = 82$ K, and the surface temperature of the deposited condensate is T_d, then the quantity of heat, q_1, abstracted by the glass through its surface S will be equal to

$\lambda_{\text{glass}}\,(T_1 - T_0)/h_0$ J s^{-1}. The thermal conductivity of the glass is $\lambda_{\text{glass}} = 10.5\times10^{-3}$ J cm^{-1} s^{-1} K^{-1}. The quantity of heat, q_2, abstracted by the deposit towards the glass surface will be $q_2 = \lambda_d(T_0 - T_d)/h$ J s^{-1}. Unfortunately, the thermal conductivity of bromine and olefins at low temperatures is unknown. For the deposited mixture it may be assumed that the thermal conductivity is 1.2×10^{-3} J cm^{-1} s^{-1} K^{-1}, which is the value usually ascribed to liquid hydrocarbons and halocarbons.

The heat supplied by the beam is abstracted at once, so $q_1 = q_2$, or

$$\lambda_{\text{glass}}\,\frac{S(T_1 - T_0)}{h_0} = \lambda_d\,\frac{S(T_0 - T_d)}{h} \tag{6.2}$$

On substituting the numerical values, we find that the temperature gradient across the deposit is $T_0 - T_d = \Delta T \approx 6$ K. The computed gradient checks with that found by experiment. From Table 6.2 it is seen, for example, that the propylene-bromine system reacts near the melting point of propylene. In the bromination of ethylene having a higher melting point than propylene, a thicker film is required in order to maintain the temperature gradient necessary for the reaction to occur. Thus, the chemical reaction in cocondensates from molecular beams may be treated as a thermal explosion which takes place when the mixture is warmed up owing to the temperature gradient. It is set off when the system reaches the temperature of the nearest phase change promoting the conversion of the pre-stabilized intermediate complexes into stable final products. Cocondensation from molecular beams creates more favourable conditions for the formation and accumulation of the molecular complexes responsible for the subsequent reaction.

6.1.3. Thermographic and Spectroscopic Investigation of the Propylene-Bromine System

From detailed thermographic studies of the propylene-bromine system it has been established that the reaction proceeds in stages and that the existence of intermediate molecular complexes is a certainty. The technique used for the purpose is described in detail in [409].

Figure 6.3 shows thermographic curves for a mixture of propylene and bromine. As is seen from curve *2*, the fast reaction is preceded by two exothermic processes. Of the two, the first is most interesting; it immediately follows the melting of the propylene and occurs in the temperature interval 88-117 K. This process is accompanied by the dissolution of the bromine and the formation of a tinted solution. The dissolution of the solid bromine in the propylene at temperatures close to the boiling point of liquid nitrogen, changes in the colour of the mixture, and the evolution of heat are indications of a strong intermolecular interaction between the bromine and the propylene, that is, the formation of molecular compounds. Assuming comparable conditions, a comparison of the areas of the peaks recorded as the bromine is dissolved in the propylene with the area of the peak associated with the melting of the propylene shows that the heat of solution for solid bromine is about 12 kJ mole^{-1}. Taking into account the heat of melting for bromine, which is 10.6 kJ mole^{-1} [379], the heat of formation for propylene-bromine molecular complexes must be not less than 20 kJ mole^{-1}. This is a reasonable figure for such complexes [410, 411].

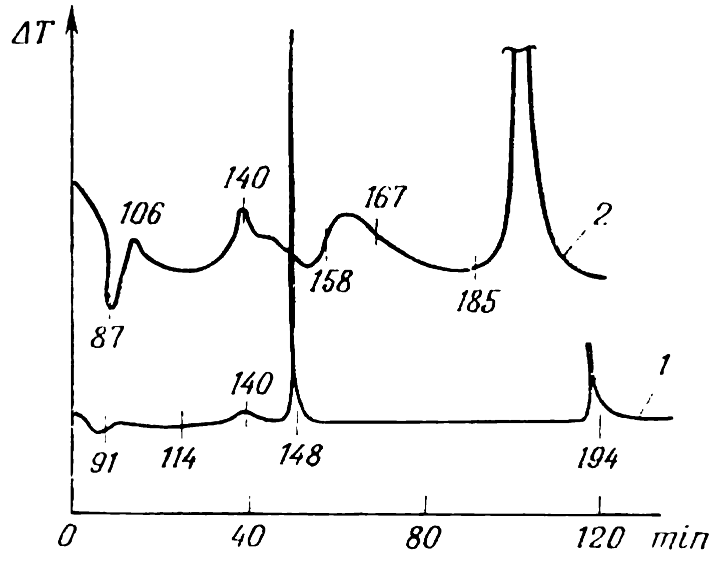

Fig. 6.3. Thermographic curves for bromine-propylene mixtures (numerals on curves give temperature in kelvins):

(1) after pre-mixing and complex accumulation; (2) multiple-layer deposition on a cooled substrate

When bromine and propylene are deposited on a cooled surface in turn, no marked reaction takes place in the temperature interval 77-117 K. Hence, the formation of complexes appears to precede the reaction.

The other exothermic process (see curve *2* in Fig. 6.3), occurring in the temperature interval 117-148 K, may, in all probability, be related to the separation of the complexes into a phase of their own or the formation of complexes differing in composition.

In addition to separating the stages of complex formation and the formation of the final product, low temperatures enable the experimentor to accumulate intermediate complexes. This can, for example, be done by repeatedly heating and cooling the propylene-bromine system in the interval 77-117 K. That this treatment leads to the accumulation of intermediate complexes is confirmed by the quantity of propylene pumped from the system at, say, 168 K. It decreases as the number of warm-up and cooling cycles is increased. From a comparison of the curves shown in Fig. 6.3, it is seen that the preliminary accumulation of complexes in sufficient amounts enables an explosive reaction to occur at 148 K.

Another indication that complex formation is connected with the bromination of propylene is that the magnitude of the exothermic peak at 148 K, associated with the reaction, varies with the number of cycles during which the mixture is warmed up and cooled in the temperature interval 77-118 K. Thus, the accumulation of complexes leads to a more homogeneous mixture and promotes the bromination of propylene at lower temperatures.

Further insight into the nature of the complexes thus formed has been gained from electron absorption spectra of the propylene-bromine system [412]. In the experiments, the starting components were deposited in alternating layers onto a cooled quartz plate. For a more even distribution, in some experiments the bromine was diluted with propane which remains practically transparent up to 200 nm at low temperatures. As is seen from Fig. 6.4, a mixture of bromine and propylene diluted with propane shows a strong band around 274 nm. In the long wavelength region, there is a well defined inflection around 312.5 nm. This is convincing evidence of a strong donor-acceptor interaction between bromine and propylene. The band at $\lambda = 274$ nm is assigned to a charge-transfer complex of bromine and propylene with a 1: 1 composition. This composition has been confirmed by experiments with the donor-acceptor interaction of bromine with olefins in nonpolar solvents [402, 413].

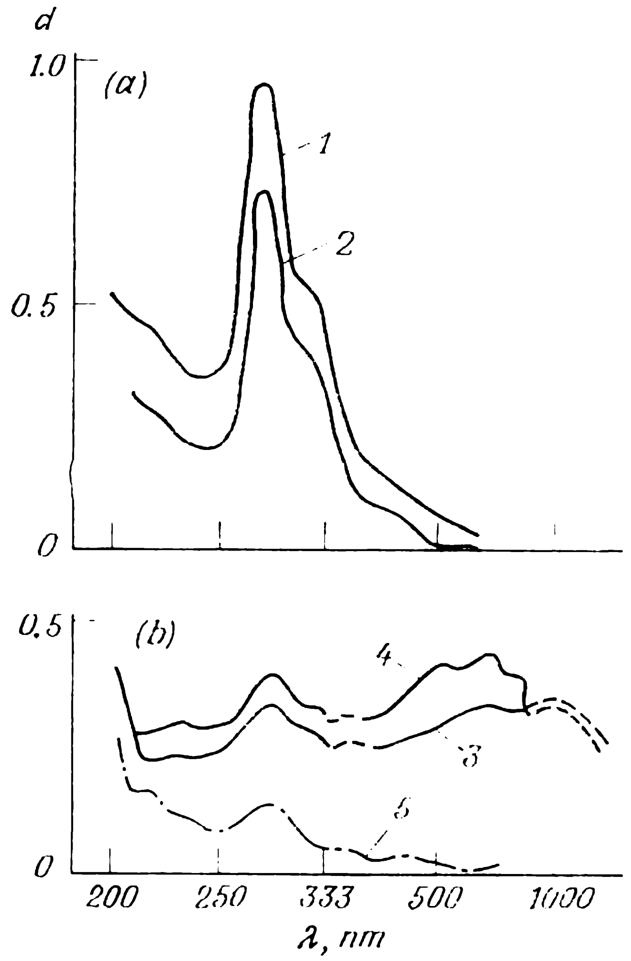

Fig. 6.4. UV absorption spectra of the system "propylene-bromine":
(*a*) with an addition of propane and (*b*) without addition:

(1) mixture warmed up from 80 to 100 K which is above T_m for propylene; the spectrum recorded at 80 K; (2) same but 90 min after maintaining at 80 K; (3) $T = 80$ K; (4) 90 min after maintaining at 80 K; (5) mixture warmed up to 100 K and cooled again to 80 K

Undiluted with propane, the propylene-bromine mixture shows a spectrum having several other bands. Of particular interest is the broad complex band in the interval 500-1 000 nm (curve *3* in Fig. 6.4). It is to be noted that maintaining the mixture at temperatures close to 77 K for a definite span of time causes this band to gain in intensity (curve *4*). If, on the other hand, the temperature of the mixture is raised to 100 K, which is higher than the melting point of propylene (equal to 87 K), absorption in the range 500-1 000 nm disappears irreversibly (curve 5). These changes in the spectra are also accompanied by a concurrent reaction. The band around 278 nm is partly retained. This evidence shows that the factors responsible for low-temperature bromination are mainly the intermediate compounds absorbing in the interval 800-1 000 nm. The broad band in the interval 500-1 000 nm is assigned to complexes of the composition $Br_2 \cdot C_3H_6 \cdot Br_2$ or associates of the form $(Br_2 \cdot C_3H_6)_n$ where $n \geqslant 2$, which coexist in equilibrium with complexes of the 1: 1 composition. The existence of similar compounds having a chain structure at reduced temperatures is described in [414]. At low temperatures, the formation of such associates is more favourable energetically than the existence of binary compounds. In all probability, the associated complexes absorbing in the interval 500-1 000 nm experience marked changes in the inter- and intramolecular spacings, which is accompanied by the loosening and strong polarization of the double bond. In the valence vibration range of the double bond (1 632 cm^{-1}), the IR spectra of frozen solid mixtures of bromine and propylene show bands at lower frequencies [415, 416], which, as it seems, confirms the above conclusion.

6.1.4. The Mechanism of the Low-Temperature Reaction

The wealth of experimental evidence gathered mainly for halogenation suggests the following mechanism for fast low-temperature spontaneous chemical reactions.

The first stage takes place during the condensation of the starting materials and leads mainly to the formation of unstable molecular complexes of the 1: 1 composition. Nonpolar molecules, such as ethylene and bromine, may likewise contribute to their formation. It is important to stress that in the halogenation of olefins the formation of such complexes is but the initial stage of the reaction. The emergence of 1: 1 complexes possessing a dipole moment favours their subsequent solvation by olefin or halogen molecules.

The spectra of the propylene-bromine system show that condensation at low temperatures favours the formation of not only 1: 1 molecular complexes, but also the more thermodynamically advantageous complexes with a higher proportion of components. The formation of strongly polarized associated molecular compounds of the donor-acceptor type in bromine-propylene mixtures at low temperatures can promote electron transfer and spontaneous ionized states. The energy involved in the nonequilibrium absorption of a light quantum (the charge-transfer band) at the long wavelength end of the absorption band at 200 nm (see Fig. 6.4) is 0.5 eV. The energy of thermal excitation may be lower, so it is natural to assume that the strongly interacting complexes which form during condensation with the evolution of a large amount of heat may favour the spontaneous production of ions or ion radicals which facilitate the subsequent addition reaction. Unfortunately, the spectra of cation radicals and negative molecular ions have not been practically investigated.

It is shown in [417] that a cation like $C_3H_6^+$ absorbs at around 560 nm. Accordingly, it may be assumed that some of the absorption in the bromine-propylene system in the interval 500-1 000 nm is due to this cation radical.

The final products form in the last stage of the reaction, usually at higher temperatures during a phase change when the molecules show a somewhat increased mobility and can overcome the activation barrier associated with the re-arrangement of the structure. The presence of molecular complexes at the time of a phase change may result in the orientation of molecules favourable for the addition reaction. In the circumstances, only one final product will be formed in good yield.

The stage of complex formation can be separated from that of final-product formation by depositing the olefin and the halogen on a cooled surface in alternate layers. Cocondensation from molecular beams leads to an intimate mixing, so that all the stages of the reaction proceed at temperatures close to the boiling point of liquid nitrogen.

Because the reaction proceeds in consecutive stages, this affects the activation energy for the overall process. According to the theory of absolute reaction rates, the formation, by molecular interactions, of unstable, probably strongly solvated exothermic molecular complexes close in structure to an intermediate state reduces the effective activation energy by the heat of solvation for the activated complex. In the presence of associates, this reduction may be appreciable and may substantially promote the production of ions and the progress of chemical reactions at low temperatures.

The mechanism described above is examined in [412, 418, 419]. According to [402], the activation energy for the formation of ions in nonpolar solvents ranges between 100 and 125 kJ $mole^{-1}$, according to the olefin involved. Therefore, low-temperature reactions involving ions in nonpolar solvents are highly unlikely to take place.

As regards fast halogenation of olefins at low temperatures, a somewhat different mechanism may be proposed for the formation of final products from molecular compounds, namely one in which the preceding production of ions does not take place. The conversion of a two-component system into a system of oriented and interacting polarized molecules brings about a marked electron density re-distribution and favours the simultaneous dissociation of old and formation of new bonds. As a result, the halogenation and hydrohalogenation of olefins can proceed in the solid phase at low temperatures.

According to the schemes discussed above, the degree of conversion η is given by

$$d\eta/dt = k_1 n \tag{6.3}$$

where n is the concentration of reactive species including in the general case ions, radicals, ion radicals, and reactive complexes, and k_1 is the respective rate constant.

Variations in the concentration of active centres can be written

$$dn/dt = k_2 n - k_3 n \tag{6.4}$$

The first term on the right-hand side of Eq. (6.4) describes the production of reactive species due to the reversible conversion of non-reactive 1: 1 complexes (k_2 is the rate constant which is a function of the equilibrium constant of the process). The second term on the right-hand side of Eq. (6.4) describes the withdrawal of active centres from the reaction, for example as a result of their trapping in the solid, with the respective rate constant k_3.

Eliminating time between Eqs. (6.3) and (6.4) and integrating gives variations in the concentration of active centres as a function of the degree of conversion and their initial concentration

$$n = n_0 + (k_2 - k_3)\eta/k_1 \tag{6.5}$$

Substituting Eq. (6.5) into Eq. (6.3) gives

$$d\eta/dt = k_1 n_0 + (k_2 - k_3)\eta$$

On integrating the above equation, we obtain the degree of conversion as a function of time and the rate constants for the separate stages of the reaction

$$\eta = \frac{k_1 n_0}{k_2 - k_3} \{\exp[(k_2 - k_3)t] - 1\} \tag{6.6}$$

It follows from Eq. (6.6) that the kinetics can markedly change according to the relative magnitudes of the constants k_2 and k_3. If $k_2 \gg k_3$, which implies that the number of active centres formed exceeds that of active centres lost, then

$$\eta = (k_1 n_0/k_2)[\exp(k_2 t) - 1] \approx (k_1 n_0/k_2)\exp(k_2 t) \tag{6.7}$$

and the final product builds up exponentially. In the circumstances, the rate of the reaction proceeding in the system under study might increase abruptly, leading to an explosion. In fact, such explosions do occur. If k_2 only slightly exceeds k_3, no sudden rise in the reaction rate will take place, but the final product will be formed by an autocatalytic process. If $k_2 \ll k_3$, which implies that the rate of loss exceeds the rate of formation of active centres, then

$$\eta = (k_1 n_0/k_3)[1 - \exp(-k_3 t)] \tag{6.8}$$

and the rate of build-up for the final product will be a maximum at the beginning. In such a case, typical kinetic curves are observed, tending to the limit with time. Thus, the halogenation and hydrohalogenation of olefins proceeding at various rates and over a broad temperature interval in the liquid and solid phases are a sufficiently convenient object for studies into the mechanism of chemical reactions at low temperatures.

6.2. REACTIONS OF ADDITION TO OLEFINS IN SOLVENTS

As a rule, experiments with chemical reactions at temperatures close to the boiling point of liquid nitrogen pose appreciable difficulties and involve the use of unverified techniques. Because of this, quantitative data are difficult to obtain. Better insight into the kinetics of low-temperature reactions can be obtained by investigating them over a broad temperature range. This can, for example, be done by letting a reaction proceed in a solvent having a low melting point and a high boiling point.

6.2.1. Chlorination

Interesting results have been obtained for the chlorination of ethylene and some other olefins in liquid hydrogen chloride and propane [420, 421]. Using propane as solvent and the calorimetric method, the investigators have been able to obtain for the first time the effective kinetic characteristics for the chlorination of ethylene at low temperatures. The activation energy for the chlorination of ethylene has been found to be 25 kJ mole $^{-1}$.

The use of hydrogen chloride as solvent in various chemical processes at low temperatures is very promising. This is because, like other hydrogen halides, hydrogen chloride can form complexes by reacting with, say, compounds having multiple bonds [422, 423]. Complex formation has also been investigated in the systems acetylene-chlorine and acetylene-hydrogen chloride [423, 424].

Various molecular complexes are also formed in the system ethylene-chlorine-hydrogen chloride. The reaction takes place at 98 K and, probably, proceeds at the instant when the eutectic mixture of chlorine-ethylene and ethylene-hydrogen chloride molecular complexes melts. The reaction produces chromatographically pure dichloroethane with a yield close to 100%. With hydrogen chloride used as solvent, the experimentor can control the rate of the reaction at will, which cannot be done in the reaction using no solvent. Also, with liquid hydrogen chloride, the low-temperature chlorination of various olefins can be conducted by streaming or bubbling the chlorine and olefin through a liquid hydrogen chloride column. On this basis, fundamentally novel chemical-engineering processes can be set up, in which synthesis can be carried out in a single stage and the expensive fractionation of the final products can be dispensed with. Also, the use of liquid hydrogen chloride as solvent is attractive because it is a by-product of many chemical processes, and its recovery and utilization pose an urgent problem.

6.2.2. Bromination

The bromination of several olefins in nonpolar solvents at low temperatures has been investigated over a broad temperature interval. Most of the experimental findings have been obtained, using the system cyclohexene-bromine in hexane. Cyclohexene has a relatively high boiling point (353 K) and a relatively low melting point (169 K), a fact which makes this compound suitable for experiments over a wide temperature range. The bromination of cyclohexene proceeds at rates convenient for measurement; the reaction has a negative temperature coefficient.

The kinetics of cyclohexene bromination has been investigated in the temperature interval 303-203 K. It has been established that the reaction is described by a general third-order equation (of order two for bromine and of order one for cyclohexene). The effective rate constant of a third-order reaction is a complex function of temperature (Fig. 6.5). The activation energy, as found from experimental data, is —62 kJ mole^{-1} in the temperature interval 303-283 K, —7 kJ mole^{-1} in the temperature interval 243-223 K, and 2.5 kJ mole^{-1} in the interval 223-203 K. The activation energy evaluated from the initial reaction rates checks with the above values [425].

Experiments with the halogenation of olefins in nonpolar solvents have discovered charge-transfer complexes of various halogens and olefins [425, 426] and also halogen-solvent complexes of the donor-acceptor type [427, 428]. The results of IR and Raman spectroscopy of the complexes formed by chlorine and bromine with olefins and acetylene and also amines are presented in [429-433]. The complexes were obtained by sputtering onto a liquid-nitrogen-cooled substrate. The degree of charge transfer in the complexes formed by chlorine and bromine with olefins is evaluated in [430]. An interesting change has been observed in the band intensity of the halogens as a result of complex formation. This may be associated with changes in the vibration mode of the halogens caused by the formation of an intermolecular bond in the complex [430]. At first, the charge-transfer bands were found in the spectra of the solid phase [401]. Later, they were found in the spectra of solutions [434] and in the spectra of complexes in a nitrogen matrix [435]. The kinetics involved in the bromination of olefins has been investigated and the presence of a radical and a molecular trend in the process has been established [402].

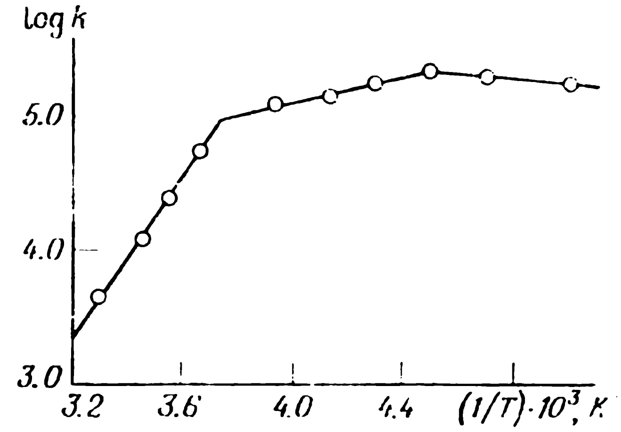

Fig. 6.5. Logarithm of the rate constant for the bromination of cyclohexene in hexane as a function of $1/T$

6.2.3. Nitration and Nitrosyl-Chlorination

Nitrogen dioxide (a dimer) reacts with most unsaturated compounds [436, 437]. The mechanism of the reaction varies with the conditions in which the reaction takes place. The reaction of N_2O_4 with isobutylene and its derivatives without a solvent is assumed to proceed by the ionic mechanism [438]. At low temperatures, such reactions occur at a very high, practically explosive, rate [401]. It has been hypothesized that such reactions involve a nitrosyl nitrate form, $N_2O_4(ON—ONO_2)$, which has a high reactivity [439]. However, there is evidence in favour of the radical mechanism of the process, usually in nonpolar solvents. For example, calorimetric measurements have shown that nitrogen dioxide begins to react with cyclohexene in hexane, with a three-fold to a ten-fold excess of the olefin, at around 223 K, the heat of the reaction being 167 ± 13 kJ mole^{-1} and the activation energy being 54 ± 4 kJ mole^{-1} [107]. The reaction is accompanied by the formation of free radicals detected by the ESR technique at low temperatures, and the radicals are produced at the same temperature as an exothermic reaction commences. After the mixture has been warmed up to 293 K, the radical concentration is 10^{16} ml^{-1}. These radicals are produced by the reaction of N_2O_4 with olefins even at room temperature [440], and their appearance is related to the secondary reactions of nitroalkyl radicals.

The above evidence and also the kinetics of addition of N_2O_4 to C_6H_{10} in a nonpolar solvent [107] suggest the radical mechanism for the reaction, including the dissociation of N_2O_4 into two NO_2 radicals, insertion of NO_2 into a double bond, and the subsequent reactions of the nitroalkyl radical:

$$\begin{aligned}
N_2O_4 &\rightleftharpoons 2NO_2 \\
NO_2 + C_6H_{10} &\rightleftharpoons \dot{C}_6H_{10}NO_2 \\
\dot{C}_6H_{10}NO_2 + NO_2 &\longrightarrow C_6H_{10}(NO_2)_2 \text{ or } C_6H_{10}(NO_2)(ONO) \\
\dot{C}_6H_{10}NO_2 + N_2O_4 &\longrightarrow C_6H_{10}(NO_2)_2 + NO_2 \\
\dot{C}_6H_{10}NO_2 + C_6H_{10} &\longrightarrow \text{Polymerization products}
\end{aligned}$$

According to the elementary rate constants, the above scheme leads to a second-order rate equation which agrees with the reaction that takes place in experiment in the absence of oxygen, with an activation energy of 62 kJ $mole^{-1}$ [107]. As the temperature is brought down to 233-223 K and the concentration of N_2O_4 in the solution is increased, the reaction mainly proceeds by the chain mechanism for which the activation energy is reduced to 39 kJ $mole^{-1}$ from the value computed from the reaction scheme. On the strength of the evidence presented in [107], it may be assumed that the fast reaction of N_2O_4 with olefins observed at low temperatures displays the characteristic features of a chain and a thermal explosion. The occurrence of the fast reaction at low temperatures and high concentrations of the reactants may be explained by an increase in the rate with which N_2O_4 dissociates into radicals as a considerable proportion of the dioxide is combined with the olefin into a complex, which fact results in loosening the N—N bond in the N_2O_4 molecule. This reaction proceeds by the mechanism of molecular-induced homolysis [441]. The molecular complex of N_2O_4 and C_6H_{10} has been found in a solution of *n*-hexane at 198 K, when no reaction can take place (the presence of the complex has been revealed by optical absorption at $\lambda_{max} = 255$ nm [107]).

As easily, olefin oxides react at low temperatures with nitrosyl chloride to give addition and telomerization products. In this case, too, the reactants first form a donor-acceptor molecular complex spectrophotometrically detected in a solution of NOCl and cyclohexene α-oxide in pentane at 153 K, where the reaction practically comes to a stop and the equilibrium is shifted towards the complex formation [442]. It has been shown that the reaction proceeds by the radical mechanism, because its rate increases when more oxygen is withdrawn from the mixture and also when the mixture is exposed to visible light. Also, in the presence of a radical trap, 2-nitroso-2-methylpropane, the ESR technique has detected free radicals. An interesting feature of this reaction is that its rate goes up as the temperature is brought down. The negative temperature coefficient is observed in the temperature range from 303 K to 228 K. With a further reduction in temperature (down to 178 K), the temperature coefficient becomes positive [442]. The effective activation energy is about —38 kJ mole^{-1} and +13 kJ mole^{-1}, respectively.

A similar change of sign by activation energy has also been observed in the bromination of cyclohexene [443]. Theoretical consideration shows that the negative activation energy is associated (in the absence of other reversible stages) with the complexes formed by the starting components and taking part in the reaction. At a certain temperature decided by the concentration of the reactants and the absolute value of enthalpy for complex formation, the negative activation energy of necessity changes to positive.

On the basis of kinetic data and thermochemical calculations, it has been hypothesized that NOCl reacts with α-oxides by a radical mechanism [442]. According to this hypothesis, the reaction is initiated by the chlorine atoms derived from NOCl. The bond in the NOCl molecule cannot be ruptured directly at low temperature (the bond energy is 159 kJ mole^{-1}). However, the formation of the complex may loosen the NO—Cl bond, so that it is eventually broken (molecular-induced homolysis) [441].

The view held currently is that many chemical reactions between electron-donor and electron-acceptor molecules proceed via a stage of intermediate molecular complexes. The role that these complexes play in the reactions has not yet been elucidated completely. Apparently, the bonds in the molecules making up the complex may in some case be loosened, and this entails a reduction in the activation energy for the reaction. If the photoexcitation of the complex at the wavelength of the charge-transfer band produces the same products as the dark thermal reaction, this may serve as an argument in favour of the complex taking part in the reaction even in the absence of radiation.

This approach has been used in investigating the role of tetranitromethane complexes in the chemical reactions involving it. It has been found that the weak complex formed by $C(NO_2)_4$ and triphenylamine shows optical absorption around $\lambda > 735$ nm where the photon energy is smaller than the energy for the dissociation of the C—N bond in the $C(NO_2)_4$ molecule (163 kJ mole^{-1}). Irradiation of frozen solutions of the reactants in benzene with infrared light produces free radicals detected by the ESR technique [444]. The ESR records clearly show the spectrum of the NO_2 radical formed by the homolytic decomposition of the complex. It has been found that photochemical action is produced by photons in the entire absorption region of the complex (Fig. 6.6). Thus, the energy sufficient to bring about the photochemical decomposition of the complex is 111 kJ mole^{-1} (at $\lambda = 1\,080$ nm). This implies that for the molecules combined into the complex the activation energy for decomposition into free radicals is substantially reduced.

The fact that the thermal and photochemical reactions of $C(NO_2)_4$ with unsaturated compounds in the liquid phase produce identical ESR signals indicates that the complex can break up into radicals in the absence of irradiation as well. The ease with which the thermal radical processes involving $C(NO_2)_4$ proceed [445] is explained by a reduction in the activation energy due to complex formation.

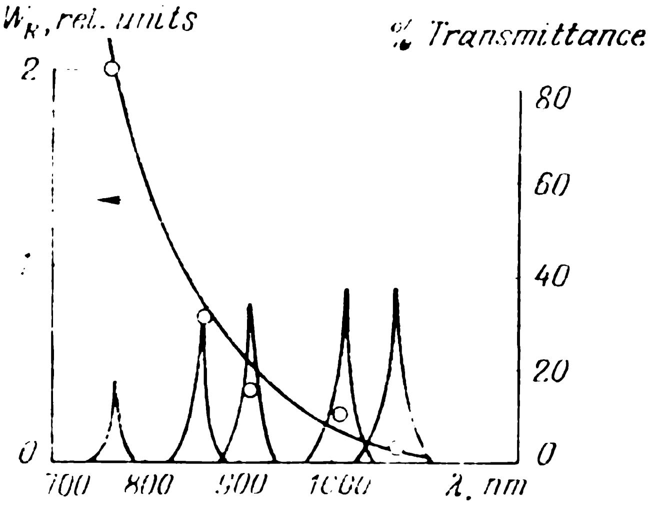

Fig. 6.6. Rate of formation of radicals from $[C(NO_2)_4 \cdot Ph_3N]$ as a function of illumination wavelength and transmission spectra of the interference filters used for irradiation

6.3. ROLE OF MOLECULAR COMPLEXES IN THE HALOGENATION OF OLEFINS

The idea that molecular complexes might take part in the halogenation of olefins was advanced by Dewar as far back as the mid-40s. It is not, however, until quite recently that the existence of such complexes has been proved experimentally and their role in liquid-phase halogenation has been investigated over a broad temperature range and in various solvents [402].

A reaction of a halogen with an olefin produces a charge-transfer complex: the olefin acts as an electron donor and the halogen as an electron acceptor. The complexes thus formed absorb in the range 240-320 nm of the UV part of the spectrum. The complexes made up of chlorine or bromine and olefins have been investigated least of all owing to the chemical reactions that occur in such systems. For proper insight into the part played by the complexes, it is vital to know their structure. Relevant theoretical analysis is presented in [446]. Analysis by the SCF-MO-LCAO CNDO/2 method is presented, taking the molecular interactions of ethylene with chlorine and bromine as a first example.

The relationship has been traced between variations in the energy of the system consisting of one molecule of ethylene and one molecule of a halogen, on the one hand, and the relative position of the molecules and variations in the internuclear distances and the valence angles inside the molecules, on the other.

The likely configurations for the complexes of ethylene and bromine or chlorine, constructed on the basis of computations, are shown in the accompanying figure (structures *a* and *c* at the top, and structures *b* and *d* at the bottom).

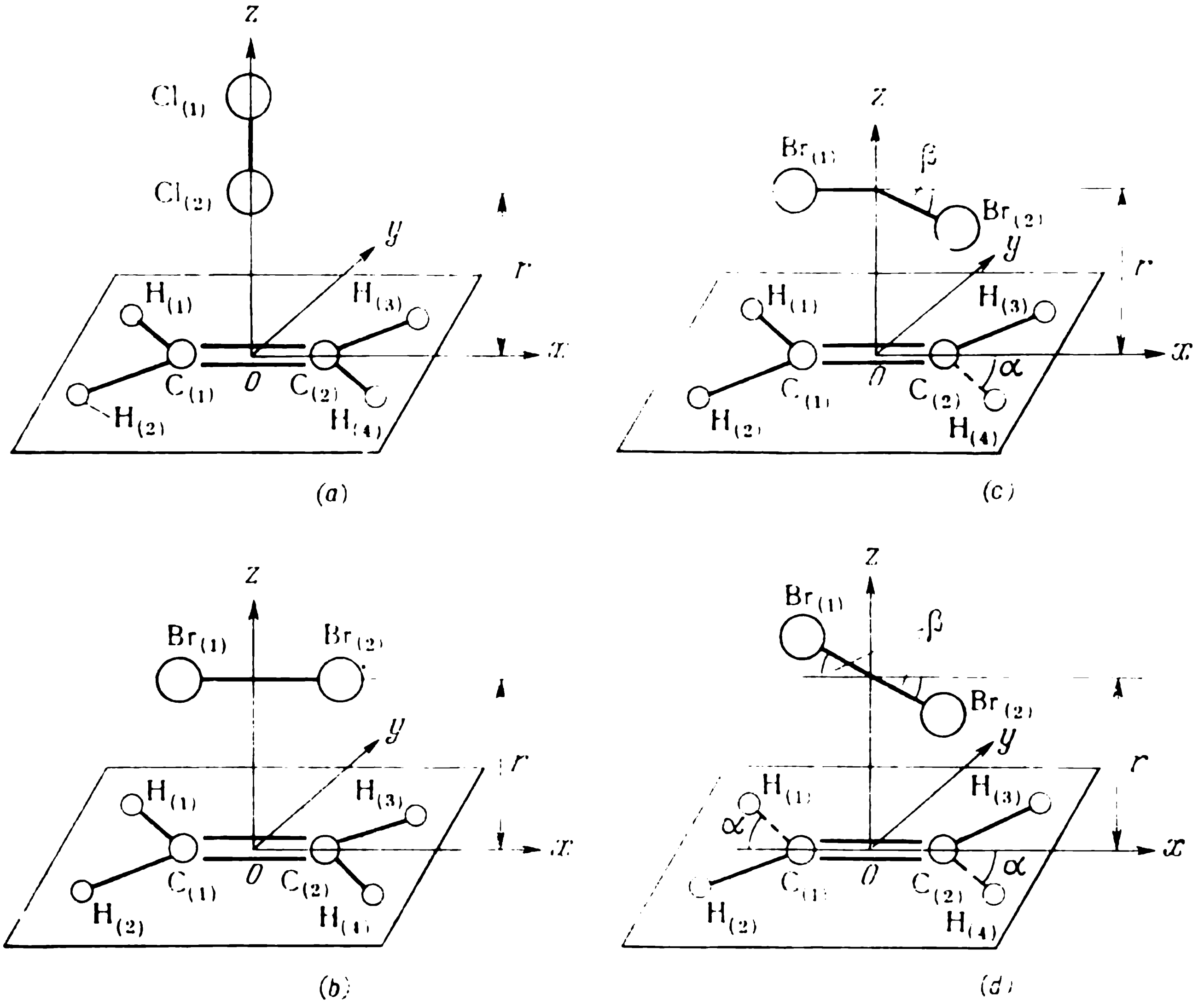

It has been found that the substantial minimum on the potential energy surface is associated with structure *a*. For the complex incorporating a chlorine molecule, only one minimum has been found on the potential surface. It corresponds to structure *a*. The chlorine molecule lies at right angles to the ethylene molecule and its z-axis runs along the C_2 axis in the ethylene. Also, the chlorine molecule is polarized so that the chlorine atom closest to the ethylene carries a positive charge. The computations for the chlorine complex agree with those carried out earlier [447, 448].

New results have been obtained for the complex containing bromine. With the bromine molecule placed close to the ethylene molecule, two minima are observed on the potential energy surface. The first minimum corresponds to the same configuration as for the chlorine complex, namely structure *a*. For the bromine complex, however, this minimum is 29.7 kJ $mole^{-1}$ lower than the minimum for the isolated molecules. The second minimum corresponds to structure *b*. In this structure, the bromine molecule is brought close to the ethylene molecule in the *xOz* plane so that the *z*-axis of the bromine molecule is parallel with the C_2 axis in the ethylene molecule, running in the direction of the double bond. This minimum is 9.2 kJ $mole^{-1}$ below that for the isolated ethylene and bromine molecules.

Halogen-olefin complexes are probably intermediate products of the reaction. From this view-point, it is very interesting to study small variations in internuclear distances and angles. A substantial gain in energy is observed in the two cases corresponding to structure *c*.

In the first case, the $H_{(4)}$ atom is turned about the *Ox* axis in a plane parallel to the *yOz* plane through an angle $\alpha = 10^\circ$ down and away from the bromine molecule. One of the bromine atoms, $Br_{(2)}$, is turned clockwise in a plane parallel to the *xOy* plane through an angle $\beta = 10^\circ$. The distance from the bromine atoms to the ethylene plane is 3 Å. The gain in energy is 21 kJ $mole^{-1}$.

The second case differs from the first one only in that the $Br_{(2)}$ atom is additionally brought 0.1 Å closer to the ethylene plane along the *Oz* axis. In this case, the gain in energy is 19.3 kJ $mole^{-1}$. It is interesting to note that the gain in energy is smaller for structure *d* which differs from structure *c* in that the $H_{(1)}$ and $Br_{(1)}$ atoms are displaced similarly.

It is an easy matter to notice that the energy of the models symmetrical about the *Oz* axis is greater than the energy of the models for which changes in the positions of the bromine and hydrogen atoms occur on one side of the *yOz* plane. Accordingly, it may be concluded that at first only one CH_2 group is re-arranged in the ethylene. It is likely that the other CH_2 group interacts with the bromine atom from the second bromine molecule lying, say, under the *xOy* plane. Indeed, preliminary computations show that the gain in energy for a system made up of an ethylene molecule and two bromine molecules is 46 kJ $mole^{-1}$. This result agrees well with the kinetics of olefin bromination in nonpolar solvents.

The halogen-olefin complexes investigated experimentally have been found to have small equilibrium constants ($K_{eq} < 1$) and small formation enthalpies ($|\Delta H| < 20$ kJ $mole^{-1}$) [402]. These values of ΔH are close to the activation energy values for many reactions of olefin halogenation and may contribute substantially to the energetics of the process.

Experiments on the halogenation of olefins in the temperature interval 303-77 K in nonpolar solvents have yielded a wealth of new data about halogen-olefin molecular complexes, their role in the reaction, and the mechanism of the process.

At the present state of the art, the following scheme may be proposed for olefin halogenation, taking into account the three likely reaction mechanisms (radical, molecular with the participation of $Ol \cdot X_2$ and $Ol \cdot (X_2)_2$ complexes, and polar involving classical and nonclassical ions):

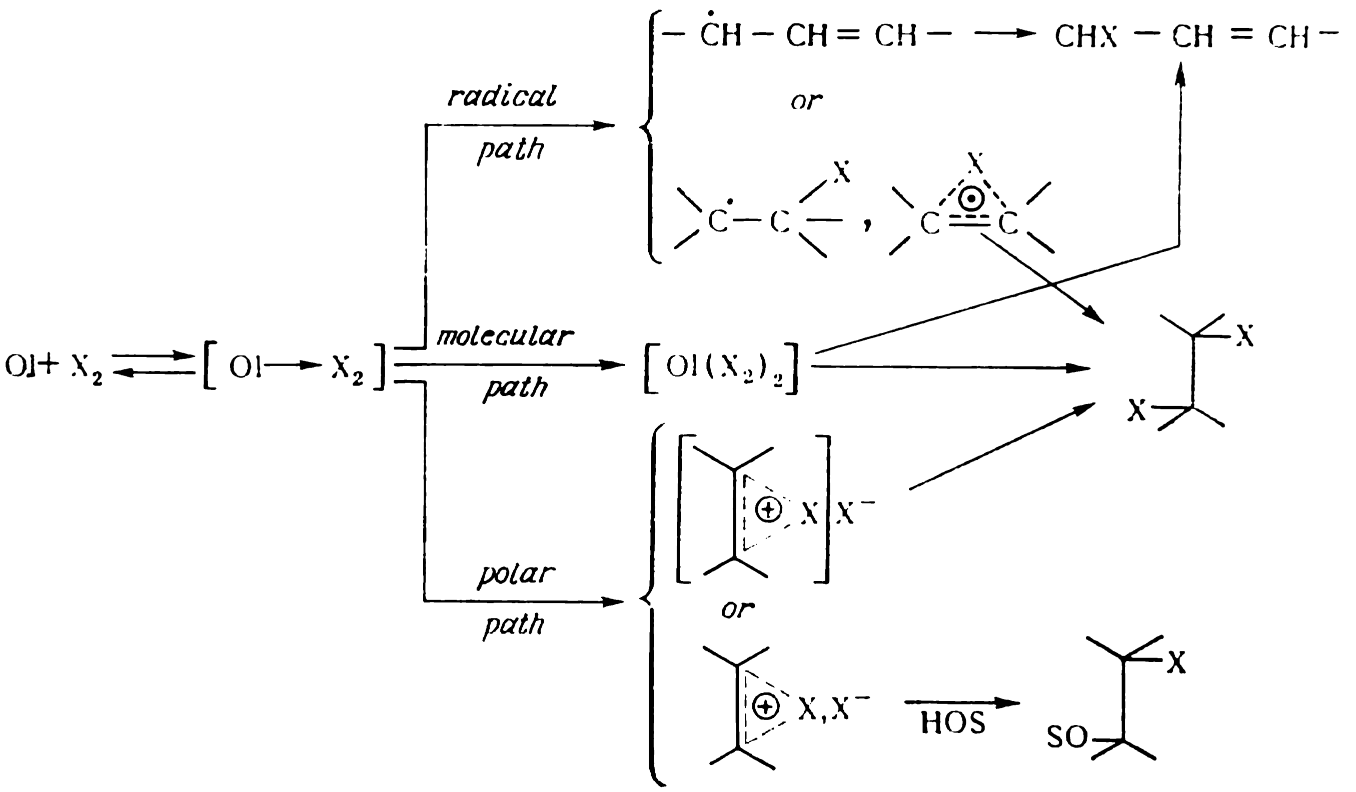

Working from the idea that the complexes may take part in the reaction, notably in polar solvents, and using an electrostatic model, a technique has been devided for evaluating the energy barriers for the various stages of the reaction [402]. In contrast to the semi-ion pair method [449], the new method has given the correct sequence of reactivities: $Cl_2 > Br_2 \gg I_2$. Other aspects of the reaction in polar solvents are examined in [402].

From the view-point of cryogenic chemistry, of special interest are reactions in nonpolar solvents. A major distinction of such reactions is the negative activation energy [235]. At present, this unusual kinetic feature has been discovered also for the chlorination of olefins [450], bromination of diphenylethylenes [451], dimerization of α-oxides [452], nitrosyl-chlorination of α-oxides [442], and conjugate reactions in the systems halogen-olefin-olefin oxide [453]. It has also been found for the radical halogenation of olefins in nonpolar solvents [416, 454].

Referring to reactions which involve halogens, notably their insertion in multiple bonds at low temperatures, [455] presents a kinetic analysis of sequential and concurrent reaction schemes and proposes criteria by which the involvement of molecular complexes in a reaction can be verified.

It has been stressed more than once in the literature that the mere detection of a molecular complex in a reacting system is no proof of its participation in the reaction [456, 457]. The formation of molecular complexes is a reversible process characterized by rate constants k_1 and k_{-1}, and the equilibrium constant $K_{eq} = k_1/k_{-1}$:

$$A + D \underset{k_{-1}}{\overset{k_1}{\rightleftarrows}} \pi \tag{6.9}$$

where A is an acceptor, D is a donor, and π is a complex.

The rate constant k_1 usually ranges between 10^9 and 10^{10} l mole^{-1} s^{-1} in value [458]. At $K_{eq} = 1$ to 10 l mole^{-1}, this implies that the lifetime of the complex must range between 10^{-8} and 10^{-9} s. The complex formation is usually complicated by the effect of the solvent [459], and this strongly affects the values of the respective rate constants [460].

Consider the simplest reaction schemes involving complexes, namely a sequential scheme (I) and a concurrent scheme (II), not complicated by the effect of the solvent:

$$\text{I} \left\{ A + D \underset{k_{-1}}{\overset{k_1}{\rightleftarrows}} \pi \xrightarrow{k_2} P \right.$$

$$\text{II} \left\{ \begin{array}{l} A + D \underset{k_{-1}}{\overset{k_1}{\rightleftarrows}} \pi \\ \\ A + D \xrightarrow{k_2} P \end{array} \right.$$

where π is the complex, and P is the reaction product.

If the reaction in a system proceeds at a fast rate and produces a reversible complex and variations in the complex concentration can easily be monitored, then schemes I and II will kinetically look identical under the usual experimental conditions at $[D]_0 \gg [A]_0$. In terms of the reaction rate, both schemes lead to a first-order kinetic equation [457].

Because of the fast, reversible stages in the scheme, associated with, say, complex formation, the observed activation energy may well show temperature dependence. The negative activation energy may serve as a kinetic criterion which confirms the participation of molecular complexes in the reaction.

The scheme in which a complex is formed concurrently with the main product does not lead to negative activation energies. Consider the two schemes from this view-point in more detail.

For scheme II, the reaction rate W is written

$$W = d[A]/dt = -k_2[A][D] \tag{6.10}$$

Molecular complexes are formed and break up at very high rates. Let $[D] \gg [A]$. For the total concentrations, $[D]_\Sigma = [D] + [\pi] \approx [D]$

and $[A]_\Sigma = [A] + [\pi]$. Because $[\pi]$ is defined in terms of the equilibrium constant K_{eq}, Eq. (6.10) can be re-written thus:

$$W = -k_2 \frac{[A]_\Sigma [D]_\Sigma}{1 + K_{eq} [D]_\Sigma} \tag{6.11}$$

or

$$k_{obs} = k_2/(1 + K_{eq} [D]) \tag{6.12}$$

Similarly, for scheme I,

$$W = -k_2 \frac{K_{eq} [A]_\Sigma [D]_\Sigma}{1 + K_{eq} [D]_\Sigma} \tag{6.13}$$

and

$$k_{obs} = k_2 K_{eq}/(1 + K_{eq} [D]) \tag{6.14}$$

Equations (6.12) and (6.14) differ from the ordinary second-order kinetic equations in that the rate constant is a function of reactant concentrations. This kind of dependence points to the formation of molecular complexes in the system and enables their equilibrium constant to be found from kinetic data.

Differentiating Eq. (6.12) with respect to the reciprocal temperature gives

$$\begin{aligned} E_{obs} &= -\partial \ln k_{obs}/\partial T^{-1} = -\partial \ln k_2/\partial T^{-1} + \partial \ln (1 + K_{eq} [D])/\partial T^{-1} \\ &= E_2 + \frac{K_{eq} [D]}{1 + K_{eq} [D]} |\Delta H|, > 0 \end{aligned} \tag{6.15}$$

where E_{obs} is the observed activation energy, E_2 is the true activation energy for a bimolecular reaction between an acceptor and a donor, $|\Delta H|$ is the absolute enthalpy, and K_{eq} is the equilibrium constant for complex formation.

It is seen from Eq. (6.15) that E_{obs} is a function of the donor concentration and increases from E_2 to $E_2 + |\Delta H|$. A similar situation exists in passing to low temperatures because of an increase in K_{eq}. An increase in K_{eq} [D] is accompanied by a gradual rise in the activation energy so that

$$E_{obs}^{max} - E_{obs}^{min} = |\Delta H| \tag{6.16}$$

Thus, the molecular complex present in the system affects the energy of the process also when it is formed concurrently with the main product of the reaction. In such a case, it is legitimate to say that the complex has an indirect effect on the reaction. It may so happen that whereas the activation energy is a function of temperature, it remains a positive quantity.

In the sequential scheme involving a molecular complex, a different situation can emerge. For a simple biomolecular scheme we may write

$$E_{obs} = E_2 - |\Delta H| + \frac{K_{eq}\,[D]}{1 + K_{eq}\,[D]} |\Delta H| \qquad (6.17)$$

If $E_2 > |\Delta H|$, then the situation is similar to that of the concurrent scheme. If $E_2 < |\Delta H|$, then at low values of K_{eq} [D], that is, at not too low temperatures and small donor concentrations it may be expected that the temperature coefficient of the reaction will be negative. In turn, the negative coefficient will tend to change sign as the temperature is lowered and the donor concentration is increased. Equation (6.16) will hold in that case, too. The more complex cases, such as trimolecular reactions, are examined in [402]. The negative temperature coefficient may arise if the reaction involves two different types of complexes.

Thus, the schemes where the complex is formed concurrently with the main product cannot explain why the activation energy becomes negative. In contrast, an explanation is offered by schemes where the complex is an intermediate product. Thus, negative activation energies may be regarded as a kinetic evidence for the direct participation of the molecular complex in the chemical reaction.

As regards the halogenation of olefins, negative activation energies are an indication that the potential energy of the intermediate state is lower than the potential energy of the starting molecules. By the theory of activated complexes, the intermediate state corresponds to a maximum of free and potential energies. The positive free energy required for the reaction to proceed is provided by the large negative values of activation entropy. Thus, the process is to a considerable degree controlled by entropy contributions. Because the molecular complexes taking part in the reaction differ in composition, the starting system adapts itself to the intermediate structure via complex formation stages. Such reactions usually proceed by simultaneous dissociation of the old and formation of the new bonds and do not call for substantial activation energies. Such a reaction may occur without any previous formation of ions or radicals, and its mechanism may be called molecular [402].

Through experiments with olefin halogenation, notably bromination, over a wide temperature range, it has been found that the molecular mechanism involves two types of molecular complexes differing in composition. For bromination, these complexes are $Br_2 \cdot Ol$ and $Br_2 \cdot Ol \cdot Br_2$, which are 1:1 and 2:1 complexes.

Presumably, the reaction proceeds according to the following scheme:

$$Br_2 + Ol \rightleftarrows Ol \cdot Br_2 \qquad (\pi_1)$$

$$Ol \cdot Br_2 + Br_2 \rightleftarrows Br_2 \cdot Ol \cdot Br_2 \qquad (\pi_2)$$

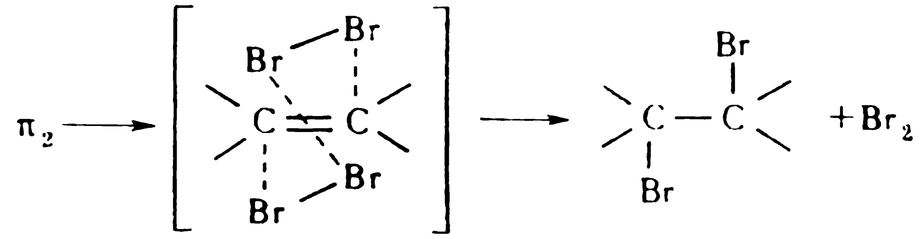

Analysis of molecular models shows that the size of the bromine molecule enables the intermediate cyclic state to form easily, without an excessive distortion of bond length. The existence of complexes of a higher composition than 1: 1 in the halogen-olefin system has been proved from inspection of UV spectra for mixtures of bromine and cyclohexene [416]. The existence of $C_6H_{10} \cdot (Br_2)_2$ has been proved by low-temperature IR and Raman spectroscopy [429, 430]. IR spectra for samples cocondensed from molecular beams onto a liquid-nitrogen-cooled sample block show bands associated with the strain vibrations of the double bond in the 1:1 and 2:1 complexes. The shift of the band in the 2:1 complex is greater, and there is every ground for believing that this complex has a higher energy of formation. Warm-up to 113 K has been found to cause the 2:1 complex to turn into dibromoalkane. The reactants not combined in the complex did not take part in the process. Raman spectroscopy shows that the 2: 1 complex has a symmetrical structure close to that of the intermediate state shown in the accompanying scheme. This is new experimental evidence in favour of the mechanism proposed some time ago for the halogenation of olefins involving two complexes.

6.4. MOLECULAR COMPLEXES IN CONVERSIONS OF α-OXIDES

Interesting data have been yielded by studies into the part played by molecular complexes in various reactions of α-oxides with halogens and their derivatives [442, 452, 453, 461, 462]. Several processes leading to complex formation have been found to take place in systems comprised of a halogen, an oxide, and an olefin. In contrast to olefin halogenation which produces complexes varying in composition, the reactions involving α-oxides produce two complexes having the same composition, but differing in structure.

Halogen-olefin oxide complexes have been obtained in the crystalline state [463] and investigated spectrally at 77 K [464]. In [462], the complexes containing Br_2, I_2, ICl, and oxides of propylene and cyclohexene are studied in solutions. The change in the optical density observed when halogen solutions are mixed with oxides in carbon tetrachloride is attributed to the formation of labile 'outer' complexes which gradually turn into the more stable 'inner' complexes. UV, IR, Raman, and NMR spectra [465] all show that the inner complex is formed owing to the reaction of the halogen with the entire ring as a kind of π-donor. For the outer complex, the structure is that typical of the conventional π-complexes. The enthalpy for the formation of the outer complex is $\Delta H = -8 \pm 2$ kJ mole ^{1}, and for the inner complex, $\Delta H = -46$ kJ mole^{-1}. Electrical conductivity measurements have shown that the inner complexes are present in an unionized form. For solutions of a mixture of cyclohexene oxide, iodine, and bromine in 1,2-dichloroethane, the electrical conductivity $\varkappa$ at 20°C has been found to be $5 \times 10^{-4}\ \Omega^{-1}\ \text{cm}^{-1}$. This value is substantially lower than that for salt-like compounds. It has been established by the *isomole series* method that the electrical conductivity is a maximum when the interacting components are present in the 1: 1 ratio.

At low temperatures, kinetic studies have been most detailed into the reactions in olefin-oxide-halogen systems [456, 466], cyclodimerization of α-oxides [465], and reactions with nitrosyl chloride [442].

Cohalogenation of olefins and α-oxides leads to 2,2-dihaloalkyl ethers. For example, in the system cyclohexene-bromine-cyclohexene oxide in a solution of carbon tetrachloride the process goes on as follows:

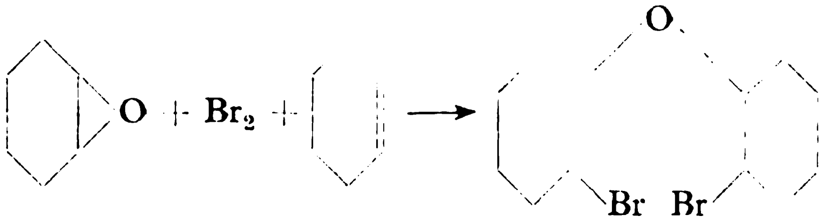

This is accompanied by the concurrent bromination of olefin. The product ratio depends on the initial concentrations of oxide and olefin. According to [466], if the concentration of α-oxide substantially exceeds that of olefin, the products are predominantly 2,2-dihaloalkyl ethers.

The reaction proceeds with a negative temperature coefficient, and the yield of the respective ethers increases with decreasing temperature. The yield of the final products is depicted by an S-shaped kinetic curve. This form of kinetics and the negative temperature coefficient point to the participation of molecular complexes in the chemical reaction. In the general form, the process can be visualized taking place as follows:

$$O + X_2 \underset{k_{-1}}{\overset{k_1}{\rightleftarrows}} \pi \underset{k_{-2}}{\overset{k_2}{\rightleftarrows}} \sigma$$

$$X_2 + Ol \underset{k_{-3}}{\overset{k_3}{\rightleftarrows}} X_2 \cdot Ol$$

$$\sigma \quad X_2 \cdot Ol \xrightarrow{k_4} \text{Product}$$

where π and σ are the outer and inner complexes of the oxide with halogen X_2, respectively; and $X_2 \cdot Ol$ is the complex of a halogen with olefin Ol.

The suggested mechanism answers the formally observed fourth order in this reaction, and the negative activation energy checks with the enthalpies for the formation of π- and α-complexes [453, 465].

The reactions of α-oxides are a graphic example of the reactions stimulated by low temperatures and complex formation [465]. Molecular complexes of halogens with α-oxides can be accumulated in appreciable amounts at temperatures between 213 K and 203 K. According to NMR evidence, the subsequent warm-up to 253 K leads to the dimerization of α-oxides. At room temperature, this process does not take place. Instead, α-oxides are slowly telomerized [467].

The likely mechanism by which α-oxides are dimerized can be depicted, taking ethylene oxide as an example, as follows:

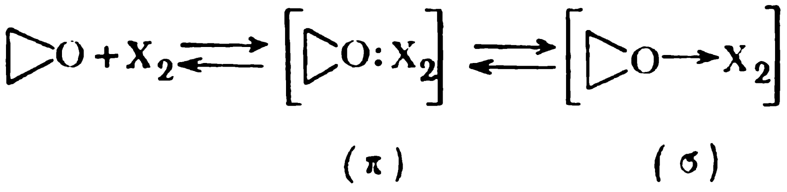

$$2\sigma \longrightarrow \text{Dioxane} + 2X_2$$

The conversion of two σ-complexes to dioxane goes via a cyclic transitory state. In addition to halogens, cyclization at low temperatures can be promoted by BF_3 and other Lewis acids. The cyclic macroethers produced at low temperatures can contain as many as eight oxygen atoms per molecule.

Depending on prevailing conditions, molecular complexes involving α-oxides can turn to the final products by different mechanisms. One of the alternatives is the radical path of the reaction [442]. It has been shown recently that the radical-chain mechanism applies to the bromination of arylcyclopropanes as well [468].

The rate with which phenylcyclopropane is brominated increases with decreasing temperature. It has been found that the bromination of styrene is abruptly speeded up in the presence of arylcyclopropanes. This points to the important part played by complexes in radical production.

Olefin oxides also form molecular complexes when they react with nitrosyl chloride [442]. Their interaction opens up the epoxy ring. The reaction has been investigated in the temperature interval 303-178 K. At room temperature, the process has a negative temperature coefficient ($E_{eff} = -38$ kJ mole^{-1}). As the temperature is brought down, the temperature coefficient becomes positive ($E_{eff} = 12$ kJ mole^{-1}). The composition of the products, and the manner in which light and oxygen affect the reaction all point to the radical mechanism of the reaction. Evidence for the formation of intermediate free radicals has been obtained from the reaction carried out in the resonator of an ESR spectrometer in the presence of 2-nitroso-2-methylpropane known to be a radical trap [468]. Apparently, complex formation substantially loosens the reactive bonds and promotes the homolytic dissociation of the bond in the nitrosyl chloride molecule. The participation of molecular complexes in the formation of radicals is difficult to prove. As a rule, the own absorption of the molecules is superimposed on the absorption of the complex. A similar superposition is observed in the system involving the α-oxide of cyclohexene and nitrosyl chloride.

The most convincing evidence for the reduction of bond energy due to complex formation has been obtained for the system tetranitromethane-triphenylamine [444].

The formation of a molecular complex loosens the bonds in the reacting molecules and can promote radical production. The various aspects of the structure, properties and role of the molecular complexes in chemical reactions are reviewed in [469]. The molecular motions occurring in molecular complexes, adducts, and other similar forms in the solid state are examined in [470], and the effect of complex formation on chemical reactions in [471]. The part played by charge-transfer complexes in acylation is reviewed in [472] which summarizes the low-temperature properties of the complexes forming in sublimed solid-phase reactant mixtures at 77 K, and notes that chemical reactions take place in the mixtures upon warming up.

Studies of the reactions involving α-oxides show that, coupled with complex formation, low temperatures substantially change the selectivity and, in some cases, the mechanism and path of the process.

The various reactions occurring in the system halogen-oxide can, in the light of the above studies, be depicted to proceed as follows:

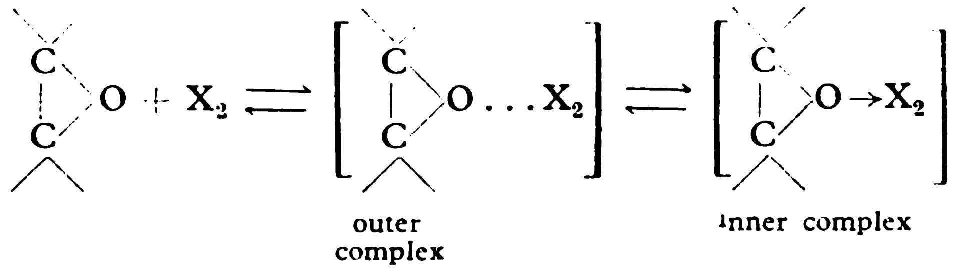

Inner complex $\xrightarrow[\text{nonpolar media}]{\text{low temperature}}$ Dioxalane derivatives (cyclodimerization)

$\xrightarrow[\text{nonpolar media}]{\text{bromination}}$ Ring opening products (radical polymerization)

$\xrightarrow[\text{low temperature}]{\text{olefins}}$ Dihaloethers (cohalogenation)

$\xrightarrow[\text{polar media}]{\text{oxide excess}}$ Polymeric products (ionic polymerization)

$\xrightarrow[\text{catalyst}]{\text{carbonyl compounds}}$ Dioxalanes (condensation)

It is seen from the above scheme that the subsequent conversions of the inner complex depend on the properties of the third component. Its part may be played by the other molecule of the complex or the substance purposefully added to the system. The temperature and polarity of the medium have a strong effect.

6.5. REACTIONS IN FROZEN SOLUTIONS

Several chemical and biochemical reactions can proceed at a high rate in a solution held at 10 to 15 kelvins below its freezing point, such as addition of triethylamine to methyl iodide [272, 473], catalytic cracking of tert-butylperoxyformiate [474], nonenzymic and enzymic solvolysis [475-477], and others [478, 479].

The mechanism of various chemical reactions in ordered systems, notably multicomponent systems and frozen solutions at low temperatures, is among the most challenging problems of present-day chemical kinetics. It is challenging from both theoretical and practical stand-points, and its knowledge can go a long way towards enhancing the efficiency of chemical synthesis.

6.5.1. Addition to Double Bonds and the Menshutkin Reaction

Olefin halogenation and hydrohalogenation at low temperatures are examples of solid-phase reactions [406] taking place in multicomponent systems. Fast addition of chlorine to ethylene at low temperatures was observed as far back as 1955 [480]. One of the earliest observations of chlorine addition to a double bond at low temperatures is described in [403]. Double-bond addition is examined in detail in Sections 6.1 and 6.2. It should be noted that such processes occur at high rates in three-component systems as well. Using the brominations of 1-hexene in frozen solutions as an example, it is shown in [481] that the rate of addition of halogens to olefins increases with decreasing temperature and as the liquid phase changes into a frozen solution (Fig. 6.7). The temperature coefficient of the reaction is negative in both the liquid phase and frozen solutions. The addition of iodine to olefins occurs in the solid phase at low temperatures [482, 483]. As is noted in [482], when diluted solutions of iodine and cyclohexene in cyclohexane or CCl_4 are frozen, the rate of the reaction increases, whereas practically no reaction occurs in the same solutions at room temperature. In the same publication, the dark addition of iodine to cyclohexene is investigated. The initial rate of the reaction at —190°C is higher than it is at —40°C, but the total amount of iodine expended in 20 minutes is greater at —40°C. Refreezing of the solution would raise the rate of the reaction at any temperature [482].

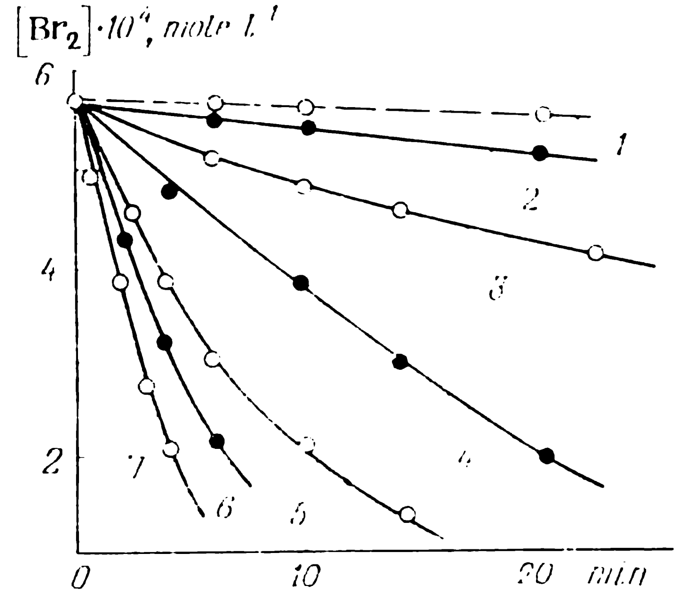

Fig. 6.7. Kinetic curves of bromine flow rate in reaction with 1-hexene in cyclohexane in (*1*) liquid and (*2*) through (*7*) frozen solutions at various temperatures ($[Ol]_0 = [Br_2]_0$ 5.8×10^{-4} mole $litre^{-1}$):
(1) 7°C; (2) 0°C; (3) —10°C; (4) —20°C; (5) —27°C; (6) —40°C; (7) —50°C

The kinetics of the Menshutkin reaction is investigated in [473] where it is noted that the freezing of the solution speeds up the reaction. The authors of [473] rationalize this occurrence on the basis of the hypothesis advanced in an earlier work [476] purporting that in a frozen solution there remain unfrozen regions — liquid inclusions where all of the reactants concentrate and the reaction proceeds by the same mechanism as in the liquid phase. A kinetic equation is derived to describe the interaction of triethylamine with methyliodide in benzene in the case of equal initial concentrations of the reactants. Unfortunately, the findings of [476] are limited in scope. For example, it leaves out of consideration the dependence of the reaction rate on the reactant concentration, the effect of the solvent on the reaction in a frozen solution, and the case when the reaction product is soluble. The temperature dependence of the rate constant is treated only qualitatively. The authors' conclusion that the addition of extraneous substances will only slow down the reaction is erroneous, as has been proved in [271, 272, 484].

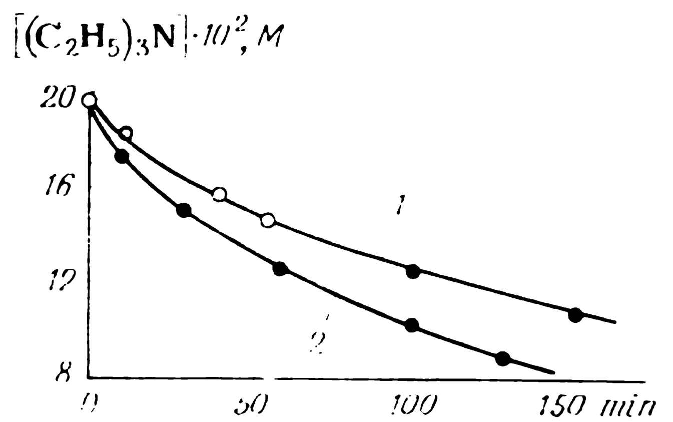

Fig. 6.8. Kinetic curves of triethylamine flow rate in reaction with methyliodide in benzene at 2.5°C ($[(C_2H_5)_3N] = [CH_3I] = 0.2$ *M*):
(1) supercooled solution; (2) frozen solution

The mechanism of the Menshutkin reaction is investigated in detail in the liquid phase. Therefore, such processes can be utilized as a model in tracing how various factors speed up the reaction with decreasing temperature. In [272], the increase in the rate of the reaction is investigated, using the reaction of triethylamine with methyliodide in frozen solutions as an example. The reaction proceeds according to the following stoichiometric equation:

$$(C_2H_5)_3N + CH_3I \longrightarrow (C_2H_5)_3CH_3N^+I^-$$

In the liquid phase, the rate of the reaction of triethylamine with methyliodide is described by a second-order kinetic equation with the rate constant given by

$$k_2 = (1.4 \pm 0.5)\times 10^4 \exp\left[-(39\,400 \pm 3\,400)/RT\right]$$

The results obtained agree well with the findings of [485].

The kinetic curves for the reaction of triethylamine with methyliodide in benzene at 2.5°C in a frozen and an unfrozen (supercooled) solution are shown in Fig. 6.8. As is seen, the reaction does go on faster in the frozen solution (curve *2*) than in the liquid phase (curve *1*). Thus, an absolute increase in the rate of the process is observed in frozen solutions. The temperature dependence of the observed rate constant for the reaction of triethylamine with methyliodide in frozen solutions yields a bell-shaped curve (6.9).

In order to find how the chemical character and concentration of an extraneous additive affects the rate of the reaction in frozen solutions, the authors of [272] have investigated the kinetics of the reaction of triethylamine with methyliodide in benzene in the presence of *p*-xylene, cyclohexane, and nitrobenzene.

By extrapolating the reaction rates found by the Arrhenius equation for the liquid phase to the temperature of frozen solutions and comparing the values thus obtained with experimental data, it is possible to evaluate the increase in the rate of the reaction when the latter is carried out at temperatures below the freezing point of the solvent. Because the order of the reaction in frozen solutions may be different from that in the liquid phase, it is preferable to compare the computed and observed values, W^{comp} and W^{obs}, of the reaction rates, rather than the rate constants. The initial rates for the reactions of triethylamine with methyliodide in frozen benzene solutions at —5°C for various initial concentrations of the reactants have been computed, using the second-order rate constants, and compared with the experimental values, W^{obs} (the observed reaction rates have been determined directly from the kinetic curves for the reactants in frozen solutions) [272]:

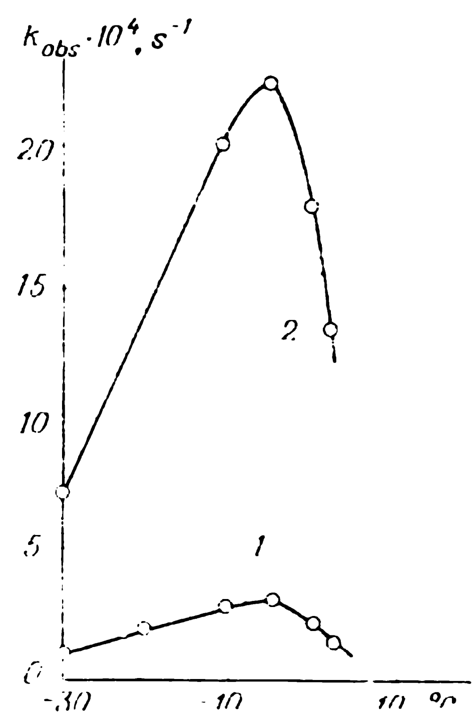

Fig. 6.9. Observed rate constant, k_{obs}, for the reaction of methyliodide with triethylamine in (*1*) benzene and (*2*) nitrobenzene as a function of temperature ($[(C_2H_5)_3N] = [CH_3I] = 0.2$ *M*)

Initial reactant concentration *M*	0.02	0.2
W_0^{obs}, mole l^{-1}s^{-1}	4.4×10^{-6}	6.2×10^{-5}
W_0^{comp}, mole l^{-1}s^{-1}	9.6×10^{-8}	9.2×10^{-6}
W_0^{obs}/W_0^{comp}	48	7

As is seen, the increase in the reaction rate is more noticeable at lower concentrations of the reactants.

6.5.2. Solvolysis Reactions

Aqueous solutions of penicillin containing imidazole and histidine quickly lose their antibiotic activity at —18°C [475]. When the same solutions are stored at +38°C, the activity of penicillin is retained.

The loss of antibiotic activity is rationalizable on the basis of β-elimination of the lactam cycle in the penicillin. This reaction is an impressive illustration of how the freezing of the system can speed up chemical reactions. Beta elimination of the lactam cycle, catalyzed by imidazole, occurs readily in the temperature interval between —5°C and —30°C. The degree of hydrolysis of penicillin is independent of the manner in which the solution is frozen or the shape and size of the vessel. In the absence of a catalyst, penicillin will not hydrolyze.

It has been found that the addition of 5% to 10% (by volume) of glycerine, ethanol or inorganic salts of alkali metals will slow down to a different degree the hydrolysis catalyzed in frozen solutions by imidazole. The addition of Na^+ ions suppresses hydrolysis in proportion to the concentration of added ions. It may be noted that K^+ ions are less effective than Na^+ ions. The authors of [475] attribute this difference to the fact that Na^+ ions are surrounded by a larger hydrate shell and can therefore break up ordered water structure better than K^+ ions.

In rationalizing the acceleration of penicillin hydrolysis in frozen solutions, the authors of [475] attach a good deal of significance to the solid phase which promotes, as they believe, the favourable orientation of the substrate and catalyst. In their opinion, a proton in ice possesses a higher mobility, thereby ensuring a high rate of catalysis. By breaking up the ice structure, the additions interfere with the proton transfer.

Unfortunately, in investigating the effect of various factors on the rate of hydrolysis in ice, the experimentors have not conducted concurrent control measurements for liquid solutions. Without such experiments, it is difficult to draw unambiguous conclusions about the relative effect of various substances on the rate of the process in frozen solutions. The temperature dependence of penicillin hydrolysis in ice in the presence of various catalysts has not practically been investigated. Reference [475] offers no experimental evidence to support the hypothesis advanced to interpret the acceleration of penicillin hydrolysis in frozen aqueous solutions.

The authors of [476] have made an attempt to verify the hypothesis according to which the reactants concentrate in liquid regions. However, measurements of reactant distribution in frozen systems have yielded no proof that the reactants tend to concentrate in isolated localities. Therefore, the experimentors have concluded that the hydrolysis is accelerated because the reactants are arranged in ice in a manner favourable for a nucleophilic reaction.

The acceleration of a reaction in a frozen solution has also been investigated, using the hydrolysis of acetic anhydride, β-propiolactone, and *p*-nitrophenylacetate [486]. The hydrolysis of acetic anhydride has been investigated in the liquid and gaseous phases. The equation of the reaction may be written

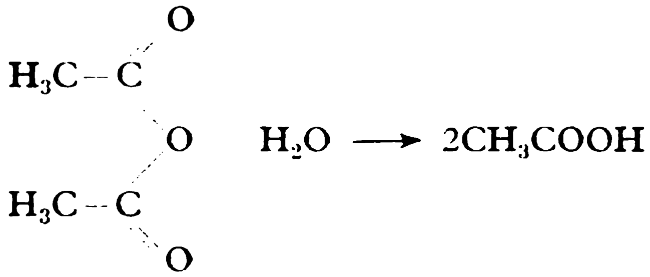

The observed rate constant of hydrolysis in ice at —10°C has been compared with the computed rate constant deduced by extrapolating the Arrhenius equation for the liquid phase. In ice, the non-catalyzed hydrolysis of acetic anhydride is slowed down in comparison with the reaction rate in liquid solutions. The rate of acidic hydrolysis is about four times as high and increases with increasing concentration of HCl. The hydrolysis catalyzed by an acetate ion is markedly accelerated in frozen solutions. The kinetics of the processes in frozen solutions obeys a first-order equation in all cases.

The rate of hydrolysis for acetic anhydride is written

$$-d[Ac_2O]/dt = (k_0 + k_{H^+}[H^+] + k_{OH^-}[OH^-] + k_{AcO^-}[AcO^-])[Ac_2O]$$

where k_0, k_{H^+}, k_{OH^-}, and k_{AcO^-} are the constants of spontaneous, acidic, alkaline, and acetic hydrolysis, respectively.

In ice at —10°C, $k_0 = 1.4 \times 10^{-3}$ min^{-1}. For supercooled water at —10°C, k_0 is found to be 1.33×10^{-2} min^{-1}. As is seen, freezing suppresses spontaneous hydrolysis.

Experimental evidence for frozen acidic solutions suggests that k_{H^+} in ice is about 22 times as great as in water at the same temperature. As regards k_{OH^-}, it has qualitatively been stated that in ice at —10°C the hydrolysis proceeds at a somewhat lower rate than in water at +5°C. Freezing increases the catalytic efficiency of acetate ions about eleven-fold. The authors of [486] rationalize the results by assuming that in frozen solutions there form liquid regions where the dissolved substances are concentrated and the reaction takes place.

The hydrolysis of β-propiolactone catalyzed by imidazole is described by an equation of the form

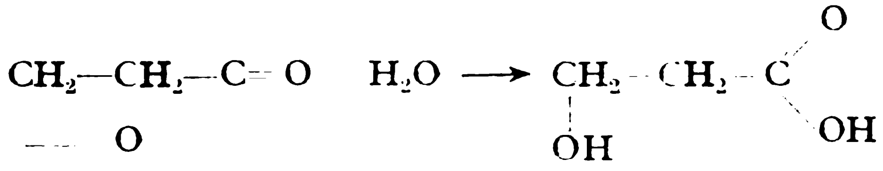

No spontaneous hydrolysis was observed in ice at —10°C for five hours. As a catalyst, imidazole is about seven times more efficient in ice than in the liquid phase [486].

The hydrolysis of *p*-nitrophenylacetate proceeds according to the scheme

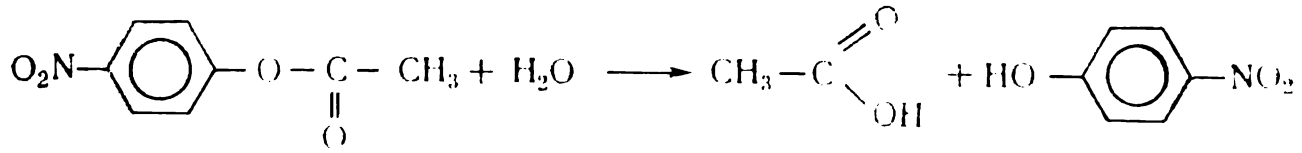

In ice at —10°C, it proceeds faster than in water at +5°C.

According to [486], the hydrolysis of acetic anhydride, β-propiolactone and *p*-nitrophenylacetate in water obeys a quasi-first-order equation which also holds for ice at —10°C. The observed acceleration or slowdown of the reaction is rationalizable on the basis of the concentration effect.

Bruice and Butler [476] have also investigated the reactions of thiolactones with morpholine in frozen and supercooled aqueous solutions. The general equation of the reaction may be written

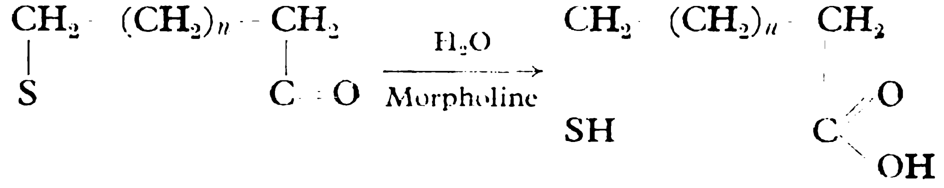

$$\underset{\displaystyle S}{CH_2}-(CH_2)_n-\underset{\displaystyle C=O}{CH_2} \xrightarrow[\text{Morpholine}]{H_2O} \underset{\displaystyle SH}{CH_2}-(CH_2)_n-\underset{\displaystyle C(=O)OH}{CH_2}$$

Thiolactones react with a large number of nucleophilic agents and are subject to attack by acids and bases. The reactions may proceed by any one of three mechanisms, namely direct nucleophilic attack k_n, acid-assisted attack k_a, and base-assisted attack k_b. Thus, the equation describing the rate of the reaction takes the form

$$-d[L]/dt = (k_n[N] + k_a[N][HA^+] + k_b[N]^2)[L]$$

where N is the base (nucleophyl), and L is the thiolactone.

The expression in the parentheses describes the observed rate constant.

In principle, any nucleophilic agent can react in the liquid phase by any one of the three mechanisms. The observations of the reaction in ice at —10°C have shown, however, that neither the acid mechanism nor the base mechanism takes place, the dominant mechanism being the direct nucleophilic attack. Hence, freezing drastically changes the mechanism of the reaction. The experimentors cooled the reactant mixture to —10°C without freezing. In the liquid phase at —10°C, the reaction proceeded by the same mechanism as in the temperature interval 3-45°C, that is, the nucleophilic component was practically nil.

In Bruice's and Butler's opinion, the observed facts are not rationalizable on the basis of the concentration effect. As they believe, the ice structure either promotes the proton transfer or ensures that the reactants are oriented so as to favour the nucleophilic attack and to speed up the reaction by this mechanism.

The hydroxylaminolysis of amides in frozen solutions has been investigated in [475, 487, 488]. The reaction is believed to proceed according to the equation

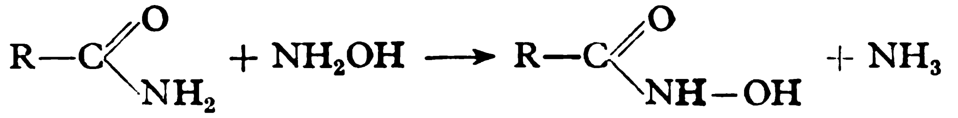

$$R{-}C\begin{matrix}{}^{\nearrow O}\\{}_{\searrow NH_2}\end{matrix} + NH_2OH \longrightarrow R{-}C\begin{matrix}{}^{\nearrow O}\\{}_{\searrow NH{-}OH}\end{matrix} + NH_3$$

The hydroxylaminolysis of simple amides at reduced temperatures is interesting in that it produces the most stable derivatives of carboxylic acids. The reaction of hydroxylamine with amide can be catalyzed by the protonized form of hydroxylamine (NH_3^+OH), a free base, and various buffer solutions. Analysis of the reaction rate as a function of pH and concentration shows that the base catalyst is more effective than the increase in reactant concentration upon freezing. It is believed that experimental evidence cannot be rationalized on the basis of the concentration effect and that it is the ice lattice that is responsible for the increase in the reaction rate.

The kinetics of the hydroxylaminolysis of acetamide in a frozen aqueous solution is examined in [475]. When the reaction is conducted in the presence of excess hydroxylamine, experimental data for both the liquid and the solid phase adequately fit a quasi-first-order kinetic equation. Exhaustive information about the temperature dependence of the rate of the reaction in a frozen solution is lacking. The same goes for the pH dependence of the rate of hydroxylaminolysis of acetamide in the liquid and solid phases. The mechanism of the reaction in a frozen solution has not been investigated.

For better insight into the mechanism of such reactions, the authors of [489] have investigated the kinetics of hydroxylaminolysis of acetamide in frozen aqueous solutions. As already noted, the hydroxylaminolysis of acetamide produces acethydroxamic acid and ammonia. The kinetics of the reaction was monitored spectrophotometrically, by measuring the optical absorption of the stable, coloured complexes of hydroxamic acid and trivalent iron ions.

During the experiments, the samples were quickly frozen in liquid nitrogen, placed in a cryostat, and maintained at the temperature of the experiment. At regular intervals, the tubes holding the frozen solutions were opened, warmed up, and analyzed. It has been found that practically no reaction takes place during phase changes upon freezing or warm-up. In other words, kinetic data interpret the process as occurring in the solid phase.

For a reaction in liquid and frozen solutions in the presence of excess hydroxylamine, the rate is described by a kinetic equation of the first order for acetamide. The experimentors have investigated the temperature and pH dependences of the observed rate constant. The values of the observed rate constants for various temperatures and values of pH are given in Table 6.3. As is seen, the plot of reaction rate versus pH has a peak. The activation energy for the reaction in liquid solutions with pH 5.5, 6.0, and 6.5 is about the same and equal to 64±4 kJ mole^{-1}.

The observed rate constant as a function of pH at various temperatures is plotted in Fig. 6.10. The values of pH given in the plot apply to liquid solutions prior to freezing. That the curve is bell-shaped is explained by the fact that the acetamide is reacted with hydroxylamine in the form of a free base and the reaction is catalyzed by hydroxylammonium ions which do not appear to react with the acetamide directly [490]. The shift of the peak of the pH dependence on freezing towards the higher values of pH (curve *4*) can be traced to the increase in the p*K* of the hydroxylammonium ion with decrease in temperature. Indeed, as is shown in [491], the decrease in temperature causes $pK_{NH_3^+OH}$ to increase to 5.70 at 44.7°C, to 6.03 at 30°C, and to 6.32 at 15°C. Linear extrapolation for —25°C gives p*K*7.2, which checks with the pH at which the rate of the reaction at —25°C is a maximum.

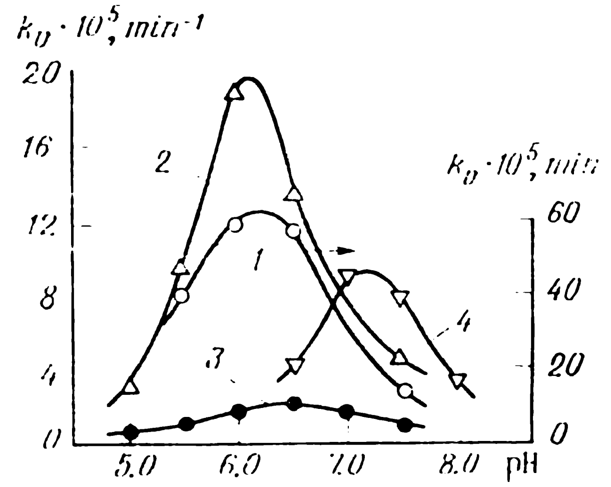

Fig. 6.10. Plot of k_v for hydroxylaminolysis of acetamide in water and ice as a function of the pH value of the reactive mixture:
(1) 39°C; (2) 22°C; (3) 0°C; (4) —25°C

TABLE 6.3

Observed Rate Constant for the Hydroxylaminolysis of Acetamide as a Function of Temperature and pH of the Solution

t, °C	$k_{obs} \times 10^5$ min^{-1}						
	pH5.0	pH5.5	pH6.0	pH6.5	pH7.0	pH7.5	pH8.0
39	—	40	60	57	—	14	—
22	3.2	9.5	19	13	—	4.7	—
0	0.7	1.1	1.8	2.1	1.7	1.1	—
−10	—	—	—	6.7	5.3	3.2	—
−25	—	—	—	4.2	8.9	7.5	3.3

The kinetic data for frozen solutions have been treated from the stand-point of formal kinetics. Such an approach brings about the differences and special features of reactions in the liquid and solid phases, and explains the causes of these differences despite some difficulty in interpreting the physico-chemical meaning of the quantities deduced.

The degree of conversion as a function of temperature for the hydroxylaminolysis of acetamide (pH7) is plotted in Fig. 6.11. As is seen, in frozen solutions at —10°C and —25°C the hydroxylaminolysis of acetamide proceeds faster than at 0°C in the liquid phase. Referring to Fig. 6.12, the experimental rate constants are substantially higher than those computed by the Arrhenius equation, which fact indicates that freezing speeds up the reaction. Thus, according to experimental evidence, it may be concluded that both freezing and reduction in the temperature of the solution bring about an absolute and a relative increase in the rate of the reaction.

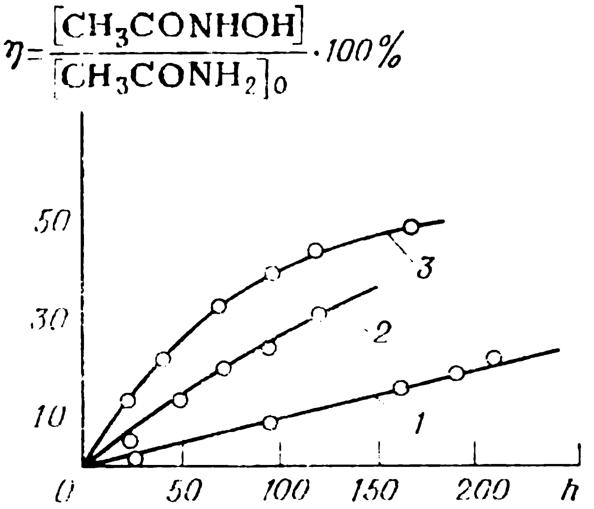

Fig. 6.11. The effect of temperature on the rate of accumulation of acethydroxamic acid at pH7:

(1) 0°C; (2)–10°C; (3)–25°C

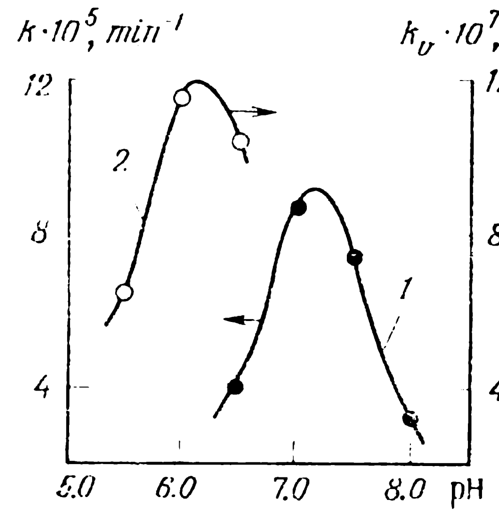

Fig. 6.12. Rate constants as functions of pH value at –25°C:

(1) experimental values; (2) values calculated by the Arrhenius equation for the reaction in the liquid phase

The decomposition of H_2O_2 has been investigated in ice with and without the addition of $CuCl_2$ and $FeCl_3$ [492]. In either case, the reaction in ice has been found to proceed faster than at 1°C in the liquid phase. The authors have rationalized the acceleration of the reaction on the basis of the catalytic action of ice in frozen solutions.

The reaction of ethylene chloride with sodium hydroxide in ice has been investigated in [493]. It has been found that the reaction in frozen solutions proceeds at a progressively higher rate as the initial concentrations of the reactants are decreased. The observed second-order rate constant has been found to depend on the initial concentrations of the reactants. Analysis of the reaction rate in ice as a function of temperature in the interval from 0 to —15°C has shown that the rate is a maximum at —5°C. The addition of salts and ethanol has been noticed to reduce the observed rate of the reaction in frozen solutions, irrespective of the nature of the added substance.

The authors of [474] and [494] have investigated the base-catalyzed decomposition of tert-butylperoxyformiate in liquid and frozen solutions of *p*-xylene. The reaction takes place according to the equation

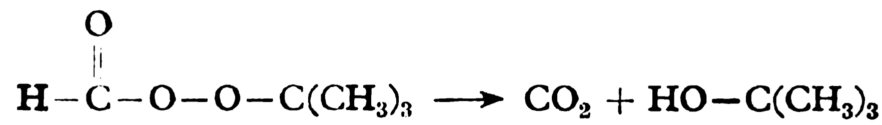

$$H-\overset{\overset{O}{\|}}{C}-O-O-C(CH_3)_3 \longrightarrow CO_2 + HO-C(CH_3)_3$$

It has been found that the reaction only takes place in the frozen solution; upon warm-up the decomposition of the peroxide practically ceases. The rate of decomposition has been found to be independent of the manner in which the samples are frozen, and to be a maximum at 2°C in the frozen solution of *p*-xylene. Although the melting point of the solvent is 13.2°C, the reaction does take place. Depending on the initial concentrations, freezing can raise the rate of reaction 30 to 400 times [474].

The authors of [474] have also investigated the effect of temperature, concentration of starting materials, and inert additions on the rate of reaction. They rationalize their experimental data on the basis of the concentration effect: they presume the existence of liquid regions with higher concentrations of reactants scattered among the crystals of the pure solvent in the frozen system. For a quantitative consideration of such reactions, they assume that in the liquid regions the dissolved substances have one and the same constant overall concentration whose value is determined by the conditions of phase equilibrium between the solution and the pure substance.

The following equation is suggested for the observed rate constant of the first-order reaction in a frozen solution:

$$k_{obs} = k_2 c_n \frac{B}{B + P + I_m}$$

where k_2 is the rate constant of the second-order reaction in the liquid phase; c_n is the total (and constant at a given temperature) concentration of the dissolved substances in the liquid regions; B, P, and I_m are the initial concentrations of the base, peroxide, and impurity, respectively [474].

The acceleration of reactions in frozen solutions has also been observed by the authors of [478] and [495]. Reference [495] is concerned with the reaction of diphenylpicrylhydrazyl with Cu-3-(butene-1-yl)-2,4-pentadionate. Reference [478] reviews some experimental results. A feature common to all the studied reactions is that at certain temperatures the reactions will proceed in frozen solutions faster than in supercooled solutions at the same temperatures, and that the rate of reaction can grow by several orders of magnitude.

As follows from the above analysis, there is no common view as yet on the mechanism of chemical reactions in frozen solutions. In [475, 476, 488, 496-498], the reactions in frozen solutions are interpreted as truly solid-phase processes, and the increase in the reaction rate is rationalized on the basis of the catalytic action of the crystalline structures. In [474, 478, 499], these reactions are attributed to the concentration of the reactants within the liquid inclusions existing in a frozen solid solvent.

Investigations of spontaneous reactions in solid multicomponent systems are of significant theoretical interest as they can throw more light on the specific features of chemical reactions at low temperatures. In more detail, the kinetics of reactions in frozen solutions is examined in the subsequent chapters. Knowledge of such reactions gives better insight into ion and radical processes at low temperatures.

CHAPTER SEVEN

KINETIC MODELS OF CHEMICAL REACTIONS IN THE SOLID PHASE

As a tool for investigating the production, accumulation and subsequent transformation of ions, radicals and other reactive species, low temperatures have been used for many years already, but the mechanism of the reactions involving such species has not yet been elucidated completely. Nor is there any complete theory to describe the kinetics of chemical reactions in the solid phase at low temperatures. However, relevant hypotheses and theoretical concepts have been advanced more than once. This chapter will be concerned with some of the theoretical models proposed to explain the kinetics of low-temperature reactions in the solid phase, with emphasis on radicals as the most known of all reactive species to date.

7.1. THE RELAXATION MECHANISM OF THE LOSS OF RADIOLYZED REACTIVE PRODUCTS

The behaviour of radicals trapped in a solid shows a specific pattern which includes, above all, stepwise recombination and loss of radicals when exposed to radiation and at the time of phase changes. These aspects of the behaviour were discovered in the late 50s when work on trapped radicals had just begun, and the effort continues.

An interesting idea about the likely causes of the specific path taken by chemical reactions in organic solids, such as solid polymers, is advanced in [500]. A distinction of such reactions is that the observed activation energy and pre-exponential factor for reactions in solid polymers are substantially higher than the "normal" values for the same processes in the liquid and gaseous phases. Often, the two quantities show a linear relationship:

$$\ln k_0 = A + BE$$

where k_0 is the pre-exponential factor, E is the activation energy, A and B are coefficients. This relation is often referred to as the compensation effect. According to [500], the compensation effect can most consistently and logically be rationalized on the basis of formal kinetic concepts advanced in [501]. If, for one reason or another, the actual activation energy decreases with decreasing temperature, the relation between the actual values E and k_0 and their effective values E_{eff} and $k_{0,\,\mathrm{eff}}$ can be established on the basis of the Arrhenius equation, using experimental data as follows:

$$\begin{aligned} E_{\mathrm{eff}} &= E - T\,\partial E/\partial T \\ k_{0,\,\mathrm{eff}} &= k_0 \exp\left[-(1/R)(\partial E/\partial T)\right] \end{aligned} \tag{7.1}$$

Furthermore, E_{eff} and $k_{0,\,\mathrm{eff}}$ are connected by the compensation relation. The suggestion made in [501] that the activation energy of a reaction strongly depends on temperature is not obvious and needs justification.

According to [500], the likely cause for the temperature dependence of activation energy may be the fact that the structural relaxation in polymers lasts longer than the chemical event proper. Because of the structural molecular relaxation in polymers, the activated complex having an energetically more favourable structure has no time to form during the reaction, and the process follows a higher energy path. For example, when a hydrogen atom is detached from a carbon atom in the polymer chain

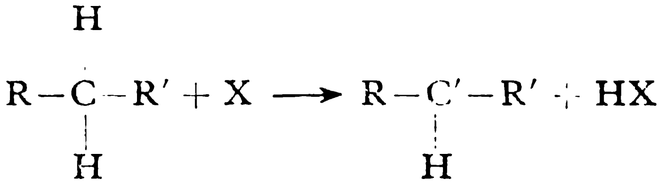

$$\mathrm{R{-}\underset{H}{\overset{H}{C}}{-}R' + X \longrightarrow R{-}\underset{H}{C'}{-}R' + HX}$$

a re-hybridization of the affected carbon atom takes place and the valence angles in that atom change from 109° to 120° (and so do the bond lengths). In the liquid phase, a hydrogen atom is abstracted and re-hybridization takes place both at the same time, whereas in a polymer matrix these events are separated in time. Re-hybridization lags behind the transfer of the hydrogen atom, because its rate is limited by the structural relaxation. This happens because, firstly, the R and R′ fragments in polymers are large and, secondly, they are bonded by van-der-Waals forces fairly strongly to other polymer molecules.

According to [500], the fact that a chemical event and re-hybridization are separated in time by structural relaxation is responsible for the increase in the actual activation energy of the reaction. Thus, the activation energy rises as the time separation between the two events increases. Schematically, the proposed relation between the activation energy and the time separation, τ, between the elementary events is shown in Fig. 7.1.

It is hypothesized in [500] that one should expect a maximum time lag in structural rearrangement relative to the reaction event at low temperatures. That the kinetics of reactions might depend on the rate of structural rearrangement of macromolecules was suggested earlier in [502] and [503].

In [504] concerned with the analysis of the isothermal loss of radiolyzed reactive products, the investigators examine the effect of relaxation molecular motion on the loss of reactive species.

According to published data, there is a close relation between molecular motion and the loss of radiolyzed reactive products. Firstly, as already noted, the rate of radiothermoluminescence caused by the loss of trapped charges, the peaks of thermally stimulated current, the loss of radicals, and the temperature intervals of structural transitions in various systems are all correlated [505-512]. Secondly, the temperature of structural transitions in polymers, the extent of radiothermoluminescence, and the magnitude of thermally stimulated current are subject to variations due to several factors, such as plastification, orientation of polymers in films, cross-linking and rate of heat build-up [513]. Thirdly, the activation energies for radiothermoluminescence, thermally stimulated current, and the loss of radicals are comparable with the values obtained for the temperature dependence of the intensity of molecular motion in polymers in the same temperature intervals [509, 511-514]. From the wealth of these and other data, it is safe to conclude that a substantial loss of radiolyzed reactive products can only occur under conditions of high molecular mobility which is observed, for example, during the structural transitions of polymers upon warm-up. According to [504], an important thing is that molecular mobility is of relaxation character, so the re-orientation of structural elements can take place even at relatively low temperatures.

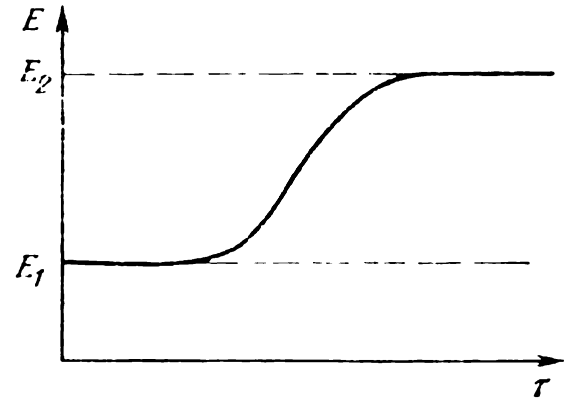

Fig. 7.1. Assumed relation between the activation energy for a chemical reaction and the time interval separating the reaction and the rehybridization [500]
[E_1 = activation energy for the reaction on the condition that both events occur at the same time ($\tau = 0$), E_2 = activation energy for the two events separated in time ($\tau > 0$)]

Let us dwell on the main result presented in [504] and examine the derivation of an equation for the isothermal loss of reactive species in irradiated polymers. The authors of [504] have worked on the following assumptions:

(1) a reactive species immobilized during low-temperature radiolysis will not escape from its trap until the instant of recombination (recombination without escape from a trap);

(2) the life time of a reactive species is equal to the relaxation time of the structural element on which it is trapped;

(3) the product of two distribution functions, namely that of structural elements by activation energies and that of reactive species by structural elements, is approximately constant.

It is important to stress that in [504] the type of reactive species and their physico-chemical characteristics are not considered, which is equivalent to assuming that the rate-controlling stage for the kinetics of loss is the rate of molecular rearrangements (the assumption under (2) above). It is presumed that a polymer specimen consists of structural elements characterized by a broad spectrum of relaxation times, τ_i. It is also assumed that the temperature dependence of relaxation time for molecular mobility in each structural element obeys an exponential law:

$$\tau_i = \tau_{i0} \exp (E/kT) \tag{7.2}$$

where E is the activation energy for molecular motion, and τ_0 is approximately 10^{-12} to 10^{-13} s [515, 516].

According to [504], the assumption under (1) above is equivalent to taking into account the experimental fact that reactive species recombine at such temperatures that they cannot be thermally released from their traps; that is, kT is by a factor of several hundred less than the depth of traps. It is to be noted that this assumption is not physically plausible and it is difficult to visualize a recombination mechanism that does not call for the reactive species involved to move closer together.

The weakest point of all, and this is admitted by the authors of [504], is the assumption under (3). As they believe, an increase in the size of a structural element is accompanied by a decrease in its mobility or, in other words, an increase in the activation energy. At the same time, the probability of trapping around such large structural elements increases. Hence, even without knowledge of the exact form of the individual distribution functions, it is reasonable to assume that their product must approximately be constant.

The rate of loss for reactive species in the *i*th structural element obeys a first-order kinetic equation of the form

$$\begin{gathered} - dn_i = n \; (1/\tau_i)dt \\ n_i' = n_{0i} \exp \left[- t\tau_0^{-1} \exp (- E_i/kT) \right] \end{gathered} \tag{7.3}$$

where n_{0i} and n_i are the number of reactive species lost in the *i*th element at the initial instant of time and at time t.

The above assumptions turn out insufficient for deriving an expression for the dependence of the number of reactive species on temperature and time in an analytical form. They have to be extended to include two more assumptions which are not stated in an explicit form in [504], namely:

(4) structural elements are distributed by relaxation times continuously (from τ_0 to ∞);

(5) there is a distribution function of reactive species by activation energies, $H(E)$, which, in view of assumption (3), is taken to be equal to a constant:

$$H(E) = \text{constant} = A_0 \tag{7.4}$$

On the basis of assumptions (4) and (5), the expression relating the number n of reactive species lost at time t to time and temperature can be derived by integrating the product of n_i given by Eq. (7.3) and $H(E)$ over the activation energy taken from zero to infinity, that is

$$n = \int_0^\infty H(E) \exp\left[-t\tau_0^{-1} \exp(-E/kT)\right] dE \quad (A_0 kT/t)\left[1 - \exp\left(-t\tau_0^{-1}\right)\right] \tag{7.5}$$

At $t > \tau_0$, Eq. (7.5) reduces to

$$n(t) = A_0 kT/t \tag{7.6}$$

where $n(t)$ is the number of reactive species lost at time t.

According to Eq. (7.6), the loss of radiolyzed reactive products must obey a hyperbolic law. The rate of isothermal glow is proportional to $n(t)$ and its decay must likewise be described by Eq. (7.6). That the hyperbolic law is obeyed has been noted by the authors of [504] for linear polyethylene, low- and high-density polyethylene, polypropylene, polybutadiene, and other polymers over a wide temperature range (at 4 K, 77 K, 90 K, 131 K, and 195 K). It is important to note that no data were obtained about the rate of isothermal glow decay in the initial portion. Recording began 5 to 10 min after irradiation had ceased. Isothermal glow has also been investigated by the authors of [517] through [519].

The total number $N(t)$ of reactive species remaining by the time t can be found by the equation

$$N(t) \quad N_0 - \int_t^{t_k} n(t)\, dt \tag{7.7}$$

where N_0 is the initial number of reactive species, and t_k is the time of the loss of all reactive species.

Also, another assumption, not so obvious at first glance, is made that t_k is finite because the number of structural elements, however great it may be, is after all finite, too. In view of Eq. (7.6), Eq. (7.7) is written

$$N(t) = A_0 kT \ln t_k/t \tag{7.8}$$

or

$$N_0 - N(t) = AT \ln t \qquad (7.9)$$

In other words, it should be expected that the loss of reactive species, including radicals, must obey a logarithmic law. In [520], the loss of radicals in irradiated polyethylene is described by an expression close to Eq. (7.9).

The authors of [504] think it important to stress that the activation energy for molecular motion is in no way related to the depth of the trap holding a given species. In their opinion, although the depth of the trap may vary within broad limits, the loss of species will occur in one and the same temperature interval which is the same as the interval of mobility warm-up for the respective structural elements. Earlier, the authors of [521] and [522] proposed charge recombination models without escape from traps.

Reference [504] also examines the stepwise loss of radicals in polymers. In the opinion of its authors, the basic kinetics of radical loss discussed in [227, 228, 523] can well be explained on the basis of the concepts advanced in [504]. The existence of "steps" is connected to instrument sensitivity. In principle, all radicals must have been lost at any temperature. Since, however, radical loss is controlled by molecular motions of relaxational character, only those radicals are lost that have been immobilized on structural elements having at a given temperature the relaxation time comparable with the observation time t:

$$(R_0 - R)/R_0 = \ln t/\ln t_k \qquad (7.10)$$

According to Eq. (7.10), all radicals must be lost, which amounts to disproving the possibility of stepwise loss. Each instrument, however, has a certain sensitivity. Let the accuracy with which radical concentration can be measured be ΔR_n (Fig. 7.2). For the radical concentration to remain unchanged during the observation interval $\Delta t = t_2 - t_1$, it is essential that

$$\Delta R = (dR/dt)\Delta t \leqslant \Delta R_n$$

or

$$\Delta t \leqslant (\Delta R_n/AT)t \qquad (7.11)$$

It follows from Eq. (7.11) that at given temperature and instrument sensitivity, the kinetic curve of radical loss will have a portion within which variations in the radical concentration are negligible. Thus, a step is a univalued function of observation time and instrument sensitivity, rather than temperature.

The empirical relation

$$R/R_0 = a - bT \qquad (7.12)$$

used in some cases to describe the temperature dependence of steady-state radical concentration [523] stems directly from Eq. (7.9). For the same observation interval, the magnitude of a step can be written

$$(R/R_0) = [(R_0 - AT \ln t_1)/R_0] = 1 - cT \tag{7.13}$$

which checks with Eq. (7.12).

The logarithmic law for the loss of radicals was derived earlier in [524] within the framework of a formal kinetic model for bimolecular reactions in a condensed phase. True, Eq. (7.9) does describe the occurrence of a step, but it fails, and so do the concepts developed by the authors of [504], to explain a very important aspect of stepwise recombination, namely, the fast loss of a good proportion of radicals at the very beginning of the transition from one isothermal condition to another, $T_1 \rightarrow T_2$. During this interval, the rate of molecular relaxation cannot, according to [504], exceed the rate at the higher temperature T_2 of the second isothermal state.

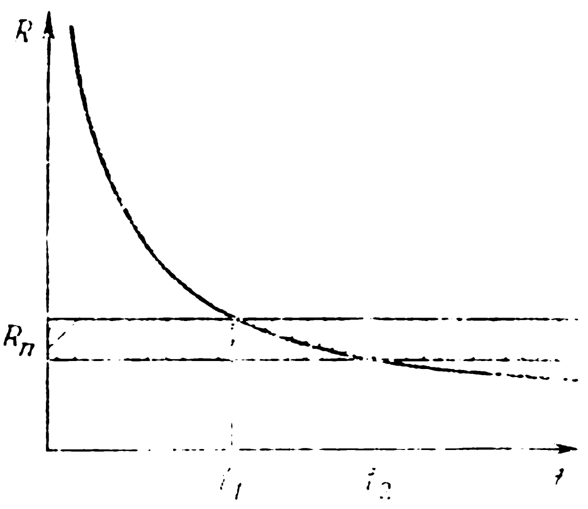

Fig. 7.2. Explaining the stepwise loss of radicals

In order to explain the fast loss of radicals during the transition period, several more assumptions need to be made. There is also some doubt about the validity of the view that the ratio R/R_0 is independent of radiation dose, based on the assumption that the polymer structure and the character of molecular mobility are independent of dose (to some limit). In contrast, the models of radical loss suggested in [525] are, in our opinion, more plausible and convincing.

7.2. THE EFFECT OF MATRIX STRUCTURE ON THE LOSS OF RADICALS

An exhaustive treatment of stepwise radical recombination is given in [525] which is largely a review. Basing himself on published data and his own observations, its author concludes that for the most part irradiation causes radicals to be formed and trapped near various lattice defects in organic solids. It is to be noted that prior to [221, 248, 250, 525-529], there were practically no publications on direct studies into the structure of organic crystals and its relation to the loss of stabilized radicals.

Referring to [525], it presents experimental verification of the hypothesis advanced earlier in [505, 530-533] that the loss of trapped radicals is related to the molecular mobility at and around structural defects in the crystalline matrix. The degree of molecular mobility was judged from the measured complex dielectric constant, $\varepsilon' - i\varepsilon''$. For ideal crystals, ε'' must be zero, whereas ε' must be independent of the temperature and frequency at which it is measured. On the other hand, it has long been found that for most organic and many inorganic compounds ε' and ε'' show dispersion over an appreciable temperature interval below the melting point. For example, it is shown in [534] that small amounts of impurities greatly affect the dielectric constant of solids, as measured at low frequencies. This conclusion is drawn from observations of nitrobenzene, aniline, phenol, benzene, ethylene chloride, dimethylsulphate, and diethylsulphate. Interesting results have been obtained for ice which, to believe experimental data, behaves as a very viscous liquid.

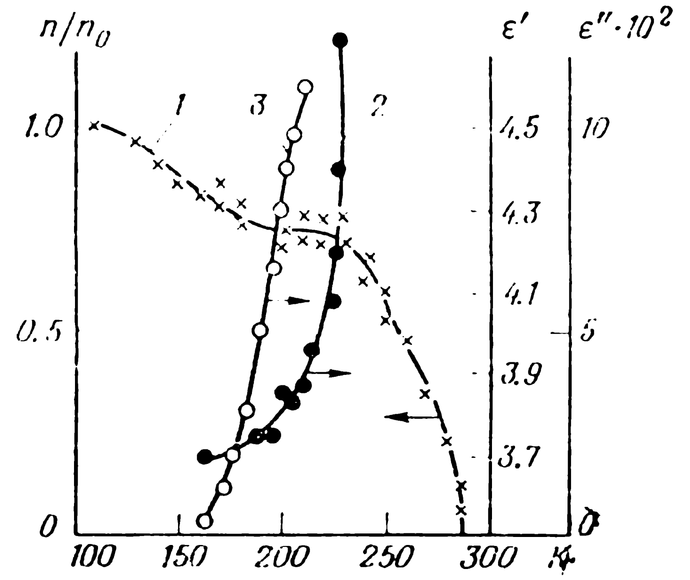

Fig. 7.3. Plots of (*1*) relative concentration n/n_0 of radicals as a function of temperature and dielectric constants ε' and ε'' in glycerine with the addition of (*2*) 7.5% H_2O and (*3*) 0.6% H_2O

Reference [525] compares the temperature dependence of radical loss in irradiated 1-octanol, acetone, phenol, succinic acid, methyl alcohol, and glycerine (with an addition of water) with their dielectric characteristics at temperatures preceding the melting point. As is clearly seen from Fig. 7.3 given as an example, both ε' and ε'' for nonirradiated materials grow in magnitude in the temperature interval of radical loss. It is assumed that radical loss is related to the "unfreezing" of molecular mobility near lattice defects and to the appearance of a liquid phase in the crystalline specimens.

To interpret the experimentally observed dependence of ε' and ε'' on temperature and frequency in the pre-fusion region, it is assumed that the increase in the magnitude of the dielectric constant may be caused by the following factors:

(1) the presence of impurities which may give rise to a liquid phase at temperatures below the melting point;

(2) the increased mobility of the molecules located at the grain boundaries, in crevices, and other lattice defects;

(3) the occurrence of heterophase fluctuations localized at and around the impurities, a few degrees below melting point.

Indirect evidence in support of the above assumptions can be found in [526-528, 534, 535].

No quantitative estimates are given in [525]. Primarily, this is because the comparison involves data taken from various sources where nothing is said about, say, the purity of the individual organic substances used.

A more exhaustive discussion can be found in the literature concerning the system glycerine-water, because the investigations have been carried out in the same laboratory [526-527]. This system has been found to have two regions of radical loss, namely a low-temperature region (120-200 K) and a high-temperature region ($>$ 200 K). In the opinion of [525], the rise in dielectric constant observed in the low-temperature region is caused by the pre-fusion of the glycerine-water eutectic. Radical recombination is likewise interpreted on the basis of radical loss in the eutectic. Coupled with the complete loss of radicals in the pure eutectic below 200 K [526], these results can, in the author's opinion, be taken as a proof that most of the radicals formed in the glycerine-water eutectic are immobilized at and around lattice defects. Among the latter, a leading part is believed to be played by the large surface area (in comparison with the individual components) of the crystals that form the eutectic.

The ideas advanced in [525] provide a basis on which the basic kinetic pattern observed in radical recombination [227, 228, 530] can be interpreted qualitatively. The assumption that the radicals are widely distributed by stabilization energies and that their loss comes about due to diffusion along the boundaries of the defects explains the stepwise shape of kinetic curves for radical loss. Interestingly, stepwise loss has been observed also for radicals adsorbed on surfaces, which fact gives support to the above assumptions [536, 537].

From our point of view, an attractive explanation of stepwise radical loss is given in [525] and [526] where it is ascribed to the formation of liquid-phase regions with rising temperature. In the circumstances, the "stationary" concentrations of radicals in isothermal conditions must be determined by the liquid-solid constitution diagram of a given substance and the impurities present.

To account for the increased rate of radical recombination at the beginning of the transition from T_1 to T_2 ($T_1 < T_2$), it is suggested in [525] that the diffusion of radicals or the attainment of equilibrium between the solid and liquid in the specimen may be speeded up by the energy liberated by radical recombination. In our opinion, a more convincing and simpler explanation lies in the relaxation mechanism of radical loss.

7.3. A MODEL FOR DIFFUSION-CONTROLLED REACTIONS IN THE CONDENSED PHASE

A theory of rates of bimolecular reactions in liquids and solids has been formulated by Waite [538, 539]. Basing himself on the theory of diffusion processes and the kinetic theory of bimolecular reactions in the gaseous phase, he has developed an expression for the rate constants of bimolecular reactions in condensed media within the framework of his formal kinetic theory. This theory may be looked upon as a generalization of the formal kinetic theory of reactions in the gaseous phase to reactions in condensed media.

By this theory, the rate of a bimolecular reaction

$$A \quad B \longrightarrow AB$$

is controlled by the following factors:

(1) the probability of collision between A and B as they move around at random;

(2) the probability that A and B will react with each other upon collision.

This leads to a known expression [540] for the rate of a bimolecular reaction in the gaseous phase:

$$dc_A/dt = Z_{AB}(r^*_{AB}, c_A, c_B)\, p \exp(-\Delta E^*/RT) \qquad (7.14)$$

where $Z_{AB}(r^*_{AB}, c_A, c_B)$ is the rate of A-B collisions (collision frequency) for species with a collision diameter r^*_{AB} and concentrations c_A and c_B; p and ΔE^* are the steric (probability) factor and the activation factor, respectively.

To develop an expression for the rate of a bimolecular reaction in condensed media in terms of r^*_{AB}, p, ΔE^* and the diffusion characteristics of the reactive species, Waite [538] makes the following additional assumptions:

(1) Any motion of a reactive species is independent of its history. This implies that a reactive species attains a state of thermal equilibrium with the surroundings immediately after each movement. Owing to this assumption, the average displacement of each particle can be computed on the basis of stochastic theory.

(2) Any set of discrete positions that species can take up owing to, say, the lattice structure in solids can be approximated by a continuum of positions such that random motion or diffusion can be

described by differential equations (otherwise, the need would arise for difference equations).

(3) There is no correlation between the distributions of two species A or two species B, and no correlation can arise between two species A either as a consequence of direct interactions between these species or their interaction with species B.

In the general form, the solution for diffusion-controlled second-order reactions, subject to the above assumptions, may be written [539]:

$$dc_A/dt = dc_B/dt = -4\pi r^{*2} D c_A c_B \beta$$

$$\times \left\{ 1 - \frac{r^*\beta}{r^*\beta + 1} \left[1 - 2e^{mt} \int_{(mt)^{1/2}}^{\infty} \frac{\exp(-\alpha^2)}{\pi^{1/2}}\, d\alpha \right] \right\} \tag{7.15}$$

where

$$m = D(r^*\beta + 1/r^*)^2 \tag{7.16}$$

and

$$\beta = [\Delta r^* \nu p \exp(-\Delta E^*/RT)]/D \tag{7.17}$$

where D is the sum of the diffusion coefficients for species A and B in the medium; r^* is the radius of the spherical shell surrounding a species A_i (the radius of capture for A_i); Δr^* is the thickness of the shell enveloping the nearest neighbours of A_i round its capture sphere; ν is the average frequency at which the nearest species B collides with species A (it is equivalent to the collision frequency in the kinetic theory of gases); p and ΔE^* are the steric and activation factors of the reactive species.

For the initial rate, where $mt \ll 1$, Eq. (7.15) reduces to

$$dc_A/dt = -4\pi r^{*2} \Delta r^* \nu p \exp(-\Delta E^*/RT) c_A c_B \tag{7.18}$$

In the steady state, at times substantially exceeding mt, the reaction rate is given by

$$dc_A/dt = -4\pi r^{*2} D \frac{\beta}{r^*\beta + 1} c_A c_B \tag{7.19}$$

It is seen from Eqs. (7.18) and (7.19) that in either case the reaction rate must be described by a second-order kinetic equation, but with the rate constants differing in magnitude. In the intermediate region, the reaction rate will be described by a more general expression, Eq. (7.15). If diffusion is not the rate-controlling stage ($r^*\beta \ll 1$), which is the case in most conventional reactions in the liquid phase, the reaction rate will be described by one and the same second-order equation over the entire time interval.

7.4. THE CAGE MODEL FOR REACTIONS IN THE SOLID PHASE

A formal-kinetic cage model for bimolecular reactions in the condensed phase has been proposed by Lebedev [524]. This model has widely been used to interpret the kinetics of the loss of radicals and other reactive species in the solid phase at low temperatures.

The model is based on the following assumptions.

1. A chemical reaction between A and B does not begin until they find themselves in the same cage. Here, the cage means some reactive volume v^*. It is assumed that $v^* \approx \gamma\lambda^3$, where λ is the lattice constant, and γ is a coefficient characterizing the specific matrix structure and the character of the reaction; it is presumed that ordinarily γ differs little from unity. Unfortunately, resort to the reactive volume v^* renders the physical picture of the process less clear.

2. Initially, the cage contains no more than one species. Here the "species" applies to any conceivable reactive centres, such as radicals, valence-unsaturated segments of macromolecules, etc. The motion of such species is construed in a wide sense and includes processes widely differing in physical character, such as diffusion of molecules and transfer of a reactive centre owing to a reaction with the molecules that make up the walls of the cage.

3. Transfer of reactive species from cage to cage due to thermal or any other activation can be described by an expression of the form

$$k_m = \nu_m^0 \exp(-E_m/RT) \tag{7.20}$$

where ν_m^0 is the pre-exponential factor and E_m is the activation energy for the migration of a reactive species from cage to cage.

4. The reaction taking place in the cage can be treated as a pseudo-monomolecular transformation (A . . . B) → AB, whose rate is described by a constant k_i equal to

$$k_i = f_i \nu_i^0 \exp(-E_i/RT) \tag{7.21}$$

where $f_i \nu_i^0$ is the pre-exponential factor and E_i is the activation energy for interaction between species A and B in the cage.

Once the species find themselves within the reactive volume v^*, they will remain in thermal equilibrium with the surroundings for a time approximately equal to $1/k_m$. Therefore, the rate of interaction between the species in volume v^* can be described by Eq. (7.21).

5. A process taking place in one cage is in no way related to that in another.

The cage model yields the following equation for the reaction rate

$$dc_A/dt = k_m^{(A)} c_A \ln\left(1 - \frac{k_i v^* c_B}{k_i + k_m^{(A)} + k_m^{(B)}}\right)$$

$$+ k_m^{(B)} c_B \ln\left(1 - \frac{k_i v^* c_A}{k_i + k_m^{(A)} + k_m^{(B)}}\right) \qquad (7.22)$$

Compare the results given by Eq. (7.22) with experimental data [524]. Subject to

$$k_i v^* c_{A,B} \ll k_i + k_m \qquad (7.23)$$

Eq. (7.22) reduces to a simple second-order kinetic equation

$$-dc_A/dt = \frac{\left(k_m^{(A)} + k_m^{(B)}\right) k_i}{k_m^{(A)} + k_m^{(B)} + k_i} v^* c_A c_B = k_{\text{eff}}\, c_A c_B \qquad (7.24)$$

The condition (7.23) is satisfied either when $k_m \ll k_i$, which implies that diffusion is not a rate-controlling stage and that the reaction proceeds in the kinetic region, or when $v^* c_{A,B} \ll 1$, which implies high degrees of conversion and that the reaction proceeds under steady-state conditions.

For the recombination of free radicals in the condensed phase, it may be taken that $k_m \ll k_i$ (which implies that the rate of recombination is controlled by diffusion). Then, subject to the condition $A \equiv B$, the rate is

$$dc/dt = 2k_m c \ln(1 - v^* c) \qquad (7.25)$$

Equation (7.25) can only be integrated numerically, which is done by Lebedev [524] for the initial condition $c_0 = c_{\text{lim}} = 1/v^*$. At $c = c_{\text{lim}}$, the rate of recombination described by Eq. (7.25) becomes infinite. The dependence of the ratio v^*/c on the generalized time $\tau = 2k_m t$, deduced by the numerical integration of Eq. (7.25), and an experimental plot for the recombination of alkyl radicals in irradiated polyethylene are shown in Fig. 7.4 borrowed from [524]. It is to be noted that even at the lowest temperature (202 K) for which [541] gives kinetic data for radical recombination, the radical concentration at zero time on the kinetic curve is as low as about 30% of the initial concentration of trapped radicals at liquid-nitrogen temperature.

It is worth mentioning the physico-chemical meaning of the expression for the rate constant, examined in [524]. The asymptotic equation (7.24) answers the following kinetic scheme:

$$A + B \underset{k_m}{\overset{k_m v^*}{\rightleftarrows}} (A \ldots B) \xrightarrow{k_i} AB \qquad (7.26)$$

such that

$$k_{\mathrm{eff}} = k_m k_i v^*/(k_m + k_i) \tag{7.27}$$

According to the above scheme, bimolecular reactions in the condensed phase proceed in two monomolecular stages. The first stage consists in the migration of the active centre and is characterized by the constant k_m. The second stage is the reaction (A . . . B) → AB in the cage. A major distinction of this stage is that the life time of the complex (A . . . B) is always longer than the time of double collisions in the gaseous phase (about 10^{-13} s) and is apparently long enough for the (A . . . B) complex to reach equilibrium with the surroundings each time. The spatial migration of active centres in condensed media may occur as a result of both ordinary diffusion of species carrying such centres, and a non-diffusion relay race of charges or free valences. Experimental verification of non-diffusion relay race would be a major discovery. At present, however, one can hardly name a single system in which non-diffusion migration of active centres may be said with certainty to take place.

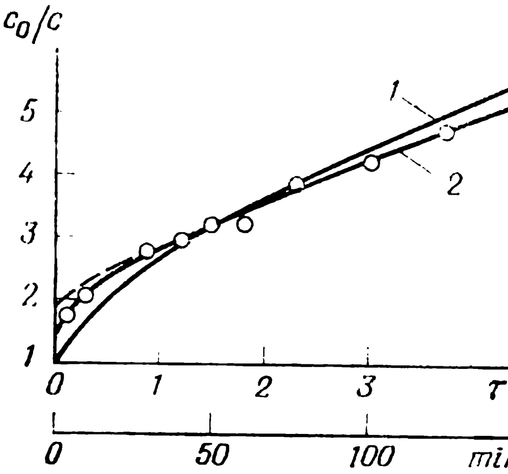

Fig. 7.4. Kinetic curves for recombination of alkyl radicals in irradiated polyethylene: (*1*) theoretically computed at $c_0 v^* = 1$ and (*2*) experimentally derived [541]

The abnormally high values of k_{eff} and E_{eff} usually obtained from experimental data processed according to Eq. (7.24) can be attributed to the fact that for a chemical reaction to take place in a solid, a number n of matrix segments must be activated simultaneously. If V is the activation energy for one segment, and ΔS_V is the entropy of the process, then for a process involving n matrix segments the constant k_m will be given by

$$k_m \approx (kT/h) \exp(n\Delta S_V/R) \exp[-(E + nV)/RT] \tag{7.28}$$

Equation (7.28) explains the abnormally high values of k^0_{eff} and E_{eff} and the compensation relation existing between them [501].

Lebedev [524] justly notes that studies of radical recombination yield practically no data about the constant k_i characterizing the rate of the reaction (A . . . B) → AB in the cage.

The cage model has further been developed by Lebedev, and also by Mikhailov *et al.* [542]. Their ideas form the basis for a polychromatic kinetic model of chemical reactions in the solid phase. Among other things, their model is based on the assumption that in a solid a continuous set of processes goes on, differing in activation energy, but involving the same reactive species. In such interpretation, this model has been applied to radical reactions at low temperatures in [543] through [546].

The polychromatic kinetic model permits a qualitative interpretation of the basic radical reactions at low temperatures. Recently, prominence has been given to the role of free volume in the kinetics of radical loss [547, 548].

7.5. THE TUNNEL MECHANISM OF REACTIONS

As already noted more than once, chemical reactions at low temperatures display a number of kinetic features that cannot be explained on the basis of the traditional concepts of chemical kinetics. Among other things, it has been found that the rate of some reactions at low temperatures depends little on temperature, so that their activation energy is zero very nearly. The reaction rate is fairly high even at very low temperature. This is especially surprising, if we recall that the diffusion of the reactants in such conditions is severely impeded. On the other hand, if the rates of low-temperature reactions were evaluated by the Arrhenius equation and from the activation energies for these reactions in the liquid phase, we would have to conclude that practically no reactions could have taken place in the circumstances. Examples of such processes are cited in the reviews by Goldansky [173] and [549].

In an attempt to explain these vagaries, recourse is had to the concept of the tunnel mechanism which is based on the quantum-chemical nature of reactive species. According to this view, a decrease in temperature causes tunnel sub-barrier transitions to play a greater part than the Arrhenius super-barrier transitions. In overall terms, the part played by the tunnel effect in low-temperature chemical reactions is examined by Goldansky [173, 549].

The role of the tunnel effect must be especially prominent in reactions involving species of low mass, such as electrons and protons. Formally, the kinetics of tunnel transfer reactions in solids is described in [255], and the likely role of the tunnel effect in post-radiation reactions of reactive species in organic solids is discussed in [550] and [551].

The likely realization of nonstationary states in the case of an electron residing in a system of two potential wells is examined in

[552]. The systems in which this situation can arise are complexes of mixed valences, containing metal atoms in identical ligand surroundings, but differing in the valent state. Examples of such systems are Fe_3O_4 and Eu_3S_4. Variations in their gamma-resonance spectra are interpreted on the basis of a fast jump of an electron between metal ions by Evans *et al.* [553] for the former (during the transition through the Vervey point) and by Berkooz *et al.* [554] for the latter (in the temperature interval from 83 K to 325 K).

The likely delocalization of an excess electron in a three-nuclear complex containing two Fe^{3+} ions and one Fe^{2+} ion has been investigated by Goldansky *et al.* [555]. Such a system can be treated as consisting of three Fe^{3+} ions and one excess electron. Gamma-resonance spectra have been analyzed for basic acetate chloroplatinate of Fe^{3+}, $[Fe_3O(CH_3COO)_6(H_2O)_3]_2PtCl_6 \cdot nH_2O$ (I), and basic acetate of iron of mixed valence, $Fe^{2+}Fe_2^{3+}O(CH_3OO)_6(H_2O)_5$ (II), in the temperature interval between 4.2 K and 360 K.

According to available data, the extra electron in three-nucleus acetate complex of iron of mixed valence experiences spatial-temporal delocalization to an extent determined by temperature. This militates for the intermediacy of the tunnel mechanism in electron transfer and the validity of the adopted structural model of complex II [556]. The other mechanism involving electron exchange [557], as Goldansky *et al.* believe, is not likely to take place.

According to experiments with the radiolysis of solid glassy matrices, an important role is played by the tunnel electron transfer for large distance exceeding the sum of van-der-Waals radii of the interacting species [252, 266, 558]. This, for example, goes for the photo-induced transfer of an electron from naphthalene (NP) and diphenylamine (DPA) to CCl_4 in glassy alcohol (CH_3OH) matrices at 77 K [558]. It is logical to expect that the tunnel effect can cause the electron transfer for large distances also in the photolysis of solid matrices containing electron-donor (D) and electron-acceptor (A) species [559].

With an electronically excited donor, the height of the energy barrier for the transfer of an electron from D to A is reduced. In the circumstances, the rate of the tunnel electron transfer must, in a first approximation, increase [560] according to the equation

$$k = a \exp \left\{ -(2rb/\hbar) \left[2m_e (V - E) \right]^{1/2} \right\}, \mathrm{s}^{-1} \tag{7.29}$$

where k is the tunnelling rate constant, a is the frequency factor, m_e is the mass of an electron, V is the ionization potential, E is the energy of the state taking part in tunnelling, $b \approx 1$ is the factor accounting for the departure of the potential barrier from a rectangular shape, and r is the width of the barrier.

At sufficiently high concentrations of A (that is, low values of r), the sub-barrier electron transfer, $D^* + A \rightarrow D^+ + A^-$ will compete with the super-barrier transfer.

In the opinion of Zhutkovsky *et al.* [558], in the light-induced electron transfer involving organic molecules this effect must manifest itself in the transition (with increasing concentration of A) from the usual two-quantum mechanism

$$D(S_0) \xrightarrow{h\nu_1} D(S_1) \rightsquigarrow D(T_1) \xrightarrow[A]{h\nu_2} D^+ + A^-$$

to a one-quantum mechanism

$$\begin{tikzcd} D(S_0) \arrow[r, "h\nu_1"] & D(S_1) \arrow[r, squiggly] \arrow[d] & D(T_1) \arrow[dl, "A"] \\ & D^+ + A^- & \end{tikzcd}$$

This transition must affect the dependence of the rate of the photo-induced electron transfer on light intensity and, as a consequence, can be detected by experiment.

According to Zhutkovsky *et al.* [558], the presence of the tunnel effect is disclosed by the fact that the exponent n in Eq. (7.32)

$$W \approx I^n \tag{7.32}$$

describing the rate of formation of $\cdot CCl_3$ radicals decreases from 2 to 1 with increasing concentration of CCl_4 (0-0.8M).

Exposure of glassy methanol solutions of naphthalene, $[NP] = 1 \times 10^{-2} M$, and diphenylamine, $[DPA] = 1 \times 10^{-3} M$, to light ($\lambda > 300$ nm) causes $\cdot CCl_3$ radicals to form. Exposure of DPA in the presence of CCl_4 leads to the formation of $\cdot CCl_3$ radicals and, at the same time, the absorption of a DPA^+ cation radical at $\lambda_{max} = 690$ nm. For a specimen containing 0.6M CCl_4, the order of magnitude for the concentration of DPA^+, estimated from the optical absorption spectrum, checks with that of $\cdot CCl_3$ concentration as determined from ESR spectra. The distance from a $\cdot CCl_3$ radical to the nearest DPA^+ cation radical, as determined from the line width of the ESR spectrum for the $\cdot CCl_3$ radical, is found to be > 1.5 nm. On the strength of these data, Zhutkovsky *et al.* believe that the observed one-quantum electron transfer from photo-excited species to CCl_4 covers a distance exceeding 1.5 nm. Zhutkovsky *et al.* [558] also believe that no photo-induced transfer occurs directly in the complex. Since no changes have been observed in the absorption spectra of NP and DPA in the investigated range of CCl_4 concentrations (0-0.8M) at 230-330 nm and 77 K, there is, apparently, every ground for excluding the super-barrier electron transfer in complexes of NP and DPA with CCl_4 [558].

In our opinion, it is not unlikely that CCl_4 forms molecular complexes with NP and DPA in the investigated systems. CCl_4 is fairly powerful acceptor and is capable of forming molecular complexes with a number of compounds [561]. That the absorption spectra show no changes in the range 230-330 nm is not a sufficient ground for deeming complex formation unlikely. For example, Sergeev *et al.* [562], using the NMR technique, have found that aniline forms molecular complexes with chloroform, whereas conventional spectroscopy fails to detect such complexes in the same experiments.

Goldansky *et al.* [563] have investigated the electron exchange reaction between Fe^{2+} and Fe^{3+} ions in ice in the temperature interval 77-195 K. In contrast to Horne [564], and Nitzan and Wahl [565] who used chemical analysis for product characterization in their study of the same reaction down to 195 K (which necessitated warming up the specimen and melting of the ice), Goldansky and associates [563] observed the process *in situ* (directly in ice) and used Moessbauer spectroscopy [330] for product identification.

The kinetics of electron exchange was investigated, using a frozen $1.94\times 10^{-2}M$ solution of $Fe(ClO_4)_2$ with a natural ^{57}Fe content of 2.19% and also a $1.76\times 10^{-2}M$ solution of $Fe(ClO_4)_3$ enriched with ^{57}Fe up to 91%. An amount of $0.5M$ perchloric acid was added to the solution. The starting solutions were mixed and frozen at the highest possible rate so as to minimize the extent of the reaction in the liquid phase as far as possible. It took several seconds to prepare and freeze the specimens to the temperature of liquid nitrogen. Yet, the exchange was only 50% even immediately after the specimen preparation. The specimens were held at a specified temperature for some time, following which their Moessbauer spectra were recorded at the temperature of liquid nitrogen. The amounts of bi- and tri-valent iron isotopes were determined from the area of the respective lines in the spectra. The kinetics of electron exchange was investigated at three temperatures, namely 195 K, 178 K, and 159 K, in addition to the temperature of liquid nitrogen at which the reaction did not practically proceed. The general equation of the reaction has the form

$$^{*}Fe^{3+} + Fe^{2+} \rightleftarrows {}^{*}Fe^{2+} + Fe^{3+} \tag{7.33}$$

The kinetics of the reaction is described by a second-order equation

$$\{[Fe^{2+}] + [Fe^{3+}]\}\,kt = -\ln(1 - x/x_\infty) \qquad B = \{[Fe^{2+}] + [Fe^{3+}]\} \tag{7.34}$$

where B is the total concentration of iron ions, k is the rate constant of the reaction, x and x_∞ are the fractions of ^{57}Fe isotope present in the Fe^{2+} form at time t and t_∞, respectively.

The term $\ln(1 - x/x_\infty)$ is a linear function of time. The rate constant of the reaction was found to be $(7.6\pm 1.5) \times 10^{-2}$ litre $mole^{-1}$ s^{-1} and $(5.2\pm 1.2) \times 10^{-2}$ litre $mole^{-1}$ s^{-1} at 195 K (two sets of measurements); $(7.0\pm 1.4) \times 10^{-3}$ litre $mole^{-1}$ s^{-1} at 178 K; and $(9.3\pm 1.8)\times$ $\times\ 10^{-4}$ litre $mole^{-1}$ s^{-1} at 159 K. The activation energy as found by the Arrhenius equation using the above data was 39.4 ± 2 kJ $mole^{-1}$.

Goldansky *et al.* [536] believe that, using a direct analysis of the isotope distribution of iron ions between the two valent states in the solid phase, they have been able to detect a fairly rapid electron exchange between Fe^{2+} and Fe^{3+} in ice. Owing to the novel technique they have also been able to evaluate the rate constants for electron exchange directly in ice, down to very low temperatures. The average distance between the iron ions at the investigated concentrations has been found to exceed more than ten-fold the distance between neighbouring water molecules, which excludes any direct contact between the ions, if they are assumed to be uniformly distributed throughout the specimen. In the opinion of Goldansky and his associates, the rate constants thus found are not due to the diffusion of ions in ice, but are related to electron transfer in the frozen solutions, probably involving the molecules of the medium. From this stand-point, it is difficult to account for the strong temperature dependence of the electron exchange rate ($E = 39.4$ kJ mole^{-1}) at temperatures exceeding 159 K, because it makes impossible for the far tunnel electron transfer from Fe^{2+} to Fe^{3+} ions to play an important role [330, 331].

To describe the radiophotoluminescence of frozen organic substances, Berlin *et al.* [551] propose a model which allows for a competition between the tunnel recombination of electrons localized in a matrix M with positive ions

$$M^+ + e^- \longrightarrow \text{Excited molecules } M^* \qquad (7.35)$$

on the one hand, and the tunnel electron capture by acceptors A without the formation of excited molecules M*, on the other:

$$e^- + A \longrightarrow A^{\bullet} \qquad (7.36)$$

This model has been extended to account for the diffusion of reactants in [566] and [567].

The time of sub-barrier transitions even for such species as electrons rapidly increases with increasing distance of tunnelling, and becomes very long at relatively small distances between the reactants. Because of this, diffusion may cause the relative position of the reacting species to change during this time interval. In [566], Berlin deduces the effective rate constant for the tunnel capture of an electron by an acceptor molecule in the stationary state with allowance for diffusion. He concludes that the tunnel mechanism can compete with the diffusion mechanism only at low temperatures typical of solid matrix experiments. At $T > 200$ K, the tunnel mechanism can no longer compete with the diffusion mechanism, if the life time of the reacting species exceeds the time t_1 required for the reaction to attain its steady-state rate. The diffusion can likewise affect the rate of the tunnel electron transfer between closely spaced reacting species in the early stages of the reaction at $t \ll t_1 \sim R_{\mathrm{eff}}/D$. Here, R_{eff} is the "effective radius" of the reaction described by Eq. (7.36). The expression for the effective radius is developed by Berlin in the same work [566].

It is to be noted that the role of diffusion must gain in importance substantially with increase in the mass of the tunnelling species. This should likewise be expected when the reacting species are distributed nonuniformly in the matrix. The quantitative contribution of diffusion to the kinetics of the reactions in multicomponent solid matrices with a nonuniform distribution of components remains to be studied yet.

The important role played by the tunnel mechanism in low-temperature polymerization of formaldehyde has already been noted in Chap. 4. This system has been found to have a low-temperature quantum limit of reaction rate and has been among the first to be assessed for the possibility of tunnelling not only for electrons and protons, but also for molecular groups [326]. In more detail, the role of low-temperature tunnelling in the kinetics of chemical reactions is examined in [173] and [549].

Even a brief overview of kinetic models shows that chemical reactions proceed in the solid phase at low temperatures by a very complex mechanism. Each model gives a good account of only some kinetic aspects and fails to do so for the other. It is, therefore, one of the important tasks facing cryochemistry to develop a unified theory for the kinetics of low-temperature reactions.

CHAPTER EIGHT

REACTIONS IN MULTICOMPONENT FROZEN SYSTEMS

Investigations carried out in recent years have shown with increasing clarity that proper insight into the mechanism of chemical reactions in ordered systems calls for detailed knowledge of their phase state. It is important to investigate the formation and propagation of defects in solids and to correlate these processes with variations in the reactivity of a given system. The effect of an inhomogeneity on a chemical reaction in a specimen will be most pronounced in a multicomponent system.

The late 50s saw the beginning of experiments with polymerization [298] and with the double-bond addition of halogens at low temperatures [403]. These experiments showed that in some cases a reduction in temperature could stimulate a chemical reaction so that a process unable to proceed at room temperature would readily do so at low temperatures. Some reactions were found to occur rapidly and spontaneously at low temperatures, chain reactions were discovered in the solid phase, and phase transitions and unstable molecular complexes of the donor-acceptor type were observed to play a special role in low-temperature chemical conversions. These and other results are reviewed in [235, 302, 401, 402, 568].

In the early 60s, investigators discovered that chemical and biochemical processes could go on in frozen solutions at temperatures below the melting point of the solvent [475, 569]. Investigations carried out both in and outside the Soviet Union demonstrated that many kinetic aspects of chemical processes could be interpreted in the light of the structural and phase inhomogeneity of frozen multicomponent systems [476, 478, 479].

8.1. THE STRUCTURE OF FROZEN SOLUTIONS ACCORDING TO ESR DATA

The sources cited in Chap. 6 show that some chemical processes can be speeded up by bringing down their temperature and by freezing the solutions. This has been assigned to several causes, including the inhomogeneous phase setup of the system. For a reaction to take place, it is important that the molecules of the reactants possess some mobility. Unfortunately, practically nothing is said in the literature about the phase state and mobility of the species in frozen solutions in the temperature interval where the processes proceed at measurable rates. The phase state of frozen solutions can conveniently be investigated by ESR and NMR techniques.

In ESR spectroscopy, the phase state of and mobility in frozen solutions are usually investigated, using the marker in the form of stable radicals (say, 2,2,6,6-tetramethyl-4-oxyl-1-piperidinyloxy radical), as a paramagnetic probe. The use of stable radicals for the study of molecular mobility is based on the relation that exists between the line width of ESR spectra and the rotational and translational mobility of these radicals [212, 570, 571]. Rotational mobility can be determined from the ESR spectra of diluted radical solutions. It is known from ESR theory [572] that the anisotropic superfine electron-nuclear and spin-orbital interactions in a radical depend on the relative orientation of the external magnetic field and the orbital of the unpaired electron. The rotation of the radical modulates these interactions, thereby bringing about fluctuations in the local magnetic fields and the broadening of ESR lines. This broadening in turn depends on the character of the unpaired electron orbital (the anisotropy of the hyperfine interaction (HFI) constant and the g-factor) and is determined by the correlation time, τ_{cor}. The correlation time characterizes the intensity of the rotational motion of the radical. Its magnitude corresponds to the time required for the radical to change its orientation by an angle of about one radian.

At $\tau_{cor} \leqslant 10^{-11}$ s, the rotation of the radical averages the anisotropic interaction, and the ESR spectrum consists of three lines of equal intensity. At $\tau_{cor} \gg 10^{-11}$ s, the rotation of the radical fails to average the anisotropic intermolecular interactions completely. As a result, in the interval $5 \times 10^{-11} < \tau_{cor} < 10^{-9}$ s, the width and, as a consequence, the intensity of the spectral lines change (the region of fast motion). The increase in τ_{cor} from 10^{-9} to 1×10^{-7} s leads to a change not only in the width, but also in the position and shape of the spectral lines (the region of slow motion). No further changes are observed in the spectrum at still longer correlation times.

Line width in the region of fast motion can conveniently be analyzed by a theory proposed by Freed and Fraenkel [573]. The equation used to find the correlation time τ_{cor} (in seconds) has the form

$$\tau_{cor} \approx 6.6 \times 10^{-10} \, \Delta H_{(+1)} \left(\sqrt{I_{(+1)}/I_{(-1)}} - 1 \right) \tag{8.1}$$

where $\Delta H_{(+1)}$ is the distance (in G) between the points of maximum slope of the spectrum component corresponding to the smaller magnetic field; $I_{(+1)}$ and $I_{(-1)}$ are the intensities of the HFI components in low and high fields, respectively.

Equation (8.1) does not hold in the region of slow motion with correlation times ranging between 10^{-9} s and 1×10^{-7} s.

Using Eq. (8.1), it is possible to determine the correlation time for the nitroxide radical from ESR spectra of frozen solutions. As an example, for 2,2,6,6-tetramethyl-4-oxyl-1-piperidinyloxy in frozen dioxane (Fig. 8.1),

$$\tau_{\mathrm{cor}} = 6.6 \times 10^{-10} \times 2.25_{(+1)} \sqrt{181_{(+1)}/128_{(-1)} - 1} = 2.8 \times 10^{-10}\ \mathrm{s}$$

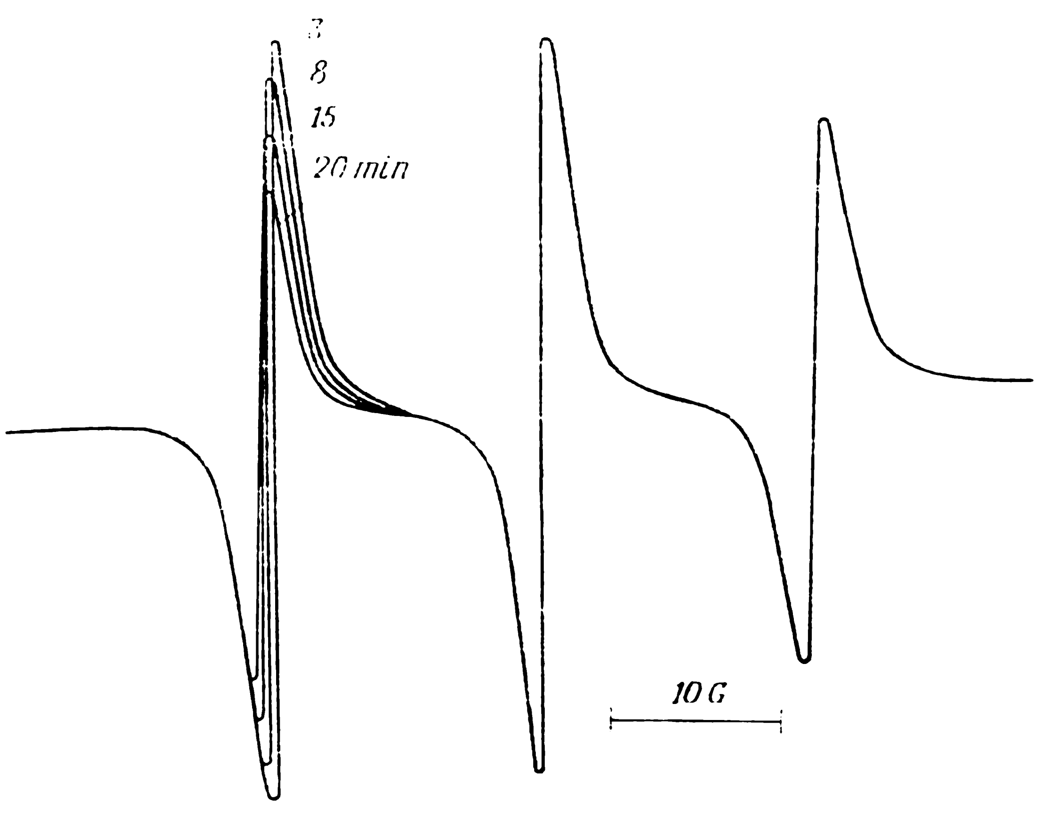

Fig. 8.1. ESR spectra for 2,2,6,6-tetramethyl-4-oxyl-1-piperidinyloxy in reaction with hydrazobenzene in frozen dioxane ($T = -28°\mathrm{C}$, $[\mathrm{R}]_0 = [\mathrm{C_{12}H_{12}N_2}]_0 = 1.1 \times 10^{-4}\,M$. Time variations in the spectrum are shown for one component)

It is seen from Fig. 8.1 that if the stable nitroxide radical is used as both a paramagnetic marker and a reactant, ESR technique will yield data about the rate of the reaction and the molecular mobility of the reactant in a frozen solution.

Binary and ternary solutions differing in composition have been investigated over a wide temperature interval from 313 K to 77 K. Each solution consisted of a solvent and a nitroxide radical or a solvent, a solute (diluent) and a nitroxide radical. In the experiments, the concentration of the radical was varied from $1 \times 10^{-6}M$ to $2 \times 10^{-4}M$. The concentration of the diluent was $0.5M$. The solvents used were benzene, nitrobenzene, dioxane, carbon tetrachloride, water, cyclohexane, *tert*-butanol, glycerine, and naphthalene. The diluents were chosen from among other solvents, and also methyliodide, triethylamine, hydrazobenzene, azobenzene, 1-hexene, ascorbic acid, inorganic salts of alkaline metals, and some other substances.

The phase state of each specimen was investigated by the ESR technique in the temperature interval from the freezing point of the solution down to 77 K. The spectra of the radical in various solvents in liquid and frozen solutions are shown in Fig. 8.2 as an example. In all solvents, except naphthalene and glycerine, the ESR spectra of liquid and frozen solutions at —18°C are triplets. The values of τ_{cor} indicate that even in a frozen solution at —18°C the radical possesses mobility comparable with that in the liquid phase.

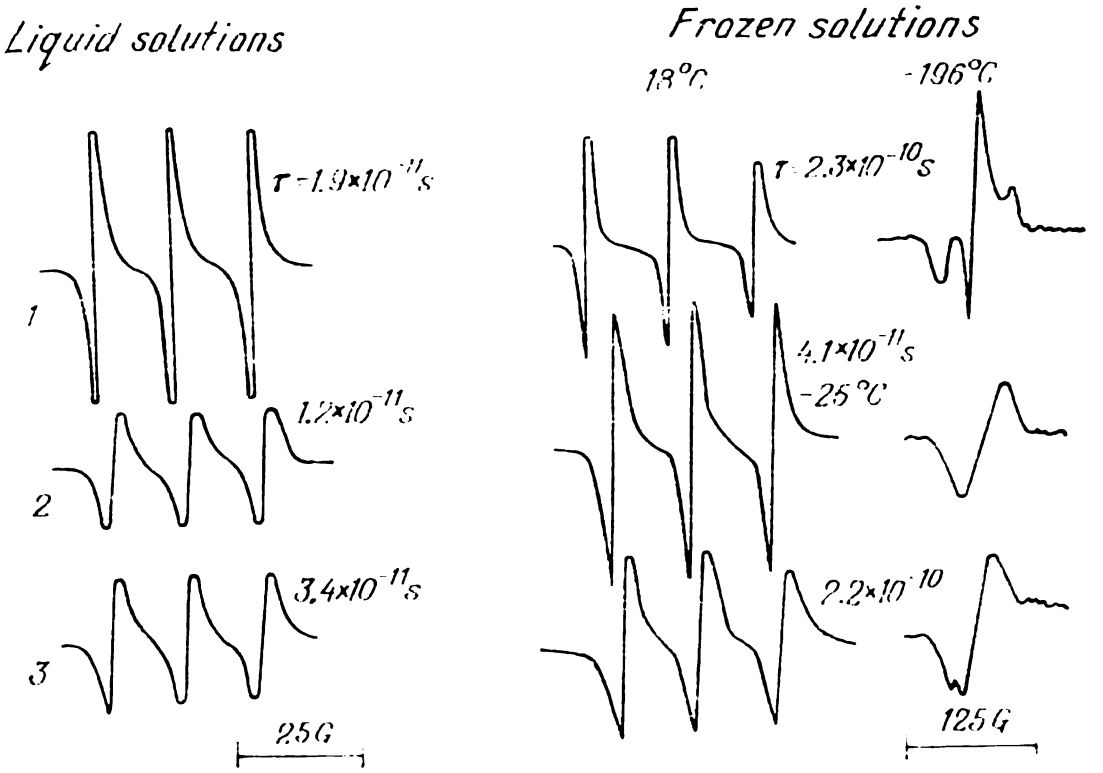

Fig. 8.2. ESR spectra and correlation times for nitroxide radical marker in liquid solutions ($T = 25°C$) and frozen solutions in various solvents ($[R] = 1.0 \times 10^{-5}$ M): (1) nitrobenzene (T_m = 5.6°C); (2) carbon tetrachloride (T_m = —23°C); (3) benzene (T_m = = 5.5°C)

The spectra of the nitroxide radical in a 10: 1 (by volume) mixture of glycerine and water have the form characteristic of those for stable nitroxide radicals in vitrifiable substances. The correlation time for such spectra is found by a more elaborate equation and is 10^{-5} or 10^{-6} s [574, 575].

Variations in ESR spectra with temperature are plotted in Fig. 8.3. Up to —90°C the radical retains a high mobility in frozen solutions. A similar picture has been observed in all the investigated solvents, except naphthalene and the glycerine-water mixture.

Freezing of the vitrifiable solutions has not produced triplet spectra for the nitroxide radical. Addition of glycerine has reduced the mobility of the nitroxide radical in frozen aqueous solutions: $\tau_{cor} = 8.3 \times 10^{-10}$ s in the presence of glycerine and 2.3×10^{-10} s in the absence of glycerine.

In neat naphthalene at room temperature, the radical has shown a singlet spectrum typical of the frozen solutions involving other solvents at liquid-nitrogen temperature. Addition of other solvents caused the singlet spectrum to change into a triplet one. For example, the introduction of 0.5*M* additions raised the mobility of the radical by several orders of magnitude, from $\tau_{cor} < 10^{-5}$ or 10^{-6} s to $\tau_{cor} = 4 \times 10^{-11}$ s.

It is interesting to consider the effect of additions on the ESR spectra of frozen solutions. As an example, Figs. 8.4 and 8.5 show the spectra of frozen solutions in dioxane, water, and naphthalene. The additions were substances whose freezing points are higher and substantially lower than the freezing point of each solvent.

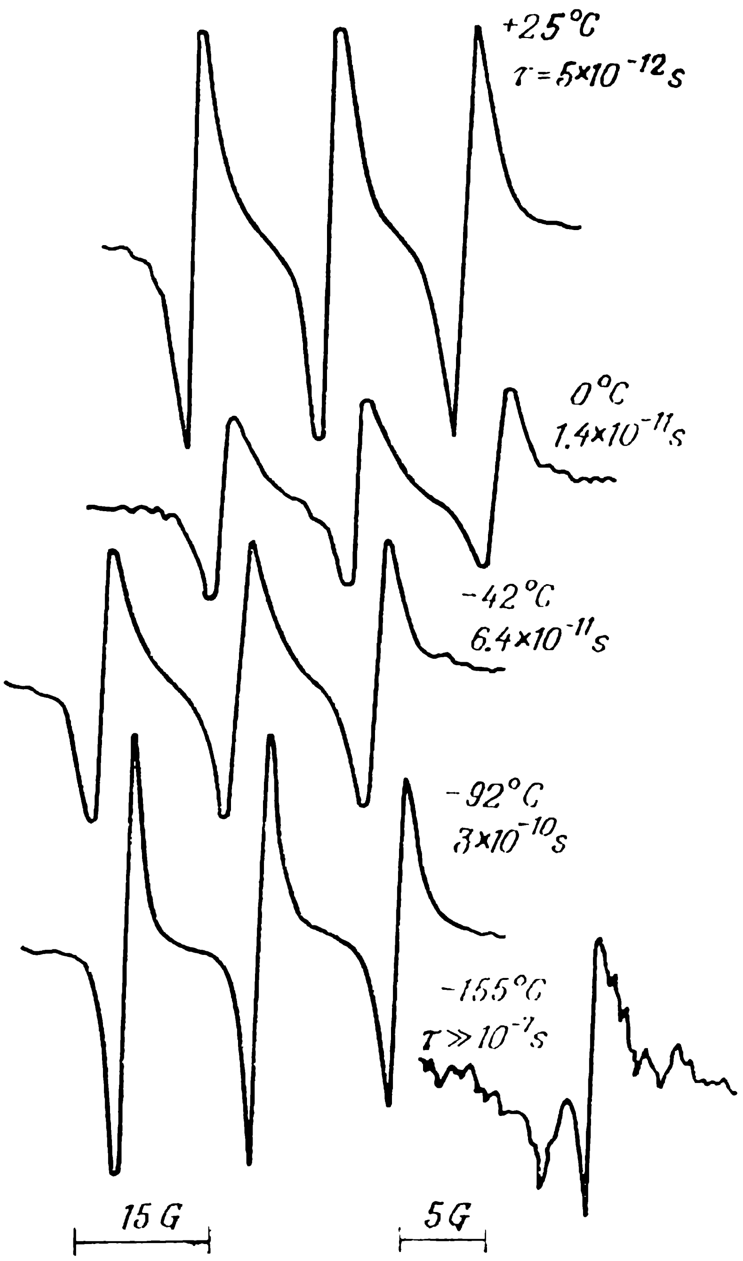

Fig. 8.3. ESR spectra and correlation times for nitroxide radical marker in benzene ($T_m = 5.4°C$) at various temperatures ($[R] = 2 \times 10^{-4}$ *M*)

The results thus obtained show that frozen solutions are inhomogeneous as regards structure and phase setup. They are complex two-phase systems consisting of a solid matrix and microinclusions whose molecular mobility is "frozen" only at the freezing point of the entire system. In the case of crystallizing solutions, practically all solutes are concentrated in the microinclusions, and the matrix is the solid solvent. The total volume of the microinclusions, as measured at medium concentrations of solutes, is considerable, so these microinclusions may be regarded as a separate microphase. Because the radical in this microphase has a mobility abnormally high for solids, we shall call this phase the liquid microphase.

It has been found that the liquid microphase remains stable for at least several days. The reduction in temperature down to —196°C causes the triplet spectrum to change into a very broad singlet spectrum. The subsequent rise in temperature, however, causes the singlet spectrum to go back to the triplet one, and the ESR spectra and the values of τ_{cor} at the same temperature are practically identical.

In addition to the above publications, several authors describe ESR studies on the phase state of frozen solutions at the boiling point of liquid nitrogen (—196°C). Khairutdinov and Zamarayev [576] have investigated the structure of frozen aqueous solutions of H_2SO_4 and $HClO_4$, using vanadyl salts as markers. They have found that the line width of ESR spectra for paramagnetic species in solids is related to their local concentration, c_{loc}. In glasses, $c_{loc} = c_0$ (the average concentration). The crystallization of any component of the solution can drive the paramagnetic markers into regions of increased c_{loc} ($c_{loc} > c_0$). In such a case, the distribution factor ρ depends on the ratio (by volume) of the crystal regions free from markers to those from which the markers have been driven. The formation of crystalline or glassy specimens depends on the concentration of the acid and the rate of freezing. Given a certain critical concentration of H_2SO_4, $c_c = 3.5M$, or at $[H_2SO_4] < 3.5M$, the aqueous solution of H_2SO_4 freezes to form an amorphous or a crystalline sample depending on the rate of freezing. In the latter case, the water in the specimen crystallizes into a solid matrix containing microregions of the composition $H_2SO_4 \cdot nH_2O$, where $n = 12 \pm 1.6$.

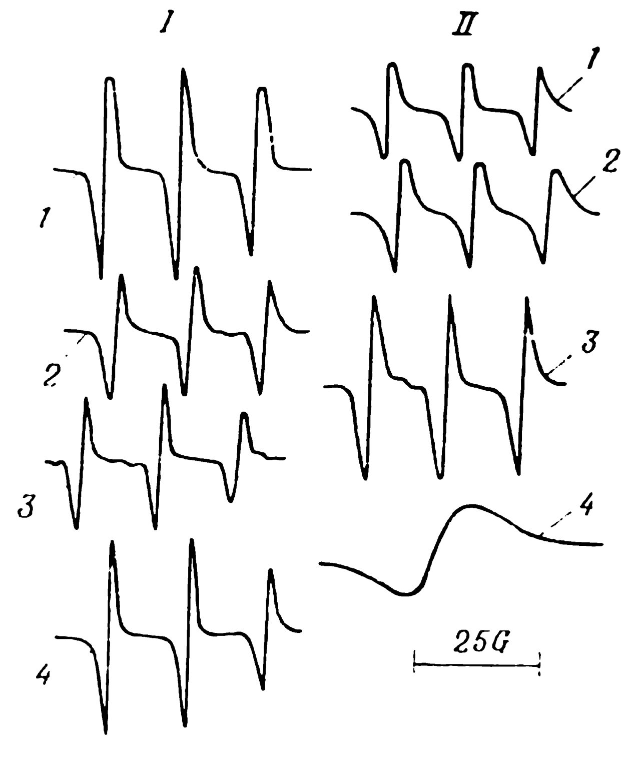

Fig. 8.4. ESR spectra and correlation times for nitroxide radical marker in (I) dioxane ($T_m = 11.8°C$, $T = -18°C$) and (II) naphthalene ($T_m = 80.1°C$, $T = 25°C$) in the presence of various diluents ($[R] = 10^{-5}\ M$, $[D] = 0.5\ M$):
I — (1) $(CH_3)_3COH$, $\tau = 1.3 \times 10^{-10}$ s; (2) CCl_4, $\tau = 4.4 \times 10^{-11}$ s; (3) H_2O, $\tau = 2.1 \times 10^{-10}$ s; (4) $C_6H_5N{=}NC_6H_5$, $\tau = 2.9 \times 10^{-10}$ s; II — (1) dioxane, $\tau = 4.0 \times 10^{-11}$ s; (2) $(CH_3)_3COH$, $\tau = 1.5 \times 10^{-10}$ s; (3) $C_6H_5NO_2$, $\tau = 2.6 \times 10^{-10}$ s; (4) no diluent

Using the stable 2,2,6,6-tetramethyl-4-oxyl-1-piperidinyl radical, Kokorin and Zamarayev [577] have investigated the structure of the following two-component solutions: heptane-ethanol, CCl_4-ethanol, and toluene-ethanol at liquid-nitrogen temperature. They have found that freezing causes the heptane-ethanol and CCl_4-ethanol solutions to separate into two phases, the solid nonpolar solvent and a solid binary mixture of a constant composition. Whereas the composition of the latter remains unchanged, the ratio (by volume) of the two phases varies according to the amount of ethanol present in the solution. Because of a higher solubility in ethanol, the radical is mainly concentrated in the ethanol-containing region. When the concentration of the radicals exceeds the solubility limit in the ethanol-containing regions, freezing causes the radical to form fine crystals that make up a separate phase. The findings of [577] agree well with those of [495, 578, 579].

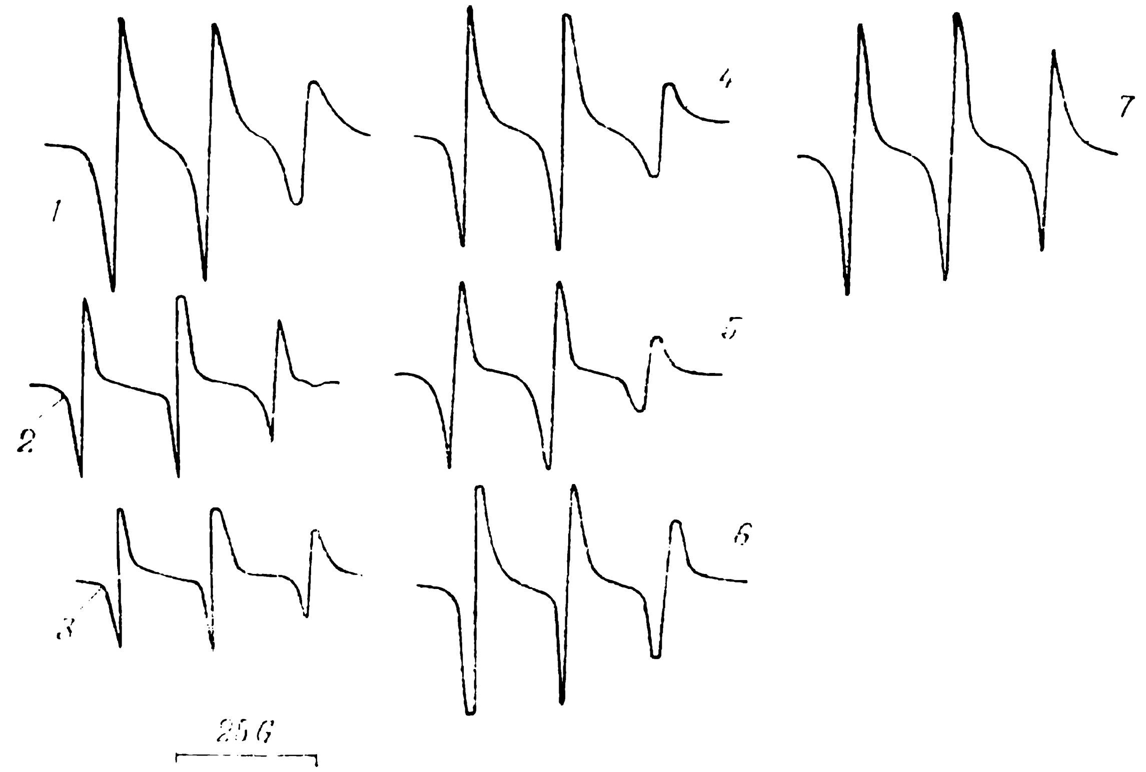

Fig. 8.5. ESR spectra and correlation times for nitroxide radical marker in frozen aqueous solutions with and without diluents present ($T = -18°C$ $[R] = 10^{-5}$ M): (1) diluents: Na_2SO_4 (1M) and $(C_2H_5)_3N$ (0.02M); $\tau = 7.8 \times 10^{-10}$ s; (2) NaCl (0.5M), $\tau = 2.2 \times 10^{-10}$ s; (3) NaCl (0.5M), and $(C_2H_5)_3N$ (0.02M), $\tau = 2.7 \times 10^{-10}$ s; (4) glycerine (0.5M), $\tau = 8.3 \times 10^{-10}$ s; (6) C_2H_5OH (0.5M), $\tau = 4.5 \times 10^{-10}$ s; (7) no diluent, $\tau = 2.3 \times 10^{-10}$ s

The ESR technique has also been used at 77 K to investigate frozen solutions of nitroxide radicals in ethanol, benzene, water, and benzene-ethanol and water-ethanol mixtures [580]. It has been found that in ethanol the radical molecules are spaced longer distances apart, whereas in benzene and water they form clusters. In frozen mixtures, a two-phase solid system is formed, consisting of the basic solvent (benzene or water) and ethanol clusters penetrated by the radical.

Mil *et al.* [581] have discovered phase inhomogeneity of the solutions of the monomers used in the production of polymers. Using a paramagnetic probe, they have carried out a detailed study on the structure of the frozen solutions.

To sum up, the ESR technique can yield valuable data about the phase state and structure of frozen solutions and has a fairly high sensitivity. Its use involves, however, the presence of paramagnetic markers in the system. Also, the ESR technique cannot give the quantitative content of nonparamagnetic components of the liquid microphase. More complete information about the phase state of frozen solutions can be obtained by NMR.

8.2. THE PHASE STATE OF FROZEN SOLUTIONS ACCORDING TO NMR DATA

The NMR spectra of a substance vary according as it is in the liquid or the solid state [572]. The absorption bands for the solid phase broaden so much in comparison with those for the liquid phase that they cannot be detected by high-resolution NMR instruments used in the study of liquid solutions. If a frozen solution comes by a liquid microphase, its high-resolution NMR spectra may be expected to display narrow resonance signals associated with the reactant and solvent molecules retaining their mobility. True to this expectation, frozen solutions generate relatively narrow resonance signals associated with the solutes and solvent [271, 582, 583].

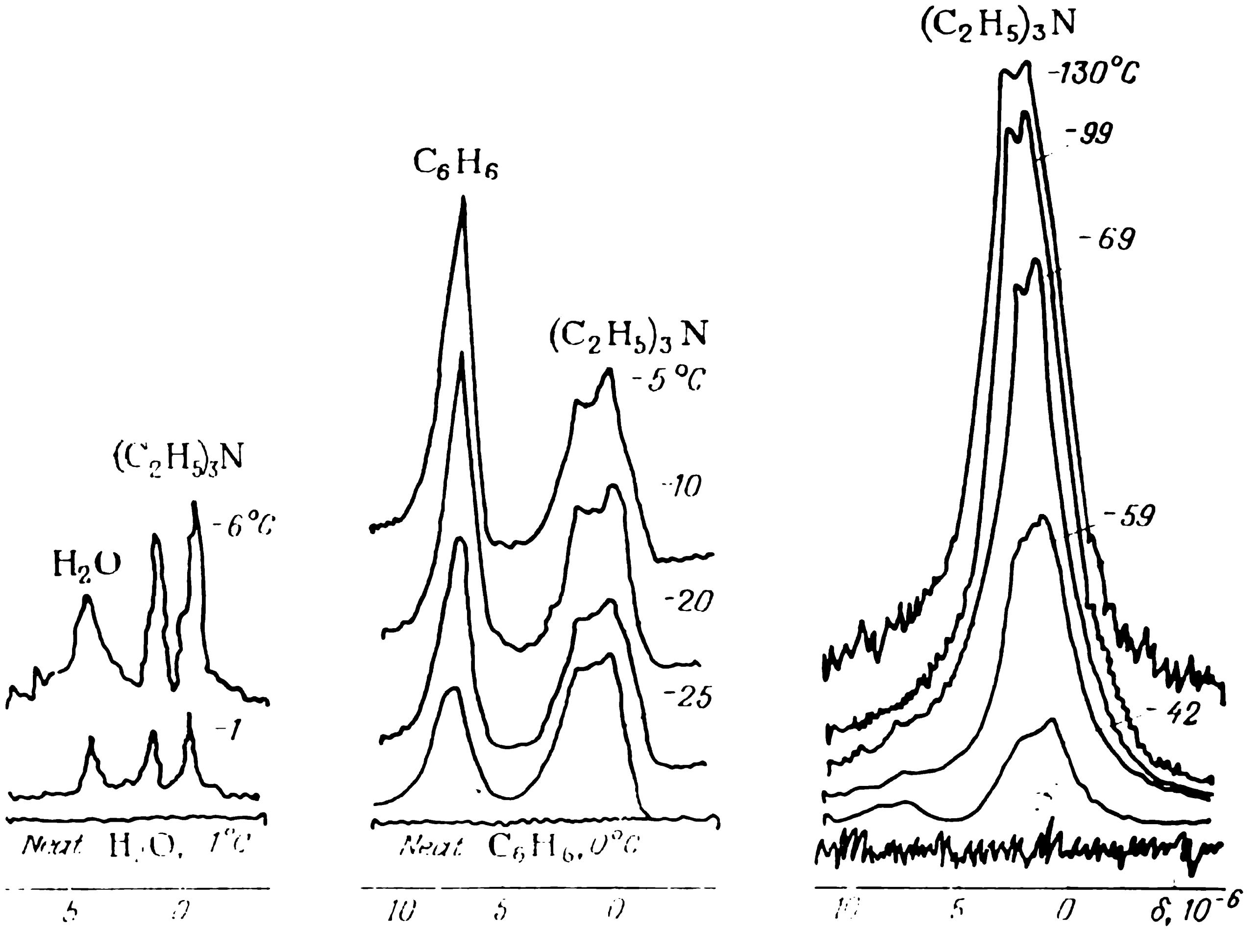

Fig. 8.6. NMR spectra for frozen neat solvents and solutions of triethylamine in water ($[(C_2H_5)_3N] = 0.04\,M$) and benzene ($[(C_2H_5)_3N] = 0.4\,M$) at various temperatures

As an example, Fig. 8.6 shows the high-resolution NMR spectra of frozen solutions of triethylamine in water and benzene. As is seen, the neat solvents, when frozen, do not produce high-resolution NMR spectra, whereas the spectra of the frozen solutions contain absorption bands assigned to triethylamine and the solvents. The presence of triethylamine which has a high molecular mobility can be detected in solution down to —130°C.

Variations in the quantitative composition of the liquid microphase with temperature and the composition of the starting liquid solutions have been traced by integrating the absorption bands in NMR spectra assigned to the various components of frozen solutions. The molar

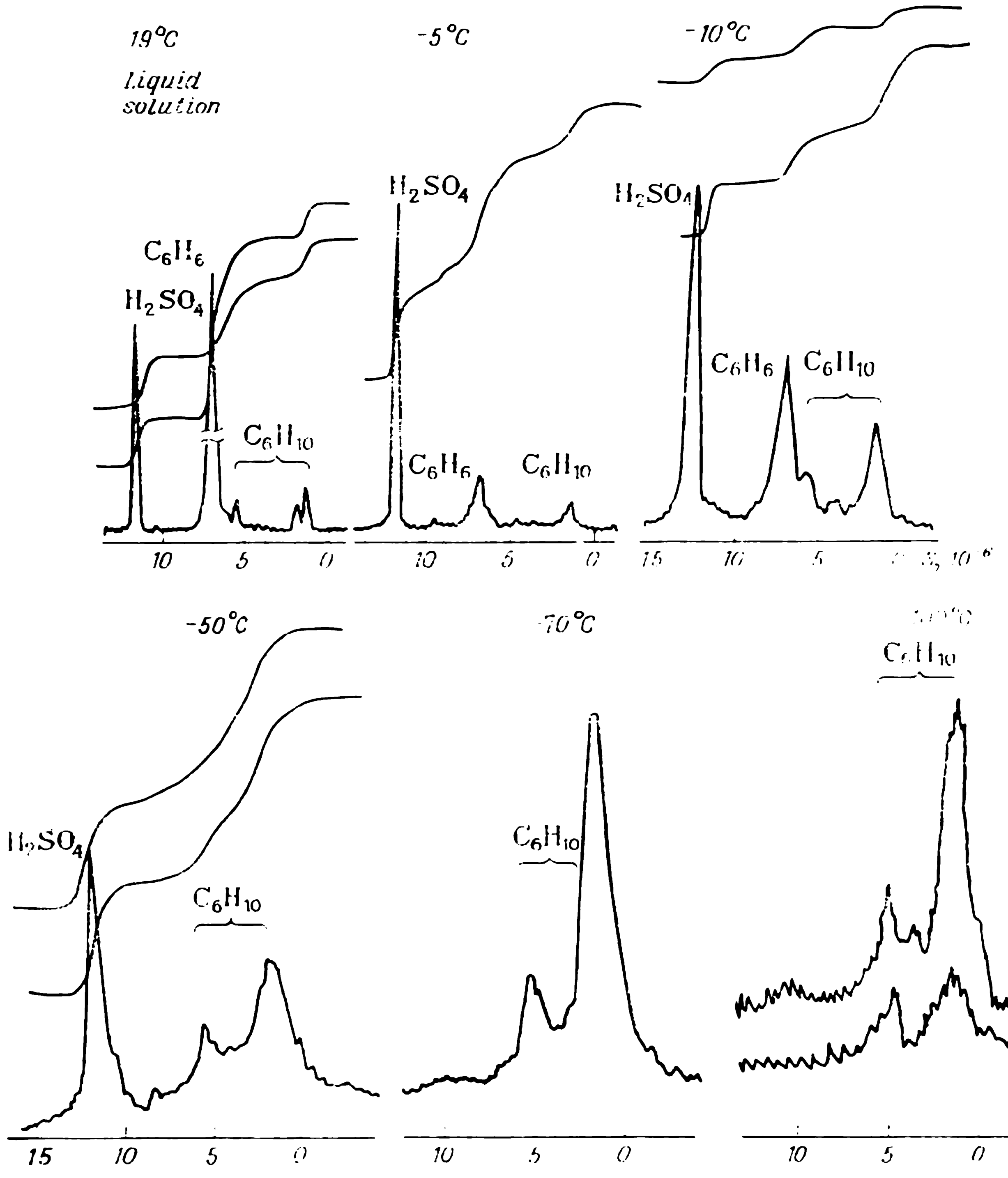

Fig. 8.7. NMR spectra for liquid and frozen solutions of cyclohexene in benzene at various temperatures ($[C_6H_{10}] = 0.2$ *M*)

ratios between methyliodide and benzene in the liquid microphase of frozen benzene solutions and in the liquid solution at various temperatures are given below ($[CH_3I] = 0.4M$):

	Liquid solution	*Frozen solutions*			
T, °C	+25	29	−47	−59	−80
$n_{CH_3I}/n_{C_6H_6}$	0.036	1.6	3.3	4.4	13.4

As is seen, the decrease in temperature from —29°C to —80°C causes the ratio of methyliodide to benzene in the liquid microphase to change by a factor of 13.4/1.6 = 8.5 and 13.4/0.036 = 370 as compared with the liquid solution at 25°C. In the circumstances, in the liquid microphase benzene may be said to be dissolved in methyliodide because the latter is present in a greater amount.

The absolute number of moles of the various substances in the liquid microphase has been determined by comparing the integrated spectra of these substances against a concentrated solution of sulphuric acid in a sealed capillary, used as a standard.

As an example, Fig. 8.7 shows the NMR spectra of liquid and frozen solutions of cyclohexene in benzene at various temperatures, and Table 8.1 presents the composition of the liquid microphase for this system and cyclohexene in CCl_4.

TABLE 8.1

Composition of the Liquid Microphase in Frozen Solutions of Cyclohexene in Benzene and CCl_4 at Various Temperatures

Solvent	T, °C	$n_{C_6H_{10}} \times 10^4$, moles	$n_{solvent} \times 10^4$, moles	V_{liq}, ml	c_{liq}, mole l^{-1}
CCl_4	+20	1.7	—	0.36 (V_0)	0.48
	−25	1.4	—	—	—
	−50	1.6	—	—	—
C_6H_6	+19	0.98	—	0.36 (V_0)	0.27
	−5	0.91	2.5	0.032	2.9
	−10	1.2	2.2	0.031	3.7

Note. $n_{C_6H_{10}}$ and $n_{solvent}$ are the molar cyclohexene and solvent contents of the liquid microphase; V_{liq} is the volume of the liquid microphase; V_0 is the volume of the starting liquid solution; c_{liq} is the concentration of cyclohexene in the liquid microphase.

It follows from Table 8.1 that the liquid microphase is present in frozen solutions in a temperature interval of several tens of degrees below the melting point. It consists of the solvent and the solutes. As the temperature is brought down, the liquid microphase shrinks in volume because the solvent is frozen out and the concentration of the solutes increases.

The volume of, and the concentration of cyclohexene in, the liquid microphase can be found by the following equations:

$$V_{liq} = \frac{n_{C_6H_{10}}}{d_{C_6H_{10}}} + \frac{n_{C_6H_6}}{d_{C_6H_6}}$$

and

$$c_{liq} = \frac{n_{C_6H_{10}}}{V_{liq}} \times 10^3$$

where $d_{C_6H_{10}}$ and $d_{C_6H_6}$ are the densities of cyclohexene and benzene in mole ml^{-1}.

NMR studies on the stability of the liquid microphase with time have shown that it remains unchanged. As the specimen is cooled from room temperature to —130°C and then warmed up until the solution is completely unfrozen, the composition of the liquid microphase remains unchanged at the same temperature. As the specimen is cooled down to —196°C, the liquid microphase gradually disappears, and the species present in it lose their high mobility. The subsequent warm-up of the specimen leads to the re-appearance of the liquid microphase. A comparison of specimens pre-cooled in liquid nitrogen with those only frozen in the resonant cavity of a spectrometer at a given temperature has shown that the composition of the liquid microphase is independent of the manner of freezing.

Thus, the available magnetic resonance data about the phase state of frozen solutions over a wide temperature range show that these solutions are complex two-phase systems. Such a system consists of a solid crystalline solvent and a microphase containing the molecules of the solutes and solvent. In some cases, the solutes can be rejected from solution to form a separate phase if their concentration exceeds their solubility. According to experiments, the investigated specimens may on the whole be regarded as being in a thermodynamic equilibrium. The substances in the liquid microphase retain a high mobility comparable with that observed in the liquid phase [271]. ESR spectra and the found correlation times indicate that the mobility of the molecules in the microphase is appreciably higher than in the matrix of the frozen solution. Even at temperatures 70 to 90°C below the melting point of the solvent this mobility is close to that in the liquid phase. The quantitative composition of the liquid microphase depends on temperature, a decrease in temperature raising the proportion of the solute. According to ESR and NMR data, the temperature interval in which the liquid microphase can exist decreases with increasing cryoscopic constant of the solvent. For example, the nitroxide radical in frozen benzene ($\Delta = 5.8$ K litre mole^{-1}) retains high mobility down to lower temperatures than in frozen dioxane ($\Delta = 4.5$ K litre mole^{-1}). In benzene at —92°C, $\tau_{cor} = 3 \times 10^{-10}$ s;

in dioxane at —60°C, $\tau_{cor} = 5.0 \times 10^{-10}$ s. The temperature interval of existence, the degree of concentration of the solutes, and the volume of the liquid microphase at a given temperature are all decided by the quantity of solutes and the physico-chemical properties of the entire system. Among these, the most important are the cryoscopic properties of the solvent and the ability to form eutectics. A decrease in temperature must reduce the volume of the liquid microphase owing to the increased concentration of the solutes in the liquid microphase and the freezing out of the solvent.

The complete reversibility of variations in ESR and NMR spectra with temperature is an indication that the state of frozen solutions produced at a freezing rate of 24 to 75 K s^{-1} is close to a state of thermodynamic equilibrium. As a consequence, the volume, V_{liq}, of microregions with highly mobile species is determined by the equation of phase state for the system. A decrease in temperature has been found to be accompanied by a decrease in V_{liq} in all the studied systems; that is, $\partial V_{liq}/\partial T > 0$. For each temperature, there is a certain definite value of V_{liq}, and if the components present in the liquid microphase are capable of interaction, a chemical reaction will occur within that volume. If the temperature is reduced by a large amount, the reactions will cease because the viscosity is increased and the mobility of the species is decreased. The formation of a liquid microphase in a frozen solution is thermodynamically more favourable than the inclusion of the solutes in the lattice of the solid solvent. This is so because the energy that must be expended to insert molecules in the lattice exceeds the free energy change associated with the rise in chemical potentials due to the increased concentration of the solutes in the liquid microphase. The concentration of the solutes that accompanies freezing may lead to an eutectic. NMR data about the composition of the liquid microphase indicate that the solutes account for 20% to 30% of the total volume of the liquid microphase at temperatures 10 to 15 degrees below the freezing point of the solution.

The microphase differs from the conventional liquid phase in properties even when the molecules in the microphase have a sufficiently high mobility. As already noted, freezing causes the NMR and ESR spectra of the solutions to broaden and the mobility of the molecules, as found from τ_{cor} of the marker radical, to decrease. Given the same temperature, the microinclusions may have a higher viscosity and a different polarity of the medium, and differ in other physico-chemical properties as compared with the supercooled liquid phase.

The total volume of microinclusions at the medium concentrations of the solutes is large. As an example, for the frozen solution of cyclohexene in benzene (see Table 8.1) at —5°C the liquid microphase accounts for 9% of the total volume of the starting solution, and its share is still larger in the presence of a diluent. For the frozen solution of triethylamine, methyliodide and cyclohexane (diluent) in benzene, V_{liq} accounts for 38% of the volume of the starting liquid solution.

8.3. KINETICS OF REACTIONS IN FROZEN SOLUTIONS

Analysis of experimental data brings out several specific aspects common to all low-temperature chemical reactions [235, 478, 479]. A plot of the reaction rate as a function of temperature shown in Fig. 8.8 is typical of the frozen multicomponent systems listed in Table 8.2. The reaction proceeds at a temperature lying below the freezing point of the solvent and formally takes place in the solid phase.

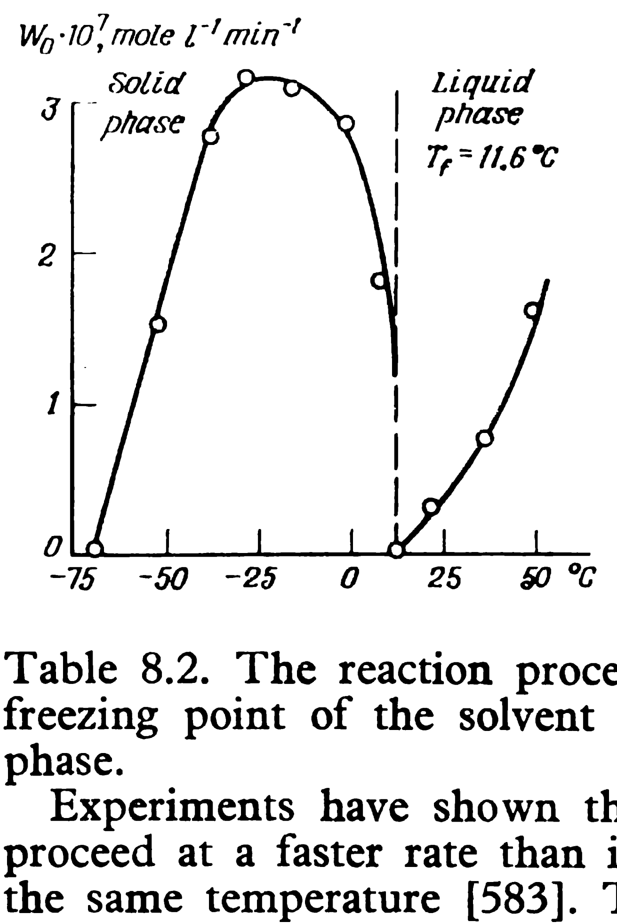

Fig. 8.8. Initial rate for the reaction of 2,2,6,6,-tetramethyl-4-oxyl-1-piperidi-nyloxy with hydrazobenzene in dioxane as a function of temperature in liquid and frozen solutions ($[R]_0 = [C_{12}H_{12}N_2]_0 = 1.1 \times 10^{-4}$ *M*)

Experiments have shown that in frozen solutions a reaction will proceed at a faster rate than in, say, liquid supercooled solutions at the same temperature [583]. The difference in rate of reaction between a frozen and a supercooled solution increases with decreasing initial concentration of the reactants. A study on the Menshutkin reaction has shown that the increase in the reaction rate in frozen solutions substantially depends on the cryoscopic constant of the solvent and increases with its decrease.

A major distinction of reactions in two-component systems, mainly investigated at low temperatures in the absence of a solvent, namely that the greater proportion of the mixture usually reacts at the instant when one of the starting materials melts, is related to phase transitions. If the reactants are capable of phase changes below the melting point of the mixture, the reaction can proceed in the solid phase. For example, in the system cyclohexene-chlorine, the reaction goes on at —170°C, that is, at the instant when the cyclohexene changes from the glassy to the crystalline state [142, 406].

TABLE 8.2

Chemical Reactions in Frozen Solutions

No.	Reaction type	Equation of reaction, reactants, products (catalyst)	Solvent	T, °C	References
1	Halogenation of olefins and aromatic compounds	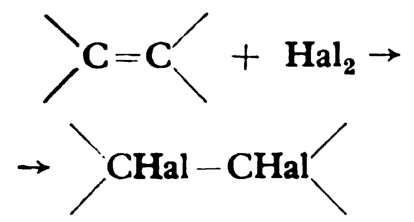 *Olefins:* ethylene, propylene, isobutylene, cyclohexene, 1-hexene *Halogens:* chlorine, bromine	None	-45 to -196	[235, 403, 482]
		Bromination of 1-hexene	Cyclohexane, benzene	0 to -110	[481]
		Bromination of toluene 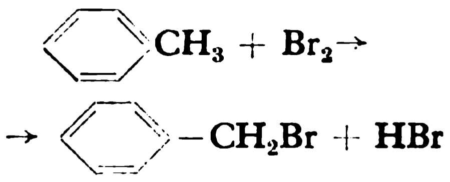	None	-70 to -142	[235]
2	Reactions of olefins with nitrogen dioxide	*Olefins:* propylene, isobutylene, 1-butene, 1-hexene, cyclohexene, cyclopentadiene, 1,3-butadiene *Main products:* dinitroalkanes, nitroalkylnitrites, and nitroalkylnitrates	None	0 to -90	[235]
3	Inorganic reactions of addition and substitution	$2NO + Cl_2 \rightarrow 2NOCl$ $HBr + Cl_2 \rightarrow HCl + ClBr$ $2NO + O_2 \rightarrow 2NO_2$	None	-116 to -165 -105 to -182 -95	[235]
4	Hydrohalogenation of olefins	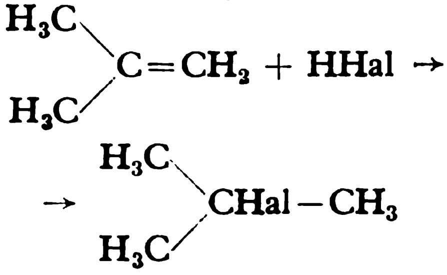 *Halogens:* chlorine, bromine, iodine	None	-100 to -190	[235]

TABLE 8.2 *(continued)*

No.	Reaction type	Equation of reaction, reactants, products (catalyst)	Solvent	T, °C	References
5	Hydrolysis	Acetanhydride 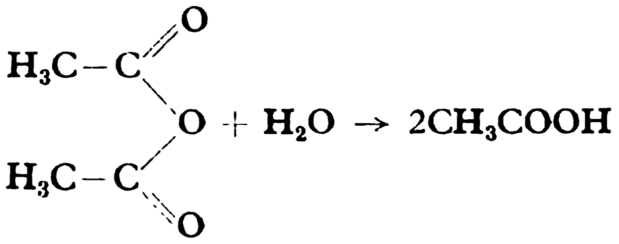 p-Nitrophenylacetate 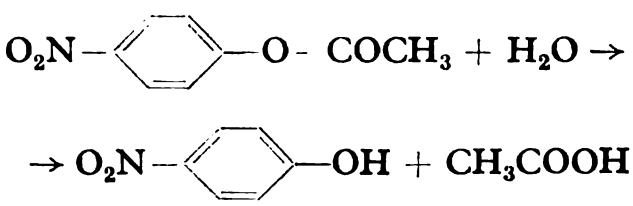 β-Propiolactone (imidazole as catalyst) 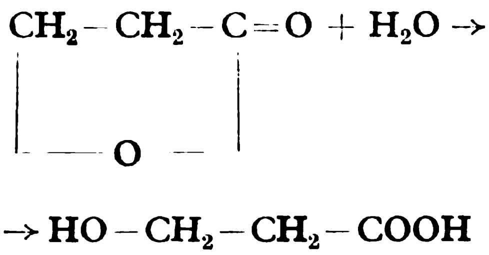	Water	−10	[476]
		δ-Thiovalerolactone and γ-thiobutyrolactone (morpholine)	Water	−10 to 45	[476, 497]
		G and V penicillins, poly-6-aminopenicillanic acid (imidazole, histidine, histamine, carnosine, OH^- ions)	Water	up to −78	[569]
6	Hydroxylaminolysis	Formamide, acetamide, propionamide, asparagine, glutamine, 2,5-diketopiperasine, cytosine, acetylcholine 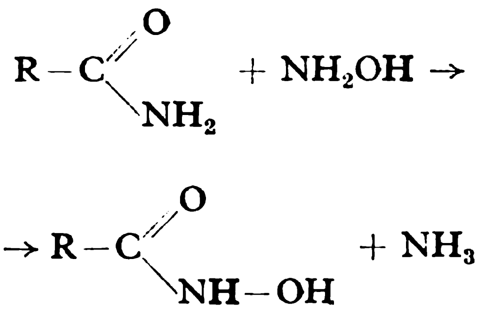	Water	up to −23	[488, 489, 498, 584]

TABLE 8.2 *(continued)*

No.	Reaction type	Equation of reaction, reactants, products (catalyst)	Solvent	T, °C	References
		Esters of glycine, serine, tyrosine, phenylalanine, and glutamic acid; ethyl ester of lysine, methyl esters of lysine, arginine (trypsin) 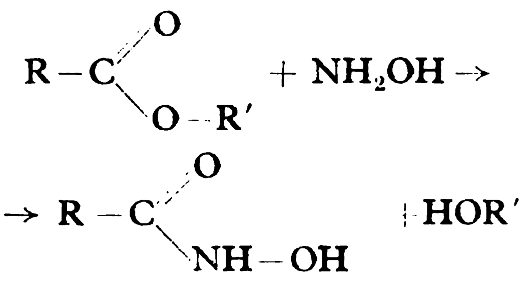	Water	-18	[477]
7	Inhibition by structural analogues (in hydroxylaminolysis)	Esters of phenylalanine, serine, lysine, tyrosine and glutamic acid	Water	-18	[585]
8	Decomposition	Hydrogen peroxide ($CuCl_2$, $FeCl_3$) $H_2O_2 \rightarrow H_2O + 1/2\ O_2$	Water		[492]
		tert-Butylperoxyformiate (2,6-lutidine, pyridine) 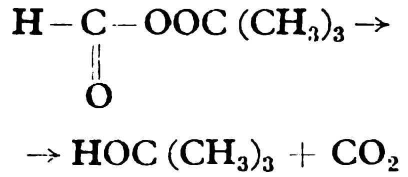 $H-C(=O)-OOC(CH_3)_3 \rightarrow HOC(CH_3)_3 + CO_2$	*p*-Xylene	up to -70	[474, 494]
9	Menshutkin's reaction	$CH_3I + (C_2H_5)_3N \rightarrow [(C_2H_5)_3NCH_3]I$	Benzene, nitrobenzene, dioxane, CCl_4, water	up to -196	[271, 272], [473], [484, 586, 587]
10	Formation of α-oxides	Ethylenechlorohydrine (reaction with NaOH) $HOCH_2CH_2Cl + NaOH \rightarrow$ 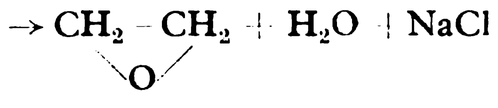	Water	up to -15	[493]

TABLE 8.2 *(continued)*

No.	Reaction type	Equation of reaction, reactants, products (catalyst)	Solvent	*T*, °C	References
11	Mutarotation	Glucose (HCl)	Water	−7	[588]
12	Polymerization	Anhydrides of N-carboxyamino acids 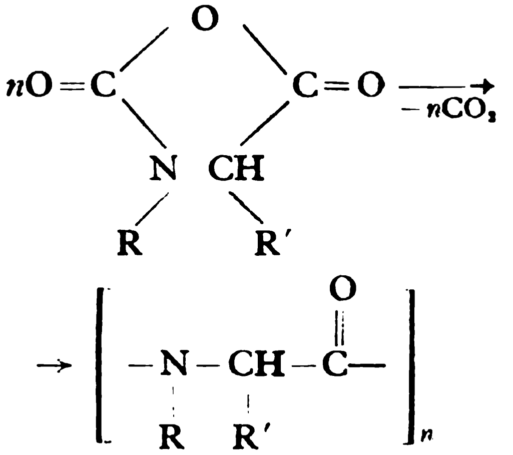	Dioxane	up to −26	[569]
		Poly-6-aminopenicillanic acid 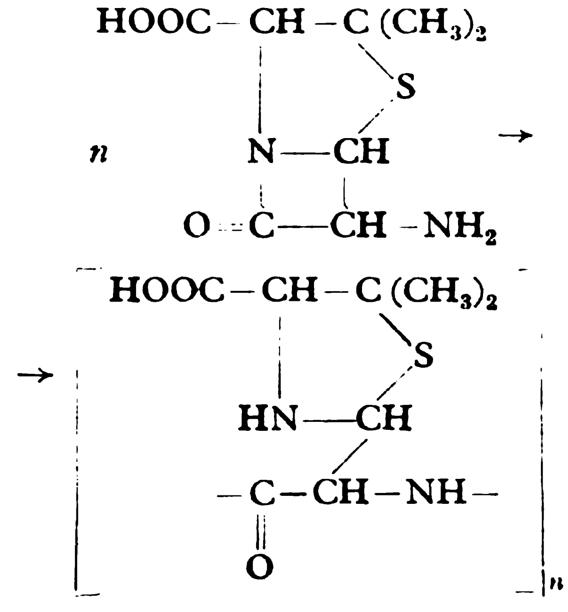	Water	up to −28	[496]
13		Adenosine-3′,5′-cyclophosphate,	Water	−15	[589]
		oligo(2′-O-methylinosine-3′-phosphate) (poly-C matrix)	Water	−15	[590]
	Oxidation	Hydrazobenzene 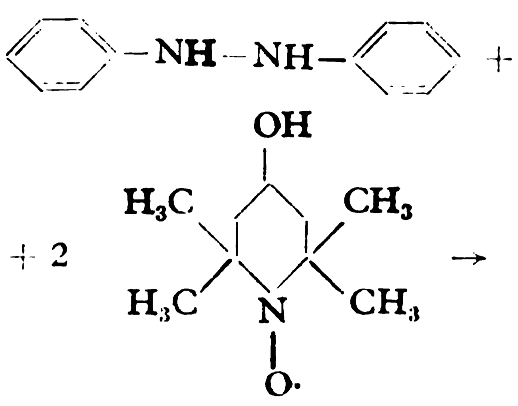	Dioxane	up to −196	[271]

TABLE 8.2 *(continued)*

No.	Reaction type	Equation of reaction, reactants, products (catalyst)	Solvent	*T*, °C	References
		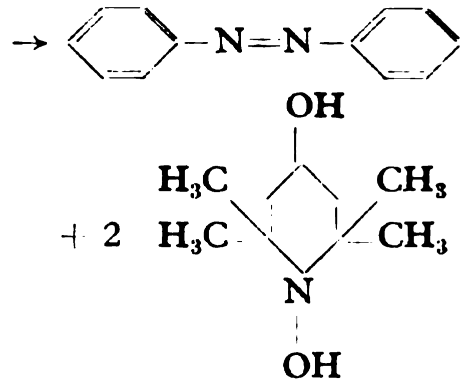 → —N=N— OH H_3C CH_3 + 2 H_3C CH_3 N OH			
14	Enzymic oxidation	Phosphoric ethers of hydroquinones (peroxidase as enzyme) 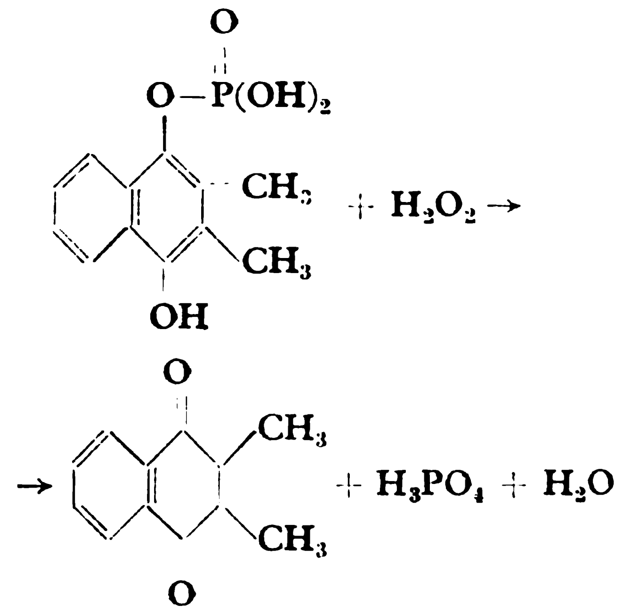 O $O-P(OH)_2$ CH_3 + H_2O_2 → CH_3 OH O CH_3 → + H_3PO_4 + H_2O CH_3 O	Water	−30 to 50	[591]-[593]
15	Nucleophilic displacement	Reaction of 2,4-dinitrophenol with glycylphenylalanine (cetyltrimethyl-ammonium bromide) 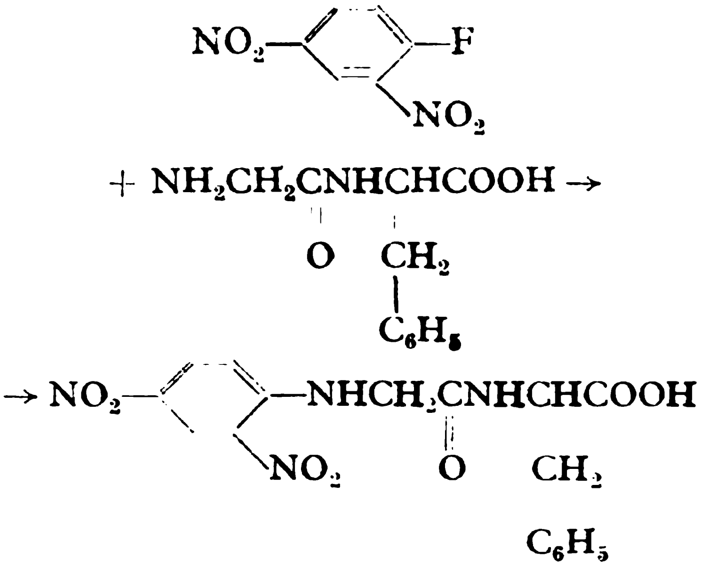 NO_2 F NO_2 + $NH_2CH_2CNHCHCOOH$ → O CH_2 C_6H_5 → NO_2 $NHCH_2CNHCHCOOH$ NO_2 O CH_2 C_6H_5	Water	−30 to 30	[594]

TABLE 8.2 *(continued)*

No.	Reaction type	Equation of reaction, reactants, products (catalyst)	Solvent	*T*, °C	References
16	Chemical inactivation of enzymes	Trypsin with imidazole, α-chymotrypsin with carbamide	Water Water	−18 up to −70	[595] [499]
17	Denaturation of DNA	In various buffer solutions with various values of pH	Water	−13 to 25	[596]

It is seen from Fig. 8.8 that the rate of a reaction bears an extremal relation to temperature in frozen solutions. The rate of a reaction in the solid matrix at a lower temperature is higher than it is in the liquid phase. Thus, the transition of a system from the liquid phase to the frozen state is accompanied by an increase in the rate of the reaction — the temperature coefficient of the reaction is thus negative.

From a comparison of the experimental rates of reactions in frozen solutions with those computed by the Arrhenius equation for a given temperature it is seen that the reaction rate can go up by several orders of magnitude. For example, the reaction of triethylamine with methyliodide in ice at —8°C proceeds at a rate about 1 000 times as high as the rate at 25°C in liquid water solutions.

The rate of a reaction can be changed by adding some inert substances (those not taking part in the chemical reaction) to the reacting mixture.

The freezing of a system stimulates the reactions involving complexes and enables the reactions proceeding in the liquid phase concurrently to be separated kinetically.

Several hypotheses have been advanced to explain the specific features of chemical reactions in multicomponent frozen systems. Among other things, the acceleration of chemical processes in frozen solutions has been attributed to changes in the mechanism of the reaction [476], to catalysis by the surface of the solid phase [475], to phase changes and various defects, and concentration of reactants in the nonfreezing regions of the solvent [473, 476], to molecular compounds [235], to the favourable spatial arrangement of the reactants, and to an increase in proton mobility in ice [477]. In our opinion, the decisive factors are the structural inhomogeneity and the associated high mobility of the reacting species, and also changes in the physicochemical characteristics of the system caused by freezing [479].

8.4. A STRUCTURAL-KINETIC MODEL OF CHEMICAL REACTIONS IN FROZEN SOLUTIONS

The basic kinetic features formulated above are characteristic of various chemical reactions. Therefore, a model intended to describe the kinetics of reactions in frozen solutions must take into account the physico-chemical properties common to all frozen systems. At the same time, such a model must reflect the specific chemistry of each individual process.

Basing themselves on the kinetics of chemical reactions in frozen solutions and on their phase state, Sergeev *et al.* [479] have proposed a structural-kinetic model for chemical reactions in solid matrices. Its main points may be summed up as follows.

Frozen multicomponent systems have an inhomogeneous phase composition. In a first approximation, they can be visualized as consisting of regions varying in composition and, as a consequence, in physico-chemical properties. In some regions solutes are predominantly concentrated, while in others — the solvent is.

Phase inhomogeneity can arise not only due to freezing, but also upon exposure of the system to radiations and other physical agencies. Even single-crystal specimens, when gamma-irradiated, become inhomogeneous, the degree of inhomogeneity being a maximum near reactive species immobilized at low temperatures.

So, it is phase inhomogeneity that controls to a considerable degree the kinetics of chemical reactions in solid matrices. The very occurrence of a chemical reaction becomes possible owing to the phase inhomogeneity produced by freezing. In regions with an increased concentration of the solutes, the interacting components are brought closer together, thereby satisfying one of the vital requirements for a reaction to take place. Also, as investigations have shown, the molecules in these regions have a higher mobility. It is close to the mobility in the liquid phase over a broad temperature range extending several tens of degrees below the freezing point of the system. Because of this, such regions may, in a first approximation, be regarded as a liquid microphase confined in a solid matrix.

The observed reaction rate, W_{obs}, may be regarded as the sum of the reaction rates in the liquid microphase, W_{liq}, and in the solid phase, W_s. Chemical reactions in frozen solutions occur mainly in the liquid microphase. In most cases, W_s is substantially smaller than W_{liq} and may be neglected. The equation for the reaction rate

$$A_{(1)} + A_{(2)} + A_{(3)} + \ldots + A_{(i)} \xrightarrow{k} P_{(1)} + P_{(2)} + \ldots \qquad (8.2)$$

under isothermal conditions at temperature T may be written

$$-V\,d[A_{(i)}]/dt = V_{liq}\,k\prod_{j=1}^{m}[A_{(j)}]_{liq}^{n_j} + W_s\quad (j, i = 1, 2, \ldots, m) \tag{8.3}$$

where k is the rate constant for the reaction in the liquid phase at a given temperature; V and V_{liq} are the volumes of the starting solution and of the liquid microphase, respectively; $[A_{(i)}]$ are the concentrations of the reactants in the liquid solution; $[A_{(j)}]_{liq}$ are their concentrations in the liquid microphase of the frozen solution; n_j is the reaction order for the jth component.

Suppose that we know the phase diagram for the system "solvent-reactants-products". Then, in addition to the differential equations, we have relations connecting the concentrations of the reactants in the liquid microphase of the frozen solution to their starting concentrations:

$$[A_{(i)}]_{liq} = f([A_{(1)}], [A_{(2)}], \ldots, [P_{(m)}], T)\qquad i = 1, 2, \ldots, m \tag{8.4}$$

and the form of the function is decided by the phase diagram of the system.

The equations describing the concentrations of reactants as functions of time, that is, the kinetics of the reaction, in frozen solutions, can be developed by solving together Eqs. (8.3) and (8.4), subject to the balance equation.

It is specially to be noted that in treating as a liquid microphase the microregions in which the reaction is predominantly localized, it is vital to bear in mind the difference in physico-chemical properties between the liquid microphase and the starting liquid solution (even in the supercooled state if there could be any).

A frozen system will not necessarily be in a state of thermodynamic equilibrium in the general case. If so, the function describing its true phase state can only be found experimentally. On the other hand, knowledge of this function is essential for achieving the principal kinetic task — that of establishing the relation between the concentrations of reactants and time in analytical form. To circumvent the difficulty, we assume that frozen solutions are in a state of thermodynamic equilibrium. This assumption has been verified by experiment and is well justified for the investigated reactions. Under this assumption, the equation of material balance may be written

$$V_0\sum_{i=1}^{m}[A_{(i)}]_0 = V_{liq}\sum_{i=1}^{m}[A_{(i)}]_{liq} + V_s\sum_{i=1}^{m}[A_{(i)}]_s \tag{8.5}$$

It is to be noted that processes in frozen systems can occur under two sets of limiting conditions. In the kinetic case, the rate of the reaction proper is lower than that of a phase change due to a change in the ambient conditions (say, temperature). The condition for the kinetic case may be written

$$V\,d\,[A_{(i)}]/dt < W_{T_1 \to T_2}$$

where $W_{T_1 \to T_2}$ is the rate of a transition from one phase state at T_1 to another at T_2.

All of the reactions studied in frozen solutions fall in the kinetic case.

Under the other set of limiting conditions which we shall call the relaxation case, the rate of a chemical transformation is decided by that of a transition from one phase state to another, that is

$$W_{T_1 \to T_2} < V\,d[A_{(i)}]/dt$$

The relaxation case covers an overwhelming majority of reactions involving trapped radicals and other reactive species, and unusual processes such as stepwise recombination are associated with the relaxation case, too.

Consider the acceleration of a reaction in a frozen solution within the framework of the structural-kinetic model. Let there be a bimolecular reaction proceeding with a change in the number of moles, $A + B \to E$. We shall use the following notation: [A], [B], and [E] are the current concentrations of the reactants and products in the unfrozen solution; [D] is the concentration of a diluent, that is an addition which does not react with either the reactants or the products; $[A]_{liq}$, $[B]_{liq}$, $[E]_{liq}$, and $[D]_{liq}$ are the concentrations of the reactants, product and diluent in the liquid inclusions in the frozen solution; V is the volume of the liquid solution; V_{liq} is the total volume of all liquid inclusions in the frozen solution. Then the expression for the reaction rate in a frozen solution may be written

$$V(d[A]/dt) = -k_2[A]_{liq}\,[B]_{liq}\,V_{liq} \tag{8.6}$$

where k_2 is the rate constant of a second-order reaction at the temperature of the reaction.

Let the reaction components be completely concentrated in the liquid inclusions in the frozen solution and let the reaction product be soluble. Then we may write

$$[A]\,V = [A]_{liq}\,V_{liq}$$

$$[B]\,V = [B]_{liq}\,V_{liq}$$

$$([A] + [B] + [D] + [E])\,V = ([A]_{liq} + [B]_{liq} + [D]_{liq} + [E]_{liq})\,V_{liq}$$

Since

$$[E] = [B]_0 - [B]$$

and

$$[E]_{liq} = [B]_{0,liq} - [B]_{liq}$$

Eq. (8.6) takes the form

$$d[\mathrm{A}]/dt = -k_2[\mathrm{A}]\,[\mathrm{B}]\,\frac{[\mathrm{A}]_{\mathrm{liq}} + [\mathrm{B}]_{0,\mathrm{liq}} + [\mathrm{D}]_{\mathrm{liq}}}{[\mathrm{A}] + [\mathrm{B}]_0 + [\mathrm{D}]} \tag{8.7}$$

From the equation of material balance,

$$[\mathrm{B}] = [\mathrm{B}]_0 - [\mathrm{A}]_0 + [\mathrm{A}]$$

and

$$d\,[\mathrm{A}]/dt = -\,k_2[\mathrm{A}]\,([\mathrm{B}]_0 - [\mathrm{A}]_0 + [\mathrm{A}]) \cdot \frac{c_{\mathrm{liq}}}{[\mathrm{A}] + [\mathrm{B}]_0 + [\mathrm{D}]} \tag{8.8}$$

where $[\mathrm{A}]_{\mathrm{liq}} + [\mathrm{B}]_{0,\,\mathrm{liq}} + [\mathrm{D}]_{\mathrm{liq}} = c_{\mathrm{liq}}$ is the total concentration of the solutes in the liquid microphase.

As we believe, this term is solely decided by the temperature of the experiment and the cryoscopic constant of the solvent:

$$c_{\mathrm{liq}} = (T_0 - T)/\Delta$$

where T_0 is the freezing point of the solvent. Then, integrating Eq. (8.8) leads to a kinetic equation of the form

$$\ln\,([\mathrm{A}] + [\mathrm{B}]_0 - [\mathrm{A}]_0) + \frac{[\mathrm{B}]_0 + [\mathrm{D}]}{[\mathrm{B}]_0 - [\mathrm{A}]_0}\,\ln\,\frac{[\mathrm{A}]}{[\mathrm{A}] + [\mathrm{B}]_0 - [\mathrm{A}]_0} = -\,k_2 c_{\mathrm{liq}} t + C \tag{8.9}$$

where C is the integration constant equal to

$$C = \ln\,[\mathrm{B}]_0 + \frac{[\mathrm{B}]_0 + [\mathrm{D}]}{[\mathrm{B}]_0 - [\mathrm{A}]_0}\,\ln\,[\mathrm{A}]_0\,/\,[\mathrm{B}]_0$$

Similarly for $[\mathrm{A}]_0 = [\mathrm{B}]_0$, we write

$$\ln\,[\mathrm{A}] - \frac{[\mathrm{D}] + [\mathrm{A}]_0}{[\mathrm{A}]} = -\,k_2 c_{\mathrm{liq}}\,t + C \tag{8.10}$$

where

$$C = \ln\,[\mathrm{A}]_0 - \frac{[\mathrm{D}] + [\mathrm{A}]_0}{[\mathrm{A}]_0}$$

An equation similar to Eq. (8.10) has been developed earlier by Pincock and Kiovsky [473] for the case in which $[\mathrm{A}]_0 = [\mathrm{B}]_0$ and the product is insoluble in benzene:

$$2\ln\,[\mathrm{A}] - [\mathrm{D}]\,/\,[\mathrm{A}] = -\,k_2 c_{\mathrm{liq}}\,t + C \tag{8.11}$$

where

$$C = 2\ln\,[\mathrm{A}]_0 - [\mathrm{D}]\,/\,[\mathrm{A}]_0$$

If $[\mathrm{A}]_0 \neq [\mathrm{B}]_0$ and the reaction product is insoluble, a more general expression applies

$$\ln\,([\mathrm{A}] - [\mathrm{A}]_0 + [\mathrm{B}]_0) + \ln\,[\mathrm{A}] = -\,k_2\,c_{\mathrm{liq}}\,t + C \tag{8.12}$$

where

$$C = \ln([B]_0[A]_0)$$

Within the framework of the adopted model, the observed rate constant k_{obs} is the product of the true rate constant and c_{liq}, that is

$$k_{obs} = k_2 c_{liq}$$

We have used Eqs. (8.9) through (8.12) to process experimental data kinetically. We have found them to fit experimental data well.

At constant temperature, the observed rate constant must not depend on the concentrations of the starting reactants, because within the limits of the adopted model c_{liq} remains constant and solely depends on the properties of the solvent.

Let us develop a general expression for the temperature at which the observed rate constant for a given reaction is a maximum. To begin with, we must rewrite Eq. (8.13)

$$\partial k_{obs} / \partial T = 0 \tag{8.13}$$

to solve it for the temperature. Since the cryoscopic constant of the solvent is

$$\Delta = (T_0 - T) / c_{liq} \tag{8.14}$$

where T_0 is the freezing point of the solvent and T is the temperature of the reaction, we get for

$$k_{obs} = c_{liq} k_2^0 \exp(-E/RT)$$

that

$$k_{obs} = \frac{T_0 - T}{\Delta} k_2^0 \exp(-E/RT) \tag{8.15}$$

Substituting Eq. (8.15) into Eq. (8.13) gives the expression for the temperature at which the rate constant is a maximum:

$$T_{max} = (E^2/4R^2 + ET_0/R)^{1/2} - E/2R \tag{8.16}$$

Equation (8.16) is identical to one developed earlier on the basis of the formal-kinetic approach [489].

Thus, within the framework of the adopted model the temperature at which the rate constant of the reaction is a maximum depends solely on the activation energy for that reaction in the liquid phase and the freezing point of the neat solvent.

8.4.1. Experimental Data

The structural kinetic model offers a tool with which to explain qualitatively the kinetics of reactions in frozen solutions and also to predict other factors. As will be seen from the discussion that follows, the kinetic equations developed on this basis adequately fit experimental data.

The Menshutkin reaction in frozen solutions has been investigated by potentiometric titration and NMR technique. It has been found that at the freezing point of the solution the rate of the reaction abruptly increases and keeps rising with decreasing temperature up to a certain limit past which it begins to decrease. The extremal dependence of the reaction rate on temperature has been observed in all the investigated solvents. The figures that follow give the temperatures at which the rate of the reaction of triethylamine with methyliodide in a frozen solution is a maximum.

Solvent	Benzene	Nitrobenzene	Dioxane	Water	CCl_4	Cyclohexane
t, °C	−5	−5	−6	−8	No reaction	

The manner in which the observed rate constant of the reaction, k_{obs}, depends on temperature in various solvents ($[(C_2H_5)_3N]_0 = [CH_3I]_0$) is illustrated below.

Nitrobenzene, $[CH_3I] = 0.02M$

t, °C	+2	0	−5	−10	−30
$k_{obs} \times 10^4$, s^{-1}	13	18	23	21	7

Dioxane, $[CH_3I] = 0.2M$

t, °C	+8	+6	+3	0	−5	−7	−9	−12	−22
$k_{obs} \times 10^4$, s^{-1}	6.0	8.0	10.0	7.0	9.0	8.5	8.5	4.3	2.0

Benzene, $[CH_3I] = 0.2M$

t, °C	2.5	0	−5	−10	−20	−30
$k_{obs} \times 10^4$, s^{-1}	1.6	2.3	3.2	2.9	2.0	1.1

Water, $[CH_3I] = 0.02M$

t, °C	−1	−3	−5	−8	−10	−14	−22
$k_{obs} \times 10^4$, s^{-1}	0.3	1.6	1.7	2.6	2.0	1.7	1.0

The rate constant for the reactions in benzene and in dioxane has been found by the equation

$$2 \ln [(C_2H_5)_3N] = k_{obs}\, t + 2 \ln [(C_2H_5)_3N]_0 \qquad (8.17)$$

With nitrobenzene and water used as solvents, the equation takes the form

$$\ln [(C_2H_5)_3N] - \frac{[(C_2H_5)_3N]_0}{[(C_2H_5)_3N]} = -k_{obs}\, t + \ln [(C_2H_5)_3N]_0 - 1 \qquad (8.18)$$

Equations (8.17) and (8.18) hold when the initial concentrations of the reactants in the solution are the same.

The increase in the rate of a reaction in a frozen solution can be assessed by comparing the observed rate with that found by the

Arrhenius equation for the same temperature. The rate of the reaction between triethylamine and methyliodide in various solvents can be taken from data on the liquid phase. As follows from Table 8.3, the increase in the reaction rate varies from solvent to solvent and is a maximum when the reactants are frozen in water, this maximum being the higher, the lower the initial concentrations of the reactants.

TABLE 8.3

Computed, W_0^{comp}, and Observed, W_0^{obs}, Initial Rates of the Reaction of Triethylamine with Methyliodide in Various Solvents at −5°C

Solvent	Δ, K litre mole^{-1}	W_0^{obs}, mole litre^{-1} s^{-1}	W_0^{comp}, mole litre^{-1} s^{-1}	W_0^{obs}/W_0^{comp}
Benzene	5.8	4.4×10^{-6}	9.2×10^{-8}	50
Nitrobenzene	4.8	2.2×10^{-5}	2.2×10^{-6}	10
Dioxane	4.5	1.8×10^{-5}	3.5×10^{-7}	50
Water	1.85	5.7×10^{-6}	5.6×10^{-9}	1 000

In some experiments with benzene as solvent, the initial concentrations of the reactants were additionally varied. The manner in which such variations affect the observed rate constant for the reaction of triethylamine with methyliodide in frozen solutions in benzene at —5°C is illustrated below.

$[(C_2H_5)_3N]_0$, mole litre^{-1}	0.20	0.02	0.02	0.02	0.02
$[CH_3I]_0$, mole litre^{-1}	0.20	0.02	0.04	0.10	0.20
$k_{obs}\times10^4$, s^{-1}	3.2 ± 0.3	3.2 ± 0.3	2.8 ± 0.3	2.8 ± 0.3	2.8 ± 0.3

In cases where the reactants were present in different concentrations, k_{obs} was found by the equation

$$\ln\{[(C_2H_5)_3N] + [CH_3I]_0 - [(C_2H_5)_3N]_0\} + \ln[(C_2H_5)_3N]$$
$$= -k_{obs}t + \ln[CH_3I]_0 + \ln[(C_2H_5)_3N]_0 \qquad (8.19)$$

The effect that the chemical character and concentration of diluent have on the rate of a reaction in a frozen solution was studied on the reaction of triethylamine with methyliodide in the presence of diluents, such as benzene, nitrobenzene, cyclohexane, and others. Both the diluent and the reactants were taken in about the same concentration. The initial rate of the reactions in frozen solutions in benzene and dioxane as a function of the concentration of nitrobenzene and cyclohexane is shown in the plot of Fig. 8.9. As is seen, the rate is a maximum when the concentration of nitrobenzene is 0.3*M*.

The relation between the observed rate constants and the chemical nature of the diluents (D) can be inferred from the data presented in Table 8.4.

TABLE 8.4

Relation Between the Kind of Diluent and the Observed Rate Constant o the Reaction of Triethylamine with Methyliodide in Benzene at —5°C, $[(C_2H_5)_3N]_0 = [CH_3I]_0 = 0.2M$, $[D] = 0.4M$

Diluent	$k_{obs} \times 10^4$, s^{-1}	ε_{dil}	[*p*-Xylene]-to-[nitrobenzene] ratio in diluent	$k_{obs} \times 10^4$, s^{-1}	ε_{dil}
None	3.2	—	1 : 3	10.1	26.6
Cyclohexane	2.8	2.02	2 : 2	7.4	18.5
p-Xylene	3.3	2.27			
Nitrobenzene	12.7	34.8	3 : 1	5.0	10.4

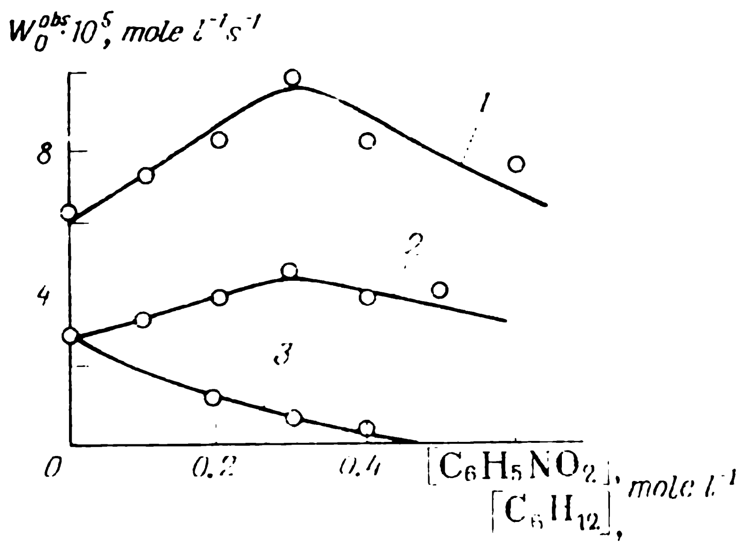

Fig. 8.9. Initial rate for the reaction of triethylamine with methyliodide in frozen solutions as a function of (*1* and *2*) nitrobenzene and (*3*) cyclohexane:

(1) dioxane, —8°C, $[(C_2H_5)_3N]_0 = [CH_3I]_0 = 0.11M$; (2) and (3) benzene, —5°C, $[(C_2H_5)_3N]_0 = [CH_3I]_0 = 0.15M$

The manner in which the observed rate constant for the reaction of triethylamine with methyliodide in frozen solutions in benzene at —5°C and in dioxane at —8°C depends on the concentration of nitrobenzene, $[(C_2H_5)_3N]_0 = [CH_3I]_0 = 0.2M$, is illustrated below.

$[C_5H_5NO_2]$, moles litre^{-1}	0.0	0.1	0.2	0.3	0.4	0.6	0.8
$k_{obs} \times 10^4$, s^{-1}							
in benzene	3.2	6.3	8.9	11	13	—	—
in dioxane	8.5	23	35	48	—	60	74

For diluents with dielectric constant $\varepsilon_{dil} \leqslant 5$, the following equation was used to find k_{obs}:

$$2\ln[(C_2H_5)_3N] - \frac{[D]}{[(C_2H_5)_3N]} = -k_{obs}t + 2\ln[(C_2H_5)_3N]_0 - \frac{[D]}{[(C_2H_5)_3N]_0} \tag{8.20}$$

For polar diluents with $\varepsilon_{dil} > 10$, the observed rate constant k_{obs} was found, using the following equation:

$$\ln[(C_2H_5)_3N] - \frac{[D] + [(C_2H_5)_3N]_0}{[(C_2H_5)_3N]} = -k_{obs}t + \ln[(C_2H_5)_3N]_0 - \frac{[D] + [(C_2H_5)_3N]_0}{[(C_2H_5)_3N]_0} \tag{8.21}$$

The effect of diluents on the reaction rate in ice has been studied on water-methanol solutions. It has been found that the addition of methanol slows down the reaction.

In order to get an idea about the effect that the structure of water may have on reactions in aqueous solutions, we have investigated the reaction of triethylamine with methyliodide in solutions of inorganic salts. We have found that the salts do not practically affect the rate of reactions in liquid aqueous solutions. A different situation has been found to exist in frozen aqueous solutions of salts. We have learned that practically no reaction can take place in 0.04*M* solutions of NaCl, KCl, and $NaClO_4$ at —8°C. A plot of the initial reaction rate as a function of salt concentration in frozen solutions is shown in Fig. 8.10. As is seen, $NaClO_4$ and NaCl retard the reaction appreciably, whereas an increase in the concentration of Na_2SO_4 speeds up the process. The relation between k_{obs} in ice and the kind and concentration of salts is illustrated in Table 8.5.

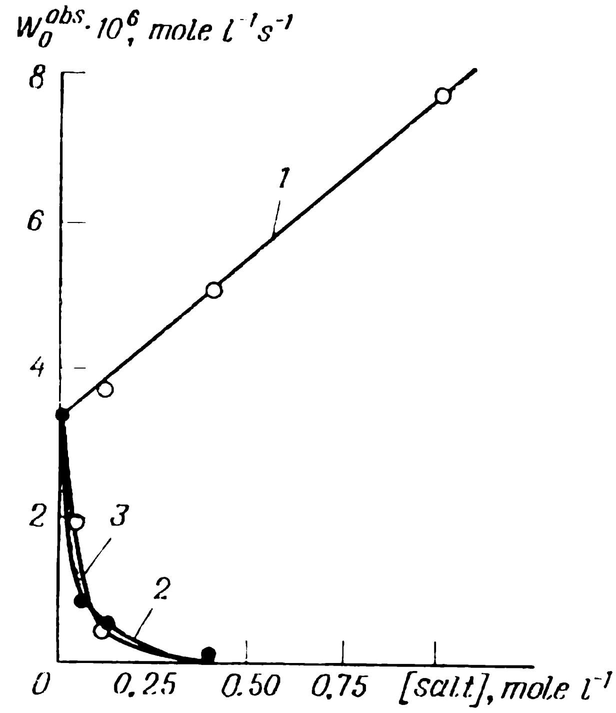

Fig. 8.10. Initial reaction rate as a function of salt concentration in a frozen aqueous solution
($t = -8°C$, $[(C_2H_5)_3N]_0 = [CH_3I]_0 = 0.02M$):
Diluents: (1) Na_2SO_4; (2) NaCl; (3) $NaClO_4$

TABLE 8.5

Observed Rate Constants for the Reaction of Triethylamine with Methyliodide in Frozen Aqueous Solutions at −8°C as a Function of Kind and Concentration of Salt ($[(C_2H_5)_3N]_0 = [CH_3I]_0 = 0.02M$)

$[NaClO_4]$, mole litre^{-1}	$k_{obs} \times 10^4$, s^{-1}	[KCl], mole litre^{-1}	$k_{obs} \times 10^4$, s^{-1}	$[Na_2SO_4]$, mole litre^{-1}	$k_{obs} \times 10^4$, s^{-1}
0.04	4.3	0.04	3.8	0.04	5.6
0.10	4.1	0.10	4.6	0.10	12
0.14	3.9			0.40	51
				1.00	132

The constants have been computed, using the following equation:

$$\ln [(C_2H_5)_3N] - \frac{2\,[D] + [(C_2H_5)_3N]_0}{[(C_2H_5)_3N]} = -k_{obs}\,t + \ln [(C_2H_5)_3N]_0 - \frac{2\,[D] + [(C_2H_5)_3N]_0}{[(C_2H_5)_3N]_0} \qquad (8.22)$$

The kinetics of the reaction of triethylamine with methyliodide directly in a frozen solution, notably in benzene, has been studied by the NMR technique at the same concentrations of reactants and diluents as in potentiometric titration.

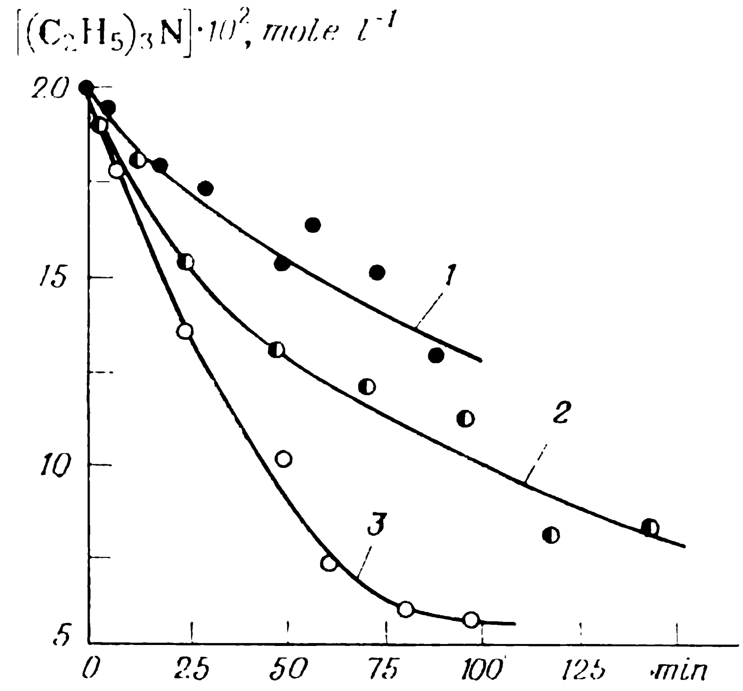

Fig. 8.11. Kinetic flow rate curves for triethylamine in the reaction with methyliodide in frozen benzene $\{[(C_2H_5)_3N]_0 = [CH_3I]_0 = 0.2M\}$:

(1) cyclohexane as diluent, [D] = 0.4*M*, *T* = —5°C; (2) no diluent, *T* = —10°C; (3) no diluent, *T* = —5°C

The kinetic flow rate curves for triethylamine are shown in Fig. 8.11. The concentration has been computed by the equation

$$[(C_2H_5)_3N] = P \times 10^3/V_0 \text{ moles litre}^{-1}$$

where V_0 is the starting volume of the unfrozen solution (0.36 ml) and P is the quantity of reactant. The observed rate constant K_{obs} obtained in the NMR studies is given below.

T, °C	−5	−5	−5	−10	−20
Diluent, [D] = 0.4M	–	C_6H_{12}	$C_6H_5NO_2$	–	–
$k_{obs} \times 10^4$, s^{-1}	4.6	1.3	2.3	2.7	1.1

The rate constant for neat solutions has been found by Eq. (8.17), for solutions diluted with cyclohexane by Eq. (8.20), and for solutions diluted with nitrobenzene by Eq. (8.21).

The results of an NMR study on variations in the progress of the reaction in the liquid microphase of volume V_{liq} and the total concentration of solutes, c_{liq}, in it are plotted in Figs. 8.12 and 8.13. As is seen, the liquid microphase in the frozen benzene decreases in volume, but the total concentration of solutes in the microphase remains practically constant and is decided above all by temperature. The plot in Fig. 8.14 illustrates variations in the volume of the reac-

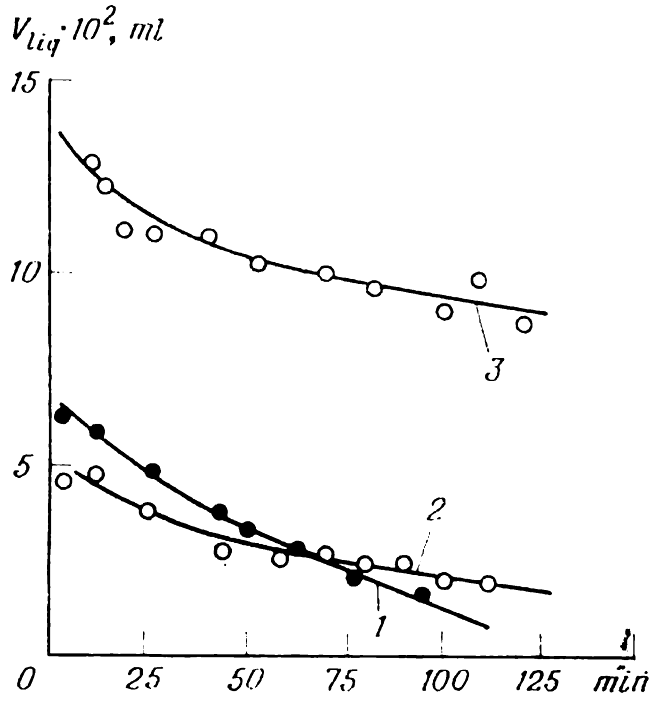

Fig. 8.12. Variations in the volume of the liquid microphase, V_{liq}, in the reaction of triethylamine with methyliodide in frozen benzene $\{[(C_2H_5)_3N]_0 = [CH_3I]_0 = 0.2M\}$:

(1) —5°C; (2) —10°C; (3) —5°C; cyclohexane as diluent, [D] = 0.4M

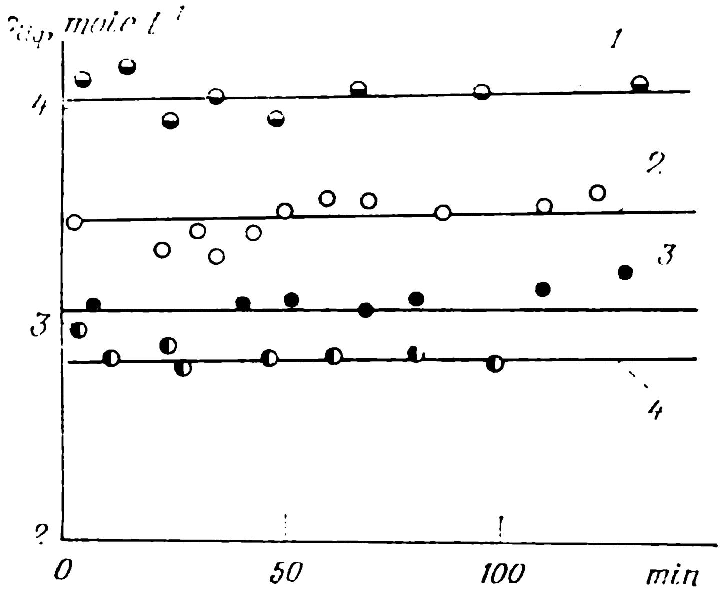

Fig. 8.13. Variations in the total concentrations of solutes, c_{liq}, in the liquid microphase in the reaction of triethylamine with methyliodide in frozen benzene $\{[(C_2H_5)_3N]_0 = [CH_3I]_0 = 0.2M$, $[D] = 0.4M\}$:

(1) —10°C, no diluent; (2) —5°C, nitrobenzene as diluent; (3) —5°C, cyclohexane as diluent; (4) —5°C, no diluent

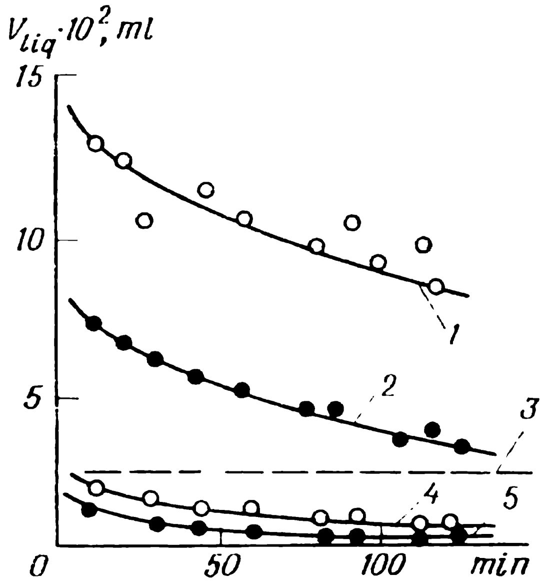

Fig. 8.14. Variations in the volumes of solvent, reactants and diluent in the liquid microphase in the reaction of triethylamine with methyliodide in frozen benzene $\{T = -5°C, [C_6H_{12}] = 0.4M, [CH_3I]_0 = [(C_2H_5)_3N]_0 = 0.2M\}$:

(1) total volume of liquid microphase; (2) volume of C_6H_6; (3) volume of $(C_2H_5)_3N$; (4) diluent volume; (5) volume of CH_3I

tants, diluent, and solvent in the liquid microphase with time. The respective volumes have been found by the following equation:

$$v_{i,\mathrm{liq}} = P_i/d_i$$

where P_i is the number of moles of the ith substance in the liquid microphase as found from NMR data, and d_i is the density of the ith substance in moles litre^{-1}. The volume of the entire liquid microphase has been found as the sum of the volumes of the individual constituents

$$V_{\mathrm{liq}} = \sum_i v_{i,\mathrm{liq}}$$

without allowance for the decrease in the volume on mixing. For the example illustrated in Fig. 8.14, it is

$$V_{\mathrm{liq}} = \frac{P_{C_6H_6}}{d_{C_6H_6}} + \frac{P_{CH_3I}}{d_{CH_3I}} + \frac{P_{(C_2H_5)_3N}}{d_{(C_2H_5)_3N}} + \frac{P_{C_6H_{12}}}{d_{C_6H_{12}}}$$

Initially, the total volume of the liquid microphase was

$$V_{\mathrm{liq}} = 7.52\times10^{-2} + 0.88\times10^{-2} + 2.1\times10^{-2} + 2.5\times10^{-2} = 13\times10^{-2}\ \mathrm{ml}$$

which corresponds approximately to the following percentages: 58% benzene, 23% reactants, and 19% cyclohexane. The total volume of the liquid microphase is 38% (0.13 ml) of that of the starting unfrozen solution (0.36 ml). The total concentration of the solutes in the liquid microphase, c_{liq}, has been found by the equation

$$c_{\mathrm{liq}} = (P_{CH_3I} + P_{(C_2H_5)_3N} + P_{\mathrm{dil}})/V_{\mathrm{liq}}$$

Thus, using the Menshutkin reaction as an example we have established that the choice of solvent and diluent (kind and concentration) affects the rate of processes in frozen solutions.

We have also studied the reactions of the nitroxide radical with hydrazobenzene and ascorbic acid in order to establish the kinetics of redox reactions in frozen solutions. Because the systems under study contained paramagnetic species, the investigations could be conducted *in situ* (directly in frozen solutions) by ESR techniques. As conveniently such systems can be investigated by UV spectroscopy. UV spectra have yielded additional information about the kinetics of such reactions in frozen solutions. Basing ourselves on ESR and UV spectra, we have been able to assess the effect of warm-up on the kinetics of the reaction.

A spectrophotometric study has shown that the oxidation of hydrazobenzene by the nitroxide radical in a frozen dioxane solution is substantially speeded up, whereas the oxidation of hydrazobenzene by atmospheric oxygen is brought to a complete stop. Curves illustrating the accumulation of azobenzene in the reaction of hydrazobenzene with the radical and with atmospheric oxygen in liquid and frozen solutions at various temperatures are shown in Fig. 8.15.

A plot of the initial reaction rate as a function of temperature for the liquid phase and frozen solution appears in Fig. 8.16. It is readily seen that in frozen solutions the reaction is speeded up and proceeds at a measurable rate down to —90°C. At —100°C, the reaction comes practically to a standstill. The reaction rate is a maximum at —20°C. The observed rate constant k_{obs} has been found by the equation

$$(1/[\mathrm{R}]_0) \ln \frac{[\mathrm{R}]_0 - [\mathrm{C_{12}H_{10}N_2}]}{[\mathrm{R}]_0 - 2\,[\mathrm{C_{12}H_{10}N_2}]} = \frac{k_{\text{obs}}\, t}{2\,[\mathrm{R}]_0 + [\mathrm{D}]} \tag{8.23}$$

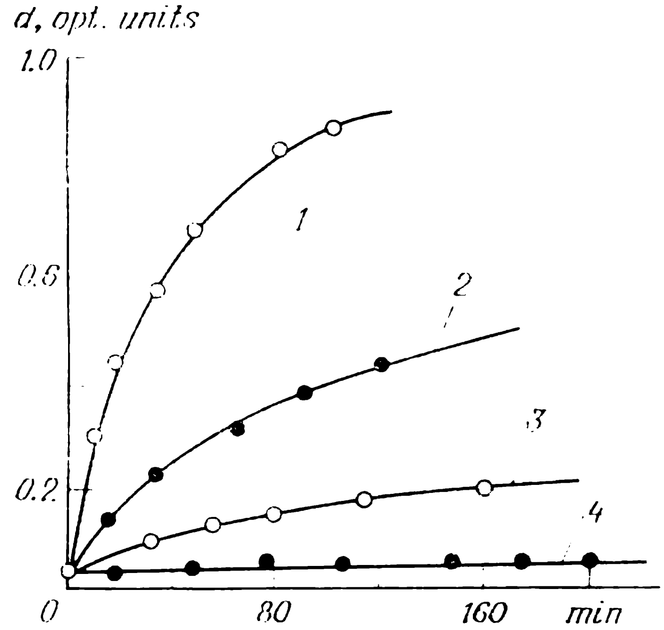

Fig. 8.15. Kinetic curves of accumulation of azobenzene in the oxidation of hydrazobenzene by (*1* and *2*) nitroxide radical and (*3* and *4*) atmospheric oxygen in liquid and frozen dioxane solutions ($[\mathrm{R}]_0 = [\mathrm{C_{12}H_{12}N_2}]_0 = 1.1 \times 10^{-4} M$, $[\mathrm{C_2H_5OH}] = 0.01 M$):
(1) frozen solution, —5°C; (2) liquid solution, 20°C; (3) liquid solution, 20°C, no radical; (4) frozen solution, —5°C, no radical (oxidation by oxygen)

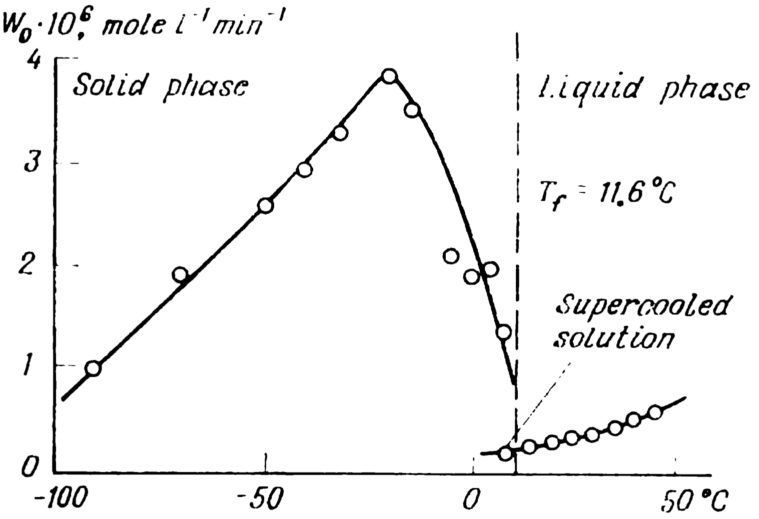

Fig. 8.16. Initial rate of oxidation of hydrazobenzene by nitroxide radical in dioxane as a function of temperature ($[\mathrm{R}]_0 = [\mathrm{C_{12}H_{12}N_2}]_0 = 1.1 \times 10^{-4} M$, $[\mathrm{C_2H_5OH}] = 10^{-2} M$)

and the values thus found are:

T, °C	+10	+5	−5	−10	−15	−20	−30	−40	−50	−70	−90
$k_{\text{obs}} \times 10$, s^{-1}	0.73	1.75	1.82	1.93	2.24	2.82	2.31	2.06	1.86	1.16	0.68

The kinetics of the oxidation of hydrazobenzene by the nitroxide radical in frozen dioxane solutions has been investigated in the temperature interval from +8° to —70°C. A plot of the initial rate of the oxidation as a function of temperature in liquid and frozen solutions is shown in Fig. 8.8. As is seen, the relation is extremal in character, the reaction rate being a maximum anywhere between —20° and —30°C. The values of k_{obs}, as found by the equation

$$(1/[R]_0)\ln\frac{[R]_0+[R]}{[R]} - (1/[R]_0)\ln 2 = \frac{k_{obs}\,t}{2\,[R]_0+[D]} \qquad (8.24)$$

are given below.

T, °C	+8	−2	−16	−29	−38	−50
$k_{obs}\times 10$, s^{-1}	1.2	2.2	2.0	2.2	1.6	1.15

Because water as solvent has specific physico-chemical properties, it was interesting to study the kinetics of the redox reaction in frozen aqueous solutions. 2,2,6,6-tetramethyl-4-oxyl-1-piperidinyloxy dissolves in water well, whereas hydrazobenzene does not dissolve at all. So, ascorbic acid was chosen as the second reactant.

The initial reaction rate as a function of temperature for two pH values is plotted in Fig. 8.17. As is seen, the relation is the same for both pH7 and pH3. In either case, the reaction rate is a maximum at —10°C.

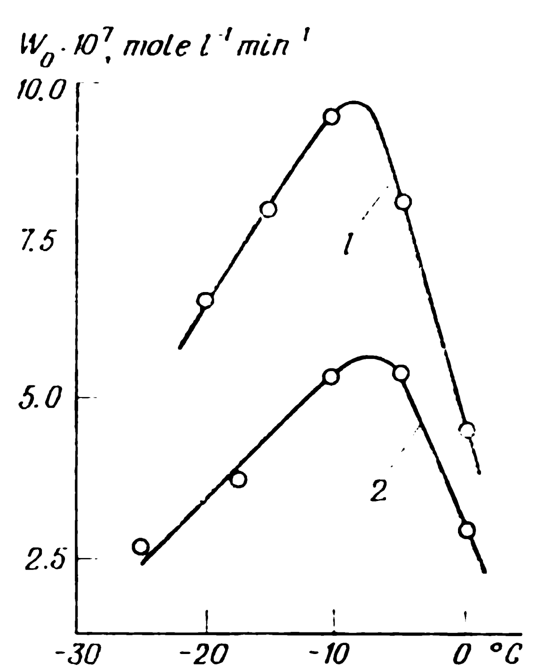

Fig. 8.17. Initial rate for the reaction of 2,2,6,6-tetramethyl-4-oxyl-1-piperidinyloxy with ascorbic acid in ice as a function of temperature ($[R]_0 = [C_6H_8O_6]_0 = 5.7\times10^{-5}\,M$): (1) pH7.0; (2) pH3.0

The values of the observed rate constants for the oxidation of ascorbic acid by the nitroxide radical in frozen aqueous solutions at various temperatures are given below.

pH7:	T, °C	0	−5	−9	−10	−15	−20	−32
	k_{obs}, s^{-1}	0.38	0.98	1.25	1.61	0.92	0.60	0.38
pH3:	T, °C	0	−5	−8	−10	−11.5	−17.5	
	$k_{obs}\times 10^2$, s^{-1}	1.6	4.3	4.7	5.3	3.5	2.2	

The observed rate constant has been computed from the equation

$$\frac{1}{[C_6H_8O_6]_0}\ln\frac{[C_6H_8O_6]}{2\,[C_6H_8O_6]-[C_6H_8O_6]_0} = \frac{k_{obs}\,t}{2\,[C_6H_8O_6]_0+[D]} \qquad (8.25)$$

where [D] is the concentration of the diluent or buffer.

In order to assess the effect of various diluents on the oxidation of ascorbic acid in frozen solutions at —5°C, we used inorganic salts and methyl alcohol as diluents.

These diluents have been found to slow down the reaction in frozen aqueous solutions. To make sure that the slow-down was not due to an increase in the ionic strength of the solution, the reaction was conducted in the liquid phase at 25°C in the presence of various amounts of diluents. It has been found that within the observed limits the concentration of a salt does not practically affect the rate of the reaction in the liquid phase.

Thus, we have found that the redox reactions involving radicals are accelerated in frozen solutions. The reaction rate has been found to be an extremal function of temperature. It has been noticed that the use of a frozen instead of a liquid solution allows the concurrent oxidation of ascorbic acid (and hydrazobenzene) by the nitroxide radical and atmospheric oxygen to be separated kinetically.

In passing from a liquid to a frozen solution, the rate of the reaction rises abruptly. This is illustrated in the plots of Figs. 8.8 and 8.16. It has been found that this abrupt rise increases with decreasing cryoscopic constant, Δ, of the solvent. For the reaction of triethylamine with methyliodide in a frozen and a liquid supercooled benzene solution ($\Delta = 5.8$ K litres mole^{-1}) at +2.5°C, the ratio of the initial reaction rates is 1.6 to 1. In dioxane ($\Delta = 4.5$ K litres mole^{-1}) at +8°C it is 2 to 1, and in water ($\Delta = 1.85$ K litres mole^{-1}) at —1°C it is 5.3×10^8 to 1 [272].

An interesting kinetic aspect of the above reactions is the extremal relation between the reaction rate and temperature. In frozen solutions, the reaction rate first rises with decreasing temperature, reaches a maximum, then falls (see Figs. 8.8, 8.16, and 8.17). For the Menshutkin reaction, the rate peaks lie 10 to 15 degrees below the freezing point of the solution. For the oxidation of ascorbic acid by the nitroxide radical, the temperature interval in which the reaction rate is a maximum is 10 degrees. For the reaction of hydrazobenzene and the nitroxide radical this interval extends to thirty-five degrees.

Comparison of the experimental reaction rate with that computed by the Arrhenius equation for the same temperature has shown that the amount by which the reaction rate goes up increases with decreasing concentration of the reactants. As follows from Table 8.3, the ratio of the two rates for reactions in various solvents increases with decreasing cryoscopic constant and reaches 10^3 in the case of the Menshutkin reaction in frozen aqueous solutions ($\Delta = 1.85$ K litres mole^{-1}). Thus, there exists some correlation between the increase in the rate of a chemical reaction in frozen solutions and the cryoscopic constant of the solvent.

Conversion of a liquid to a frozen solution can stimulate chemical reactions. For example, the oxidation of hydrazobenzene (see Fig. 8.8) by the nitroxide radical in frozen dioxane ($T_{\text{melt}} = 11.8°\text{C}$) proceeds at a fairly high rate ($W_0 = 1.7 \times 10^{-7}$ mole litre^{-1} min^{-1} at +8°C). The reaction does not practically occur in the liquid phase at temperatures close to 12°C. These results are related to the phase inhomogeneity of frozen solutions. Freezing causes the effective concentration of the reactants to increase and the rate of the process to rise abruptly. Owing to the competition between the increase in the local concentration of the reactants and the decrease in the rate constant with decreasing temperature, the relation between the reaction rate and temperature is extremal in character. The degree of concentration of the solutes depends above all on the cryoscopic properties of the solvent and increases as use is made of solvents with progressively decreasing cryoscopic constants. For one and the same solvent, the ratio of the reaction rates in the frozen and supercooled solutions at the same temperature increases with decreasing initial concentrations in the starting solution, if the concentration is primarily determined by the temperature of the experiment and the cryoscopic constant of the solvent.

The observed rate constants for the Menshutkin reaction in frozen benzene, based on NMR and titration studies, are given in Table 8.6.

TABLE 8.6

Observed Rate Constants of the Reaction of Triethylamine with Methyliodide in Frozen Benzene Solutions {$[(C_2H_5)_3N]_0 = [CH_3I]_0 = 0.2M$}

c_{dil}, moles litre^{-1}	T, °C	$k_{\text{obs}} \cdot 10^4$, s^{-1}	
		NMR studies	titration studies
—	−5	4.6±2.3	3.2±0.3
—	−10	2.7±1.4	2.9±0.3
$[C_6H_{12}] = 0.4$	−5	1.3±0.7	2.8±0.3
$[C_6H_5NO_2] = 0.4$	−5	2.3±1.2	13±3

The rate constants for the oxidation of hydrazobenzene by the nitroxide radical in frozen dioxane, based on ESR and UV spectroscopy studies, are given below, $[R]_0 = [C_{12}H_{12}N_2] = 1.1 \times 10^{-4}M$; $[C_2H_5OH] = 0.1M$ (ESR) and $0.01M$ (UV).

ESR: T, °C	+8	−2	−16	−29	−38	−50
$k_{\text{obs}} \times 10$, s^{-1}	1.2±1	2.2±1	2.0±1	2.2±1	1.6±1	1.2±1

UV: T, °C	+10	+5	−5	−10	−15	−20	−30	−40	−50	−70
$k_{\text{obs}} \times 10$, s^{-1}	0.7 ±0.2	1.8 ±0.5	1.8 ±0.5	1.9 ±0.6	2.2 ±0.7	2.8 ±0.8	2.3 ±0.7	2.1 ±0.6	1.9 ±0.6	1.2 ±0.3

It is seen from Table 8.6 and the above data that the values of k_{obs} determined by different methods agree within the error of experiment. Thus, the phase change associated with the unfreezing of the solutions and the history of the solutions do not affect the end results appreciably.

There is a good deal of interest in processes with a negative temperature coefficient. We have investigated for this purpose the bromination of 1-hexene in frozen cyclohexane. In the liquid phase, this reaction involves the molecular complexes formed by the reactants, and its effective activation energy is $E_{eff} = —38$ kJ mole^{-1}. In frozen solutions, the negative temperature coefficient has been observed over a wide temperature interval extending from +7° to —50°C. The effective activation energy depends on temperature and is —96 kJ mole^{-1} in the temperature interval from zero to —20°C and —13 kJ mole^{-1} from —30°C to —50°C.

In frozen solutions, a decrease in the temperature speeds up the reaction owing to the negative temperature coefficient, and also because the reactants are concentrated in the liquid microphase. As the temperature is varied from 0 to —50°C, the rate of the bromination of 1-hexene rises 21 times, whereas that of the Menshutkin reaction and of the oxidation of hydrazobenzene and ascorbic acid by the nitroxide radical in frozen solutions under comparable conditions increases 1.5 to 2.5 times as the temperature is brought down.

At below —50°C, the concentration of the complexes practically ceases to grow, and the effective activation energy for the process changes from negative to positive with the result that the reaction in frozen solutions is slowed down.

Thus, the negative temperature coefficient in the liquid phase is responsible for a marked acceleration of the reaction in frozen solutions and a sizeable expansion of the temperature region where the rate of the process increases and attains its maximum value. For the bromination of 1-hexene, the temperature interval where the rate of the reaction in frozen solutions increases exceeds 60°C. For the other reactions under study it is from 10° or 15°C (the Menshutkin reaction, oxidation of ascorbic acid by the nitroxide radical) to 30-35°C (oxidation of hydrazobenzene). It is seen that reactions can be stimulated by carrying them out in frozen solutions and that this is especially effective for reactions involving complexes.

8.4.2. Effect of the Solvent

In the liquid phase, the rate of the reaction between triethylamine and methyliodide decreases in the following sequence: nitrobenzene > dioxane > benzene > water > carbon tetrachloride > cyclohexane

(Table 8.7). For the sake of comparison, Table 8.7 gives the rate constants for the Menshutkin reaction in liquid and frozen solutions.

TABLE 8.7

Rate Constants for the Reaction of Triethylamine with Methyliodide in Liquid and Frozen Solutions (ε is the dielectric constant of the solvents, Δ is the cryoscopic constant of the solvents)

Solvent	k_2^{+25} 10^4, litre $mole^{-1}$ s^{-1}	k_{obs}^{-5} 10^4, s^{-1}	ε	Δ, K litre $mole^{-1}$
Nitrobenzene	335	23	34.75	4.8
Dioxane	32	9.0	2.4	4.5
Benzene	17.6	3.2	2.3	5.8
Water	9.0	1.7	81	1.85
Carbon tetrachloride	0.75	—	2.2	18.7
Cyclohexane	—	—	2.2	26.0

In frozen solutions, the sequence of the solvents in decreasing order of reaction rate remains the same (see Table 8.7). Practically no reaction takes place in frozen cyclohexane and carbon tetrachloride. This is attributed to the low rate constants and high cryoscopic constants of the solvents.

In principle, there can be an inversion in the sequence of solvents in frozen solutions. If some solvent in the sequence has a cryoscopic constant Δ_2 which is substantially smaller than that of the preceding solvent, Δ_1, the reactants will concentrate more in the solvent with Δ_2, and the reaction rate may exceed that in the solvent with Δ_1. The inversion can be caused by some other factors. For example, it will take place owing to a change in the relative solubility of the reactants at the temperature necessary for a liquid microphase to exist in frozen solutions of several solvents.

The addition of inert diluents should be expected to slow down reactions in frozen solutions, because they minimize the effect of reactant concentration. The concentration of solutes in the liquid microphase of a frozen solution is then such that the diluent accounts for a sizeable proportion of the entire volume of the liquid microphase. NMR studies show (see, for example, Fig. 8.13) that this is exactly the case. The addition of nitrobenzene has a similar diluting effect, but the rate constant for the reaction in a diluted polar solvent is substantially higher than it is in neat benzene or dioxane. The reason for this effect is as follows. On the one hand, the addition of nitrobenzene causes the rate of the reaction to increase owing to an increase in the polarity of the medium. On the other, the increased concentration of the diluent produces an increased diluting effect on the reactants in the liquid microphase as its volume changes. The joint action of these opposing factors results in extrema on the curves relating W_0 to the diluent concentration (curves *1* and *2* in Fig. 8.9).

Experimental evidence suggests the following general pattern. The addition of an inert diluent will slow down the reaction in a frozen solution if the rate of the process in that diluent (when used as a solvent) in the liquid phase is lower than in the solvent in question. The addition of an inert diluent can both decrease and increase the rate of the reaction in frozen solutions, if the rate of the process in that diluent in the liquid phase is higher than in the solvent in question.

It is also important to note that in all the observed cases the concentration of the diluent was comparable with that of the reactants and accounted for less than 5% of the volume of the entire system. It may therefore be concluded that, although they do not affect kinetics of the reaction in the liquid phase, diluents can control the rate of the process in frozen solutions.

To learn how the surface of the solid phase and other factors could possibly affect the rate of chemical processes in ice, we have investigated the influence of various salts on the Menshutkin reaction and the oxidation of ascorbic acid by the nitroxide radical.

As regards their effect on the structure of water in liquid solutions, all salts may be classed into two groups, chaotropic and nonchaotropic [597]. The former include salts with Cl^-, I^-, and ClO_4 anions which break up the hydrogen-bonded structure of water. Salts with SO_4^{2-} and HPO_4^{2-} anions "strengthen" the water structure. In frozen solutions, the addition of NaCl, $NaClO_4$ or Na_2SO_4 in a $0.1M$ concentration slows down the oxidation of ascorbic acid by the nitroxide radical, the strongest in this effect being NaCl, then $NaClO_4$ and, finally, Na_2SO_4. They affect in the same sequence the reaction of triethylamine with methyliodide in ice. The only exception is sodium sulphate. As is seen from Fig. 8.10, the addition of $0.1M$ Na_2SO_4 (curve *1*) speeds up the Menshutkin reaction in frozen aqueous solutions. The increase in the concentration of sodium sulphate has a similar effect. In contrast, an increase in the concentration of NaCl and $NaClO_4$ brings about a decrease in the rate of the reaction (curves *2* and *3*).

To understand why salts affect reactions in ice, it is important to know whether they are incorporated in the ice crystals or remain in the liquid microphase. An ESR study on the phase state of frozen aqueous solutions has shown that the addition of salts, notably sodium sulphate, controls the mobility of the nitroxide radical. At —18°C and in the presence of $1M$ Na_2SO_4 the correlation time is $\tau_{cor} = 7.8\times \times 10^{-11}$ s; in the absence of diluents, $\tau_{cor} = 2.3\times10^{-10}$ s. This may be interpreted as pointing to the presence of the diluent salts in the liquid microphase. According to [598] and [599], no solid solutions are formed in water. Thus, it may be thought that the salts are concentrated in the liquid microphase.

Inorganic salts act in the same way as organic diluents — they increase the volume of the liquid microphase and dilute the reactants. The higher the concentration of a diluent, the lower the rate of the process. An important distinction of inorganic salts from other diluents seems to arise from the fact that anions and cations carry charge. Electrostatic forces can produce various effects in solutions. The abnormal behaviour of sodium sulphate in the case of the Menshutkin reaction is probably related to the fact that its presence causes the solution in the liquid microphase to separate into an organic phase (the reactants) and an inorganic phase (the reactants, water, and diluent). Triethylamine and methyliodide freeze at —115° and —64°C, respectively. In frozen solutions of CH_3I and $(C_2H_5)_3N$ in benzene, CCl_4 and other solvents, the presence of the liquid microphase is detected down to —100°C (see Fig. 8.6). Besides, CH_3I and $(C_2H_5)_3N$ dissolve in water but little. Taken together, these factors promote the separation of the solution in the liquid microphase. The addition of Na_2SO_4 can reduce the solubility of organic reactants in water. Thus, the reaction can proceed in two different phases, one of which is neat reactants. Obviously, the overall rate of the process must rise. If the starting reactants are solids, such as the nitroxide radical and ascorbic acid, then the addition of sodium sulphate will not lead to the separation of the solution in the liquid microphase, and the process will be slowed down [586].

There is considerable interest, both theoretical and practical, in the effect of freezing upon concurrent reactions. This has been studied on the oxidation of ascorbic acid and hydrazobenzene by 2,2,6,6-tetramethyl-4-oxyl-1-piperidinyloxy. In the liquid phase, either reaction is accompanied by the action of ascorbic acid and hydrazobenzene with the dissolved oxygen. The ascorbic acid and hydrazobenzene are present in solution in excess with respect to the oxygen, so both processes are described by a quasi-first-order kinetic equation. In the liquid phase, the rate of oxidation of hydrazobenzene by oxygen at 20°C contributes substantially to the rate of the overall process in the presence of the nitroxide radical (see curves *3* and *2*, respectively, in Fig. 8.15).

A different picture is to be seen in frozen solutions. The oxidation by the dissolved oxygen is practically suppressed (curve *4*), whereas the reaction of hydrazobenzene with the nitroxide radical is abruptly speeded up (curve *1*). The reaction of oxygen with hydrazobenzene in frozen solutions comes to a standstill because the concentration of the solutes in the liquid microphase does not affect reactions of the first and quasi-first order. A similar situation is observed in the oxidation of ascorbic acid by the nitroxide radical and oxygen. Thus, conversion of a system from the liquid to the frozen state can in some cases be utilized for kinetically separating the reactions proceeding concurrently in a system.

8.4.3. Correspondence Between Experiment and the Model

The evidence cited above points out that the reactions in frozen solutions take place in the liquid microphases contained within solidified solution matrices.

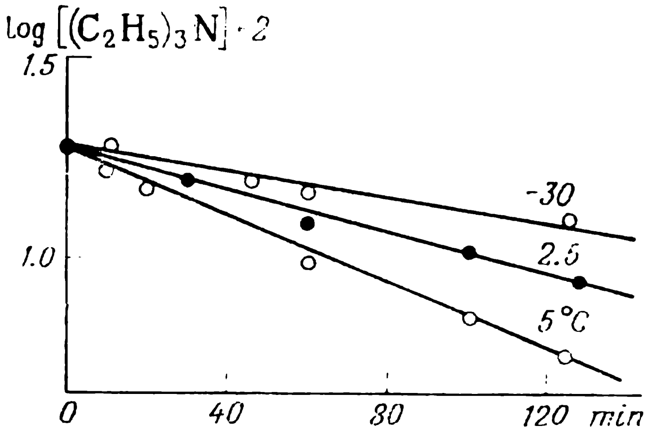

Fig. 8.18. Logarithm of triethylamine concentration in reaction with methyliodide in frozen benzene as a function of time at various temperatures $\{[(C_2H_5)_3N]_0 = [CH_3I]_0 = 0.2M\}$

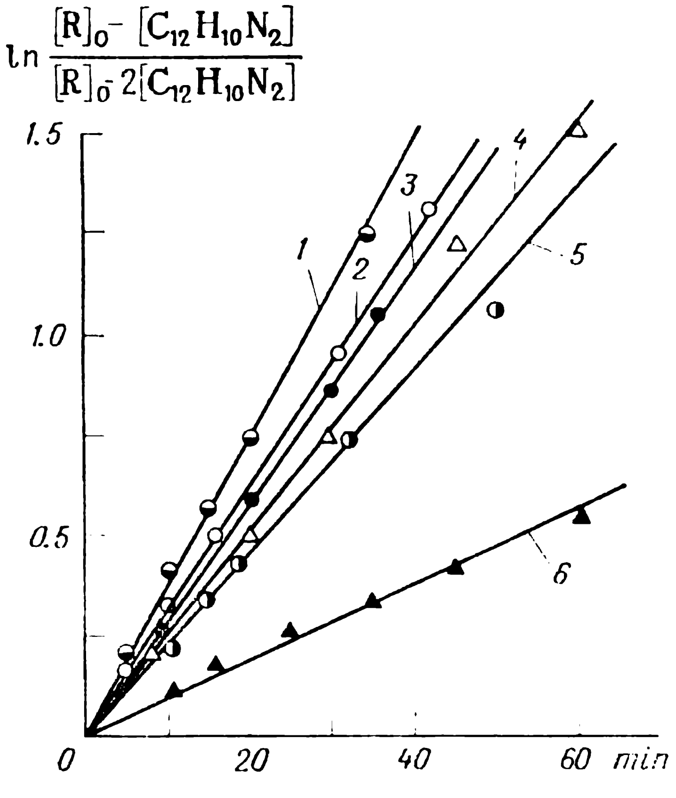

Fig. 8.19. Kinetic curves of azobenzene formation in the oxidation of hydrazobenzene by 2,2,6,6-tetramethyl-4-oxyl-1-piperidinyloxy in frozen dioxane solutions at various temperatures:

(1) —20°C; (2) —30°C; (3) —15°C; (4) —10°C; (5) —5°C; (6) —10°C

The kinetic equations resulting from the model examined in Sec. 8.4 adequately describe the kinetics of the reactions in frozen solutions. As examples, the plots in Figs. 8.18 and 8.19 illustrate the consumption of triethylamine in its reaction with methyliodide in benzene and the accumulation of azobenzene in the reaction of the nitroxide radical with hydrazobenzene in dioxane, as found by appropriate equations.

The bromination of 1-hexene in frozen solutions at $[Br_2]_0 = [Ol]_0$ is described by the following equation:

$$\ln \frac{[Br_2]_0}{[Br_2]} = k_{obs} t = k'(c_{liq}/2)^2 t \tag{8.26}$$

on the assumption that in frozen solutions $[Br_2]_{liq} > [Br_2 \cdot Ol]_{liq}$ and $[Br_2]_{liq} > [P]_{liq}$, where $[P]_{liq}$ is the concentration of the product in the liquid microphase. In the liquid phase, this reaction is described by a third-order equation:

$$-d[Br_2]/dt = k\,[Br_2]^3$$

From an analysis of data about the bromination of 1-hexene in frozen solutions it has been found that the kinetics of the reaction is described by Eq. (8.26) and does not obey the third-order equation.

For the reaction of bromine with 1-hexene, the effective activation energy is

$$E_{eff} = E - 2RT^2/(T_0 - T) \tag{8.27}$$

As is seen, it is the difference between the activation energy in the liquid phase and a positive term, $RT^2/(T_0 - T)$. Since $T < T_0$, it follows that $(T_0 - T) > 0$. The magnitude of this term depends on both the temperature of the frozen solution, T, and the freezing point of the solvent, T_0. At $T_{max} < T < T_0$, the term $RT^2/(T_0 - T)$ exceeds E, which implies that in this temperature interval the reaction in frozen solutions will have a negative temperature coefficient. The factor 2 in Eq. (8.27) accounts for the fact that bromination is a trimolecular reaction. Thus, in the general case the expression for E_{eff} also depends on the type of reaction. For bromination, which has a negative temperature coefficient in the liquid phase, E_{eff} in frozen solutions will be smaller than zero over the entire temperature interval, whereas its absolute value will decrease with decreasing temperature.

For bromination at —5°C,

$$E_{eff} = -37.7 - 2 \times 2 \frac{4.2 \times 268^2 \times 10^{-3}}{279.4 - 268} = -143 \text{ kJ mole}^{-1}$$

For the oxidation of hydrazobenzene by 2,2,6,6-tetramethyl-4-oxyl-1-piperidinyloxy at the same temperature,

$$E_{eff} = 20 - \frac{2 \times 268^2 \times 4.2 \times 10^{-3}}{279.4 - 268} = -33 \text{ kJ mole}^{-1}$$

With all other conditions being equal, the region in which a negative temperature coefficient may be expected will, according to Eq. (8.27), be the greater, the lower the activation energy for the liquid phase, because the difference $(T_0 - T_{max})$ will then be greater.

To illustrate, for the reaction of triethylamine with methyliodide in benzene ($E = 39.4$ kJ mole^{-1}) this difference is $T_0 - T_{\max} = 278 - 268 = 10$ K, and for the oxidation of hydrazobenzene by the nitroxide radical ($E = 25$ kJ mole^{-1}) it is $T_0 - T_{\max} = 285 - 253 = 32$ K.

The marked influence of the chemical nature of diluents on the rate of reactions in frozen solutions (assuming that the concentrations of the diluents and reactants are nearly the same) can likewise be explained within the framework of the model in question. The point is that, apart from diluting the reactants as it increases the volume of the liquid microphase, the diluent may appreciably affect the chemical properties of the medium in the microphase and, as a consequence, the magnitude of k_2 (this is true, for example, of nitrobenzene in the Menshutkin reaction).

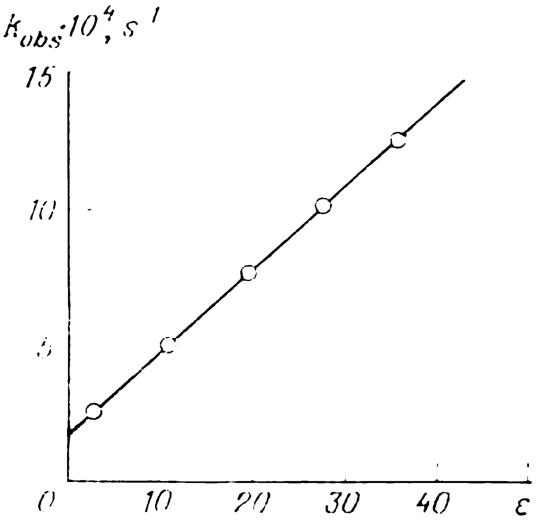

Fig. 8.20. Observed rate constant, k_{obs}, for the Menshutkin reaction in frozen benzene as a function of the dielectric constant ε of the diluent ($T = -5$°C, $[CH_3I]_0 = [(C_2H_5)_3N]_0 = 0.2M$, $[D] = 0.4M$)

The acceleration of reactions in benzene and dioxane by nitrobenzene can be attributed to the increase in the polarity of the medium in the liquid microphase and the accompanying rise in the rate constant for the bimolecular reaction. The plot in Fig. 8.20 illustrates the dependence of k_{obs} on the dielectric constant of the diluent. As is seen, the rate constant increases with increasing concentration of nitrobenzene owing to the increased polarity of the medium. From some point on, the decrease in the concentration of the reactants in the liquid microphase owing to the increase in its volume caused by the diluent begins to be felt. It is the joint action of these two conflicting factors that causes extrema to appear on the curves relating W_0 to the diluent concentration (see Fig. 8.9).

For a quantitative evaluation of the effect of a diluent, it is important to know how the rate constant for the bimolecular reaction depends on the properties of the medium. As regards variations in ε_{liq} in the case of the Menshutkin reaction in frozen solutions, this can be done in the following way [484]. Suppose that the dielectric constant of the liquid microphase is related to the value of ε of the individual components by an equation of the form

$$\varepsilon_{\text{liq}} = \sum_i n_i \varepsilon_i \tag{8.28}$$

where ε_i and n_i are the dielectric constant and the molar fraction of the ith component.

Suppose also that variations in the volume of the solution with decreasing temperature and in the volume of the microphase with the progress of the reaction are negligibly small. In view of the above assumptions, it is an easy matter to compute the dielectric constant for the medium in the liquid microphase. In one of the experiments, the reactants were present in the same concentration equal to $0.2M$, the concentration of the nitrobenzene diluent was $0.4M$. Thus, the total concentration of the solutes in the liquid solution was $0.8M$, and its value for the liquid microphase, c_{liq}, can be found by Eq. (8.14). For a reaction in benzene ($T_0 = 278.4$ K) in the presence of nitrobenzene at —5°C, its value is $1.8M$. As is seen, freezing the solution down to —5°C increases the concentration of the solutes $1.8/0.8 = 2.25$ times. If, for example, the volume of the unfrozen solution is $V = 4$ ml, the volume of the liquid microphase will be $V_{\text{liq}} = V \div 2.25 = 1.78$ ml. Using the initial concentrations of the reactants and nitrobenzene and also the volume of the unfrozen solution, we can readily find the quantity of solutes in the liquid microphase and the volume they take up. In the case on hand, it is 0.32 ml. Thus, the volume of benzene in the liquid microphase is $1.78—0.32 = 1.46$ ml, which corresponds to 16.5×10^{-3} mole. Nitrobenzene accounts for 1.6×10^{-3} mole, and methyliodide and triethylamine for 8×10^{-4} mole each. Using the above figures and Eq. (8.28), we can readily compute the dielectric constant for the medium in the liquid microphase:

$$\varepsilon_{\text{liq}} = 0.838 \times 2.3 + 0.081 \times 34.75 + 0.041 \times 2.42 + 0.041 \times 7.1 = 5.1$$

Data on the dielectric constant, ε, for unfrozen solutions of triethylamine and methyliodide in benzene and dioxane and the dielectric constant, ε_{liq}, of the liquid microphase in frozen benzene at —5°C and in frozen dioxane at —8°C as function of nitrobenzene concentration, $[(C_2H_5)_3N]_0 = [CH_3I]_0 = 0.2M$, are given below.

$[C_6H_5NO_2]$, moles litre^{-1}	0.0	0.1	0.2	0.3	0.4	0.6	0.8
ε:							
in benzene	2.39	2.68	2.96	3.25	3.63	—	—
in dioxane	2.32	2.59	2.87	3.14	3.42	3.99	4.55
ε_{liq}:							
in benzene	2.70	3.64	3.82	4.66	5.13	—	—
in dioxane	4.51	9.61	13.2	15.7	17.5	20.1	21.8

A plot of the dielectric constant of the medium as a function of nitrobenzene concentration in unfrozen solutions and the liquid microphase appears in Fig. 8.21. The addition of 0 to 0.8*M* nitrobenzene brings about an insignificant rise in the dielectric constant of unfrozen solutions. In contrast, as is seen from 8.21, the dielectric constant of the liquid microphase, especially in frozen dioxane, rises substantially. This happens because dioxane has a lower cryoscopic constant as compared with benzene ($\Delta_{C_6H_6} = 5.8$ K litres mole^{-1}; $\Delta_{dioxane} = 4.5$ K litres mole^{-1}), and, as a consequence, its concentration produces a stronger effect.

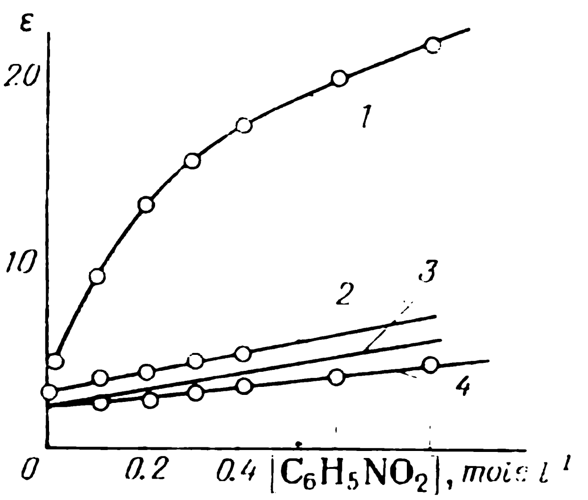

Fig. 8.21. Dielectric constant of the medium as a function of nitrobenzene concentration $\{[(C_2H_5)_3N]_0 = [CH_3I]_0 = 0.2M\}$:

(1) frozen dioxane solution, —8°C; (2) frozen benzene solution, —5°C; (3) unfrozen benzene solution; (4) unfrozen dioxane solution

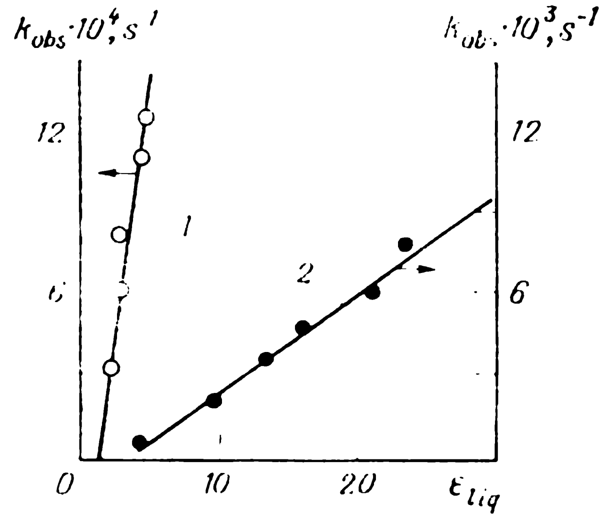

Fig. 8.22. Observed rate constant for the reaction of triethylamine with methyliodide as a function of dielectric constant of the liquid microphase $\{([C_2H_5)_3N]_0 = [CH_3I]_0 = 0.2M\}$:

(1) benzene, —5°C; (2) dioxane, —8°C

A plot of the observed rate constant, k_{obs}, as a function of ε_{liq} is shown in Fig. 8.22. As is seen, k_{obs} increases with the dielectric constant of the medium in the liquid microphase in the investigated interval of diluent (nitrobenzene) concentration. The extremal dependence, actually observed in experiments, of the reaction rate in frozen solutions on the nitrobenzene concentration arises from the joint action of two conflicting factors, namely the increased polarity of the medium and the reduced concentration of the reactants.

It should be expected that the dependence of the rate of the Menshutkin reaction in frozen solutions on the dielectric constant of the liquid microphase will qualitatively be the same as in the liquid phase. In a number of solvents, the Menshutkin reaction in the liquid phase has been found to obey the Kirkwood equation with some constraints [600, 601]. As is seen from Fig. 8.23, the dependence of the observed rate constant for the Menshutkin reaction in frozen solutions on the dielectric constant of the liquid microphase does obey the Kirkwood equation. We shall write this equation, limiting it to the term explicitly dependent on the dielectric constant:

$$k_2 = k_0 \exp\left(\frac{\beta}{kT} \cdot \frac{\varepsilon - 1}{2\varepsilon + 1}\right) \tag{8.29}$$

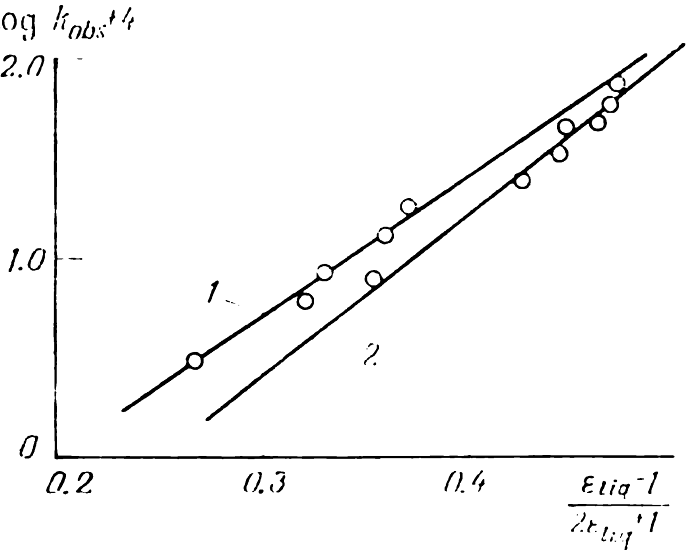

Fig. 8.23. Logarithm of observed rate constant for the reaction of triethylamine with methyliodide as a function of $(\varepsilon_{liq} - 1)/(2\varepsilon_{liq} + 1)$ $\{[(CH_3I]_0 = [(C_2H_5)_3N]_0 = 0.2\ M\}$: (1) benzene, —5°C; (2) dioxane, —8°C

where

$$\beta = \mu_A^2/r_A^3 + \mu_B^2/r_B^3 - \mu_{AB}^{2\neq}/r_{AB}^{3\neq}$$

Suppose that the dielectric constant of the liquid microphase, ε_{liq}, is a linear function of the diluent concentration, $[D]_{liq}$

$$\varepsilon_{liq} = \varepsilon_0 + \alpha[D]_{liq} \tag{8.30}$$

where ε_0 and α are the constants for a given system.

On substituting Eqs. (8.30) and (8.29) into Eq. (8.6) and re-arranging, we get

$$d[A]/dt = -k_0 \exp\left(\frac{\beta}{kT} \cdot \frac{\varepsilon_0 - 1 + \alpha[D]_{liq}}{2\varepsilon_0 + 1 + 2\alpha[D]_{liq}}\right) \frac{[A]\,[B]\,c_{liq}}{[A]_0 + [B]_0 + [D]} \tag{8.31}$$

From analysis of the above equation it follows that the reaction rate is a maximum at a certain definite diluent concentration which is a function of α, β, and ε_0.

Thus, the proposed model takes into account the effect of the dielectric constant of the medium on the rate of the reaction in frozen solutions and permits a quantitative description of the reaction rate as a function of the polarity of the medium.

Let us compare the rates of concurrent chemical reactions in the liquid phase and in frozen solutions, using the above model.

Let, for example, there be two concurrent bimolecular chemical reactions

$$A + B \xrightarrow{k_1} E + F \tag{8.32}$$

$$C + D \xrightarrow{k_2} K + H \tag{8.33}$$

When the substance D is present in excess, the reaction (8.33) becomes pseudo-monomolecular, and it may be written

$$C \xrightarrow{k_3} K + H \tag{8.34}$$

The rates of the reactions (8.32) and (8.34) in the liquid phase are written

$$W_{(a)} = k_1[A]\,[B] = k_1^\circ \exp(-E_1/RT)\,[A]\,[B] \tag{8.35}$$

$$W_{(b)} = k_3\,[C] \quad k_3 = k_2\,[D] = k_2^\circ \exp(-E_2/RT)\,[D] \tag{8.36}$$

where [A], [B], [C], and [D] are the reactant concentrations in the liquid phase; k_1° and k_2° are the pre-exponential factors for the first and second reactions; E_1 and E_2 are the activation energies for these reactions in the liquid phase.

According to the kinetic model, the rates for the reactions (8.32) and (8.34) are written

$$W_{(a),\,\mathrm{liq}} = k_{\mathrm{obs}(a)}\,[A]\,[B] = \frac{T_0 - T}{\Delta([A]_0 + [B]_0)} \cdot k_1^\circ \exp(-E_1/RT)\,[A]\,[B] \tag{8.37}$$

$$W_{(b),\,\mathrm{liq}} = k_{\mathrm{obs}(b)}\,[C] = k_2^\circ \exp(-E_2/RT)\,[D]\,[C] \tag{8.38}$$

where T_0 is the freezing point of the solvent and Δ is its cryoscopic constant, K litre mole^{-1}.

If at T_1 the reactions (8.32) and (8.34) proceed in the liquid phase at the same rate, then

$$k_1^\circ \exp(-E_1/RT_1)\,[A]\,[B] = k_2^\circ \exp(-E_2/RT_1)\,[D]\,[C]$$

or

$$\frac{[A]\,[B]}{[C]\,[D]} = \frac{k_2^\circ \exp(-E_2/RT_1)}{k_1^\circ \exp(-E_1/RT_1)} \tag{8.39}$$

The ratio of the rates for these reactions in the supercooled liquid phase at temperature T will be

$$W_{(a)}(T)/W_{(b)}(T) = \frac{k_1^\circ \exp(-E_1/RT)}{k_2^\circ \exp(-E_2/RT)} \cdot \frac{[A]\,[B]}{[C]\,[D]} \tag{8.40}$$

The ratio of the rates for the same reactions in frozen solutions at temperature T will be

$$W_{(a)\,\mathrm{liq}}(T)/W_{(b\,\mathrm{liq}}(T) = \frac{T_0 - T}{\Delta([A]_0 + [B]_0)} \cdot \frac{k_1^\circ \exp(-E_1/RT)}{k_2^\circ \exp(-E_2/RT)} \cdot \frac{[A]\,[B]}{[C]\,[D]} \tag{8.41}$$

On substituting Eq. (8.39) into Eq. (8.41), we get

$$\frac{W_{(a)\,\mathrm{liq}}(T)}{W_{(b)\,\mathrm{liq}}(T)} = \frac{T_0 - T}{\Delta([\mathrm{A}]_0 + [\mathrm{B}]_0)} \cdot \frac{\exp(-E_1/RT)}{\exp(-E_2/RT)} \cdot \frac{\exp(-E_2/RT_1)}{\exp(-E_1/RT_1)} \tag{8.42}$$

From comparison of Eqs. (8.40) and (8.42) it is an easy matter to see that the same change in temperature brings about a different change in the ratio of the rates for two concurrent chemical reactions in the liquid phase and in frozen solutions. The difference in the reaction rates brought about by conversion of the system from the liquid to the frozen state is

$$\frac{W_{(a)\,\mathrm{liq}}(T)/W_{(b)\,\mathrm{liq}}(T)}{W_{(a)}(T)/W_{(b)}(T)} = \frac{T_0 - T}{\Delta([\mathrm{A}]_0 + [\mathrm{B}]_0)} \tag{8.43}$$

If we take the oxidation of hydrazobenzene by the nitroxide radical and dissolved atmospheric oxygen in dioxane ($T_0 = 285$ K, $\Delta = 4.5$ K litres mole^{-1}, $[\mathrm{A}]_0 = [\mathrm{B}]_0 = 1 \times 10^{-4} M$), and the temperature of the maximum reaction rate ($T_{\max} = 253$ K), the above equation will give a value of 3.6×10^4, which implies that the rate of oxidation by dissolved oxygen is 1/35 000 of that by the nitroxide radical. On the other hand, the oxidation of hydrazobenzene by the nitroxide radical is accelerated in frozen solutions in comparison with the liquid phase. For the reaction involving ascorbic acid, the oxidation by atmospheric air is slowed down in comparison with the main reaction by a factor of about 50 000.

Thus, conversion of a system from the liquid to the frozen state offers a means for a kind of kinetic selection.

For a more detailed verification of the proposed model, we have compared experimental and computed rate constants. In the absence of phase diagrams, the total concentration of the solutes in the liquid microphase, c_{liq}, has been found by Eq. (8.14). The values of c_{liq} deduced from NMR data and computed by Eq. (8.14) are given in Table 8.8.

TABLE 8.8

Total Concentration of Solutes in the Liquid Microphase for the Reaction of Triethylamine with Methyliodide in Frozen Benzene Solutions, $[\mathrm{CH_3I}]_0 = [(\mathrm{C_2H_5})_3\mathrm{N}]_0 = 0.2M$

c_{dil}, mole litre^{-1}	T, °C	c_{liq}, mole litre^{-1}	
		deduced from NMR data	computed
—	−5	3±1.5	1.8
—	−10	4±2	2.7
$[\mathrm{C_6H_{12}}] = 0.4$	−5	3±1.5	1.8
$[\mathrm{C_6H_5NO_2}] = 0.4$	−5	3.5±1.7	1.8

The computed and experimental temperatures at which the rate of some of the investigated reactions is a maximum are given in Table 8.9.

TABLE 8.9

Computed, $T_{\max}^{\text{comp}}$, and Observed, $T_{\max}^{\text{obs}}$, Maximum-Rate Temperatures for Various Solvents and Activation Energies in the Liquid Phase and in Frozen Solutions

System	Solvent	E, kJ mole^{-1}	E_f, kJ mole^{-1}	$T_{\max}^{\text{comp}}$, °C	$T_{\max}^{\text{obs}}$, °C
$CH_3I + (C_2H_5)_3N$	Benzene	39 ± 4	48	-9 ± 2	-5
	Nitrobenzene	41 ± 4	49	-8 ± 2	-5
	Dioxane	28 ± 4	40	-9 ± 2	-6
	Water	85 ± 4	97	-8 ± 2	-8
	CCl_4	52 ± 4	--	-32 ± 2	—
$R + C_{12}H_{12}N_2$	Dioxane	25 ± 4	27	-14 ± 2	-20 (UV) -20 to -25 (ESR)
$R + C_6H_8O_6$	Water	50 ± 8, pH7	71	-10.5 ± 3	-10
		54 ± 8, pH3	79		-10

The values of E_f used in Table 8.9 have been found from plots of $\ln \{k_{obs}/[(T_0 - T)/\Delta]\}$ as a function of $1/T$. An example of such a plot for the Menshutkin reaction in benzene is shown in Fig. 8.24. As is seen, when plotted in these coordinates the curve is linear.

Figure 8.25 shows, as an example, experimental and computed plots of rate constants as a function of temperature for the reaction of the nitroxide radical with hydrazobenzene.

As is seen from Tables 8.8 and 8.9 and Fig. 8.25, the structural kinetic model makes it possible not only to interpret experimental facts, but also to compute the rates of processes in frozen solutions on the basis of the characteristics of the reactions in the liquid phase. This offers a novel, physically tangible insight into events such as the kinetic cessation of chemical reactions, including stepwise recombination of radicals in frozen solutions.

The kinetic cessation of processes under isothermal conditions, notably the stepwise recombination of radicals observed in a large number of processes [172, 602, 603] may be associated with the phase inhomogeneity of the investigated systems. A rise in temperature causes the system to pass into a new state of phase equilibrium in which some of the trapped reactive species gain in diffusion mobility, and are lost in the course of chemical reactions. Since the process is actually limited by the warm-up rate of the specimen, simple first- and second-order kinetic equations often fail to describe the kinetics involved, as might be expected if the chemical stage were the controlling one. The stepwise recombination of radicals must then have obeyed a second-order equation, which does not actually happen.

Experimental evidence available at the time of writing as regards the kinetic cessation of chemical reactions at low temperatures can be rationalized as follows. When, say, a monomer crystal is exposed to ionizing radiation, there form, in the spurs, various reactive intermediates which interact with the monomer molecules and with one another to form a polymer. Just as they are produced, the primary reactive species possess a substantial excess energy over the energy they have when they are in thermal equilibrium with the surroundings.

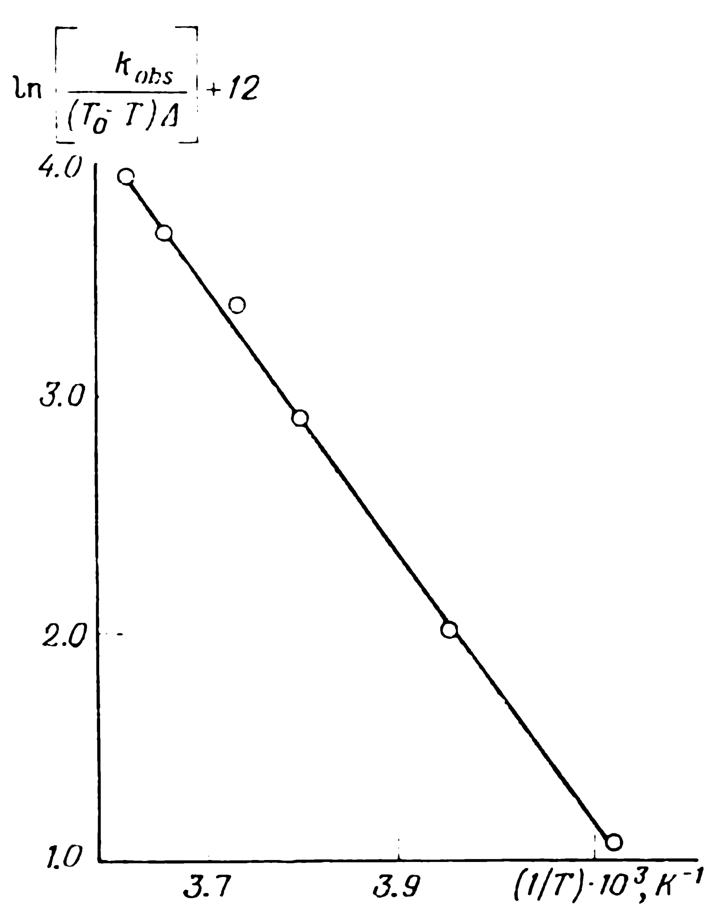

Fig. 8.24. Plot of ln $\frac{k_{obs}/(T_0 - T)}{\Delta}$ as a function of $1/T$ for the Menshutkin reaction in frozen benzene

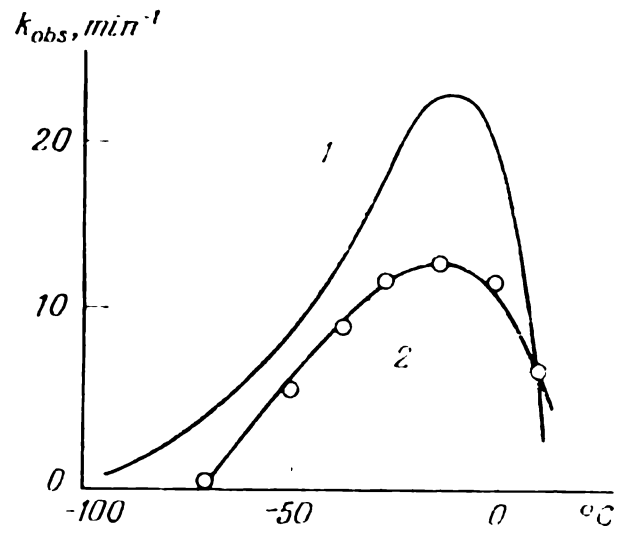

Fig. 8.25. Rate constant for the oxidation of hydrazobenzene by nitroxide radical in frozen dioxane as a function of temperature:
(1) calculated value; (2) experiment

The calorimetric method characterizes the entire specimen, whereas the regions of the microscopic surroundings where the polymerization takes place may differ from the specimen as a whole in physico-chemical properties. The kinetic cessation of polymerization with decreasing temperature may, therefore, be traceable to the fact that the rate of energy generation by the primary processes and its rate of dissipation are such that the conditions favour the formation in the specimen of some microscopic regions where the mobility of the species exceeds that in the matrix for some time. The chain reaction of polymerization induced by gamma irradiation takes place exactly in those microscopic regions which may be treated as sufficiently large assemblages of species displaying macroscopic physico-chemical properties. These microscopic regions can be brought into being by exposure of the specimen to radiation and by the subsequent primary radiation-chemical processes.

The time during which the species in such microscopic regions retain high mobility depends on the type of radiation, the character of primary and secondary physical and chemical processes, and the physical properties of the specimen. It is reasonable to assume that, starting at a certain temperature, this time is above all controlled by the type of radiation and the primary processes, and, as a consequence, it will vary but little with decreasing temperature. In practice, this will result in that the rate of polymerization will only slightly depend on temperature, that is, there will exist a low-temperature limit for the rate of the chemical reaction.

Arguments in favour of the above rationalization can be found in [172] dealing with the postpolymerization of gamma-irradiated formaldehyde at 20-150 K. It is important to stress that the yield for polymerization of formaldehyde has always been determined upon melting and warming up the specimens to room temperature. The warm-up of specimens irradiated at low temperatures has been found to be accompanied by an effective postpolymerization [322] which, according to [172], proceeds at a significant rate already at 15-20 K. According to available evidence, the chain polymerization of formaldehyde occurs at very low temperatures and is carried on by the reactive species and centres accumulating during the irradiation period. In fact, two temperature regions of postpolymerization have been registered, labelled as *A* and *B* in the reference quoted. Interestingly, the temperature boundaries of region *B* lying at higher temperatures depend on the integral dose of radiation and are independent of the temperature of pre-irradiation. The temperature boundary of postpolymerization in region *A* goes down with decreasing temperature of irradiation. It has been found that for the polymerization of formaldehyde the kinetic cessation of the process occurs under isothermal conditions.

The arguments set forth above explain why the lower boundary (the onset) of postpolymerization of formaldehyde depends on the radiation dose [172]. An increase in the dose accentuates the phase inhomogeneity and stimulates the local concentrations of the products and trapped reactive species. The net result is that the lower temperature boundary is brought down.

The kinetic cessation of postpolymerization under isothermal conditions is traceable to the phase equilibrium that is established between the matrix and the microscopic regions as the temperature of the specimen is raised. Thus, the reaction kinetics observed as the temperature of the specimen is raised from T_1 to T_2 reflects in fact the manner in which the specimen originally residing in a state of equilibrium at T_1 approaches the state of equilibrium at T_2. The rate of the observed reactions involving reactive species is controlled by diffusion rather than the chemical interactions proper.

Given the same temperature, the diffusion mobility of the species in the microscopic regions is substantially higher than in the more rigid matrix. Qualitatively, it can be accounted for by invoking analogy with, say, the lowering of the freezing point for solutions of substances by diluents. In the case on hand, the "diluents" are the irradiation products which usually have a smaller molecular mass and a lower melting point than the reactants, and also the reactive species such as ions and radicals. It is, therefore, logical, in our opinion, to ask how much the melting point of the microscopic regions of a specimen can be brought down by the ions, radicals, and other reactive species found there. More generally, this question can be stated thus: What are the physico-chemical properties of specimens showing phase inhomogeneity, how do these properties vary within the bulk of a specimen, and how much do they differ from those of specimens with phase homogeneity? Unfortunately, little is known as yet about the structure and physico-chemical characteristics of multicomponent frozen solutions.

The idea that the phase inhomogeneity of frozen solutions is closely related to the kinetics of the processes occurring in them may, as we believe, be used to interpret the mechanism of radiophotoluminescence for organic substances at low temperatures [551, 604, 605]. Berlin *et al.* [551] have proposed a mechanism based on the tunnel charge transfer. They have studied samples of methylcyclohexane gamma-irradiated at 77 K. In the experiments conducted to verify the proposed model, tetramethylparaphenylenediamine was added to the specimens as phosphor to enhance radiophotoluminescence, and it was presumed that the phosphor was distributed uniformly throughout the specimen upon freezing. Actually, the phosphor could as well be concentrated locally and produce specimens with phase inhomogeneity. If this was actually so, the experimental results might be interpreted differently. Interestingly, isothermal luminescence has been found to show experimental kinetics basically similar to that found for the irradiation-induced polymerization of formaldehyde [172].

The stepwise recombination of radicals can likewise be rationalized within the framework of the structural kinetic model, if it is assumed that freezing or irradiation produces a structurally inhomogeneous specimen [606, 607]. Let us assume for simplicity that trapped radicals are uniformly distributed throughout the bulk of a frozen specimen and that the products of primary irradiation-induced chemical reactions are distributed nonuniformly. Because one has to allow for the nonuniform distribution of radicals, which does occur in reality, a mathematical description of the process grows more complicated, but the results are basically the same.

As the temperature of a specimen is raised, the molecular mobility increases in both the matrix and the microscopic regions, but the increase is materially greater in the latter. As a point of departure, let us assume that a phase transition of the solid-liquid type takes place in the microscopic regions at a temperature T decided by the concentration of all impurity molecules. The mobility of the radicals found in the microscopic regions rises so much that their recombination is no longer controlled by diffusion and proceeds practically instantaneously. The equation connecting the temperature T and the composition of the specimen and defining the volume of the microscopic regions where the phase transition has taken place can be written

$$T_0 - T = f(N_A, N_B) \tag{8.44}$$

where T_0 is the melting point of the matrix material, $f(N_A, N_B)$ is the equation of the liquidus for the system "matrix material-impurity molecules", N_A and N_B are the molar fractions of the matrix material and the impurity molecules in the microscopic regions of a given composition.

Unfortunately, the equation of the liquidus and phase diagrams for the systems in question are not available.

In a first approximation, we may use a linear relation of the form

$$T_0 - T = KN_B \tag{8.45}$$

where K is a numerical coefficient having the sense of cryoscopic constant.

For each value of T there will be a particular value of the volume of the microscopic regions "molten" at that temperature. The value of the volume is a function of many factors, the principal ones being the temperature of the specimen, the physico-chemical properties of the components (above all, the cryoscopic constant and the ability to form eutectics), the quantitative composition of the microscopic regions, the character of the radicals and reaction products, and the manner of freezing. An increase in temperature entails an increase in the volume within which recombination can occur. Under isothermal conditions, the radicals remaining in the solid phase recombine at a very low rate, and their rate of loss is diffusion-controlled.

The loss of radicals upon an instantaneous rise in the temperature of the outer wall of the specimen from T_1 to T_2 may then be visualized to occur as follows. As the temperature rises, the volume of the "molten" microscopic regions increases; an equation describing the loss of radicals in the increased volume can be developed by solving the equation of thermal conductivity for the specimen, with allowance for the volume distribution density of the various microscopic regions [607]. On the loss curve (Fig. 8.26), this is represented by the region of fast recombination involving a considerable proportion of radicals. For a rectangular specimen (with dimensions $d \times d \times l$) having an average concentration of trapped radicals n and an average volume density of the microscopic regions m, the time dependence of R (the number of lost radicals) as the specimen temperature is raised by $\Delta T = T_2 - T_1$ can be described by the equation developed in [607]:

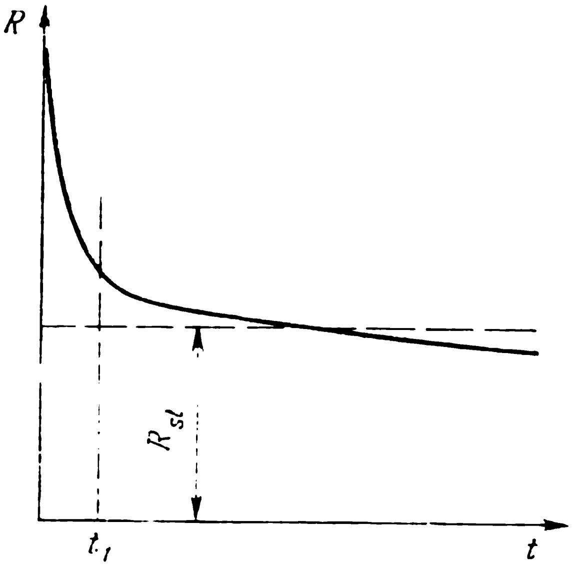

Fig. 8.26. Number R of recombining radicals in a specimen as a function of time

$$R(t)/R_0 = nV_0/R_0 - (m\beta/\alpha^2 \Delta T)\,[1 - c \exp(-t/\tau)] \tag{8.46}$$

where R_0 is the initial number of radicals in the specimen; n is the average concentration of trapped radicals at time $t = 0$; V_0 is the volume of the specimen; m is the volume density of the microscopic regions; $\Delta T = T_2 - T_1$ is the temperature rise of the outer wall of the specimen initially at temperature T_1; $\alpha = (T_0 - T_2)/(T_2 - T_1)$; T_0 is the melting point of the matrix material; τ is the characteristic time defined as

$$\tau = \pi^{-2} a^{-2} [(2/d^2) + (1/l^2)]^{1}$$

(a is the temperature conductivity, β is a numerical coefficient varying with the cryoscopic properties of the matrix material, and c is a numerical coefficient which can be found by solving the equation for thermal conductivity and equal to about 0.5).

The fast loss of radicals ceases after the temperature at all points of the specimen has risen to T_2. In Fig. 8.26, this time is labelled as t_1. At $\Delta T \approx 25$ K and $\tau \approx 30$ s, t_1, as found by Eq. (8.46), is about 40 s. Unfortunately, there are no reliable data on the kinetics of radical recombination during the initial periods of time.

At $t > t_1$, the loss of radicals takes place under isothermal conditions owing to their diffusion in the solid. Now the rate of loss is considerably lower than during the initial period, and the transition from recombination under non-isothermal conditions to recombination under isothermal conditions is perceived as the kinetic cessation of radical recombination (the stationary concentration corresponding to a step in the kinetic curve is designated as R_{st} in the plot of Fig. 8.26). The shape of the radical loss curve relating the concentration of radicals to time is decided by the rate at which the specimen attains an equilibrium phase state corresponding to T_2 after an abrupt change in temperature, rather than by the kinetics of radical recombination itself. Thus, the structural kinetic model offers a plausible explanation for the kinetic cessation of reactions proceeding under conditions of relaxation of the sample.

Naturally, the character of trapped species depends on the chemical and physical nature of the system under study, temperature, and the type of radiation used. The trapped species and the irradiation products of primary processes are distributed in the specimen nonuniformly. The microscopic regions with increased concentrations of such species and products possess physical and chemical properties different from those of the specimen as a whole prior to and after irradiation. Among other things, irradiation products usually have a lower molecular mass than the starting reactants, and it should be expected that the melting point of the microregions will be substantially lower than that of the specimen.

In studying the behaviour of reactive species in solids, it is important not to overlook the following. The microscopic regions surrounding the trapped radicals have substantially different properties than the matrix prior to irradiation. The yield of radicals in the microscopic regions with the new structure will differ from their yield in the regions of the solid not yet damaged by irradiation. Thus, one must reckon with the fact that the processes observed in these regions of the solid will differ in both mechanism and effectiveness. Notably, it should be expected that there will be an increase in the yield of the newly formed radicals (owing to a decrease in the cage effect) in the radiation-damaged regions, that is, where trapped radicals already exist.

This approach explains the increased probability of radical formation near the already existing ones, and, as a consequence, the increase in their rate of loss with increasing radiation dose, and other experimental facts. In view of the foregoing, we can explain qualitatively the high energy yield for the loss of radicals (in reference [34], page 347, the reader will find that the number of peroxide radicals lost in PTFE and polypropylene per 100 eV of energy absorbed by these radicals alone is 5×10^3), the low virtual activation energies, and nearly the same rate constants for radical loss in various substances (reference [34], p. 346). The process in question can be expected to change the manner in which the kinetics of radical accumulation depends on radiation dose, and this has been observed experimentally [608, 609]. This also throws light on the formation of recombination products, including those formed directly in the solid phase (for example, the formation of ethylene glycol upon irradiation of methanol [610]).

At present, only macrokinetic aspects have been elucidated on the basis of the structural kinetic model for multicomponent frozen systems. It is important to conduct further studies on the relation between the structure and phase state of a system, on the one hand, and the rate constant, on the other, and to evaluate quantitatively the effect that various factors (such as the migration of inclusions, history, thermodynamic and kinetic factors) have on chemical transformations in frozen solid matrices. These problems are all of important theoretical and practical significance. Experiments with chemical and biochemical reactions at low temperatures will expand our knowledge about the mechanism of chemical transformations under extremal conditions, suggest new approaches to controlled chemical synthesis, and offer a means for predicting conditions for the preservation of medical and biochemical materials, and foodstuffs.

CHAPTER NINE

BIOCHEMICAL REACTIONS AT REDUCED AND LOW TEMPERATURES

Low temperatures have long been used to slow down reactions and to preserve food for extended periods of time. Recent years have seen an increased interest in the long-term storage and preservation of simple and complex biological material and living organisms. This interest has above all been stimulated by the needs of medicine, notably in the wake of advances in hypothermia and cryothermia. At present, international banks have been set up for organs and biological preparations such as used, for example, in organ and tissue transplantations. Of course, this cannot but run into difficulties. For example, if biological material is to be preserved for a long time (months or even years), it must be completely frozen and cooled to liquid nitrogen temperatures which are beyond the capabilities of conventional refrigerators and freezers. Also, biological material, even a simple one, can be destroyed by freezing. The main cause of its loss is physical damage to the cells by ice crystals forming inside them and by the chemical reactions induced by changes in concentration and temperature. These difficulties can be circumvented through the use of cryoprotectants, such as glycerine, ethylene glycol or dimethylsulphoxide. With their aid, it has been possible to accomplish prolonged reversible preservation of biological material such as leucocytes, sperm, marrow, and cartilage. Work is under way on methods of reversible preservation for the more complex biological systems and even organs.

Obviously, it is impossible to cover in a single chapter all matters related to cryobiochemistry, the more so that purely biological applications of low temperatures lie outside the scope of this monograph. The reader may refer to specialized publications, such as [611] and [612]. We shall only dwell on the chemical and physico-chemical aspects of cryobiochemistry.

For the low-temperature preservation of biological material to be solved successfully, it is essential to get insight into the mechanism of biochemical processes occurring at reduced temperatures.

Studies have shown that living organisms can adapt themselves to low temperatures by synthesizing increased amounts of cryoprotectants — mainly polyatomic alcohols, above all glycerine [611, 613]. The function of cryoprotectants basically consists in that they bring down the freezing point of solutions, so that, on freezing, water does not turn to ice crystals. In addition to the already mentioned glycerine, ethylene glycol and dimethylsulphoxide, some inorganic salts may likewise act as cryogenic protectors. For example, sodium acetate at $5M$ concentration brings down the freezing point of an aqueous solution to —18.5°C.

When added to a solution, a cryoprotectant prevents some unwanted processes and controls the progress of the desired biological processes, for example enzyme activity.

Nature has seen to it that the cryoprotectants that form in living organisms capable of adaptation to low temperatures are not toxic and leave the organism in due time. With man-made cryoprotectants used for low-temperature preservation, this must be provided for by the experimentor.

It is important that enzyme activity should change reversibly on cooling and that enzymes should not be denatured in storage. It has been found that some organic compounds can control the activity of enzymes at normal and reduced temperatures [614]. For example, sugars can act as cryoprotectants by preventing the denaturation of enzymes in storage. Obviously, this and other tasks make it essential to investigate the activity of enzymes in liquid and frozen solutions at low temperatures.

Studies on biochemical processes at low temperatures, apart from giving insight into their mechanisms, help to detect and examine reactive intermediates. If a process goes on in several stages, which is typical of enzymic processes, and at a sufficiently low temperature, it can be arranged so that the process in question will come to a stop at the stage yielding the intermediate of interest [615].

In investigations concerned with the mechanism of low-temperature biochemical reactions, it is important to know how the physico-chemical properties of the system change with decreasing temperature. Unfortunately, there are no systematic data about the dielectric constant, viscosity, conductivity, pH value, and other physico-chemical properties even for the most commonly used solvents at present.

9.1. PHYSICO-CHEMICAL PROPERTIES OF ORGANO-AQUEOUS SOLVENTS AT LOW TEMPERATURES

Enzyme solutions that do not freeze at low temperatures are usually prepared by using a mixture of organic solvents and water. The organic diluent controls the dielectric constant, viscosity, and ionic strength of solutions [616] and enzyme activity. Practically nothing is known about these effects at low temperatures, because in an experiment it is difficult to model variations in only one of the physico-chemical variables of the system, especially variations in the rate of enzymic reactions with temperature.

It is only recently that Douzou and his associates [616-624] have investigated the dependence of the physico-chemical variables of such mixed organo-aqueous solvents on composition at low temperatures. Let us sum up, at least in brief, what is known about variations in the physico-chemical variables of mixed solvents at low temperatures and about the effect of these variations on enzyme activity in such solvents.

It has been found that the physico-chemical properties of mixed organo-aqueous solvents change substantially with decreasing temperature. The figures that follow refer to a mixture of water, ethylene glycol, and methanol taken in various proportions at two temperatures [624]:

Proportion (by volume) of water, ethylene glycol, and methanol	2:2:1	2:1:1	4:1:5	3:1:6
T_f, °C	−71	−50	−69	< −80
Dielectric constant:				
at −30°C	48	34	19	14
at −50°C	195	145	69	42
Viscosity, Pa s $\times 10^{-3}$				
at −30°C	79.1	82.2	76.2	70.2
at −50°C	88.3	91.9	85.5	79.3
Density, g cm^{-3}.				
at −30°C	1.04	1.02	0.96	0.94
at −50°C	1.07	1.04	0.99	0.98

It is seen that the viscosity of the mixtures increases with decreasing temperature so that near the freezing point it may be by several orders of magnitude higher than the viscosity of water under normal conditions. In a first approximation, the viscosity is a linear function of the inverse temperature. High viscosity might impede the normal diffusion of the substrate, change the life time of enzyme-substrate complexes, and thereby affect the reaction rate.

If enzyme activity is to be preserved, it is important that the dielectric constant of the medium should be close to its value in water under normal conditions (for pure water at +20°C, it is 80), and the enzyme molecule should be in a conformation characteristic of its native state. The dielectric constant of mixed organo-aqueous solvents is markedly lower under the same conditions, but it increases with decreasing temperature (in a first approximation, as a linear function of $1/T$). Because of this, it is possible to model in mixed organo-aqueous solvents a macroscopic dielectric constant close to its value in aqueous solutions under normal conditions.

What follows are the temperatures of water-methanol mixtures at which the dielectric constant is 80, and also the freezing points, T_f, of the mixtures [624]:

Composition, % (by volume)	30:70	40:60	50:50	60:40
T, °C	-80	-45	-30	-20
T_f, °C	-115	-90	-55	-35

However, the maintenance of the dielectric constant in mixtures equal to its value in aqueous solutions is not in itself sufficient for many proteins to retain their native conformation essential for the preservation of enzyme activity. Even in a water-methanol mixture having a dielectric constant of 80, it has been observed that some enzymes, such as dehydrogenases and reductases, are irreversibly inhibited. On the other hand, other enzymes, such as trypsin, α-chymotrypsin, aminotransferases and peroxidases, retain a high level of enzymic activity even in mixtures for which the dielectric constant differs substantially from 80. This behaviour is also characteristic of mixtures of glycerine and water.

The activity and stability of enzymes strongly depend on the activity of protons in the solution. As important is the ionic strength of the solution. Organic diluents and decreasing temperature bring down the degree of ionization of electrolytes, and this leads to reduced solubility and reduced proton activity. The solubility of weak acids and bases in the above water-methanol mixtures near their freezing point is about a mere $10^{-2}M$.

Strong electrolytes, such as hydrogen chloride, are in a fully dissociated state in water-methanol mixtures containing up to 70% (by weight) of methanol, down to their freezing point [618]. Sodium chloride at a concentration of 1×10^{-2} M is fully dissociated down to —80°C in a solution containing 44% (by weight) of methanol, whereas at a concentration of $1\times10^{-1}M$ this is so only down to —50°C [619]. Sodium and potassium iodides dissolve more readily in mixed solvents than sodium chloride. They can be utilized to secure the desired ionic strength over a broad temperature range.

At pH close to pK in systems used in the preparation of buffer solutions and containing weak electrolytes and their salts, the same changes have been noted as in strong electrolytes. The virtual pH values of solutions and the actual index of activity for protons, pa_{H^+}, at low temperatures can be measured spectrophotometrically, with the aid of suitable indicators.

The manner in which the proton activity, pa_{H^+}, of buffer solutions ($c_b = 1\times10^{-2}M$) changes with decreasing temperature and in various mixtures of water, ethylene glycol, and methanol can be seen from the figures given below [624].

2:2:1 Mixture (proportion by volume)

T, °C	+20	0	−10	−20	−30	−40
pa_{H^+}						
tris-buffer	8.05	8.65	9.00	9.30	9.70	10.15
phosphate buffer	7.45	7.45	7.45	7.45	7.50	7.50

2:1:1 Mixture (proportion by volume)

T, °C	+20	0	−10	−20	−30	−40
pa_{H^+}						
tris-buffer	8.40	9.05	9.35	9.70	10.05	10.55
phosphate buffer	7.85	7.90	7.90	7.95	8.00	8.05

As measured in water at +20°C, the pH values were 8.0 and 6.5 for tris- and phosphate buffers, respectively. It is to be noted that the pa_{H^+} of the tris-buffer is strongly dependent on temperature, being a linear function of $1/T$. As the temperature is brought down from +20° to —50°C, pa_{H^+} increases by two or three units in such weak electrolytes as tris- and glycine buffer solutions. As is seen from the above tabulation, the value of pa_{H^+} for the phosphate buffer solution varies according to the composition of organo-aqueous mixtures, but does not practically depend on temperature. Interestingly, a reduction in temperature brings about an increase in the proton activity of borate buffer solutions; this is, in all probability, related to the polymerization of boric acid. This has been utilized to protonize purine polynucleotides at low temperatures [620]. Processes leading to variations in the dissociation constant and pH are temperature-reversible, which means that the pH of a medium can be controlled by varying temperature, without changing the chemical composition of the system.

9.2. ENZYME ACTIVITY AT REDUCED TEMPERATURES

Reduction in temperature and freezing usually lead to a reduction in enzyme activity in the system. For some yet unknown reason, reactions involving xanthinoxidase and D-amino acid oxidase are fully retarded at —20°C. However, this retardation is reversible, and enzyme activity can be restored by warming up and dilution with water. This behaviour of oxidases cannot be interpreted in terms of a simple increase in the viscosity of organo-aqueous solutions. In some cases involving the same mixtures, other enzymic reactions with nearly the same activation energies would proceed at a considerable rate even at —60°C. Retardation can be attributed to the change in the activation energy with decreasing temperature. It may be due to changes in the solvation of enzyme molecules with decreasing temperature, and also to the formation of clusters around the active centre of a protein or to changes in the conformation of the protein leading to irreversible inactivation. Reversible inactivation has been observed at ordinary temperature and can explain the gradual decrease in enzyme activity with the addition of an organic solvent [625].

The joint effect of solvents and temperature on enzyme activity may take some other forms. For example, enzyme activity can be brought down by an increase in the interaction between water molecules and substrates owing to the formation of hydrogen bonds. A similar result can be produced by the association of enzyme molecules into polymer forms with decreasing temperature owing to a build-up of van der Waals forces, as exemplified by the insoluble cryogenic forms of globulins [625].

It has been found that enzymes consisting of several subunits are markedly less stable in organo-aqueous mixtures than catalase, peroxidase, and similar enzymes each consisting of a single polypeptide chain. Irreversible inactivation of enzymes consisting of several subunits is, in all probability, due to the incomplete re-association of previously dissociated subunits as the system goes back to normal conditions. The dissociation and re-association of subunits occurring under the action of an organic solvent and freezing may lead to the appearance of polymer forms not possessing enzymic activity. For example, the freezing of solutions of two electrophoretically individual forms of lactodehydrogenase, followed by melting in the presence of sodium chloride, results in the production of five different forms. Organic solvents like ethylene glycol, propylene glycol, glycerine or dimethylsulphoxide, when added to a solution, will completely inhibit the production of such forms and, except propylene glycol, promote the preservation of enzyme activity [626, 627]. As a rule, the solubility of the substances, including enzymes and substrates, decreases with decreasing temperature even in the presence of organic solvents. Nevertheless, it is often sufficient to have not very high concentrations of substrates in order to detect intermediates at low temperatures, because a decrease in temperature brings about an increase in stationary concentrations [615, 628]. It is important, however, to check if the intermediates thus detected are the same as exist under normal conditions, because the pathway of the process may have changed. The activity of enzymes found in biomembranes and fixed to lipids falls off as they are transferred to aqueous buffer solutions. It is known, for example, that cytochrome P-450 is inactivated when extracted into an aqueous solution (this is also accompanied by functional changes) [629], but remains in its native state and reactive with respect to lipids. For such enzymes to retain activity, it is important that they should remain in the conformation in which they are found in the membrane. The activity of such enzymes can be enhanced by diluting the aqueous buffer solutions with organic solvents which bring down the dielectric constant of the solution. In order that some enzymes (such as those extracted from mitochondria) may function normally, the addition of phospholipids is a must [629].

Noguchi and Freed [630] have been able to dissolve membrane enzymes in organo-aqueous solutions at low temperatures without recourse to the generally practised method of solubilization involving the use of detergents, by causing micelles to form in aqueous solutions. Upon removal of the lipid components at —75°C, the protein remained in its native state and retained its activity. Thus, enzyme activity is not lost at low temperatures in solvents like mixtures of chloroform and methanol, and this opens up an opportunity for studying membrane proteins.

Freed and Sack [631] describe several analytical operations, such as homogenization, centrifugation, chromatographic separation, extraction, and some others, performed on biochemical preparations of brain tissue at low temperatures (between —35° and —196°C). Their results show that biochemical analysis of tissue at low temperature is quite feasible and enables the experimentor to study the mechanism of biochemical processes, as it yields a direct information less distorted by secondary processes.

One of the crucial problems in biochemistry at present is the behaviour of polyenzymic organized systems. Studies are under way on the hydroxylating polyenzymic system from microsomes from a rat's liver in membrane structures, and attempts are being made to include some enzymes in synthetic polypeptide aggregates soluble in organo-aqueous solutions at low temperatures [632]. In the latter case, investigations can be conducted in a homogeneous and clear medium, so that spectroscopic measurements can be made.

Temperature perturbation spectroscopy [633] and solvent perturbation [634] have successfully been applied by Hui Bon Hoa [635] and Guinand *et al.* [636] to the study of the conformation state of β-lactoglobulin at low temperatures. They have been able to show that the molecule of β-lactoglobulin contains two types of tryptophan residues differing in their surroundings and detected spectroscopically at 306 nm and 296 nm. The ionization constant for one of the tryptophan residues noticeably varies with temperature, which, in the authors' opinion, is caused by a charged group next to the chromophore and the increase in the dielectric constant of the medium with decreasing temperature. From a comparison of the effect that thermal perturbation has on differential spectra of the protein and model compounds, it has been found that there are two ordinary tryptophan residues located on the surface of the β-lactoglobulin molecules and accessible to the solvent. The above examples show that low-temperature studies can yield valuable information about the structure of proteins.

It is a well known fact that the activation energy for some enzymes in aqueous buffer solutions at temperatures considered normal for biological material (0 to 40°C) increases with decreasing temperature, so that there is a break in the Arrhenius relation at certain temperature [637, 638]. A similar departure of the reaction rate from the Arrhenius relation has also been found for some enzymic reactions at low temperatures [639]. A plot of the rate constant for the oxidation of guaiacol by hydrogen peroxide, with peroxidase as catalyst, as a function of temperature [625] is shown in Fig. 9.1

A detailed discussion of the physical aspects of enzymes will be found in [640] and [641]. The rationale of the main concept is that the kinetics of enzymic reactions may fail to obey the Arrhenius equation. Supposedly, the conformational relaxation of the enzyme-substrate complex is an essential elementary act of an enzymic reaction and that the rate of product formation is decided by the rate at which its conformation is re-arranged.

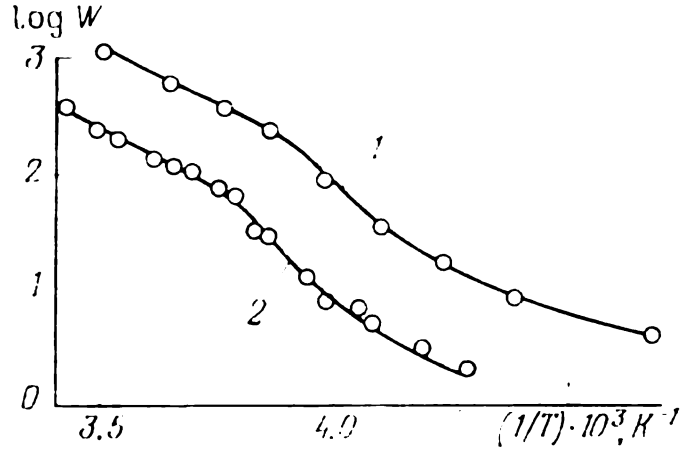

Fig. 9.1. Arrhenius relations for the rate W of oxidation of guaiacol ($2\times10^{-3}M$) by hydrogen peroxide ($2\times10^{-3}M$) catalyzed by peroxidase (E) [625]:

(1) in a mixture of aqueous buffer solution (p^aH^+6) and methanol (40: 60 by volume); $[E]=10^{-6}M$; (2) in a mixture of aqueous buffer solution (p^aH^+6) and ethylene glycol (50: 50 by volume), $[E] = 6.7\times10^{-8}M$

The activation energies can change and the reaction rates can depart from the Arrhenius law also, as has been shown in [642], in consequence of changes in the physico-chemical properties of the system with temperature. The effect of temperature on the activation energy and entropy has been studied on the hydrolysis of *p*-nitrophenylacetate in such a way that the likely effect of changes in the conformation of the enzyme was excluded.

The respective plots of the reaction rate as a function of temperature in the interval from 0 to 40°C for phosphate and tris-buffer solutions appear in Fig. 9.2. As is seen, the activation energy for phosphate buffer solution is 57 kJ mole^{-1}, and for tris-buffer solution, 13 kJ mole^{-1}. This discrepancy in activation energy between different buffer solutions arises from the different effect of temperature on the pH value of the medium.

The activation energy as given by the Arrhenius equation is practically always an effective quantity and, in addition to the direct contribution by the temperature dependence of the reaction rate, it contains the contribution by the temperature-dependent variations in many variables of the system, directly or indirectly affecting the kinetics and thermodynamics of the reaction. Among them are changes in the phase state of the system and its heat capacity in the course of the reaction, the shift in the acid-base and other equilibria in the system leading to changes in the concentrations of reactants (ions, molecules) [643], pH value of the medium, p*K* of ionogenic groups, and dielectric constant.

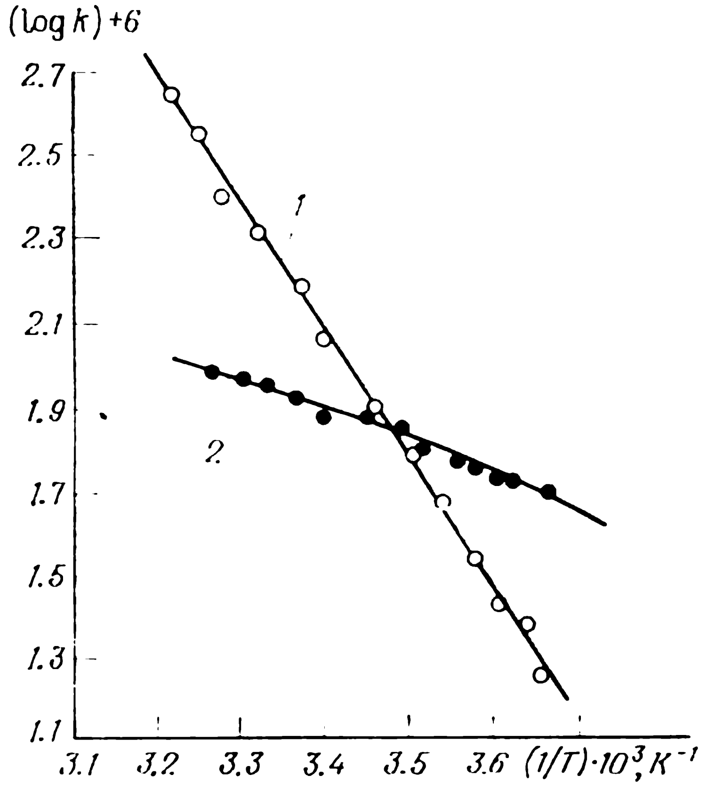

Fig. 9.2. Rate constant for the hydrolysis of *p*-nitrophenylacetate (*p*-NPA) in (*1*) 0.1*M* phosphate buffer solution and (2) 0.1*M* tris-buffer solution as a function of time {[*p*-NPA] = 1 × × 10^{-4} *M*, 5% (by vol.) dioxane, 20°C, $pH_{1,2}$ 8.0}

Consider the effect of temperature on the experimentally found activation energy. Let E_{exp} be the activation energy as found from the temperature dependence of the experimental rate constant, k_{exp}, as given by the Arrhenius diagram. This value of activation energy is utilized to determine the experimental enthalpy, $\Delta H^{\ddagger}_{exp}$, and experimental entropy, $\Delta S^{\ddagger}_{exp}$, of the activation. Let E_0, $\Delta H_0^{\ddagger}$, and $\Delta S_0^{\ddagger}$ be the activation variables solely dependent on the chemical nature of the reactive species. The values of E_{exp}, $\Delta H^{\ddagger}_{exp}$, and $\Delta S^{\ddagger}_{exp}$ found in an actual experiment in the liquid phase are only approximate estimates of E_0, $\Delta H_0^{\ddagger}$ and $\Delta S_0^{\ddagger}$. The degree of discrepancy between the experimental and true activation variables depends to a large extent on how correct the experimentor is in estimating the effect of the temperature-dependent variables of the medium on the reaction kinetics. With allowance for the contribution by changes in the temperature-dependent properties of the medium, *i*, the experimental activation energy may be written

$$\begin{aligned} E_{exp} &= -2.3R\frac{\partial \log k_{exp}}{\partial(1/T)} - 2.3R\sum_i \frac{\partial \log k_{exp}}{\partial i}\,\frac{\partial i}{\partial(1/T)} \\ &= E_0 - 2.3R\sum_i \frac{\partial \log k_{exp}}{\partial i}\cdot\frac{\partial i}{\partial(1/T)} \end{aligned} \tag{9.1}$$

It is seen from Eq. (9.1) that the extra term appearing on the right-hand side in addition to E_0 may cause E_{exp} to be greater or smaller than E_0. The term $2.3R\sum(\partial \log k_{exp}/\partial i)\,[\partial i/\partial(1/T)]$ may exceed E_0 in absolute value, in which case the reaction will have a negative temperature coefficient. In the general case, the term $\sum(\partial \log k_{exp}/\partial i) \times [\partial i/\partial(1/T)]$ is temperature-dependent, and this will inevitably lead to a departure from the Arrhenius law.

The contribution of the temperature-dependent variations in the properties of the medium to E_{exp} is responsible for the fact that the activation enthalpy is, too, temperature-dependent:

$$\Delta H^{\ddagger}_{exp} = \Delta H^{\ddagger}_0 - 2.3R \sum_i \frac{\partial \log k_{exp}}{\partial i} \cdot \frac{\partial i}{\partial(1/T)} \tag{9.2}$$

As a consequence, the value of $\Delta S^{\ddagger}_{exp}$ as found from k_{exp} and $\Delta H^{\ddagger}_{exp}$ is different from that obtained upon correction. In a series of experiments conducted under varying conditions of the reaction, the unaccounted-for contributions by the temperature-dependent variations in the properties of the medium may lead to the so-called compensation effect. The point is that using an exaggerated activation enthalpy as compared with the true one, the computation would result in an exaggerated activation entropy as well. If, in another experiment of the series, the temperature-dependent variations in the properties of the medium lead to a decreased value of $\Delta H^{\ddagger}_{exp}$ compared with $\Delta H^{\ddagger}_0$, the computation would yield a decreased value of $\Delta S^{\ddagger}_{exp}$, because these terms enter the equation for the reaction rate constant with opposite signs. In fact, experiments yield directly only the rate constant. Thus, to determine the actual compensation, it is essential first to exclude the seeming balancing effect.

It is to be noted that the contributions by the temperature-dependent variations in the properties of the medium to E_{exp} depend on the values of the derivatives $\partial \log k_{exp}/\partial i$ and $\partial i/\partial(1/T)$ at fixed values of i and T. In other words, the narrowing of the temperature interval within which the activation variables are determined does not lead to a decrease in these contributions. As a consequence, for the effect of temperature on the activation energy for a given reaction to be determined correctly, it is important to know the temperature dependence of the properties of the medium and their effect on the rate constant. The literature gives only scattered data about the effect of various physico-chemical variables and their temperature dependence. Analyzed together, these data offer a quantitative evaluation of the contribution to the experimental activation energy by the temperature-dependent variations in the properties of the medium.

To evaluate $\partial \log k_{\mathrm{exp}}/\partial i$ in cases where the (i) variables are pH or pK values, recourse may be had to the Brönsted equations relating the reaction rate to pH and pK:

$$\log k = a\mathrm{pH} + b \quad \text{and} \quad \log k = a' \ \mathrm{p}K + b' \tag{9.3}$$

whence,

$$\frac{\partial \log k_{\mathrm{exp}}}{\partial \mathrm{pH}} = a \quad \text{and} \quad \frac{\partial \log k_{\mathrm{exp}}}{\partial \mathrm{pK}} = a'$$

The form of the temperature dependences of pH for buffer solutions is defined in [619, 644, 645]. Using them, we can readily determine value of ∂ pH/∂ (1/T).

Let us analyze experimental results, using Eq. (9.1). The rate constant for the hydrolysis of *p*-nitrophenylacetate strongly depends on the pH of the medium because, according to [646], $\partial \log k_{\mathrm{exp}}/\partial (\mathrm{pH}) = 0.8$. On the other hand, the pH value for tris-buffer solution varies markedly with variations in temperature. According to [619], $\partial \ \mathrm{pH}/\partial (1/T) = 2.3 \times 10^3$ pH K.

Then, using $E_{\mathrm{exp}} = 13$ kJ mole^{-1} for tris-buffer solution, we get from Eq. (9.1) that $E_0 = 45$ kJ mole^{-1}. According to [619], the pH value for phosphate buffer solution depends on temperature only slightly, so the contribution of $2.3R \sum_i (\partial \log k_{\mathrm{exp}}/\partial i) [\partial i/\partial (1/T)]$ to E_{exp} for the hydrolysis of *p*-nitrophenylacetate in phosphate buffer solution may be neglected. As is seen, $E_0 = 45$ kJ mole^{-1}, deduced with allowance for the contribution due to variations in the pH value for tris-buffer solution with temperature, is close to the activation energy for phosphate buffer solution, equal to 57 kJ mole^{-1}. The difference in E_{exp} between tris- and phosphate buffer solutions is due to the difference in the temperature dependence of the pH value in either case rather than the difference in their nucleophylic properties.

Analysis shows that the activation energy determined for tris-buffer solution is by 32 kJ mole^{-1} lower than E_0. The value of E_0 equal to 45 kJ mole^{-1} is close to that given in the literature for the alkaline hydrolysis of *p*-nitrophenylacetate (46 kJ mole^{-1}) [647, 648]. The activation energies for the aqueous, alkaline, acidic, and imidazol-catalyzed hydrolysis of *p*-nitrophenylacetate quoted in [647] respectively are 87, 46, 72, and 35 kJ mole^{-1}. In our opinion, the striking difference in activation energy is related to variations in the properties of the medium with temperature.

In order to obtain undistorted activation variables and to interpret them adequately, it is essential to take proper account of the temperature-induced variations in the properties of the medium and their effect on the reaction kinetics. In the case of enzymic reactions, this effect is far more noticeable, because the enzymes undergo changes in their conformational state.

9.3. FROZEN SOLUTIONS AND HYDRATION OF MACROMOLECULES

The water molecules directly surrounding macromolecules form a solvate shell. Their behaviour differs from that of water molecules in the bulk. The number of water molecules forming the solvate shell determines the degree of hydration of macromolecules and depends on the manner in which the macromolecules interact with water. Kuntz *et al.* [582], Kuntz and Brassfield [649], and Kuntz [650] have proposed to determine the degree of hydration of macromolecules from NMR (^1H) absorption spectra for the frozen aqueous solutions of the substances involved. They have observed relatively narrow (250-900 Hz) resonance absorption signals due to the water protons in the NMR spectra (60 MHz) of frozen aqueous solutions of proteins and nucleic acids at —35°C. They have found that for each gram of protein there was 0.3 to 0.5 g of water of hydration. Nucleic acids have been found to be two to five times more hydrated than proteins.

Several facts corroborate that the observed absorption signals are associated with water protons. For one thing, the signals decrease in intensity by more than 90% when H_2O is replaced by D_2O. For another, the chemical shifts in the signals are equal or close to that for water. Last but not least, the signal strength is too high for the signals to be assignable to protons capable of exchange in dissolved substances. The absorption line of ice proper is substantially wider than the observed signals.

The lack of a well defined freezing point for the fixed water is an indication that it has no well organized structure, although it is less mobile than liquid water. The activation energy for the temperature dependence of proton mobility is 17 to 21 kJ mole^{-1}, which is comparable with the energy of formation of one hydrogen bond [651]. For the sake of comparison, it may be noted that the activation energy in ice is 50 kJ mole^{-1} [652].

As is justly noted by Kuntz *et al.* [582], the crucial point is the nature of the fixed water. According to their hypothesis, the water detected on the basis of NMR spectra is not included in the ice lattice. In their opinion, one can visualize a state in which water does not freeze to ice. Water chemically or physically adsorbed on a surface freezes at a lower point. A similar effect may exist in frozen solutions of macromolecules where a thin film (probably, a monolayer) of water separates the solute from the ice. This film or layer may reflect the form of the macromolecule. Such water might be held by hydrogen bonds or reside in regions where the normal structure of ice is disturbed by “hydrophobic” interactions. The existence of a film of liquid water on the ice surface at subzero temperatures has been demonstrated by Kiselev *et al.* [653] and Ushakova [654].

Kuntz *et al.* [582] and Kuntz [650] have investigated the hydration of polypeptides and their conformation in frozen aqueous solutions by NMR (^1H) techniques at temperatures down to —60°C. In our opinion, experimental data that can be obtained by this method are not directly related to the quantity of water of crystallization if the latter is taken to mean the water immediately surrounding the molecules of biopolymers. Rather, these data characterize the phase inhomogeneity of frozen biopolymer solutions.

A method for determining the degree of hydration of macromolecules on the basis of calorimetric data for frozen solutions is examined in [174].

9.4. PHOTOCHEMICAL PROCESSES IN FROZEN BIOPOLYMER SOLUTIONS

The disclosure of mechanisms by which mutations occur in biologically important molecules such as nucleic acids is of paramount importance and hardly needs any further justification.

Mutations, for example, occur when DNA is exposed to UV radiation. In order to elucidate the mechanism underlying the photodimerization of purine and pyrimidine bases in DNA [655, 656], Varghese [657] has investigated simpler model systems. Pisarevsky *et al.* [658] have studied the mechanism by which thymine dimers are formed in aqueous solutions frozen to liquid-nitrogen temperature upon UV irradiation. The photochemical reactions of nucleic acid bases, including thymine, depend on the presence of diluents in frozen solutions, whose effect has not yet been fully elucidated. For example, the presence of naphthalene ($1.5 \times 10^{-4} M$) in a frozen aqueous solution of thymine ($3 \times 10^{-3} M$) causes an increase of 15% in the yield of dimers, whereas the presence of acetone ($5 \times 10^{-4} M$) under the same conditions causes the yield to decrease by about 75%. According to Pisarevsky *et al.*, the photodimerization of thymine involves the singlet state of thymine, and the observed sensibilization and inhibition of dimer yield are due to the respective effects of naphthalene and acetone on that state.

Unfortunately, Pisarevsky *et al.* have analyzed their results without allowance for the structure of the frozen solutions. In our opinion, the photodimerization of nucleic acid bases and of their derivatives in frozen solutions actually proceeds by the same mechanism as in the liquid phase, and all the anomalies observed during experiment are caused by the structural and phase inhomogeneity of the frozen solutions. Freezing causes the dissolved molecules to move closer together. This, among other things, explains the increase in dimer yield upon freezing [657-659].

The presence of additions markedly affects the phase inhomogeneity of frozen solutions. This effect depends on the physical and chemical properties of the additions. If an addition and water form a vitrifiable mixture, there will be no increase in the concentration of the dissolved bases, and the dimer yield will decrease. An addition which dilutes the bases in the microphase and increases its volume will bring down the dimer yield if it does not possess sensibilizing properties as well. In our opinion, the phase inhomogeneity of frozen solutions explains the decrease in the dimer yield in frozen water-alcohol (1:1 by volume) solutions [658, 659] in which the alcohol acts as a diluent, and also the noticeable luminescence of the thymine in such solutions in contrast to aqueous solutions. Varghese and Wang [660] have shown that frozen aqueous solutions of thymine even carry microcrystals of thymine whose structure has been investigated by X-ray diffraction analysis.

Irradiation of frozen solutions of nucleic acid bases may bring about the formation and trapping (for example, at liquid-nitrogen temperature) of the intermediates which undergo transformation during the subsequent warm-up. That the formation of intermediates may take place is borne out by the fact [661] that the fluorescence due to the thymine dimer is observed during the subsequent warm-up rather than directly during irradiation at —196°C.

Studies on the photochemistry of nucleic acids and their components, including frozen solutions, are reviewed in [662] and [663].

The structure of biopolymers in the crystalline state is often difficult to investigate at low temperatures. The freezing of individual protein crystals presents a big problem, because the expansion of the water of crystallization during the phase change from water to ice will, as a rule, break up the crystal. To avoid this, Thomanek *et al.* [664] have proposed to freeze cachalot's myoglobin crystals at a hydrostatic pressure of 250 MPa. Their method is based on the fact that at a pressure of 210 to 350 MPa ice exists in two phase states known as ice III and ice IX. As water changes to ice III, there is a decrease rather than an increase in volume as happens with ordinary ice (ice I) when freezing takes place at atmospheric pressure.

Crystal growth from appropriate solutions has widely been used in practice [665]. For example crystals of L-asparagine have been grown from ethyl alcohol ($T_m = —117.3$°C). Recently, marked progress has been recorded in the production of enzymes and enzyme-substrate complexes in crystalline forms at low temperatures [666]. X-ray diffraction studies on enzyme-substrate complexes will undoubtedly give better insight into the action of enzymes [667].

It is of considerable interest to be able to carry out chemical reactions in frozen, high-pressure specimens, and to investigate the kinetics of such reactions. To these authors' knowledge, such studies have not yet been attempted.

9.5. BIOCHEMICAL PROCESSES AND STABILIZATION OF DYNAMIC BIOPOLYMER CONFORMATIONS IN FROZEN SOLUTIONS

Knowledge of the general pattern of various chemical and biochemical reactions at reduced temperatures, notably in frozen aqueous solutions, is of both theoretical and practical interest. The reactivity of proteins is mainly investigated in conditions close to those existing in living organisms. Studies of enzymes under extremal conditions are important for a better insight into the mechanism involved in their activity and changes in their specificity.

The hydroxylaminolysis of cytosine, acetylcholine, glutamine, asparagine, 2,5-diketopiperasine and esters of glycerine, serine, thyrosine, phenylalanine and glutamic acid in frozen aqueous solutions has been investigated by Grant and Alburn [488]. At —11, —18 and —23°C, the reactions have been found to proceed faster than in liquid solutions at +1°C. In the investigators' opinion, the speed-up of the reactions in frozen solutions can be rationalized on the basis of the catalytic action of solid surfaces. Basing himself on his own work and the published data, Grant [668] believes that structured water may likewise serve as catalyst in biological systems.

According to Grant and Alburn [585], structural analogues inhibit the nonenzymic hydroxylaminolysis of esters of amino acids which are substrates in the enzyme-catalyzed reaction.

The kinetics of the peroxydase oxidation of quinol phosphates by hydrogen peroxide in frozen aqueous solutions has been investigated by Sergeev *et al.* [591-593]. The nonenzymic oxidation of quinol phosphates in the liquid phase has been studied in detail by Sergeev and Batyuk [669].

It has been found that the activity of peroxydase decreases with increase in both the number of freeze-thaw cycles and the duration of stay in the frozen state. For example, eight consecutive freeze-thaw cycles have caused an enzymic solution to lose about 40% of its original activity, and a 10-hour stay of a frozen enzymic solution at —10°C has halved its activity under the experimental conditions.

A comparative study on the kinetics of oxidation of 2,3-dimethyl-1,4-naphthohydroquinol-1-phosphate by hydrogen peroxide in the presence of peroxydase has been carried out in the temperature interval from —25°C to 30°C. A plot of the reaction rate as a function of temperature for liquid and frozen solutions is shown in Fig. 9.3. As is seen, in frozen solutions at —17°C the rate of the reaction is 20 times that of the reaction in the liquid phase at 0°C. Thus, the enzymic reaction proceeds in ice, and it shows a negative temperature coefficient [592]. The acceleration of enzymic hydrolysis had been observed earlier by Grant and Alburn [477].

A study on the relation between the reaction rate and the concentration of peroxydase and hydrogen peroxide has shown that the direct proportion between the two variables is retained in both liquid and frozen solutions down to —17°C. In the investigated interval of hydrogen peroxide concentrations (from 1.8×10^{-5} to $4.2 \times 10^{-4} M$), the rate of the reaction in solutions frozen at —17°C has been found to remain practically constant.

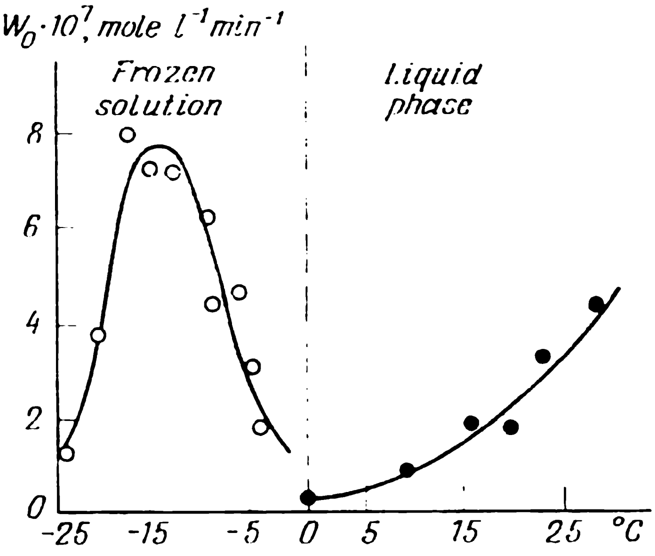

Fig. 9.3. Initial rate W_0 for peroxidase oxidation of 2,3-dimethyl-1,4-naphthohydroquinol-1-phosphate (DNQP) by hydrogen peroxide in water and ice ($[E] = 7.5 \times 10^{-9}$ M, $[DNQP] = 2.5 \times 10^{-5}$ M, $[H_2O_2] = 3.5 \times 10^{-5}$ M, $[NaCl] = 0.1 M$, pH 7.0)

Figure 9.4 shows plots relating the reaction rate to the concentration of the substrate in liquid and frozen solutions. As is seen, there is a good deal of difference between the plots for 2,3-dimethyl-1,4-naphthohydroquinol-1-phosphate in the liquid phase at 23.5°C (curve *1*) and in frozen solutions at —17°C (curve *2*).

The increase in the activity of enzymes in frozen solutions and some other manifestations of an unusual kinetic behaviour can be rationalized on the basis of the structural kinetic model suggested in Chap. 8. The reaction mixture contains a diluent (a buffer, NaCl) whose concentration is many times that of the remaining solutes. The volume of the liquid microinclusions is decided by the properties of the solvent, the temperature of the experiment, and the concentration of the diluent. In the circumstances, the concentration factor may be written as

$$\beta = (T_0 - T)/(\Delta[D]) \qquad (9.4)$$

where T_0 is the freezing point of the neat solvent, T is the temperature of the experiment, Δ is the cryoscopic constant of the solvent, and [D] is the concentration of the diluent.

Introducing the concentration factor, β, in the Michaelis-Menten equation yields an expression which, according to the model, must describe the rate of a simple, two-stage enzymic reaction in a frozen solution in the presence of the diluent:

$$W = \frac{k_2\,[\mathrm{E}]\,[\mathrm{S}]}{\{K_m\Delta[\mathrm{D}]/(T_0 - T)\} + [\mathrm{S}]} \tag{9.5}$$

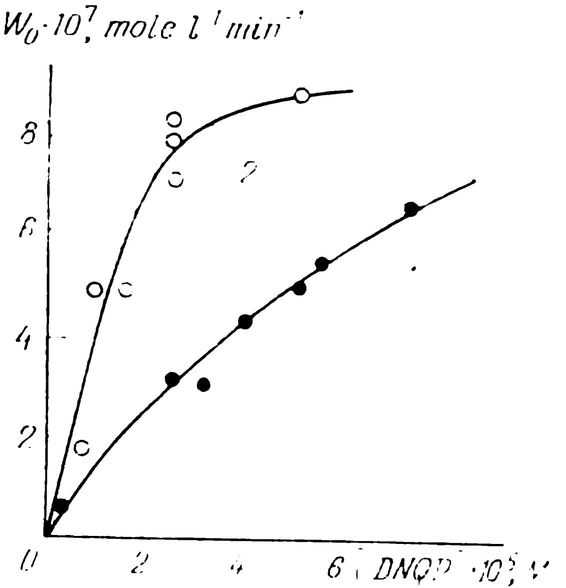

Fig. 9.4. Rate of peroxidase oxidation of 2,3-dimethyl-1,4-naphthohydroquinol-1-phosphate by hydrogen peroxide as a function of its concentration in liquid and frozen solutions at various temperatures ($[\mathrm{E}] = 7.5\times10^{-9}M$, $[\mathrm{H_2O_2}]=3.5\cdot10^{-5}M$, $[\mathrm{NaCl}]=0.1M$, pH 7.0): (1) 23.5°C; (2) —17°C

where K_m is the Michaelis constant, [E] is the concentration of the enzyme, and [S] is the concentration of the substrate. Alternatively,

$$W = k_2[\mathrm{E}]\,[\mathrm{S}]/K'_m + [\mathrm{S}]$$

where

$$K'_m = K_m\Delta\,[\mathrm{D}]/(T_0 - T)$$

It is seen from Eq. (9.5) that the two-stage enzymic reaction in frozen solutions must formally be described by the Michaelis scheme using another constant, K'_m, adjusted for the degree of concentration of the reactants.

The following scheme is proposed by George [670] for the action of peroxydase:

$$\mathrm{E} + \mathrm{H_2O_2} \xrightarrow{k_2} \mathrm{E_I} \tag{9.6}$$

$$\mathrm{E_I} + \mathrm{AH_2} \xrightarrow{k_3} \mathrm{E_{II}} + \dot{\mathrm{A}}\mathrm{H} \tag{9.7}$$

$$\mathrm{E_{II}} + \mathrm{AH_2} \xrightarrow{k_4} \mathrm{E} + \dot{\mathrm{A}}\mathrm{H} \tag{9.8}$$

$$2\dot{\mathrm{A}}\mathrm{H} \xrightarrow{kd} \mathrm{AH_2} + \mathrm{A} \tag{9.9}$$

where k_2, k_3, k_4, and k_d are the reaction constants for the individual stages; E_I and E_{II} are compounds I and II, that is, peroxydase in various states of oxidation; AH_2 is the oxidized substrate (S) which in this case is 2,3-dimethyl-1,4-naphthohydroquinol-1-phosphate; and A is the oxidation product which in this case is 2,3-dimethyl-1,4-naphthoquinone.

Let us extend the scheme to include the sorption of the H_2O_2 molecule on the active centre of peroxydase:

$$E + H_2O_2 \underset{k_{-1}}{\overset{k_1}{\rightleftarrows}} E \cdot H_2O_2 \tag{9.10}$$

Let $k_1 \gg k_2$ and $k_2 > k_3 > k_4$, and introduce

$$K_S = [E]\,[H_2O_2]/[E \cdot H_2O_2]$$

Applying the method of stationary concentrations to E_I, E_{II}, and $E \cdot H_2O_2$ and analyzing kinetically the scheme extended to include the stage (9.10) with allowance for the degree of concentration β, we obtain the following expression for the reaction rate in ice:

$$W = \frac{2k_4[E]\,[DNQP]}{1 + k_4/k_3 + (k_4/k_2)\,[DNQP]\left(\dfrac{T_0 - T}{\Delta[D]} + \dfrac{K_S}{[H_2O_2]}\right)} \cdot \frac{T_0 - T}{\Delta \cdot [D]} \tag{9.11}$$

The freezing of solutions and a reduction in their temperature slow down the reaction according to the Arrhenius equation. On the other hand, the solvent is frozen out and the reactants are concentrated in liquid inclusions. It is the competition between these two conflicting factors that makes extremal the temperature dependence of the reaction rate in frozen solutions. A shift in the position of the maximum on the temperature dependence with increasing concentration of the diluent (NaCl) occurs because in reactions involving several consecutive stages the diluent affects both the reaction rate and the position of the maximum on the temperature dependence plot.

The effect that the concentration of solutes has on the reaction rate in frozen solutions becomes still more pronounced with the addition of substances that depress the activity of the enzyme. It has been found that 0.1*M* and 0.5*M* concentrations of methanol do not practically affect the rate of the peroxydase oxidation of 2,3-dimethyl-1,4-naphthohydroquinol-1-phosphate by hydrogen peroxide at 25°C in the liquid phase. In ice at —17°C, the presence of 0.1*M* and 0.5*M* methanol brings down the reaction rate by a factor of 2.6 and 8.7, respectively. The reaction is slowed down mainly owing to the inactivation of the enzyme.

The concentration effect is not the only factor that introduces peculiar effects in the reaction kinetics at low temperatures. No analysis of kinetic data can be complete without considering the temperature-induced variations in the physico-chemical properties of the medium and of the solutes. A decrease in temperature has a marked effect on the dielectric constant and viscosity of the medium [616], the pH value of buffer solutions and the pK value of ionic groups in the substrates and enzymes [619]. Naturally, these variations cannot but affect the reaction rate. Precisely these factors are responsible for the change in the general aspect of the pH dependence of the reaction rate at —17°C in comparison with the same relation for the liquid phase at +25°C (Fig. 9.5).

In the general case, variations in the physico-chemical properties of the medium and reacting molecules with temperature will also affect the temperature dependence of reaction rate and rate constant, thereby causing a departure from the Arrhenius law. A study [592] on the temperature dependence of the rate of the peroxydase oxidation of 2,3-dimethyl-1,4-naphthohydroquinol-1-phosphate by hydrogen peroxide in the liquid phase has shown that some departure from the Arrhenius relation can be caused not only by the temperature-induced variations in the properties of the medium, but also by the difference in temperature coefficient between the intermediate stages of oxidation. In the case of multistage reactions, the difference in temperature may be responsible for a change in the contribution that each stage makes to the overall effect [671].

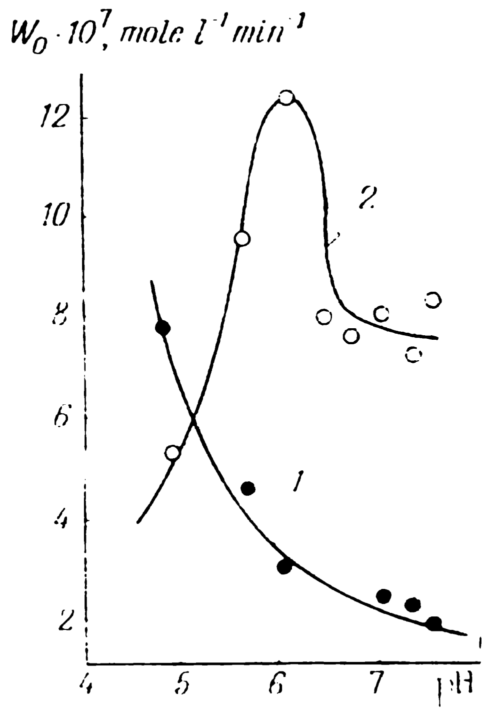

Fig. 9.5. Effect of pH of the medium on the rate of peroxidase oxidation of 2,3-dimethyl-1,4-naphthohydroquinol-1-phosphate by hydrogen peroxide in (*1*) the liquid phase at 25°C and (*2*) in ice at -17°C ($[E]=7.5\times10^{-9}M$, $[DNQP]=2.5\times10^{-5}M$, $[H_2O_2] = 3.5\times10^{-5}M$, $[NaCl] = 0.1M$)

(The acceleration of enzymic reactions in ice is interesting from the view-point of understanding the mechanism by which enzymes act under extremal conditions.) Reactions of micellar catalysis have been found to proceed with ease in frozen solutions [594]. A similar effect related to additional structurization may well have played an important part in the origin of life on the Earth.

Another interesting example is the increased rate of polymerization of hydrogen cyanide in dilute aqueous solutions at —10° to —22°C described in [672]. The polymerization proceeds with the formation of a tetramer, $H_2NC(CN)C(CN)NH_2$, which, when UV-irradiated and reacted with HCN, changes to adenine. In this way, an important component of DNA is produced in a dilute solution of HCN upon freezing under conditions that might exist on the Earth at the time when life originated.

The physical concept of the mechanism by which enzymes act has already been mentioned in discussing the causes for the departure of the reaction rate from the Arrhenius equation [640]. Given low temperatures and rigid matrices, the conformational states of macromolecules, labile under normal conditions, can exist for a long time and they can be observed by spectroscopic methods. Blumenfeld *et al.* [673-675] have been able to observe nonequilibrium states for several hemo-containing proteins by reducing them with solvated electrons produced by radiolysis of protein solutions in a water-ethylene glycol matrix at 77 K.

The study reported in [673] and carried out in the visible region of the spectrum, has been concerned with variations that occur in the spectra of cytochrome C at 77 K in water-ethylene glycol (50%) glasses gamma-irradiated from a Co-60 source. In the opinion of Blumenfeld *et al.*, their hypothesis seems to be corroborated by the pulse radiolysis of aqueous solutions of cytochrome C investigated in [676] and [677].

In [673], the investigators have attempted to "trap" a nonequilibrium conformation of cytochrome C in which, as they believe, the protein resides immediately after it has been reduced by electrons. The investigators have recorded absorption spectra for the frozen solutions of oxidized cytochrome C and of irradiated solutions in which cytochrome C was reduced by electrons. For comparison, they have also recorded spectra for the frozen solutions of cytochrome C chemically reduced at normal temperature in the liquid phase (in a pH7 solution of sodium ascorbate). As has been found, the spectra of electron-reduced cytochrome C in a rigid matrix at 77 K differ from the reference spectra as regards the position of absorption bands. In some cases, the shift was as large as 6 nm. It is to be noted that the absorption spectra of the chemically reduced cytochrome C did not change upon irradiation, and the differences that were observed reversed with a change in temperature.

Available evidence favours the hypothesis by which conformational changes play a decisive role in the mechanism of enzymic catalysis. In principle, the differences observed by Blumenfeld *et al.* in the absorption spectra may well be caused by some other factors, such as variations in the properties of the medium with temperature and their nonequivalence in the compared specimens. It is relevant to mention the investigators' reference to an unpublished report where the character of the observed differences is attributed to the nature of protein, the composition and pH value of the solutions used.

In [674], Blumenfeld *et al.* cite data about hemoglobin. The experimental technique was the same as they used in [673]. The experiments were conducted on human hemoglobin. The investigators have come to the conclusion that the reduction of methemoglobin by gamma-generated electrons in a frozen solution leads to the formation of an active centre in the reduced low-spin ferro-state which is unusual for hemoglobin. As Blumenfeld *et al.* believe, this non-equilibrium state arises because the iron of hemoglobin is reduced under conditions such that the structure of the active centre and of the protein as a whole cannot change. Warm-up to room temperature brings about relaxation, and the hemoglobin returns to the equilibrium state.

We have thus seen that biochemical processes at reduced temperatures show a peculiar behaviour in many respects. Some biochemical reactions can take place even at very low temperatures. Studies on the behaviour of biochemical systems at low temperatures provide better insight into their functioning. Work in this direction will help to solve problems of long-term cryopreservation of biological material in the future.

CHAPTER TEN

APPLICATIONS OF LOW TEMPERATURES IN SCIENCE AND ENGINEERING

Knowledge accumulated to date about low-temperature chemical reactions has laid foundation for cryochemistry — a new and rapidly expanding science.

Now that various reactions have been implemented and others have been stimulated by low temperatures, the task to be achieved next is to develop an appropriate technology. In some cases, low temperatures can drastically change the properties of materials. This chapter quotes examples of how low temperatures can be put to use in various fields of science, engineering and economy in general. Mention is made of the yet unresolved problems of practical interest.

In chemistry, low temperatures offer a means for trapping and studying reactive intermediates. In this connection, it is interesting to cite Gordon *et al.* [678] who have used an original technique to produce high stationary concentrations of nitrogen atoms ($> 1.6\%$) stabilized in superfluid helium (at 1.5 K). According to their estimate, the activation energy for recombination is 0.4 kJ mole^{-1}. It has not yet been possible to obtain such concentrations of reactive species by condensation on a cooled substrate and by exposure of specimens to penetrating radiations. Upon irradiation, the concentration of reactive species has been found to be by an order of magnitude lower, being a few tenths of one per cent. It has also been found that the recombination of nitrogen atoms is an activation process with a low activation energy. These findings add more substance to the concepts which have served as a basis for a theory describing the trapping of reactive species in solids.

Of late, helium temperatures and matrix isolation have been gaining ground in the synthesis and study of species unstable under normal conditions. Matrix-isolated condensates are thermodynamically nonequilibrium systems and, as a consequence, various processes can occur in them.

Using argon matrix isolation and IR spectroscopy, Serebryanikov [679] has detected unusual boron compounds of the BO_2 type and some oxide compounds of other metals.

In such investigations, it is important to know how low the temperatures can be at which particular reactions can still proceed with a measurable rate and how such systems behave at low temperatures. An attempt to answer these questions has been made by Bos and Howe [680] who have studied the diffusion and reactivity of SnO, Sn_2O_2, Sn_3O_3, and other SnO-based polymer molecules trapped in a solid nitrogen matrix. According to them, SnO and, though less, Sn_2O_2 are sufficiently mobile down to 34 K. At this temperature, as they have found, the coefficient of diffusion for SnO in the crystalline modification of nitrogen, $\alpha = N_2$, ranges between 1×10^{-20} and $4 \cdot 10^{-20}$ $m^2\,s^{-1}$, which is the same as for Sn atoms in $\alpha = N_2$ at 34 K, found earlier. At around 34 K, the prevalent process has been found to be the reaction of SnO with SnO-based polymers, because the activation energies for the reactions

$$2SnO \longrightarrow Sn_2O_2 \text{ and } SnO + Sn_2O_2 \longrightarrow Sn_3O_3$$

are non-zero, and they are inhibited at this temperature.

There is a good deal of interest in studies concerned with tunnel transitions as they must play a prominent role at low temperatures. Unfortunately, no direct experimental verification of tunnelling (notably for heavy species) in low-temperature reactions has been obtained yet. Studies in this field, along with investigations of electric conductivity under conditions of low-temperature chemical reactions, are of value to the manufacture of superconducting materials [681].

Low-temperature polymerization is another promising and industrially important direction in cryochemistry. Using the gamma-induced radical polymerization of butylmethacrylate in the presence of zinc chloride [682] and the polymerization of methylmethacrylate in the presence of orthophosphoric acid, H_3PO_4 [683], Georgiyev *et al.* and Garina *et al.*, respectively, have shown that the introduction of complex-forming agents, such as protonic and aprotonic acids, in monomers stimulates radical polymerization at low temperatures by the "living chain" mechanism which is characteristic of ion polymerization. When conducted at low temperatures, polymerization by the "living chain" mechanism shows an abrupt decrease in the rate of bimolecular termination.

In low-temperature polymerization, the gamma-irradiation of crystalline acrylonitrile leads to the oriented propagation of polymer chains. To explain this anisotropic polymerization, Kotin *et al.* [684] have advanced an interesting idea of an unequal partition of energy among the degrees of freedom of the crystal. The addition of a monomer molecule to the propagating chain apparently occurs at a faster rate than the re-arrangement of the lattice near the propagating chain.

Using a combination of low temperatures and high pressures, Yenikolopov *et al.* [685] have been able to polymerize compounds nonpolymerizable under normal conditions.

Research in the field of low-temperature polymerization has raised quite a number of urgent problems. No conclusive evidence has yet been obtained in support of the mechanisms proposed for low-temperature polymerization and based on the concepts of cooperative transfer of energy and excitation. A great number of yet unclear facts await their interpretation. Among other things, it is unclear why the yield of products depends to a marked degree on the phase state. For example, it is different for alkyl halides irradiated in the glassy and the polycrystalline state [686]. It is yet to be explained why the radiation polymerization of *n*-alkyl-*n*-vinylsulphonamides gives a greater yield in the solid than in the liquid phase or why irradiation at 198 K can induce polymerization in the crystalline state and cannot in the glassy state [687]. Nor is it yet understood why minute quantities of impurities produce a disproportionately strong effect on processes in the solid phase.

Studies on the chemical reactions induced in multicomponent systems by light and other radiations have shown that the yields of products are often other than additive. To explain this and other anomalies, it is customary to have recourse to the hypothesis of free valence and excitation transfer.

Irradiation produces various species, and the originally single-component system (for example, a single crystal of an individual chemical compound) becomes multicomponent in the regions where radiation has interacted with matter. In matrices, regions appear, consisting of tens or even hundreds of molecules. The properties of such regions cannot be described in terms of phenomenological variables related to the macroquantities of the condensed phase or within the framework of the generally accepted formalism, whereas their determination from molecular characteristics is a formidable task indeed.

Shpolsky *et al.* in the 50s have demonstrated that, although in the liquid phase at normal temperatures complex molecules may produce smeared, structureless spectra, they will give quasi-line, well-defined spectra in solid matrices at low temperatures [688, 689]. The physical foundations of the phenomenon are examined in [688], but an unambiguous explanation is still lacking. A very important fact, as we believe, is that quasi-line spectra can only be observed at certain temperatures and that structured spectra for each of the compounds can only be produced in certain solvents.

A problem common to all investigators concerned with low-temperature chemical reactions is that most of the physico-chemical variables applying to low temperatures have not yet been defined or, less so, evaluated. This, above all, holds for the solid phase. Among such variables are the pH value, dielectric constant, and others.

In tackling many problems, it is most fruitful to take into account not only the chemistry of a given process, but also the effect of the phase state of the system. Even today we know very little about the structure of multicomponent systems at low temperatures, notably when they are exposed to the action of various physical agencies, including radiations.

The joint action of low temperatures and other physical factors, such as radiations, on a system offers an especially versatile tool for changing the properties of materials and for initiating various chemical processes.

In reference [690] it is shown that the frost resistance of low-density polyethylene can substantially be improved by irradiating it with 2 MeV electrons. The investigators attribute this improvement to two causes. For one thing, already at low doses irradiation produces an increased number of "through" chains owing to the formation, in the amorphous regions, of cross-links between the chains reaching into the amorphous regions from the neighbouring crystalline ones. For another, heavy doses of irradiation cause the formation of a skeleton of cross-links, predominantly in the amorphous regions.

Special promise is held out by studies on the behaviour of various systems under the joint action of low temperatures and high and very high pressures. Before such studies can become a practical proposition, it will be necessary to resolve a number of fundamental difficulties and to tackle complex engineering problems. For example, very low temperatures complicate the transfer of hydrostatic pressure and render most substances brittle. These difficulties can be circumvented by applying a high pressure to the system of interest at moderate temperature and then to freeze the system. As has been found, this technique leaves the stress distribution in the compressed medium almost unaffected. Very often, experiments at low temperatures can be conducted under a quasi-hydrostatic pressure.

Adadurov *et al.* [691] summarize the results of pioneer experiments in which impact compression is applied to liquefied and frozen gases and solids at low temperature, in order to bring about chemical transformations. Experiments of this kind are important, for example, to the production of metallic hydrogen. Such experiments are described in [692] and [693].

Adadurov *et al.* [691] have also been concerned with the preservation, after impact compression, of liquefied gases, frozen gases and liquids, and their mixtures and solutions containing various substances at $T_0 = 77$ K. The preservation of gases in the original condensed state after impact compression poses a very difficult problem. Apparatus has already been developed which permits gaseous and solid products to be preserved after impact compression to a pressure of up to 6×10^4 MPa in the case of a planar loading system, and solid products after an impact compression to a pressure of about 1×10^5 MPa in the case of a cylindrical loading system. Some of the results are discussed below.

A mixture of gaseous, anhydrous HCl and C_2H_2 taken in a 1:1 proportion and condensed in a vacuum at 77 K was impact-compressed to a pressure of 6×10^4 MPa by a planar loading system. The products were analyzed gas-chromatographically in a column filled with silica gel at 80°C. The main gaseous product of the chemical decomposition of the HCl-C_2H_2 mixture was methane. Apart from methane, there also formed a solid carbon residue — finely divided carbon black carrying a considerable proportion of fixed chlorine.

A mechanical mixture of solid carbon dioxide and powdered niobium with a grain size of 50 μm was impact-compressed at 77 K to a pressure of 1×10^5 MPa by a cylindrical loading system. X-ray diffraction analysis showed the presence of niobium carbide in the solid product.

A 1.05% solution of polyacrylamide in water was impact-compressed by a cylindrical loading system to a pressure of 2.5×10^4 MPa at 173 K. The characteristic viscosity of the solution and the molecular mass of the starting polyacrylamide were 0.48 and 5×10^4, respectively. The impact compression had raised these characteristics to 1.3 and 2.3×10^5, respectively. Analysis of the polyacrylamide in an electron microscope showed an increase in the size of the globules.

It may be hoped that the work commenced on converting impact compression to isoentropic compression will permit starting materials to be heavily compressed with a low temperature rise owing to the low initial temperature, T_0. Then experiments will in effect be carried out under nearly isothermal conditions, and it will be possible to compress large volumes of materials to a pressure of 1×10^5 MPa and even higher [691, 694].

A reduction in temperature and a change in the phase state of a system entail changes in practically all properties of that system. The change is especially pronounced when the system passes from one phase state to another.

Cryochemical investigations offer a better insight into the behaviour of substances at low temperatures and for improving the properties of materials. For example, cryogenic quenching at rates of 10^5 or 10^6 degrees per second imparts metal alloys with extremely unusual properties [695-697]. Also, low temperatures can be used to turn out semiconductor materials possessing high service qualities [698].

The hypothesis that low-temperature chemical reactions in solids proceed predominantly on structural defects is being confirmed in many fields. From a consideration of the activation energy for the migration of grain boundaries in metals, Osipov [699] concludes that thermal activation for the migration of grain boundaries in pure metals is analogous to local melting, that is, local amorphization of crystals in certain activated volumes. Interestingly, it was detected that the melting point of indium present in a finely divided state is depressed by several tens of degrees.

By maintaining suitable conditions, it is possible to produce amorphous states for substances that normally exist in the crystalline state. Condensation of water vapours onto a metal surface cooled to low temperatures produces amorphous solid water [700]. It can serve as a convenient object in developing and testing models, because it can be investigated experimentally under conditions in which the effects due to the thermal excitation of molecules and their statistical distribution are well separated. Comparative studies on the reaction kinetics in crystalline ice and amorphous solid water can help with the understanding of the mechanism involved in solid-phase processes and the part played by the phase state of the matrix.

It is of important practical interest to combine the action of low temperatures and mechanical factors on substances. The ensuring processes lie in the domain of mechanochemistry. It has been demonstrated that mechanical agents can produce radicals in most various systems [701]. A far more attractive case, however, is where a sudden change in temperature and the transition of a system from the liquid to the solid state produce mechanical stresses. If, upon freezing and thawing, a system undergoes a chemical transformation, it is often said that cryolysis has taken place, usually attributed to the action of mechanical factors [701, 702]. This statement is valid if it is proved that no reactions other than associated with mechanical factors take place at low temperatures.

Phase changes, like solid-to-solid transitions, are related to mechanical stresses which can lead to chemical transformations, such as in the case of the beta-to-alpha transition in solid methanol (at 157.8 K). The cooling of solid methanol during its beta-to-alpha transition causes it to decompose with the formation of hydrogen, carbon monoxide, and methane. Also, the transition is accompanied by the break-up of large crystals of beta-methanol to grains of alpha-methanol, and by light emission [703]. It has been shown that both the chemical decomposition and the light emission are mainly caused by electric discharges occurring near the surface of the crystals during the phase transition. On the basis of the above findings, a mechanism for the decomposition of methanol during the phase transition has been proposed [703]. It is to be noted that the degree of decomposition during the phase transition is low ($< 10^{-5}\%$).

In view of the low thermal effect of the beta-to-alpha transition (710 J mole^{-1}), the investigators rationalize the fairly high intensity of triboluminescence by assuming that a considerable amount of energy stored up in the form of stress energy is apparently released in methanol during the phase transition.

Chemical reactions may probably be initiated by cracks and tears forming at the vertices and propagating with the mechanical destruction of crystals or grains in nonequilibrium states. This idea has been advanced in [704], and the detection of gaseous products upon the decomposition of $NaNO_3$ seems to corroborate it [705].

Interestingly, Hochstrasser and King [706] believe that photochemical reactions in solids at low temperatures may selectively favour molecules having a particular isotope composition. For example, by exposing *sym*-tetrazine, $C_2N_4H_2$, in benzene at low temperatures (1.6-10 K) to the beam of a narrowband tunable laser, they have been able to photolyze selectively the $C_2N_4H_2$ molecules containing ^{12}C and ^{14}N isotopes according to the reaction

$$C_2N_4H_2 \xrightarrow{h\nu} N_2 + 2HCN$$

In this way the percentage of ^{13}C and ^{15}N isotopes in the product was substantially increased over the natural figures. By conducting photolysis in a matter of a few minutes, the remaining $C_2N_4H_2$ molecules were enriched in ^{13}C and ^{15}N by a factor of 10^4. It is noted in [706] that the photolyzed products naturally have an increased content of the respective isotopes. The isotopic selectivity of photolysis is traced to the selective optical excitation of the molecules carrying a particular isotope. Thus, the joint use of low temperatures and highly monochromatic radiation can reveal an exceedingly small difference in energy between molecules of the same chemical compound built from various isotopes of the same element. The isotopic selectivity of photochemical reactions at low temperatures can be utilized for the isotope enrichment of compounds, including labile ones, and for studies on the mechanism of photochemical processes. The photochemical synthesis of isotope-enriched chemical compounds may prove a paying proposition already in the near future.

UV-induced low-temperature chemical reactions play an important part in the stratosphere. According to Rowland [707], chlorine atoms and ClO radicals enter into chain reactions with ozone in the upper atmosphere. In the stratosphere, chlorine atoms are produced by the action of light on freons finding their way there as a result of diffusion of industrial wastes. The chain reactions involving ozone tend to break up the ozone blanket performing an important protective function in the atmosphere.

Cryochemistry can also tackle some problems facing space chemistry. As will be recalled, interstellar matter accounting for 10% of all mass in the Galaxy consists of compact, cold gaseous clouds (with a number density of 10 particles per cubic centimetre or more and a kinetic temperature of less than 100 K), which are surrounded by a hot rarefied gas (with a number density of 2 particles per 10 cm^3 or less and a kinetic temperature of more than 1 000 K). Also, interstellar matter includes more massive "dark" and "black" clouds whose kinetic temperature is very low and whose density is appreciably higher. Knowledge of what is going on there is important because these clouds give birth to stars and hold the overwhelming majority of the molecules existing in interstellar space [708].

Interstellar space is filled with various radiations. As regards chemical transformations in space, it is UV radiation with a wavelength of over 91.2 nm that is most important, because it is responsible for both the formation and decomposition of molecular products in the interstellar space and black-body radiation at 2.7 K. In the absence of other interactions, notably collisions, this radiation controls the local thermodynamic equilibrium of molecules.

Investigations of interstellar space have detected various radicals (for example, $\cdot$OH) and organic compounds (for example, formic acid, methyl alcohol, and formamide) [708].

Proper understanding of the chemical processes taking place in the Universe cannot be obtained without conducting related studies in the laboratory. In particular, this is true of studies on low-temperature processes in the gaseous and heterogeneous phases. Special importance is attached to investigations into the chemical behaviour of molecules under nonequilibrium conditions which are characteristic of not only space processes, but also all radiation-induced processes.

Some aspects of molecule formation and decomposition in interstellar space are taken up in [708] which also sums up some laboratory studies. The formation of molecules and radicals has been observed in the gaseous phase and on the surface of solid forms (grains) whose temperature was usually below 50 K.

Among other things, the kinetics and rate of molecule formation on grains are discussed in [709]. It is likely that highly reactive radicals are trapped in ice grains. Local warm-up by cosmic space or light quanta may initiate a chain reaction involving such radicals, leading to the break-up of the entire grain with the likely formation of complex organic molecules.

Low temperatures are gaining more and more ground in the chemical industry. Undoubtedly, the number of low-temperature chemical processes will keep growing as time passes by. At present, wide use is made of liquid-nitrogen cooling of adsorbents used in gas purification. For example, cryogenic gas purification is employed in ammonia synthesis. Cryogenic scrubbing of nitrogen and hydrogen used in ammonia synthesis was first used commercially in the USSR and abroad in the early 60s. As will be recalled, the catalysts used in ammonia synthesis are readily poisoned by minute amounts of impurities. In the USSR, the hydrogen used for ammonia synthesis is ordinarily produced by the high-temperature conversion of natural gas. In addition to hydrogen, the products of this conversion contain impurities in the form of various saturated and unsaturated hydrocarbons. Among them, ethylene, acetylene, allene, propane and other similar compounds may account for 1.0 to 0.01 cm^3 per cubic metre [710]. The nitrogen used for ammonia synthesis is taken from air, and it contains various impurities, too, mainly in the form of nitrogen oxides such as NO, NO_2, and N_2O_3. Cryogenic scrubbing in liquid-nitrogen-cooled towers freezes out the impurities and improves both the capacity of the catalysts and the yield of ammonia.

At some factories outside the USSR, cryogenic scrubbing has been accompanied by explosions. Inquiries have shown that explosions can be set off by the cryogenic reactions of nitrogen oxides with unsaturated compounds which accumulate in the system in the course of scrubbing. The reactions leading to such explosions commence as the pieces of equipment are warmed up for their clean-outs. The findings of the inquiries have served as a basis for recommendations on the prevention of explosions [710].

At present, the chemical reactions used commercially are expected to meet ever-growing requirements for selectivity. These requirements can be satisfied by low temperatures because they offer a means of selection on an energy basis and can raise the yield of chemical end products. The use of low temperatures is especially advantageous in reactions having relatively low activation energies. Some processes can be stimulated by low temperatures. This is true, above all, of halogenation and hydrohalogenation of olefins, addition reactions, and cyclodimerization of α-oxides. Undoubtedly, the field of application for cryogenic reactions will be expanded still more before long.

Special promise is held out by studies on the low-temperature reactions of diene synthesis, the Friedel-Crafts reaction, and insertion reactions. It is particularly important to combine low temperatures with complex formation. Molecular complexes whose concentration usually increases with decreasing temperature affect the reactivity of the reacting molecules. They make it possible to produce substances whose synthesis by other paths is either expensive or unfeasible at all. The range of chemical processes which basically take place at low temperatures is continually extended. Special significance is attached to the cryogenic production of various organometallic compounds and the use of low temperatures in the processes involving such compounds. Some of such reactions are described in [711].

Recently, dihalides of inert gases have been obtained by photolysis at 16 K, using a mercury-arc lamp and an argon laser [712]. In some cases, the gas mixture had been passed through a microwave discharge prior to condensation. The following dihalides of inert gases have been obtained: KrF_2, XeF_2, $XeCl_2$, and XeClF. The investigators have been able to identify the IR bands of $XeCl_2$ and XeClF and to detect the frequencies appearing in the Raman spectra for all the four compounds.

The use of low temperatures in the chemical and other industries has continuously been expanding with the growing scale of liquefied gas production. At present, liquid nitrogen has found an exceptionally wide use as refrigerant. In fact, it would be close to impossible to list all the fields where it is being used. There is a continuous increase in its use for the preservation of biological materials. Interestingly, it has been proposed to use liquid nitrogen in conjunction with a heat sink as fuel for propulsion [713]. This form of propulsion, it is believed, will not pollute the air at all. Its use is highly promising in cases where safety requirements are especially stringent, such as in mines. Liquid oxygen is being used on as large a scale, too. At the time of writing the world's consumption of liquid oxygen was estimated at about 400 000 tons a year. It is used to intensify combustion so as to obtain higher temperatures, and as refrigerant in the chemical and microbiological industries. Liquid oxygen is more readily available and less expensive than liquid nitrogen, but special care must be exercised in handling it. Because of this, it cannot be used in some cases at all. In the future, the use of liquid oxygen in low-temperature chemical processes will undoubtedly be extended because it can act as both a refrigerant and a reactant. Liquid neon is used as refrigerant in cases where the temperature need not be below 27 K ($T_b = 27.2$ K). Neon is more convenient and safer to handle than, say, liquid hydrogen. Cryogenic liquids, too, are widely used in industry [714].

Liquefied natural gas (LNG) already now is being used as fuel. Undoubtedly, the scale of use will grow as it will gain more and more in value as a source material in chemical industry.

In the power-supply field, a very important part will be played by liquid hydrogen in the future. Hydrogen-burning engines will not pollute the environments, because the only product of hydrogen combustion is water. Apparently it will be more advantageous to use liquid hydrogen first as coolant for superconducting power transmission lines, then as a fuel. The large-scale consumption of hydrogen will undoubtedly entail radical changes in many chemical processes [713-715].

The use of low temperatures has been expanding in step with advances in facilities for their production. Naturally, it is stimulated by the fact that many processes are more economical to carry out at low temperatures than under ordinary conditions. In turn, the economy of a process depends on the cost of refrigeration which tends to rise with decreasing temperature.

The efficiency of refrigeration systems, expressed as the fraction of the ideal thermodynamic coefficient of performance (the Carnot coefficient) is a function of many factors, notably the working temperature T and the cooling capacity q. In such a case, the power requirement of a refrigerator, W_r, is given [96] by:

$$W_r = q(T_0/T - 1)/\eta$$

where η is the efficiency.

For present-day refrigerators, η is 0.1-0.3 at $T = 4.5$ K, from 0.2 to 0.4 at $T = 20$ K, and between 0.4 and 0.5 at $T = 80$ K [96]. Plots of the power requirement per unit cooling capacity at various temperatures are given in Fig. 10.1. Notably, it is seen from Fig. 10.1 that the total power requirement, W_t, decreases when electricity is transmitted at low temperature. It has been estimated that transmission of elecric power over an aluminium cable held at 20 K will reduce power losses by 90% [96].

The economic gain from the use of low temperatures also depends on the capital and running costs of refrigeration equipment. Reference [96] gives the following approximate relations which can be used in estimating the capital cost C of refrigerating plant according to the cooling capacity q (in kW):

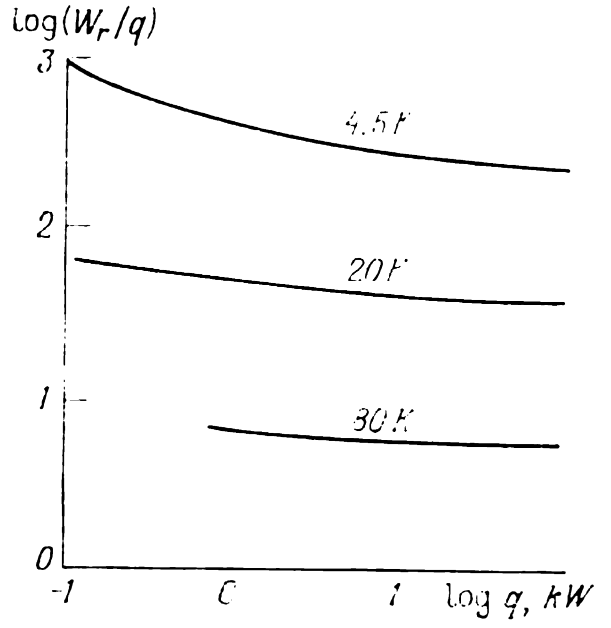

Fig. 10.1. Power requirement per unit cooling capacity as a function of cooling capacity at various working temperatures

— at $T = 80$ K: $\log C = -0.33 \log q + (0.5 \pm 0.3)$

— at $T = 20$ K: $\log C = -0.33 \log q + (1.45 \pm 0.3)$

— at $T = 4.5$ K: $\log C = -0.6 \log q + (2.25 \pm 0.3)$

The cost of refrigeration, R (per kWh), at various temperatures can be found from the relation

$$\log R = -1.5 \log T + 1.6$$

In evaluating the economic efficiency of various chemical processes at low temperatures, it is important also to take into account factors other than the cost of refrigeration. For example, low-temperature synthesis usually yields products of a very high purity making any subsequent refining unnecessary. Freedom from additional refining or preheating will more than offset the cost of cooling in many cases.

Low temperatures have substantially extended the capabilities of communication systems. Some of the outstanding discoveries recently made in radio astronomy have been made possible by the use of receivers operating under low-temperature conditions [715]. Also, low temperatures play an exceptionally important role in the operation of various systems on board space craft. The use of low temperatures in microwave communication equipment is discussed, for example, in [715] which also describes various types and designs of the cryostats used for the purpose.

The current trend is towards the use of progressively lower temperatures. Many fields of engineering are extending their use of liquid helium (its limited use to date has been due to its scarcity and high cost). Transition to helium temperatures opens up basically novel capabilities, notably the utilization of superconductivity in engineering [717].

Low temperatures are helpful in vacuum techniques. There are already cryogenic pumps which can build up an exceptionally high vacuum (about 10^{-13} Pa). Special promise is held out by adsorption cryogenic pumps which are simple in design and convenient to use.

Temperatures of a few kelvins or very close to absolute zero have come to be used for research purposes in metallography, optics, and many other divisions of science. A progressively increasing practical importance is gained by superconductivity discovered at the beginning of this century. Today it is successfully being used in many fields of research and practical applications, such as the controlled fusion (thermonuclear) reaction and MHD-generators. Superconductivity has served as the basis for many novel scientific instruments, such as high-resolution NMR spectrometers which substantially extend the capabilities of research workers. Advances in the chemistry and physics of low temperatures bring us closer to the advent of superconducting materials capable of operating at higher temperatures. Such materials will bring about a veritable revolution in engineering. The search for chemical systems in which fast reactions take place at low temperatures can go a long way towards achieving this goal.

Of special interest are systems in which charge-transfer complexes are formed. Research in this field will also bring in new materials for electron optics.

The radical changes in the physico-chemical properties of materials occurring at low temperatures hold out the promise of fundamentally new engineering implementation for even traditional processes. An example is comminution equipment (such as grinders and mills) operating with the aid of liquid nitrogen. They can produce finely divided, fluid and well-mixing powders from viscous and ordinarily elastic materials such as polymers, natural rubber, and various resins.

It is often difficult even to imagine how versatile low temperatures can be. In effect, they are frequently put to uses which might appear unexpected at first glance. It has been found among other things that paper that has been severely damaged by water can best be restored by freezing and subsequent sublimation of ice [716]. Low temperatures can successfully be used in a trade as ancient and traditional as fabric dyeing.

A discussion of the electronic and optical properties of various materials at low temperatures and instruments specifically designed for measurements and research in the field of low-temperature physics can for example be found in [717]. Large-scale research is under way on commercial methods for the desalination of seawater by freezing (see, for example [718]).

In practical activities, it is often important to take into account the effect of natural subzero temperatures occurring in winter or in permafrost areas. Soil congelation must for example be taken into account in construction, farming, and some other fields. Low temperatures have a complex effect on soil formation. It has been found, for example, that active oxidation processes [719] and the formation of various salts can take place in winter in the top layer of permafrost soil distinguished by temperature variations and lack of free water. Low temperatures can produce an unexpectedly strong accelerating effect on chemical and biological processes in biological material. It is a well-known fact, for example, that many biological processes occur at an increased rate in the littoral area of the northern seas and oceans, especially during transitions through zero degrees at the time of ice formation and thawing. Understanding of the processes occurring spontaneously in nature or accompanying man's activity is important for proper control of ecological equilibrium.

Low temperatures are widely used in agriculture, notably in animal husbandry to preserve the semen of some pedigree livestock. Noticeable advance has been made in the low-temperature preservation of semen in pigstry. Used in conjunction with artificial insemination, this offers an effective means for the faster and wider selective breeding of animal varieties, thereby enhancing the productivity of livestock.

There is one more example of an unusual application of low temperatures in farming. It has been found that the best way to brand animals is with a frozen rather than a white-hot iron. A "cryogenic" iron destroys hair roots without affecting the skin. As a result, the hair falls out, giving way to hair of a different colour.

Resistance to low temperatures is a valuable quality of any crops. If we learn the mechanism by which plants adapt themselves to cooling, we shall be able to cut down substantially the loss of crops in winter and to develop new, more frost-resisting varieties [720]. At present, a physico-chemical method for determining the frost resistance of plants (with reference to grapes) has already been developed, based on measuring the luminescence of the leaves at low temperatures.

It is hard to overestimate the importance of low temperatures for the food industry. Since their first use in 1918 when the first consignments of refrigerated meat were delivered to Great Britain from Australia, the scale of use for low temperatures has increased so much that this industry is simply inconceivable without refrigeration. Some aspects of food refrigeration and various relevant patents are described in [721] and [722]. The best approach to date has been to quick-freeze the products, as this leaves their nutritional qualities, vitamins, and flavour only slightly changed. It may be added that there is a growing tendency towards using ever lower temperatures. At present, household refrigerators with freezers capable of maintaining a temperature of about —20°C have become a commercial merchandise.

At present, there is no way of supplying man with food without resort to low temperatures. This will be even more so in the future. If food is to be distributed uniformly and if food supply is to be uninterrupted, it is vitally important to stock-pile foodstuffs and to have advanced methods for their storage and delivery. One approach to this problem is to preserve food at low temperatures [723]. Preservation methods currently in use are applicable to many kinds of food, but they are not free from drawbacks. A major limitation is that long cold storage impairs the quality of the stored foodstuffs. The impairment in flavour and nutritional quality is mainly the outcome of the undesirable chemical and biochemical processes that take place at low temperatures.

It is an urgent and commercially attractive task to produce concentrated fruit juices, notably from aqueous solutions, by freezing. This process yields a better product than distillation and osmosis. Examples are the production of coffee extract and apple juice [724]. A scheme for the concentration of aqueous solutions by freezing [724] is given below:

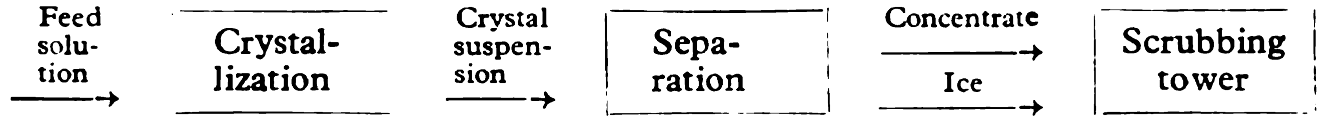

The scrubbing tower can practically separate all ice from the concentrate without any loss of volatile aromatic substances, with the solutes left in the waste liqour not exceeding one part in 10^4.

In biology and medicine, low temperatures are mainly used for the preservation of various biological materials and medical preparations [725, 726]. The most remarkable examples are the preservation of blood plasma and other blood components, mother's milk, and marrow.

A decisive contribution to the cryopreservation of blood and marrow has come from Soviet scientists. Owing to studies conducted mainly at the Institute for the Problems of Cryogenic Biology and Medicine and at the Central Institute of Hematology and Blood Transfusion, blood and marrow can now be cryopreserved for years and then used successfully for medical purposes [727, 728].

The advent of miniature cryogenic systems [729] provides a firm basis for the extensive use of low temperatures in medicine.

The cryopreservation of red blood cells is examined in [730]. The long storage of blood and other biological materials is possible only if all metabolic processes are brought to a practically complete standstill. As regards blood cryopreservation [728], this can be done by any one of two techniques already used under clinical conditions, namely: quick freezing in the presence of 15% (by volume) of glycerine as cryoprotectant at the final stage and storage in liquid nitrogen at 77 K, or slow freezing in the presence of 40% (by volume) of glycerine and storage at 203 K. The results are practically equally good in either case. It must be stressed, however, that there still remain unresolved problems related mainly to the retention of biological functions by the blood. One of the problems is how to extend the period, upon thawing, during which red blood cells can retain the properties they possess at 4°C. The point is that cryopreserved samples show an appreciable hemolysis (high-rate loss of hemoglobin, APT, and other compounds) which is an indication that irreversible processes occur during storage and, in all probability, mainly at freezing and thawing. Because of this, in transfusions clinics only use the blood unfrozen not more than 24 hours earlier.

Studies have shown that the freeze-thaw cycle does hidden damage to the membranes of blood cells, and this is the cause of rapid hemolysis [731]. Among other things, investigators have observed conformational changes of protein components, leading to a change in the permeability of the membranes. Fortunately, this damage to the membranes is not irreversible, so it can be hoped that the problem will be solved successfully. As already noted, to keep cells and tissue intact upon cryopreservation, resort is made to cryoprotectant agents, notably glycerine. However, it takes some time and effort to remove glycerine from the blood upon thawing. The simplification of the operation or, still better, the replacement of glycerine by some better cryoprotectant is another still unresolved problem. Other promising cryoprotectants are such compounds as polyvinylpyrrolidone and polyethyleneoxides answering the general formula $HO—CH_2(CH_2—O—CH_2)_nCH_2—OH$. They are stable, readily dissolve in water and organic solvents, and are of low toxicity [732]. At present, the search is under way for still better, mainly polymeric, cryoprotectants.

The rate of freezing and the presence of cryophylactic agents have a marked effect on the survival of bone tissue and the differentiation and multiplication of cells [733]. Studies on animals have shown that hypothermia can prolong the state of clinical death [734], which is extremely essential to successful reanimation. Using dimethylsulphoxide and bull's albumin from plasma as cryoprotectants, a technique has been developed for storing mitochondria from rat's liver in solutions frozen at liquid nitrogen temperature [735]. Mitochondria act as power plants in the cell and are complex biological species. The prolonged storage of mitochondria without detriment to their ultimate functioning has been a major achievement.

A successful attempt to deep-freeze man's lymphocytes is described in [736]. It has been found that if the cells are to survive super-fast freezing, they must be maintained at an intermediate temperature of about —26°C for some time. This enables the cells to adapt themselves to the action of unfavourable factors at freezing and thawing. The mechanism of this adaptation is still to be discovered. In our opinion, when the cells are maintained at an intermediate temperature, they enter into exchange reactions with the surroundings, which leads to a relative equilibrium. In the meantime, the cells are partly dewatered and the concentrations of various substances (above all, salts) in the surroundings and the cells are equalized. As a result, the cells turn out better prepared for exposure to abrupt freezing and the subsequent thawing. Studies on the effect of various factors on the behaviour of cells at freezing are discussed, for example, in [726, 727, 737, 738].

Studies in the field of cryobiology will help in the future with solving the problem of long-term anabiosis for mammals and man. Already today, advances in hypothermia open up promising perspectives before biology and medicine, notably in operations on the heart and organ transplantations [739]. Even shallow cooling brings about radical changes in all vital processes. As experiments with bees have shown, cooling can bring to a stop the built-in physiological "clock", its action being stronger than that of light.

Experiments in the USSR have shown that, when held under deep hypothermia, animals can stand up to overloads tens of times as great as under normal conditions.

To sum up, probing into the secrets of artificial anabiosis can open up broad vistas before medicine and space exploration; with it, man will ultimately be able to harness time itself.

REFERENCES

1. Bass A.M. and Broida H.P. (Eds.) *Formation and Trapping of Radicals*. New York, 1960.
2. Minkoff G.J. *Frozen Free Radicals*. London, 1960.
3. McGee H.A. The 5th International Symposium on Free Radicals. Upsalla, Sweden, 1961.
4. Grosse A.V., Kirschenbaum A.D. *J. Am. Chem. Soc.*, **77**, 19, 5012-13 (1955).
5. Shilov A. Ye. In: "Chemical Kinetics and Chain Reactions", pp. 229-42, Nauka, Moscow, 1966 (in Russian).
6. Semenov N.N. *Chemical Physics*. Ins. Khim. Fiz. Akad. Nauk SSSR, 1975 (in Russian).
7. Glasstone S., Laidler K., Eyring H. *The Theory of Rate Processes*. New York, 1941.
8. Rice F.O., Potocki R., Gosselin K. *J. Am. Chem. Soc.*, **75**, 8, 2003-04 (1953).
9. Rice F.O., Freamo M. *J. Am. Chem. Soc.*, **73**, 12, 5529-30 (1951).
10. Geib K.H., Harteck P. *Ber.*, **65**, 8, 1551-55 (1932).
11. Briner E., Ricca M. *Helv. Chim. Acta*, **38**, 340-48 (1955).
12. Broida H.P., Pellam J.R. *J. Chem. Phys.*, **23**,, 2, 409 (1955).
13. Broida H.P., Lutes O.S. *J. Chem. Phys.*, **24**, 2, 484-85 (1956).
14. Minkoff G.J., Scherber F.I., Galacher J.S. *J. Chem. Phys.*, **30**, 3, 753-58 (1959).
15. Ruehrwein R.A., Hashman J.S. *J. Chem. Phys.*, **30**, 3, 823-26 (1959).
16. Avramenko L.I. *et al. Izv. Akad. Nauk SSSR, Ser. khim.*, 11, 2079-81 (1962).
17. Bennet J.E., Thomas A. *Proc. Roy. Soc., Ser. A*, **280**, 123-38 (1964).
18. Poljakow M., Lefanov E., Nosenko D. *Acta Physicochimica, USSR*, **10**, 3, 441-50 (1939).
19. Egerton A.C., Minkoff G.J. *Proc. Roy. Soc., Ser. A*, **191**, 1025, 145-68 (1947).
20. Everett A.J., Minkoff G.J. *Trans. Faraday Soc.*, Part 7, **52**, 971-79, 980-85, 986-96 (1956).
21. Minkoff G.J. *Disc. Faraday Soc.*, 14, 141 (1953).
22. Papazian H.A. *J. Chem. Phys.*, **34**, 5, 1614-16 (1961).
23. Rice F.O., Sparrow C.J., *J. Am. Chem. Soc.*, **75**, 4, 848-50 (1953).
24. Rice F.O., Scherber F. *J. Am. Chem. Soc.*, **77**, 2, 291-93 (1955).
25. Rice F.O., Grelecki. *J. Am. Chem. Soc.*, **79**, 11, 2679-80 (1957).
26. Meyer B., Schumacher E. *Nature*, **186**, 4727, 801-03 (1960).
27. Rice F.O., Luckenbach T.A. *J. Am. Chem. Soc.*, **82**, 11, 2681-82 (1960).
28. Gager W.B., Rice F.O. *J. Chem. Phys.*, **31**, 2, 564 (1959).
29. Papazian H.A. *J. Chem. Phys.*, **32**, 2, 456-60 (1960).
30. Foner S.N., Hudson R.L. *J. Chem. Phys.*, **28**, 4, 719-20 (1958).
31. Pshezhetsky S.Ya. *Mechanism and Kinetics of Radiation Chemistry Reactions*. Khimiya, Moscow, 1968 (in Russian).
32. Pikayev A.K. *The Solvated Electron in Radiation Chemistry*. Nauka, Moscow, 1969 (in Russian).
33. Voyevodsky V.V. *The Physics and Chemistry of Elementary Chemical Processes*. Nauka, Moscow, 1969 (in Russian).
34. Pshezhetsky S. Ya. *et al. Free Radical ESR in Radiation Chemistry*. Khimiya, Moscow, 1972 (in Russian).
35. *Free-Radical States in Chemistry*. Nauka, Novosibirsk, 1972 (in Russian).
36. Briner E. *Advances in Chem. Ser.*, **21** (1959).

37. McNesby J.R. *J. Chem. Phys.*, **31**, 1, 283-84 (1959).
38. Pshezhetsky S. Ya., Myasnikov I.A., Buneyev N.A. In: "Collection on Radiation Chemistry". Izd. Akad. Nauk SSSR, 1955 (in Russian).
39. Kircher J.F. *et al. Radiation Res.*, **13**, 3, 452-65 (1960).
40. Lewis G.N., Lipkin D. *J. Am. Chem. Soc.*, **64**, 12, 2801-08 (1942).
41. Reznitsky L.A. *et al. Zhur. fiz. khim.*, **32**, 1, 87-92, (1958).
42. Skorokhodov I.I. *et al. Zhur. fiz. khim.*, **35**, 4, 905-10 (1961).
43. Nekrasov L.I., Skorokhodov I.I., Kobozev N.I. *Zhur. fiz. khim.*, **38**, 9, 2198-2203 (1964).
44. Yagodovskaya T.V., Nekrasov L.I. *Zhur. fiz. khim.*, **41**, 1, 211-15 (1967).
45. Yagodovskaya T.V. *et al. Zhur. fiz. khim.*, **41**, 3, 714-17 (1967).
46. Maltsev Yu. A., Nekrasov L.I. *Zhur. fiz. khim.*, **44**, 2, 431-36 (1970).
47. Yagodovskaya T.V., Nekrasov L.I. *Zhur. fiz. khim.*, **44**, 7, 1718-20 (1970).
48. Antipenko E. Ye. Candidate's dissertation. Moscow University, 1975 (in Russian).
49. Solomon I.J. *et al. J. Am. Chem. Soc.*, **84**, 1, 34-36 (1962).
50. Moll N.G., Clutter D.R., Thompson W.E. *J. Chem. Phys.*, **45**, 12, 4469-81 (1966).
51. Weissberger E., Breckenridge W.H., Taube H. *J. Chem. Phys.*, **47**, 5, 1764-69 (1967).
52. Lebeau P., Damiens A. *Compt. Rend.*, **185**, 14, 652-54 (1927).
53. Frisch P., Schumacher H.J. *Z.anorg. und allg. Chem.*, **229**, 4, 423-28 (1936).
54. Kirschenbaum A.D., Grosse A.V. *J. Am. Chem. Soc.*, **81**, 6, 1277-79 (1959).
55. Grosse A.V., Streng A.G., Kirschenbaum A.D. *J. Am. Chem. Soc.*, **83**, 4, 1004-05 (1961).
56. Streng A.G., Grosse A.V. *J. Am. Chem. Soc.*, **88**, 1, 169-70 (1966).
57. Solomon I.J. *et al. J. Am. Chem. Soc.*, **89**, 9, 2015-17 (1967).
58. Nebgen J.W., Metz F.I., Rose W.B. *J. Am. Chem. Soc.*, **89**, 13, 3118-21 (1967).
59. Arkell A. *J. Am. Chem. Soc.*, **87**, 18, 4057-62 (1965).
60. Solomon I.J. *et al. J. Am. Chem. Soc.*, **90**, 20, 5408-11 (1968).
61. Solomon I.J. *et al. Inorg. Chem.*, **3**, 3, 457 (1964).
62. DesMarteau D.D. *Inorg. Chem.*, **11**, 1, 193-95 (1972).
63. Lawless E.W., Smith I.C. *Inorganic High-Energy Oxidizers*. Marcel Decker, New York, 1968.
64. Sessa P.A., McGee H.A. *Inorg. Chem.*, **10**, 9, 2066-68 (1971).
65. Klein R., Scheer M.D., *J. Chem. Phys.*, **31**, 1, 278 (1959).
66. Klein R., Scheer M.D. *J. Am. Chem. Soc.*, **80**, 4, 1007 (1958).
67. Klein R., Scheer M.D. *J. Phys. Chem.*, **62**, 7, 1011-14 (1958).
68. Scheer M.D., Klein R. *J. Phys. Chem.*, **63**, 9, 1517-18 (1959).
69. Klein R., Scheer M.D. *J. Phys. Chem.*, **65**, 2, 375-77 (1961).
70. Klein R., Scheer M.D. *J. Phys. Chem.*, **66**, 12, 2677-81 (1962).
71. Lomanov Yu. P., Ponomarev A.N., Talrose V.L. *Kinetika i kataliz*, **3**, 1, 49-57 (1962).
72. Ponomarev A.N., Talrose V.L. *Kinetika i kataliz*, **4**, 5, 657-61 (1963).
73. Ponomarev A.N. *Kinetika i kataliz*, **4**, 6, 859-62 (1963).
74. Makarov V.A., Filatov E.S., Nesmeyanov A.N. *Khimiya vysokikh energii*, **4**, 5, 465-66 (1970).
75. Makarov V.A., Filatov E.S., Nesmeyanov A.N. *Khimiya vysokikh energii*, **3**, 5, 413-20 (1969).
76. Makarov V.A., Filatov E.S., Nesmeyanov A.N. *Khimiya vysokikh energii*, **3**, 5, 413-20 (1969).
77. El Saffar Z.M., Eades R.G., Llewellyn J.P. *J. Chem. Phys.*, **50**, 8, 3462-66 (1969).
78. Dixon P.S., Stefani A.P., Szwarc M. *J. Am. Chem. Soc.*, **85**, 17, 2551-56 (1963).
79. Makarov V.A., Filatov E.S. *Khimiya vysokikh energii*, **4**, 5, 467-68 (1970).
80. Kapralova G.A., Shilov A. Ye. *Kinetika i kataliz*, **2**, 3, 362-64 (1961).
81. Kapralova G.A. *et al. Kinetika i kataliz*, **16**, 5, 1164-68 (1975).
82. Kapralova G.A., Chaikin A.M., Shilov A. Ye. *Kinetika i kataliz*, **8**, 3, 485-92 (1967).
83. Surin S.A. *et al. Khimiya vysokikh energii*, **8**, 1, 43-8 (1974).

84. Shvets V.A., Vorotyntsev V.M., Kazansky V.B. *Kinetika i kataliz*, **10**, 2, 356-63 (1969).
85. Tench A.J., Lawson T. *Chem. Phys. Lett.*, **7**, 4, 459-60 (1970).
86. Williamson W.B., Lunsford J.H., Naccache C. *Chem. Phys. Lett.*, **9**, 1, 33-4 (1971).
87. Naccache C. *Chem. Phys. Lett.*, **11**, 3, 323-25 (1971).
88. Surin S.A., Shelimov B.N., Kazansky V.B. *Khimiya vysokikh energii*, **5**, 443-49 (1971).
89. Nikisha V.V. *et al. DAN SSSR*, **214**, 4, 858-60 (1974).
90. Lyubimova O.I., Kotov A.G. *Khimiya vysokikh energii*, **4**, 1, 62-7 (1970).
91. Lyubimova O.I., Kotov A.G. *Khimiya vysokikh energii*, **8**, 4, 364-65 (1974).
92. Mayor F. In: "Formation and Trapping of Free Radicals" (Bass A.M. and H.P. Broida, eds.), New York, 1960.
93. White G.K. *Experimental Techniques in Low-temperature Physics*. Clarendon Press, Oxford, 1959.
94. Scott R.B. *Cryogenic Engineering*. Van Nostrand, Princeton, New Jersey, Toronto, 1959.
95. Rose-Innes A.C. *Low Temperature Techniques*. English Univ. Press, London, 1964.
96. Haselden G.G., ed. *Cryogenic Fundamentals*. Academic Press, New York-London, 1971.
97. Timmerhaus, ed. *Advances in Cryogenic Engineering*. Plenum Press. New York, 1971.
98. Adelberg M., Buchhold T.A., Clark J.A. (Eds.) *Cryogenic Technology*. Wiley and Sons, New York-London, 1963.
99. Below J.F., Connick R.E., Coppel C.P. *J. Am. Chem. Soc.*, **80**, 12, 2961-67 (1958).
100. Badylkes I.S. *Properties of Refrigerants*. Pishchevaya promyshlennost, Moscow, 1974 (in Russian).
101. Dodd R.E., Robinson P.L. *Experimental Inorganic Chemistry*. Elsevier, Amsterdam, 1954.
102. Gordon A., Ford R. *The Chemist's Companion. A Handbook of Practical Data, Techniques and References*. New York, 1972.
103. Gurman V. S., Sergeev G.B. *Zhur. fiz. khim.*, **44**, 3, 803-04 (1970).
104. Gurman V.S., Pergushov V.I. *Zhur. fiz. khim.*, **49**, 7, 1839-40 (1975).
105. Korolev V.V., Plyusin V.F., Bazhin N.M. *Zhur. fiz. khim.*, **49**, 9, 2440-42 (1975).
106. Cho F., Covindjee R. *Biochim. Biophys. Acta*, **216**, 139-50 (1970).
107. Sergeev G.B., Leyenson I.A., Garbuzov V.G. *Kinetika i kataliz*, **14**, 6, 1394-1401 (1973).
108. Schoen L.J., Kuentzel L.E., Broida H.P. *Rev. Sci. Instr.*, **29**, 7, 633-38 (1958).
109. Duerig W.H., Mador I.L. *Rev. Sci. Instr.*, **23**, 8, 421-24 (1952).
110. Nuner J.H., Payne W.J. *Anal. Biochem.*, 355-62 (1973).
111. Simons J.P. *J. Sci. Instr.*, Series 2, **1**, 872-73 (1968).
112. Kiyozo Kawai. *Anal. Biochem.*, **25**, 264-70 (1968).
113. Claisse M.L. *et al. Eur. J. Biochem.*, **16**, 3, 430-38 (1970).
114. Dutton P.L. *Biochim. Biophys. Acta*, **226**, 63-80 (1971).
115. Hagihara B., Iizuka T., *J. Biochem.*, **69**, 355-62 (1971).
116. Bilger H.R., Nicolet M.A. *Rev. Sci. Instr.*, **41**, 3, 346-47 (1970).
117. Bigeleisen J. *et al. Rev. Sci. Instr.*, **39**, 3, 353-56 (1968).
118. Pickup C.P., Kemp W.R.G. *Cryogenics*, **9**, 2, 90-94 (1969).
119. McSweeney D., Levy P.W. *Rev. Sci. Instr.*, **36**, 9, 1324-26 (1965).
120. Sharon B., Treves D. *Rev. Sci. Instr.*, **37**, 9, 1252-54 (1966).
121. Duda C.R., *Rev. Sci. Instr.*, **39**, 10, 1484-87 (1968).
122. Kessler H.K., *Rev. Sci. Instr.*, **37**, 4, 517-18 (1966).
123. Knox W.P., Cuthbert J.D. *Rev. Sci. Instr.*, **39**, 8, 1181-83 (1968).
124. Maltsev A.K., Mikayelyan R.G., Nefedov O.M. *Pribory i tekhnika eksperimenta*, 1, 249-51 (1971).
125. Maltsev A.K., Kagramanov N.D., Nefedov O.M. *DAN SSSR*, **224**, 3, 630-33 (1975).

126. Maurel P., Travers F., Douzou P. *Anal. Biochem.*, **57**, 555-63 (1974).
127. Kolenko Ye. A. *Thermoelectric Cooling Devices*. 2nd ed., Nauka, Leningrad, 1967 (in Russian).
128. Goldsmid H.J. *Thermoelectric Refrigeration*. Plenum Press, New York, 1964.
129. Kolenko Ye.A., Zakrevskaya M.A. *Pribory i tekhnika eksperimenta*, 1, 274 (1971).
130. Kaplin A.P. *Zav. lab.*, **35**, 9, 1143 (1969).
131. Kuliyev A.Z. *Izmerit. tekhn.*, 12, 90-1 (1967).
132. Nayer V.A., Khirich I.Ya., Kravchenko P.N. *Pribory i tekhnika eksperimenta*, 4, 260 (1971).
133. Caldin E.F., Trickett. *Trans. Faraday Soc.*, **49**, p. 772 (1953).
134. Ainscough J.B., Caldin E.F. *J. Chem. Soc.*, 2528-49 (1956).
135. Caldin E.F., Jackson R.A. *J. Chem. Soc.*, 2411-20 (1960).
136. Whittle E., Dows D.A., Pimentel G.C. *J. Chem. Phys.*, **22**, 11, 1943 (1954).
137. Norman I., Porter G. *Proc. Roy. Soc.*, *Ser. A*, **230**, 1182, 399-414 (1955).
138. *Advances in Chemical Physics*. Vol. 10. Molecular Beams. Ed. by J. Ross. New York, 1966.
139. Semenov N.N., Shalnikov A.I. *Zhur. r. kh. o.*, *fiz. chast*, **60**, **4**, 303-08 (1928).
140. Kargin V.A., Kabanov V.A., Zubov V.P. *Vysokomol. soed.*, **1**, 2, 265-68 (1959).
141. Kargin V.A. *et al. Vysokomol. soed.*, **3**, 3, 426-34 (1961).
142. Prokofyev A.I., Sergeev G.B. *Vestn. MGU*, *Ser. khim.*, 4, 24-7 (1966).
143. Meyer B. *Low Temperature Spectroscopy*. Elsevier, New York, 1971.
144. Sakhrovsky M.Yu., Smolinsky Ye.S. *Pribory i tekhnika eksperimenta*, 5, 181-83 (1971).
145. Hirshberg Y., Fisher E. *Rev. Sci. Instr.*, **30**, 3, 197-99 (1959).
146. Nakane R. *et al.*, *Bull. Chem. Soc. Japan*, **36**, 11, 1376-81 (1963).
147. Lappo M.T., Serafimovich A.I. *Zhur. prikl. spectr.*, **17**, 1, 174-75 (1972).
148. Dmitriyev A.G., Tsarenkov B.V., Chiabrishvili N.G. *Pribory i tekhnika eksperimenta*, 1, 207-08 (1971).
149. Higashimura T. *et al. J. Chem. Phys.*, **53**, 3, 1152-55 (1970).
150. Labbe P., Chaix P. *Anal. Biochem.*, **39**, 2, 322-26 (1971).
151. Kawai K. *Anal. Biochem.*, **57**, 1, 190-99 (1974).
152. Sergeev G.B., Papisova V.I., Fedorova S.E. *Vestn. MGU*, *Ser. khim.*, 6, 76-78 (1967).
153. Petrus A.A. *Khimiya vysokikh energii*, **8**, 3, 280-81 (1974).
154. Kulakov V.V., Nikolsky V.G. *Khimiya vysokikh energii*, **6**, 6, 514-18 (1972).
155. Nikolsky V.G., Sapozhnikov D.N., Tochin V.A. *Vysokomol. soed.*, **Б12**, 1, 19-22 (1970).
156. Caldin E.F. *Fast Reactions in Solution*. Oxford, 1964.
157. Allen C.R., Brook A.J.W., Caldin E.F. *Trans. Faraday Soc.*, **56**, 788-93 (1960).
158. Dewald R.R., Brooks J.M. *Rev. Sci. Instr.*, **41**, 11, 1612-13 (1970).
159. Hui Bon Hoa, Douzou P. *Anal. Biochem.*, **51**, 127-36 (1973).
160. Strickland E.H., Horwitz J., Billups C. *Biochem.*, **8**, 8, 3205-13 (1969).
161. Horwitz J., Strickland E.H., Billups C. *J. Am. Chem. Soc.*, **91**, 1, 184-90 (1969).
162. Strickland E.H. *et al. J. Biol. Chem.*, **245**, 16, 4168-77 (1970).
163. Beckman E., Rass R. *Cryogenics*, **11**, 2, 147 (1971).
164. Koningstein J. *Introduction to the Theory of the Raman Effect*. Dordrecht, 1972.
165. Maltsev A.A., Mikayelyan R.G., Nefedov O.M. *Pribory i tekhnika eksperimenta*, 1, 249-51 (1971).
166. Dreufus R.W., Okrasinski M. *Rev. Sci. Instr.*, **41**, 3, 476 (1970).
167. Zundel G. *Hydration and Intermolecular Interaction*. Acad. Press, 1969.
168. Osipov Yu.V. *PTE*, 2, 256-58 (1971).
169. Zasavitskii I.I., Metsonashvili B.N., Shotov A.P., *Cryogenics*, **11**, 2, 136-37 (1971).
170. Lishnevsky V.A., Uzhinov B.M., Sergeev G.B. *DAN SSSR*, **142**, 2, 1116-19 (1962).
171. Cheng Tong Kha, Sergeev G.B., Kunskaite L.Yu., *Vestn. MGU*, *Ser. khim.*, 2, 28-30 (1967).

172. Kiryukhin D.P. *et al.* *DAN SSSR*, **211**, 3, 632-35 (1973).
173. Goldansky V.I. *Usp. khim.*, **44**, 12, 2121-49 (1975).
174. Andronikashvili E.L. *Biofizika*, **17**, 6, 1068-82 (1972).
175. Rubin L.G. *Cryogenics*, **10**, 1, 14-22 (1970).
176. Weyhmann W. Thermometry at Ultra Low Temperatures. In: "Methods of Experimental Physics" (L. Marton, ed.) v. 10-11, 1973.
177. Marson G.B. *International Laboratory*, 5, 43-51 (1973).
178. *Thermocouples and resistance thermometers.* A Handbook, Kiev, 1970 (in Russian).
179. Balzovsky V.B., Orzhevsky O.B. *Zav. lab.*, **35**, 8, 1016-17 (1969).
180. Kutz M. *Temperature Control.* Wiley and Sons, New York, 1968.
181. Bligh J., ed. *Essays on Temperature Regulation.* North Holland, 1972.
182. Pado G.S., Astrov D.N. *Pribory i tekhnika eksperimenta*, 1, 207-09 (1968).
183. Logvinenko S.P., Brovkin Yu.N. *Pribory i tekhnika eksperimenta*, 1, 212-13 (1968).
184. Mironov S.V., Rudashevsky Ye.G., Chernykh V.I. *Pribory i tekhnika eksperimenta*, 5, 192-93 (1969).
185. Davydov Yu.S., Mikhailov I.T. *Kholodilnaya tekhnika*, 11, 50-51 (1969).
186. Vasilyev Ya.I. *et al.* *PTE*, 5, 187-90 (1969).
187. Van Hecke P., Van Gerven L. *Cryogenics*, **10**, 5, 386-88 (1970).
188. Gromyshev A.V., Lutsenko E.L., Sinitsky V.V. *Pribory i tekhnika eksperimenta*, 5, 206-07 (1970).
189. Zyukin N.A., Shalnikov A.I. *Pribory i tekhnika eksperimenta*, 1, 222 (1969).
190. Rovinsky A.Ye., Abramov G.I. *Pribory i tekhnika eksperimenta* 2, 247-48 (1970).
191. Lopyrev V.A., Mukhin N.K. *Pribory i tekhnika eksperimenta*, 3, 214-17 (1971).
192. Kaporovsky B.M. *et al.* *Pribory i tekhnika eksperimenta*, 1, 253 (1971).
193. Benyaminovich S.M., Fisher L.M. *Pribory i tekhnika eksperimenta*, 2, 258-59 (1971).
194. Kanter B.Z. *Pribory i tekhnika eksperimenta*, 3, 211-13 (1971).
195. Klipping G., Schönherr W.D., Schulze W. *Cryogenics*, **10**, 6, 501-03 (1970).
196. Vasilyev V.G., Verein N.V., Leontyev Yu.V. *Pribory i tekhnika eksperimenta*, 2, 234 (1969).
197. Izvozchikov V.A., Kishmaria S.R. *Pribory i tekhnika eksperimenta*, 5, 179-80 (1970).
198. Maznitsa A.M., Derbenev I.P. *Pribory i tekhnika eksperimenta*, 5, 181-82 (1970).
199. Kuchnir M. *et al.* *Rev. Sci. Instr.*, **42**, 4, 536-37 (1971).
200. *Chemical Applications of Mössbauer Spectroscopy.* Ed. by V. Goldanskii, R. Herber. New York, 1968.
201. Irkayev S.M., Kuzmin R.N., Opalenko A.A. *Nuclear Gamma Resonance.* Moscow University Press, 1970 (in Russian).
202. Golovin V.A. *et al.* *PTE*, 1, 111-12 (1969).
203. Wertz J., Bolton J. *Electron Spin Resonance.* New York, 1972.
204. Salikhov K.M., Semenov A.G., Tsvetkov Yu.D. *Electron Spin Echo and Its Applications.* Nauka, Novosibirsk, 1976 (in Russian).
205. Jen C.K. *et al.* *Phys. Rev.*, **112**, 4, 1169-82 (1958).
206. Moiseyev V.A., Pshisukha A.M., Zvyagin A.I. *Pribory i tekhnika eksperimenta*, 5, 197 (1969).
207. Kabanov V.A. *et al.* *Vysokomol. soed.*, **1**, 12, 1859-61 (1959).
208. Molin Yu.N. *et al.* *Pribory i tekhnika eksperimenta*, 6, 73-7 (1960).
209. Blumenfeld L.A., Voyevodsky V.V., Semenov A.G. *Use of ESR in Chemistry.* Sib. Otd. Akad. Nauk SSSR Press, Novosibirsk, 1962 (in Russian).
210. Lebedev Ya.S., Muromtsev V.I. *ESR and Relaxation of Trapped Radicals.* Khimiya, Moscow, 1972 (in Russian).
211. Lebedev Ya.S. *Usp. khim.*, **37**, 5, 934-67 (1968).
212. Buchachenko A.L., Vasserman A.M. *Stable Radicals.* Khimiya, Moscow, 1973 (in Russian).
213. Jackson J.L., Montroll E.W. *J. Chem. Phys.*, **28**, 6, 1101-09 (1958).
214. Golden S. *J. Chem. Phys.*, **29**, 1, 61-71 (1958).

215. Jackson J.L. *J. Chem. Phys.*, **31**, 1, 154-57 (1959).
216. Jackson J.L. *J. Chem. Phys.*, **31**, 3, 722-29 (1959).
217. Talrose V.L., Vasilyev G.K. *Kinetika i kataliz*, **4**, 4, 497-507 (1963).
218. Tikhomirov L.A., Belyaeva V.A., Buben N.Ya. *Izv. Akad. Nauk SSSR, Ser. khim.*, 4, 594-98 (1965).
219. Trofimov V.I., Chkheidze I.I., Buben N.Ya. *Zhur. fiz. khim.*, **39**, 7, 1662-68 (1965).
220. Tikhomirov L.A., Buben N.Ya. *DAN SSSR*, **163**, 2, 414-17 (1965).
221. Tolkachev V.A., Sokolov I.B. *Khimiya vysokikh energii*, **4**, 4, 367-68 (1970).
222. Roginsky V.A., Chervonenko V.S., Vyboishchikov F.P. *Khimiya vysokikh energii*, **4**, 4, 364-65 (1970).
223. Kotov A.G. *et al. Kinetika i kataliz*, **4**, 6, 926-29 (1963).
224. Gurman V.S., Yakovenko Ye.I., Papisova V.I. *Zhur. fiz. khim.*, **34**, 10, 2372 (1960).
225. Sergeev G.B. *et al.* Fifth International Symposium on Free Radicals. Uppsala, 1961.
226. Popovich G.M., Golubev V.B., Bugayenko L.T. *Khimiya vysokikh energii*, **7**, 2, 159-65 (1973).
227. Mikhailov A.I., Lebedev Ya.S., Buben N.Ya. *Kinetika i kataliz*, **5**, 6, 1020-27 (1964).
228. Mikhailov A.I., Lebedev Ya.S., Buben N.Ya. *Kinetika i kataliz*, **6**, 1, 48-55 (1965).
229. Serdobov M.V., Aleksandrov A.I., Lebedev Ya.S. *Khimiya vysokikh energii*, **7**, 5, 439-44 (1973).
230. Roginsky V.A., Miller V.B. *DAN SSSR*, **213**, 3, 642-45 (1973).
231. Dzyuba S.A., Tolkachev V.A., Burshtein A.I. *DAN SSSR*, **223**, 3, 633-35 (1975).
232. *Solids under Pressure.* Ed. by W. Paul and D. Warschauer. New York, 1963.
233. Radzig V.A., Rainov M.M. In: "Kinetics and mechanism of chemical reactions in solids", pp. 265-69, Minsk (1975).
234. Gurman V.S. *et al.* In: "Chemistry of peroxide compounds", 46-9, Nauka, Moscow, 1964 (in Russian).
235. Sergeev G.B. *Usp. khim.*, **35**, 4, 747-74 (1966).
236. Pospelova M.A., Belokon V.G., Gurman V.S. *DAN SSSR*, 212, 2, 414-16 (1973).
237. Kroh J.B., Green B.C., Spinks J.W.T. *J. Am. Chem. Soc.*, **83**, 9, 2201-02 (1961).
238. Kaitmazov S.D., Prokhorov A.M. *FTT*, **5**, 1, 347-48 (1963).
239. Gurman V.S., Sergeev G.B. *Zhur. fiz. khim.*, **44**, 4, 1086-88 (1970).
240. Gurman V.S., Batyuk V.A., Sergeev G.B. *Kinetika i kataliz*, **8**, 3, 527-31 (1967).
241. Smith R.C., Wyard S.J. *Nature*, **191**, 4791, 897-98 (1961).
242. Raitsimring A.M., Moralev V.M., Tsvetkov Yu.D. *Khimiya vysokikh energii*, **7**, 2, 125-28 (1973).
243. Raitsimring A.M., Pomytkin A.P., Tsvetkov Yu.D. *Khimiya vysokikh energii*, **4**, 4, 369-70 (1970).
244. Raitsimring A.M., Moralev V.M., Tsvetkov Yu.D. *Khimiya vysokikh energii*, **4**, 2, 180-82 (1970).
245. Starenky A.G., Lavrentovich Ya.I., Kabakchi A.M. *Vysokomol. soed.*, **Б14**, 5, 377-83 (1972).
246. Pasalsky B.K. *et al. Khimiya vysokikh energii*, **8**, 5, 451-54 (1974).
247. Trofimov V.I. Abstract of a doctor's dissertation. Chernogolovka, 1974 (in Russian).
248. Tolkachev V.A., Sokolov I.B., Kovalevsky V.I. *Khimiya vysokikh energii*, **4**, 5, 455-56 (1970).
249. Tolkachev V.A., Kovalevsky V.I. *Zhur. fiz. khim*, **44**, 5, 1365 (1970).
250. Tolkachev V.A., Sokolov I.B. *Khimiya vysokikh energii*, **4**, 5, 469-70 (1970).
251. Abdrashitov E.F. *et al. Khimiya vysokikh energii*, **7**, 3, 274-76 (1973).
252. Zamarayev K.I. *et al. DAN SSSR*, **199**, 3, 640-42 (1971).

253. Khairutdinov R.F., Zhutkovsky R.B., Zamarayev K.I. *Fiz. tverd. tela*, **17**, 3, 929-30 (1975).
254. Khairutdinov R.F., Zamarayev K.I. *DAN SSSR*, **222**, 3, 654-56 (1975).
255. Parmon V.N., Khairutdinov R.F., Zamarayev K.I. *Fiz. tverd. tela*, **16**, 9, 2572-77 (1974).
256. Andreyev N.S. *et al. Liquation in Glasses*. Nauka, Leningrad, 1974 (in Russian).
257. Girina Ye. L., Yershov B.G., Pikayev A.K. *Khimiya vysokikh energii*, **8**, 5, 470-71 (1974).
258. Girina Ye. L., Yershov B.G., Pikayev A.K. *Khimiya vysokikh energii*, **8**, 4, 334-38 (1974).
259. Girina Ye. L., Yershov V.G. *Izv. Akad. Nauk SSSR*, 2, 278-81 (1972).
260. Kroh J., Stradowski Cz. *Radiochem. Radioanal. Letters*, **9**, 3, 169-77 (1972).
261. Kroh J., Stradowski Cz. *Int. J. Radiat. Phys. Chem.*, **5**, 2, 243-45 (1973).
262. Bugayenko L.T., Povolotskaya O.S. *DAN SSSR*, **174**, 2, 378-81 (1967).
263. Bugayenko L.T., Povolotskaya O.S. *Khimiya vysokikh energii*, **1**, 5, 480-86 (1967).
264. Batyuk B.A. *et al. Khimiya vysokikh energii*, **4**, 2, 143-48 (1970).
265. Hase H., Kevan L. *J. Phys. Chem.*, **74**, 18, 3358-61, (1970).
266. Khairutdinov R.F., Mikhailov A.I., Zamarayev K.I. *DAN SSSR*, **200**, 4, 905-08 (1971).
267. Steen H.B., Kaalhus O., Kongshaug M. *J. Phys. Chem*, **75**, 13, 1941-46 (1971).
268. Byakov V.M., Yershov B.G. *DAN SSSR*, **222**, 3, 637-40 (1975).
269. Byakov V.M. In: "Mechanism of water radiolysis" (Bugayenko L.T. ed.), Moscow University Press, 1970 (in Russian).
270. Pernikova T.Ye. *et al. Khimiya vysokikh energii*, **7**, 5, 429-33 (1973).
271. Sergeev G.B. *et al. DAN SSSR*, **213**, 4, 891-94 (1973).
272. Sergeev G.B. *et al. Kinetika i kataliz*, **15**, 2, 333-40 (1974).
273. Zhdanov G.S., Milinchuk V.K., Pshezhetsky S.Ya. *Khimiya vysokikh energii*, **7**, 2, 190-91 (1973).
274. Milinchuk V.K., Zhdanov G.S., Pshezhetsky S.Ya. *Vysokomol. soed.*, **Б12**, 9, 658-61 (1970).
275. Skvortsov V.G., Zhdanov G.S., Milinchuk V.K. *Khimiya vysokikh energii*, 5, 5, 466-67 (1971).
276. Karasev A.L. *Khimiya vysokikh energii*, **6**, 6, 519-24 (1972).
277. Bagdasaryan Kh. S. *Kinetika i kataliz*, **8**, 5, 1073-93 (1967).
278. Kondratyev V.A., Bagdasaryan Kh. S. *Khimiya vysokikh energii*, **1**, 3, 197-201 (1967).
279. Vasilyev V.G., Verein N.V., Piskunov A.K. *Khimiya vysokikh energii*, **4**, 5, 409-12 (1970).
280. Bazhin N.M. *Khimiya vysokikh energii*, **8**, 4, 310-15 (1974).
281. Stepanov B.I., Gribkovsky V.P. *Introduction to the Theory of Luminescence*, Izd. AN BSSR, Minsk, 1963 (in Russian).
282. Kiryukhin Yu. I., Sinitsina Z.A., Bagdasaryan Kh.S. *DAN SSSR*, **203**, 5, 1111-1114 (1972).
283. Korolev V.V., Bazhin N.M. *Khimiya vysokikh energii*, **8**, 6, 506-12 (1974).
284. Dzantiev B.G. *et al. Khimiya vysokikh energii*, **8**, 6, 552-53 (1974).
285. Merkel P.B., Hamill W.H. *J. Chem. Phys.*, **53**, 9, 3414-16 (1970).
286. Cadogan K.D., Albrecht A.C. *J. Chem. Phys.*, **51**, 6, 2710-25 (1969).
287. Kulakov V.V., Nikolsky V.G. *Khimiya vysokikh energii*, **8**, 4, 376-77 (1974).
288. Korobeinikova V.N., Kazakov V.P., Chuvilin Yu.N. *DAN SSSR*, **213**, 4, 884-86 (1973).
289. Nikolsky V.G., Burkov G.I. *Khimiya vysokikh energii*, **5**, 5, 416-21 (1971).
290. Yershov B.G., Mustafayev A.I., Pikayev A.K. *Intern. J. Rad. Phys. and Chem.*, **3**, 2, 71-6 (1971).
291. Butterfield A.W., Ericson L.C. *Molecular Cryst. and Liquid Cryst.*, **11**, 145-51 (1970).
292. Randall J.T., Wilkins M.H.F. *Proc. Roy. Soc.*, **A184**, 366-90 (1945).
293. Novikov G.F., Ametov K.K., Yakovlev B.S. *Khimiya vysokikh energii*, **7**, 2, 136-42 (1973).

294. Bolshakova S.I., Kuzminsky A.S. *Khimiya vysokikh energii*, **8**, 1, 61-7 (1974).
295. Kohlshutter H.W., Sprenger L. *Z. phys. Chem.*, **16**, 282-86 (1932).
296. Letort M. *Comp. Rend.*, **202**, 9, 767-68 (1936).
297. Travers M.W. *Trans. Faraday Soc.*, **32**, 246-50 (1936).
298. Semenov N.N. *Khim. i tekhnol. polimerov*, 7-8, 196-221 (1960).
299. Maga M. *Khim. i tekhnol. polimerov*, 3, 8-28 (1963).
300. Shapiro A. *Khim. i tekhnol. polimerov*, 4, 52-68 (1964).
301. Bruk M.A. In: "Advances in Polymer Chemistry" (Z.A. Rogovin, ed.) 42-100, Khimiya, Moscow, 1966 (in Russian).
302. Kargin V.A., Kabanov V.A. *Zhur. V. Kh. O. im. Mendeleyeva*, **9**, 6, 602-19 (1964).
303. Ivanov V.S. *Radiation Polymerization*. Khimiya, Leningrad, 1967 (in Russian).
304. Terenin A.N. *Photonics of Molecules of Dyes and Related Organic Compounds*. Nauka, Leningrad, 1967 (in Russian).
305. Kargin V.A. *et al. DAN SSSR*, **141**, 2, 389-92 (1961).
306. Finkelshtein Ye.I., Abkin A.D. *DAN SSSR*, **174**, 4, 887-90 (1967).
307. Finkelshtein Ye.I., Abkin A.D. *Khimiya vysokikh energii*, **3**, 5, 447-48 (1969).
308. Bamford C.H., Bibby A., Eastmond G.C. *Polymer*, **9**, 12, 653-61 (1968).
309. Bruk M.A. *et al. DAN SSSR*, **157**, 6, 1399-402 (1964).
310. Bolshakov A.I. *et al. Khimiya vysokikh energii*, **5**, 1, 57-62 (1971).
311. Broude V.L., Goldanskii V.I., Gordon D.A. *Khimiya vysokikh energii*, **2**, 2, 165-71 (1968).
312. Broude V.L., Petrus A.A., *Vysokomol. soed.*, **Б15**, 3, 197-99 (1973).
313. Gordon D.A., Migunova I.I., Mikhailov A.I. *DAN SSSR*, **213**, 2, 368-71 (1973).
314. Perec-Spritzer L., Spritzer C., *J. Chem. Phys.*, **72**, 5, 685-87 (1975).
315. Perec L. *J. Chim. phys.*, **66**, 10, 1742-59 (1969).
316. Masterova M.N. *et al.* Resume of a Report at the 11th Mendeleyev Congress, 2, 155-56, Nauka, Moscow, 1975 (in Russian).
317. Petrus A.A. *Khimiya vysokikh energii*, **8**, 3, 280-81, (1974).
318. Nikitin L.Ya., Fedoseyeva T.S., Kuzminsky A.S. *Khimiya vysokikh energii*, **8**, 6, 557-58 (1974).
319. Berlin A.A. *et al. DAN SSSR*, **187**, 6, 1339-42 (1969).
320. Tabata I. *Khim. i tekhnol. polimerov*, 9, 3-24 (1965).
321. Pshezhetsky V.S., Tupikov V.I. In: "Heterocyclic High-Molecular Compounds" (G.S. Kolesnikov, ed.), 220-225, Nauka, Moscow, 1963.
322. Kiryukhin D.P. *et al. Vysokomol. soed.*, **A14**, 10, 2115-19 (1972).
323. Goldanskii V.I., Kiryukhin D.P., Barkalov I.M. *Khimiya vysokikh energii*, **8**, 3, 279 (1974).
324. Roshchupkin V.P. *et al. DAN SSSR*, **222**, 2, 396-98 (1975).
325. Kiryukhin D.P. *et al. Vysokomol. soed.*, **Б12**, 7, 491-92 (1970).
326. Goldanskii V.I., Frank-Kamenetskii M.D., Barkalov I.M. *DAN SSSR*, **211**, 1, 133-36 (1973).
327. Goldanskii V.I., Frank-Kamenetskii M.D., Barkalov I.M. *Science*, **182**, 4119, 1344 (1973).
328. Kiryukhin D.P. *et al. DAN SSSR*, **199**, 4, 857-60 (1971).
329. Kiryukhin D.P. *et al. DAN SSSR*, **206**, 1, 147-50 (1972).
330. Goldanskii V.I. *DAN SSSR*, **124**, 6, 1261-64 (1959).
331. Goldanskii V.I. *DAN SSSR*, **127**, 5, 1037-40 (1959).
332. Siebrand W. *J. Chem. Phys.*, **46**, 2, 440-47 (1967).
333. Lin S.H., Eyring H. *PNAS*, **69**, 11, 3192-94 (1972).
334. Panasenko A.A. Candidate's dissertation. Moscow University, 1968 (in Russian).
335. *Chemistry of the Solid State*, Ed. by W. Garner. London, 1955.
336. Kabanov V.A. Doctor's dissertation, Moscow University, 1966 (in Russian).
337. Barkalov N.M. *et al. J. Pol. Sci.*, Part C, **4**, 31-7 (1964).
338. Shulgina E.S. *et al. Vysokomol. soed.*, **8**, 11, 1942-51 (1966).
339. Papisov I.M. *et al. DAN SSSR*, **156**, 3, 669-72 (1964).
340. Papisov I.M. Candidate's dissertation, Moscow University, 1964 (in Russian).

341. Brown J.F., White D.M. *J. Am. Chem. Soc.*, **82,** 21, 5671-78 (1960).
342. White D.M. *J. Am. Chem. Soc.*, **82,** 21, 5678-85 (1960).
343. Bolshakov A.I. *et al. DAN SSSR,* 222, 3, 633-36 (1975).
344. Amagi Y., Chapiro A. *J. Chim. Phys.*, **59, 6,** 537-57 (1962).
345. Gusakovskaya I.G., Goldanskii V.I. *Khimiya vysokikh energii,* **2, 1,** 46-53 (1968).
346. Gusakovskaya I.G., Nikolsky V.G., Goldanskii V.I. *Khimiya vysokikh energii,* **4,** 5, 434-38 (1970).
347. Buben N.Ya. *et al. Vysokomol. soed.*, **A9,** 10, 2275-83 (1967).
348. Nikolsky V.G., Alfimov M.V., Buben N.Ya. *Izv. AN SSSR, Ser. khim.*, 5, 955 (1963).
349. Nikolsky V.G., Alfimov M.V., Buben N.Ya. *Kinetika i kataliz,* **5,** 2, 268-76 (1964).
350. Charlesby A., Partridge R.H. *Proc. Roy. Soc., Ser. A,* **271,** 188-206 (1963).
351. Alger R.S., Anderson T.H., Webb L.A. *J. Chem. Phys.*, **30,** 3, 695-706 (1959).
352. Panasenko A.A. *et al. Vysokomol. soed.*, **Б9,** 12, 890-93 (1967).
353. Panasenko A.A. *et al. Vysokomol. soed.*, **Б10,** 2, 139-42 (1968).
354. Lipatov Yu.S., Vilensky V.A. *Vysokomol. soed.*, **A17,** 9, 2069-75 (1975).
355. Ferry J. *Viscoelastic Properties of Polymers.* New York, 1961.
356. Gerasimov G.N. *et al. DAN SSSR,* **216,** 5, 1051-54 (1974).
357. Gerasimov G.N. *et al. DAN SSSR,* **222,** 4, 865-68 (1975).
358. Suzuki F. *et al. J. Polymer. Sci.*, **A1,** 7, 753-57 (1969).
359. Teitelbaum B.Ya. *DAN SSSR,* **222,** 5, 1155-58 (1975).
360. Stacey F.W., Sauer J.C., *McKusick* B.C. *J. Am. Chem. Soc.*, **81,** 4, 987-92 (1959).
361. Tobolsky A.V. *et al. J. Am. Chem. Soc.*, **86,** 19, 3925-30 (1964).
362. Maryin A.P., Shlyapnikov Yu. A. *DAN SSSR,* **215,** 5, 1160-63 (1974).
363. Lukashina N.N., Shlyapnikov Yu. A. *Kinetika i kataliz,* **16,** 5, 1169-72 (1975).
364. Vasserman A.M. *et al. DAN SSSR,* **222,** 2, 384-87 (1975).
365. Korst N.N. *et al. Teoret. i eksper. khim,* **8,** 1, 63-70 (1972).
366. Atkins P., Symons M. *The Structure of Inorganic Radicals.* Amsterdam, 1967.
367. Semenov N.N. *Chain Reactions.* Goskhimtekhizdat, Leningrad, 1934 (in Russian).
368. Semenov N.N. *On Some Problems of Chemical Kinetics and Reactivity.* Izd. AN SSSR, Moscow, 1958 (in Russian).
369. *Chemical Kinetics and Chain Reactions.* Nauka, Moscow, 1966 (in Russian).
370. Meinhold T.F. *et al. Chem. Proc.*, **26,** 24-31 (1963).
371. Kovalev G.N. *et al. DAN SSSR,* **142,** 2, 396-98 (1962).
372. Noyes W.A., Leighton P.A. *The Photochemistry of Gases.* Reinhold Publishers, 1941.
373. Schneider W.G., Bernstein H.I., Pople J.A. *J. Chem. Phys.*, **28,** 4, 601-07 (1958).
374. Rank D.H., Rao B.S., Wiggins T.A. *J. Chem. Phys.*, **37,** 11, 2511-15 (1962).
375. Moger G.G., Sergeev G.B. *Vestn. MGU, Ser. khim.*, 2, 14-16 (1963).
376. Chiltz G. *et al. Chem. Rev.*, **63,** 4, 355-72 (1963).
377. Fettis G.C., Knox J.H. *Progress in Reaction Kinetics,* v. 2, 165-96, Pergamon Press, 1964.
378. Trotman-Dikenson A.F. *Chem. and Ind.*, 9, 379 (1965).
379. Glushko V.P., ed. *Thermodynamic Properties of Individual Substances.* Izd. AN SSSR, Moscow, 1962 (in Russian).
380. Lane M.R., Linnett J.W., Ostin H.G. *Proc. Roy. Soc., Ser. A,* **216,** 361-74 (1953).
381. Kovalev G.N., Sergeev G.B. In: "Elementary Processes of High-Energy Chemistry", pp. 276-78, Nauka, Moscow, 1965 (in Russian).
382. Kovalev G.N., Sergeev G.B. *DAN SSSR,* **160,** 2, 390-93 (1965).
383. Semenov N.N. *Pure and Appl. Chem.*, **5,** 353-74 (1962).
384. Maass O., Wright C.H. *J. Am. Chem. Soc.*, **46,** 12, 2664-73 (1924).
385. Kovalev G.N. Candidate's dissertation. Moscow University, 1967 (in Russian).
386. Powles J.G. *Trans. Faraday Soc.*, **48,** 430-39 (1952).
387. Huffman H.M., Eaton M., Oliver G.D. *J. Am. Chem. Soc.*, **70,** 9, 2911-14 (1948).

388. Eades R.G., Feinch N.D., Elsaffar Z.M. *Arch. Sci.*, **12**, 109-16 (1959).
389. Terres E., Assemi M.T. *Brennstoff-Chem.*, **37**, 257-66 (1956).
390. Kovalev G.N., Sergeev G.B. *Zhur. fiz. khim.*, **47**, 10, 2573-76 (1973).
391. Sugimoto K., Ando W., Oae S. *Bull. Chem. Soc. Japan*, **37**, 3, 365-68 (1964).
392. Fokin A.V., Skladnev A.A., Knunyants I.L. *DAN SSSR*, **138**, 1132-36 (1961).
393. Kobeko P.P. *Amorphous Substances*. Izd. AN SSSR, Moscow-Leningrad, 1952 (in Russian).
394. Becker H. *Einführung in die Elektronentheorie organischchemischer Reactionen*. Berlin, 1964.
395. Kovalev G.N., Masterova M.N., Sergeev G.B. *DAN SSSR*, **165**, 2, 351-53 (1965).
396. Strella S. *J. Appl. Polymer. Sci.*, **7**, 569-73 (1963).
397. Simha R., Boyer R.E. *J. Chem. Phys.*, **37**, 5, 1003-07 (1962).
398. Winter-Klein A. *Silicates Industr.*, **21**, 157-63 (1956).
399. Nakhapetyan L.A. *et al. Zhur. prikl. khim.*, **37**, 8, 1808-11 (1964).
400. Yakovenko Ye. I., Sergeev G.B., Rakhimov M.M. *DAN SSSR*, **171**, 4, 890-93 (1966).
401. Sergeev G.B. In: "Present-Day Problems of Physical Chemistry", pp. 20-65, Moscow University Press, Moscow, 1970 (in Russian).
402. Sergeev G.B., Serguchev Yu.A., Smirnov V.V. *Usp. khim.*, **42**, 9, 1545-73 (1973).
403. Lishnevsky V.A., Sergeev G.B. *DAN SSSR*, **128**, 4, 767-68 (1959).
404. Bodrikov I.V., Smolyan Z.S. *Usp. khim.*, **35**, 5, 853-80 (1966).
405. De la Mare P., Bolton R. *Electrophilic Additions to Unsaturated Systems*. Amsterdam, 1966.
406. Sergeev G.B. In: "Problems of Kinetics and Catalysis", v. 15, pp. 220-25, Nauka, Moscow, 1973 (in Russian).
407. *Selected Values of Physical and Thermodynamic Properties of Hydrocarbons and Related Compounds*. Carnegie Press, 1953.
408. Merzhanov A.G., Dubovitsky F.I. *Usp. khim.*, **35**, 4, 656-83 (1966).
409. Lishnevsky V.A., Sergeev G.B. *Kinetika i kataliz*, **5**, 3, 407-13 (1964).
410. Foster R. *Organic Charge-Transfer Complexes*. Academic Press, London-New York, 1969.
411. Mulliken R.S., Person W.B. *Molecular Complexes*. Wiley Interscience, New York, 1969.
412. Lishnevsky V.A. *et al. DAN SSSR*, **172**, 4, 863-66 (1967).
413. Sergeev G.B., Cheng Tong Kha. *Vestn. MGU, Ser. khim.*, 1, 62-4 (1969).
414. Hassel O., Romming G. *Quart Rev.*, **16**, 1, 1-18 (1962).
415. Lishnevsky V.A. Candidate's dissertation, Moscow University, 1964 (in Russian).
416. Sergeev G.B. *et al. DAN SSSR*, **203**, 2, 394-97 (1972).
417. Barachevsky V.A., Terenin A.N. *Opt. i spectroscop.*, **17**, 2, 304-06 (1964).
418. Lishnevsky V.A. *DAN SSSR*, **172**, 3, 641-44 (1967).
419. Lishnevsky V.A. *DAN BSSR* **17**, 7, 617-20 (1973).
420. Shvedchikov A.P. *et al. Zhur. org. khim*, **42**, 12, 2753-55 (1972).
421. Shvedchikov A.P. *et al.* Inventor's Certificate No. 393258, "Otkrytiya. Izbr. Prom. obraztsy. Tovarn. znaki", 33, 117 (1973).
422. Goldanskii V.I. *et al. DAN SSSR*, **224**, 1, 128-30 (1975).
423. Kevdina I.B., Shantarovich V.P., Shvedchikov A.P. *Khimiya vysokikh energii*, **10**, 4, 375-77 (1976).
424. Kimelfeld Ya. M., Lumer E.V., Shvedchikov A.P. *Izv. Akad. Nauk SSSR*, 8, 1714-19 (1974).
425. Smirnov V.V. Candidate's dissertation. Moscow University, 1973 (in Russian).
426. Sergeev G.B., Cheng Tong Kha. *Teor. eksp. khim.*, **3**, 3, 422-24 (1967).
427. Serguchev Yu. A., Stetsyuk G.A., Smirnov V.V. *Zhur. org. khim.*, **11**, 1, 16-22 (1975).
428. Serguchev Yu.A., Stetsyuk G.A. *Ukr. chim. zhur.*, **39**, 96-101 (1973).
429. Kimelfeld Ya. M., Mostovoi A.B., Fainshtein L.I. *DAN SSSR*, **209**, 5, 1105-08 (1973).

430. Kimelfeld Ya. M., Mostovoi A.B., Mostovaya L.M. *DAN SSSR*, **222,** 5, 1130-33 (1975).
431. Kimelfeld Ya. M., Mostovoi A.B. *DAN SSSR*, **213,** 2, 382-85 (1973).
432. Kimelfeld Ya. M., Lumer E.V., Shvedchikov A.P. *DAN SSSR*, **214,** 1, 142-45 (1974).
433. Kimelfeld Ya. M., Mostovoi A.B., Mostovaya L.M. *Zhur. fiz. khim.*, **49,** 2, 284-88 (1975).
434. Dubois J.E., Garnier F. *Spectrochim. Acta*, **23A,** 2279-84 (1967).
435. Fredin L., Melander B. *J. Mol. Struct.*, **16,** 205-11 (1973).
436. Gray P., Joffe A.D. *Chem. Rev.*, **55,** 1069-98 (1955).
437. Zhekhter G. *Usp. khim.*, **35,** 1722-53 (1966).
438. Ustavshchikov B.F. *et al. DAN SSSR*, **157,** 143-47 (1964).
439. Parts L., Milter J.T. *J. Phys. Chem.*, **73,** 3088-96 (1969).
440. Sergeev G.B., Leyenson I.A. *Vestn. MGU, Ser. khim.*, **2,** 184-95 (1970).
441. Sergeev G.B., Leyenson I.A. *Usp. khim.*, **42,** 1566-93 (1972).
442. Sergeev G.B. *et al. Zhur. org. khim.*, **12,** 3, 506-13 (1976).
443. Sergeev G.B., Pokholok T.V., Cheng Tong Kha. *Kinetika i kataliz*, **10,** 47-53 (1969).
444. Leyenson I.A., Sergeev, G.B. *DAN SSSR*, **205,** 6, 1400-03 (1972).
445. Leyenson I.A., Sergeev G.B. *Khimiya vysokikh energii*, **5,** 4, 370-71 (1971).
446. Stepanov N.F. *et al. Adv. in Molec. Relax. and Interac. Processes*, **12,** 325-332 (1978).
447. Bach R.D., Henneike H.F. *J. Am. Chem. Soc.*, **92,** 19, 5589-5602 (1970).
448. Nelander B. *Tetrahedron*, **30,** 11, 1337-39 (1974).
449. Benson S.W., Haugen G.R. *J. Am. Chem. Soc.*, **87,** 18, 4036-44 (1965).
450. Konyushenko V.P., Serguchev Yu.A., Stetsyuk G.A. *Teor. i eksp. khim.*, **9,** 3, 343-49 (1973).
451. Zalukayev L.P. *et al. Kinetika i kataliz*, **12,** 3, 754-56 (1971).
452. Sergeev G.B. *et al. Vestn. MGU, Ser. khim.*, 3, 290-94 (1975).
453. Movsumzade M.M. *et al. DAN SSSR*, **206,** 2, 391-94 (1972).
454. Sergeev G.B., Smirnov V.V. *Kinetika i kataliz*, **16,** 3, 611-17 (1975).
455. Sergeev G.B. *Zh. V. Kh. O. im. Mendeleyeva*, **19,** 3, 285-94 (1974).
456. Banthorpe D.V. *Chem. Rev.*, **70,** 3, 295-322 (1970).
457. Selter S. *Adv. Alicycl. Chem.*, **2,** 19-27 (1968).
458. Brevard C., Lehn J.M., *J. Am. Chem. Soc.*, **92,** 16, 4987-89 (1970).
459. Sergeev G.B., Smirnov V.V., Sytilin M.S. *Zhur. fiz. khim.*, **47,** 3, 704-06 (1973).
460. Sergeev G.B., Zenin S.V., Polyakov V.A. *DAN SSSR*, **218,** 3, 620-23 (1974).
461. Sergeev G.B., Naizarek Z., Smirnov V.V. *Zhur. fiz. khim.*, **49,** 9, 2417-18 (1975).
462. Sergeev G.B., Smirnov V.V., Naizarek Z. *Vestn. MGU, Ser. khim.*, 3, 476-81 (1976).
463. Sergeev G.B. *et al. Uch. zap. Azerbaij. Gos. Un-ta, Ser. khim.*, 1, 42-48 (1973).
464. Alexanyan V.T., Gevorkyan B.Z. *Zhur. struct. khim.*, **15,** 3, 450-53 (1974).
465. Sergeev G.B. *et al. Vestn. MGU, Ser. khim.*, 2, 174-79 (1975).
466. Shabanov A.L. *et al. Zhur. org. khim.*, **7,** 6, 1109-10 (1971).
467. Movsumzade M.M., Shabanov A.L., Gurbanov P.A. Trudy AzINEFTEKHIM, **27,** 11-17 (1969).
468. Sergeev G.B. *et al. Kinetika i kataliz*, **18,** 1, 70-75 (1977).
469. Foster R.L. (ed.) *Molecular Complexes.*, **1,** Elek Science, 1973.
470. Fyfe C.A. In: "Molecular Complexes (R.L. Foster, ed.)", v. 1, pp. 209-29, Elek Science, 1973.
471. Colter A.K., Dack M.R. In: "Molecular Complexes (R.L. Foster, ed.)", v. 1, pp. 301-62, Elek Science, 1973.
472. Kardash I.Ye., Pravednikov A.N. *Zh. V. Kh. O. im. Mendeleyeva*, **20,** 1, 14-19 (1975).
473. Pincock R.E., Kiovsky T.E. *J. Am. Chem. Soc.*, **88,** 1, 51-55 (1966).
474. Pincock R.E., Kiovsky T.E. *J. Am. Chem. Soc.*, **87,** 18, 4100-07 (1965).
475. Grant N.H., Clark D.E., Alburn, H.E. *J. Am. Chem. Soc.*, **83,** 21, 4476-77 (1961).

476. Bruice T.C., Butler A.R. *J. Am. Chem. Soc.*, **86**, 19, 4104-07 (1964).
477. Grant N.H., Alburn H.E. *Nature*, **212**, 194-97 (1966).
478. Pincock R.E. *Accounts of Chem. Res.*, **2**, 4, 97-103 (1969).
479. Sergeev G.B., Batyuk V.A. *Usp. khim.*, **45**, 5, 793-826 (1976).
480. Chaikin A.M. Candidate's dissertation. Moscow University, 1955 (in Russian).
481. Sergeev G.B. *et al. Kinetika i kataliz*, **17**, 6, 1441-46 (1976).
482. Lissi E.A., Sanhueza E. *Rev. Latinoamer. Quim.*, **5**, 1, 26-31 (1974).
483. Lissi E.A., Ogaz J., Sanhueza E. *Rev. Latinoamer. Quim.*, **3**, 4, 183-88 (1973).
484. Sergeev G.B. *et al. Kinetika i kataliz*, **16**, 3, 629-34 (1975).
485. Laidler K.J., Hinshelwood C.N. *J. Chem. Soc.*, 858-62 (1938).
486. Butler A.R., Bruice T.C. *J. Am. Chem. Soc.*, **86**, 313-19 (1964).
487. Grant N.H. *Cryobiology*, **6**, 3, 182-87 (1969).
488. Grant N.H., Alburn H.E. *Arch. Biochem. Biophys.*, **118**, 2, 292-96 (1967).
489. Sergeev G.B., Batyuk V.A., Sergeev B.M. *Kinetika i kataliz*, **15**, 2, 326-32 (1974).
490. Jencks W.P., Gilchrist M. *J. Am. Chem. Soc.*, **86**, 24, 5616-20 (1964).
491. Bruice T.C., Fedor L.R. *J. Am. Chem. Soc.*, **86**, 22, 4886-97 (1964).
492. Grant N.H., Alburn H.E. *Science*, **150**, 1589-90 (1965).
493. Pincock R.E., Kiovsky T.E. *J. Am. Chem. Soc.*, **88**, 19, 4455-59 (1966).
494. Pincock R.E., Kiovsky T.E. *J. Am. Chem. Soc.*, **87**, 9, 2072-73 (1965).
495. Uehara K. *et al. Bull. Chem. Soc. Japan*, **45**, 4, 1221-23 (1972).
496. Grant N.H., Clark D.E., Alburn H.E. *J. Am. Chem. Soc.*, **84**, 5, 876-77 (1962).
497. Fedor L.R., Bruice T.C. *J. Am. Chem. Soc.*, **86**, 19, 4117-23 (1964).
498. Alburn H.E., Grant N.H. *J. Am. Chem. Soc.*, **87**, 18, 4174-77 (1965).
499. Pincock R.E., Lin Wen-Shu. *J. Agr. Food Chem.*, **21**, 1, 2-5 (1973).
500. Pudov V.S., Yasina L.L., Buchachenko A.L. *Kinetika i kataliz*, **15**, 5, 1110-14 (1974).
501. Lebedev Ya.S., Tsvetkov Yu.D., Voyevodsky V.V. *Kinetika i kataliz*, **1**, 4, 496-502 (1960).
502. Bagdasaryan Kh.S. *Theory of Radical Polymerization*. Nauka, Moscow, 1966 (in Russian).
503. Kooyman E.C., Strang A. *Rec. trav. chim.*, **72**, 4, 329-41 (1953).
504. Aulov V.A., Sukhov F.F. *Khimiya vysokikh energii*, **7**, 5, 412-17 (1973).
505. Yermolayev V.K., Molin Yu.N., Buben N.Ya. *Kinetika i kataliz*, **3**, 1, 58-64 (1962).
506. Nikolsky V.G., Buben N.Ya. *DAN SSSR*, **134**, 1, 134-36 (1960).
507. Aulov V.A. *et al. Khimiya vysokikh energii*, **2**, 2, 191, (1968).
508. Aulov V.A. *et al. Khimiya vysokikh energii*, **3**, 5, 452 (1969).
509. Aulov V.A. *et al. Vysokomol. soed.* **Б12**, 10, 757-58 (1970).
510. Koritsky A.T. *et al. Vysokomol. soed.*, **1**, 8, 1182-93 (1959).
511. Nara S. *et al. Rept. Progr. Polymer. Phys. Japan*, **10**, 483-89 (1967).
512. Nara S., Kashiwabara H., Sohma I. *Rept. Progr. Polymer. Phys. Japan*, **10**, 479-82 (1967).
513. Nikolsky V.G., Buben N.Ya. *Vysokomol. soed.*, **4**, 6, 922-25 (1962).
514. Pechahold W., Blasenbrey S., Woerner S. *Kolloid. Z.*, **189**, 14-23 (1963).
515. Woodward A., Sawyer J. In: "Physics and Chemistry of the Organic Solid State". New York, 1965.
516. Kargin V.A., Slonimsky G.M. *An Outline of the Physics and Chemistry of Polymers*. Khimiya, Moscow, 1967 (in Russian).
517. Bagdasaryan Kh.S., Milyutinskaya R.I., Kovalev Yu.V. *Khimiya vysokikh energii*, **1**, 2, 127-35 (1967).
518. Milyutinskaya R.I., Kovalev Yu.V., Bagdasaryan Kh.S. *Khimiya vysokikh energii*, **5**, 1, 10-15 (1971).
519. Burton M., Funabashi K. *Molec. Cryst. Liquid Cryst.*, **9**, 153-59 (1969).
520. Charlesby A., Libby D., Ormerod M.G. *Proc. Roy. Soc., Ser. A*, **262**, 207-18 (1961).
521. Nikolsky V.G., Tochin V.A., Buben N.Ya. *Fiz. tverd. tela*, **5**, 8, 2248-56 (1963).
522. Frankevich Ye.L. *Usp. khim.*, **35**, 7, 1161-85 (1966).

523. Lebedev Ya.S., Mikhailov A.I., Buben N.Ya. In: "Elementary Processes of High-Energy Chemistry", pp. 183-87, Nauka, Moscow, 1965 (in Russian).
524. Lebedev Ya.S. *Kinetika i kataliz*, **8,** 2, 245-51 (1967).
525. Tolkachev V.A. *Khimiya vysokikh energii*, **4,** 4, 322-27 (1970).
526. Yermolayev V.K., Milov A.D., Tolkachev V.A. *Khimiya vysokikh energii*, **3,** 3, 224-30 (1969).
527. Tolkachev V.A. *et al. Zhur. struct. khim.*, **10,** 5, 791-96 (1969).
528. Tolkachev V.A., Chernobrov A.S. *Zhur. fiz. khim.*, **44,** 9, 2147-51 (1970)
529. Tolkachev V.A. *et al. Zhur. struct. khim.*, **9,** 5, 798-802 (1968).
530. Yermolayev V.K., Molin Yu.N., Buben N.Ya. *Kinetika i kataliz*, **3,** 3, 314-20 (1962).
531. Szwarc H. *J. Chim. Phys.*, **59,** 10, 1067-71 (1962).
532. Szwarc H. *J. Chim. Phys.*, **63,** 1, 137-41 (1966).
533. Bensasson R. *et al. Disc. Faraday Soc.*, **36,** 177-83 (1963).
534. Smyth C.P. *Dielectric Behaviour and Structure*. McGraw Hill, New York, 1955.
535. Smice O. In: "Physics and Chemistry of the Organic Solid State". New York, 1965.
536. Golubev B.V. *Zhur. fiz. khim.*, **39,** 10, 2606-08 (1965).
537. Zalevskaya R.I., Tsvetkov Yu.D. *Kinetika i kataliz*, **8,** 3, 542-49 (1967).
538. Waite T.R. *J. Chem. Phys.*, **28,** 1, 103-06 (1958).
539. Waite T.R. *Phys. Rev.*, **107,** 2, 463-78 (1957).
540. Kondratyev V.N., Nikitin Ye.Ye. *Kinetics and Mechanism of Gas-Phase Reactions*. Nauka, Moscow, 1974 (in Russian).
541. Cracco F., Arvia A.J., Dole M. *J. Chem. Phys.*, **37,** 10, 2449-57 (1962).
542. Mikhailov A.I. *et al. Fiz. tverd. tela*, **14,** 4, 1172-79 (1972).
543. Mikhailov A.I. *et al. DAN SSSR*, **204,** 383-86 (1972).
544. Lebedev Ya.S. *et al.* In: "Problems of the Kinetics of Elementary Chemical Reactions", pp. 80-92, Nauka, Moscow, 1973 (in Russian).
545. Yakimchenko O.E. *et al. Izv. AN SSSR, Ser. khim.*, 354-59 (1974).
546. Mikhailov A.I. *et al. Vysokomolec. soed.*, **18A,** 6, 1226-30 (1976).
547. Burshtein A.I., Tsvetkov Yu.D. *DAN SSSR*, **214,** 369-72 (1974).
548. Lebedev Ya.S., Burshtein A.I. Abstract of a Report at the 6th All-Union Conference on the Kinetics and Mechanism of Chemical Reactions in Solids, pp. 25-28, Minsk, 1975 (in Russian).
549. Goldanskii V.I. *Ann. Rev. Phys. Chem.*, **27,** 85-126 (1976).
550. Mikhailov A.I. *DAN SSSR*, **197,** 1, 136-39 (1971).
551. Berlin Yu.A., Kulakov V.V., Nikolsky V.G. *DAN SSSR*, **215,** 4, 887-90 (1974).
552. Blumenfeld L.A. *et al. Zhur. struct. khim.*, **8,** 5, 854-63 (1967).
553. Evans B.J., Hafner S.S. *J. Appl. Phys.*, **40,** 3, 1411-13 (1969).
554. Berkooz O., Melamud M., Strikman S. *Solid State Commun.*, **6,** 155-58 (1968).
555. Goldanskii V.I. *et al. DAN SSSR*, 1973, **213,** 4, 867-70 (1973).
556. Chernavsky D.S. *Usp. fiz. nauk*, **107,** 157-83 (1972).
557. Lupu D. *et al. J. Inorg. and Nucl. Chem.*, **34,** 9, 2803-10 (1972).
558. Zhutkovsky R.B., Khairutdinov R.F., Zamarayev K.I. *Khimiya vysokikh energii*, **7,** 6, 558-59 (1973).
559. Okada T., Oohari H., Mataga N. *Bull. Chem. Soc. Japan*, **43,** 9, 2750-58 (1970).
560. Landau L.D., Lifshitz Ye.M. *Quantum Mechanics*. Fizmatgiz, Moscow, 1963 (in Russian).
561. Polyakov V.A. *et al. Zhur. fiz. khim.*, **49,** 2, 541-43 (1975).
562. Sergeev G.B., Zenin S.V., Polyakov V.A. *DAN SSSR*, **218,** 3, 620-23 (1974).
563. Goldanskii V.I., Stukan R.A., Tolmachev A.N. *DAN SSSR*, **191,** 2, 380-83 (1970).
564. Horne R.A. *J. Inorg. and Nucl. Chem.*, **25,** 9, 1139-46 (1963).
565. Nitzan E., Wahl A.C. *J. Inorg. and Nucl. Chem.*, **28,** 12, 3069-71 (1966).
566. Berlin Yu.A. *DAN SSSR*, **223,** 625-28 (1975).
567. Berlin Yu.A. *DAN SSSR*, **223,** 6, 1387-90 (1975).

568. Sergeev G.B., Shvedchikov A.P. *Zh. V. Kh. O. im. Mendeleyeva,* **18,** 52-63 (1973).
569. Grant N.H., Clark D.E., Alburn H.E. *J. Am. Chem. Soc.*, **88,** 17, 4071-74 (1966).
570. Buchachenko A.L., Troitskaya A.S. *Izv. AN SSSR, Ser. khim.*, 4, 602-09 (1966).
571. Sukhorukov B.I. *et al. DAN SSSR,* **177,** 2, 454-57 (1967).
572. Carrington A., McLachlan A. *Introduction to Magnetic Resonance with Applications to Chemistry and Chemical Physics.* New York, 1967.
573. Freed J.H., Fraenkel G.K. *J. Chem. Phys.*, **39,** 2, 326-48 (1963).
574. Hamilton C.L., McConnel G.M. *Usp. khim.*, **39,** 3, 531-59 (1970).
575. Buchachenko A.L., Wasserman A.M., Kovarskii A.L. *Int. J. Chem. Kinetics,* **1,** 361-66 (1969).
576. Khairutdinov R.F., Zamarayev K.I. *Izv. AN SSSR, Ser. khim.*, 7, 1524-28 (1970).
577. Kokorin A.I., Zamarayev K.I. *Zhur. fiz. khim.*, **46,** 11, 2914-15 (1972).
578. A. van Roggin, L. van Roggen, Gordy W. *Phys. Rev.*, **105,** 1, 50-5 (1957).
579. Lord N.W., Blinder S.M. *J. Chem. Phys.*, **34,** 5, 1693-1708 (1961).
580. Golikov V.P., Muromtsev V.I. *Zhur. struct. khim.*, **13,** 2, 332-33 (1972).
581. Mil Ye.M., Kovarsky A.L., Vasserman A.M. *Izv. AN SSSR, Ser. khim.*, 10, 2211-16 (1973).
582. Kuntz I.D. *et al. Science,* **163,** 1329-31 (1969).
583. Stepanov M.B. Candidate's dissertation. Moscow University, 1974 (in Russian).
584. Sergeev B.M. Candidate's dissertation. Moscow University, 1975 (in Russian).
585. Grant N.H., Alburn H.E., *Biochem.*, **4,** 10, 1913-16 (1965).
586. Sergeev G.B. *et al. Kinetika i kataliz,* **16,** 3, 635-38 (1975).
587. Sergeev G.B., Batyuk V.A., Stepanov M.B. Dep. VINITI, No. 2785, Nov. 4, 1974; *Vestn. MGU,* 2, 250 (1975).
588. Kiovsky T.E., Pincock R.E. *J. Am. Chem. Soc.*, **88,** 20, 4704-10 (1966).
589. Renz M., Lohrman R., Orgel L.E. *Biochem. Biophys. Acta,* **240,** 463-71 (1971).
590. Uesugi S., Ts'o P.O. *Biochem.*, **13,** 3142-47 (1974).
591. Sergeev G.B., Batyuk V.A., Sergeev B.M. *DAN SSSR,* **214,** 6, 1354-57 (1974).
592. Sergeev G.B. *et al. Vestn. MGU, Ser. khim.*, 5, 557-62 (1975).
593. Sergeev G.B. *et al. Vestn. MGU, Ser. khim.*, 2, 182-89 (1976).
594. Sergeev G.B., Batyuk V.A., Sergeev B.M. *DAN SSSR,* **221,** 2, 384-87 (1975).
595. Anson M.L. *J. Gen. Physiol.*, **22,** 79-86 (1938).
596. Sergeev G.B. *et al.* In: "Abstracts of Reports at the All-Union Symposium on Bioorganic Chemistry". Vladivostok, 1975 (in Russian).
597. Hanstein W.G., Dewis K.A., Hatefi Y. *Arch. Biochem. and Biophys.*, **147,** 534-41 (1971).
598. Zaromb S., Brill R. *J. Chem. Phys.*, **24,** 4, 895-902 (1956).
599. Mironov K.Ye., Bergman A.G. *DAN SSSR,* **81,** 6, 1081-83 (1951).
600. Tommila F. *Acta Chem. Scand.*, **13,** 3, 622-23 (1959).
601. Laidler K.J., Eyring H. *Ann. New York Acad. Sci.*, **39,** 303-07 (1940).
602. Emanuel N.M., Zaikov G.Ye. *Vysokomol. soed.*, **17A,** 9, 2122-32 (1975).
603. Roginsky V.A., Miller V.B. *DAN SSSR,* **215,** 5, 1164-67 (1974).
604. Ceccaldi D., Bullot J. *Chem. Phys. Lett.*, **9,** 6, 551-54 (1971).
605. Kieffer F., Meyer C., Rigaut J. *Chem. Phys. Lett.*, **11,** 3, 359-61 (1971).
606. Sergeev G.B., Batyuk V.A., Stepanov M.B. Dep. VINITI, No. 153, Jan. 23, 1975; *Vestn. MGU Abstracts,* 3, 380 (1975).
607. Sergeev G.B. *et al.* Dep. VINITI, No. 1281-76, Apr. 15, 1976; *Vestn. MGU Abstracts,* 5, 635 (1976).
608. Trofimov V.I., Buben N.Ya. *Khimiya vysokikh energii,* **3,** 2, 116-20 (1969).
609. Kabi A. *et al. Int. J. Radiat. Phys. Chem.*, **1,** 1, 45-51 (1969).
610. Tikhomirov L.A., Pavelyev V.S., Buben N.Ya. *Khimiya vysokikh energii,* **2,** 3, 284-86 (1968).
611. Lozina-Lozinsky L.K. *Essays on Cryobiology.* Nauka, Leningrad, 1972 (in Russian).
612. Smith Au. *Biological Effects of Freezing and Supercooling.* London, 1961.
613. Samygin G.A. *Zhur. obshch. biol.*, **34,** 5, 691-709 (1973).

614. Tappel A.L. In: "Cryobiology (H.T. Meryman, ed.)", pp. 163-177, Academic Press, 1966.
615. Fink A.L. *Biochem.*, **15,** 7, 1580-86 (1976).
616. Douzou P. *Biochimie,* **53,** 1135-45 (1971).
617. Travers F., Douzou P. *J. Phys. Chem.*, **74,** 10, 2243-44 (1970).
618. Shedlowsky T., Kay R.L. *J. Phys. Chem.*, **60,** 2, 151-55 (1956).
619. Hui Bon Hoa G., Douzou P. *J. Biol. Chem.*, **248,** 13, 4649-54 (1973).
620. Hui Bon Hoa G., Douzou P., Michelson A.M. *Biochim. Biophys. Acta,* **182,** 334-41 (1969).
621. Hui Bon Hoa G., Gaboriaud R., Douzou P. *C.R. Acad. Sci. Paris,* **270, Ser. C,** 4, 373-76 (1970).
622. Balny C., Becker L. *J. Chim. Phys.*, **68,** 6, 1008-09 (1971).
623. Travers F., Douzou P. *Biochimie,* **56,** 4, 509-14 (1974).
624. Travers F. *et al. Biochimie,* **57,** 1, 43-8 (1975).
625. Douzou P. *Mol. and Cellular Biochem.*, **1,** 1, 15-27 (1973).
626. Meryman H.T., ed. *Cryobiology.* Academic Press, New York, 1966.
627. Douzou P., Sircix R., Travers F. *Proc. Nat. Acad. Sci.*, **66,** 3, 787-92 (1970).
628. Douzou P., Leterrier F. *Biochim. Biophys. Acta,* **220,** 338-40 (1970).
629. Jurtshuk P., Sczuku I., Green D.E. *Biochim. Biophys. Research Comm.*, **6,** 76-82 (1961).
630. Noguchi T., Freed S. *Nature, New Biology,* **230,** 165-67 (1971).
631. Freed S., Sack R. *Anal. Biochem.*, **43,** 492-508 (1971).
632. Debey P., Balny C., Douzou P. *FEBS Lett.*, **35,** 1, 86-90 (1973).
633. Bello J. *Biochem.*, **8,** 4542-50 (1969).
634. Herskovits T.T., Laskowski M., Jr. *J. Mol. Chem.*, **237,** 2481-85 (1962).
635. Hui Bon Hoa G. *et al. Biochimie,* **55,** 269-76 (1973).
636. Guinand S., Hui Bon Hoa G., Pantaloni C. *Biochimie,* **56,** 863-71 (1974).
637. Kemp A., Groot G.S.P., Reitsma H.J. *Biochim. Biophys.* Acta, **180,** 1, 28-34 (1969).
638. Chilson P.O., Costello L.A., Kaplan N.O. *Fed. Proc.*, **15,** 555-58 (1966).
639. Maier V.P., Tappel A.L., Volman D.H. *J. Am. Chem. Soc.*, **77,** 1273-77 (1955).
640. Blumenfeld L.A. *Problems of Biological Physics.* Nauka, Moscow, 1974 (in Russian).
641. Blumenfeld L.A. *J. Theor. Biol.*, **58,** 269-84 (1976).
642. Sergeev G.B., Batyuk V.A., Sergeev B.M. *DAN SSSR,* **224,** 2, 387-90 (1975).
643. Jencks W. *Catalysis in Chemistry and Enzymology.* New York. 1969.
644. Good N.E. *et al. Biochem.*, **5,** 2, 467-71 (1966).
645. Bates R.G. *Determination of pH. (Theory and Practice.)* John Wiley and Sons, New York, London, Sydney, 1964.
646. Goren H.J., Fridkin M. *Europ. J. Biochem.*, **41,** 263-69 (1974).
647. Bruice T.C., Schmir G.L. *J. Am. Chem. Soc.*, **79,** 1663-67 (1957).
648 Tommila E., Hinshelwood C.N. *J. Chem. Soc.*, 1801-04 (1938).
649. Kuntz I.D., Brassfield T.S. *Arch. Biochem. Biophys.*, **142,** 660-64 (1971).
650. Kuntz I.D. *J. Am. Chem. Soc.*, **93,** 2, 514-18 (1974).
651. Fuller M.E., Brey W.S. *J. Biol. Chem.*, **243,** 2, 274-80 (1968).
652. Blears D.J., Danyluk S.S. *Biochim. Biophys. Acta,* **154,** 1, 17-27 (1968).
653. Kurzayev A.B., Kvlividze V.I., Kiselev V.F. *Biofizika,* **20,** 3, 533-34 (1975).
654. Ushakova L.A. Abstract of a Candidate's Dissertation. Moscow University, 1975 (in Russian).
655. Smith K.C. *Radiat. Res. Suppl.*, 6, 54-79 (1966).
656. Setlow R.B. *Science,* **153,** 379-86 (1966).
657. Varghese A.J. *Biochem.*, **9,** 24, 4781-87 (1970).
658. Pisarevsky A.N., Tatarinov B.A., Cherenkevich S.N. *Biofizika,* **15,** 154-56 (1970).
659. Eisinger J., Shulman R.G. *Proc. Acad. Soc.*, **58,** 895-98 (1967).
660. Varghese A.J., Wang S.Y. *Biochem. Biophys. Res. Commun.*, **33,** 102-06 (1968).
661. Rahn R.O., Hosszu J.L. *Photochem. Photobiol.*, **10,** 2, 131-37 (1969).
662. Kochetkov N.K. *et al. Organic Chemistry of Nucleic Acids.* Khimiya. Moscow, 1970 (in Russian).

663. Duchesne J., ed. *Physico-Chemical Properties of Nucleic Acids*, v. 1, Academic Press, London, New York, 1973.
664. Thomanek U.F. *et al. Acta Crystallogr., Sec. A*, **29**, 3, 263-65 (1973).
665. Brice J.C. *The Growth of Crystals from Liquids*. North Holland, London-New York, 1973.
666. Douzou P., Hui Bon Hoa G. *J. Mol. Biol.*, **96**, 367-80 (1975).
667. Petsko G.A. *J. Mol. Biol.*, **96**, 381-92 (1975).
668. Grant N.H. *Discovery*, **27**, 8, 26-30 (1966).
669. Sergeev G.B., Batyuk V.A. *DAN SSSR*, **190**, 6, 1399-1402 (1970).
670. George P. *Biochem. J.*, v. 55, pp. 220-26 (1953).
671. Kumamoto J., Raison J.K. *J. Theor. Biol.*, v. 31, 47-56 (1971).
672. Orgel L.E., Lohrmann R. *Accounts Chem. Res.*, **7**, 11, 368-77 (1974).
673. Blumenfeld L.A. *et al. FEBS Lett.*, 45, 1, 256-58 (1974).
674. Blumenfeld L.A. *et al. FEBS Lett.*, 49, 2, 246-48 (1974).
675. Blumenfeld L.A. *et al. Biochim. Biophys. Acta*, 379, 2, 512-16 (1975).
676. Pecht I, Faraggi M. *Proc. Natl. Acad. Sci. U.S.*, **68**, 902-06 (1972).
677. Lichtin U.N., Shafferman A., Stein G. *Biochim. Biophys. Acta*, **314**, 117-35 (1973).
678. Gordon Ye.B., Mezhov-Deglin L.P., Pugachev O.F. *Letters to ZhETF*, **19**, 2, 103-06 (1974).
679. Serebryanikov L.V. *Vestn. MGU. Ser. khim.*, 3, 363 (1975).
680. Bos A., Howe A.T. *J. Chem. Soc., Faraday Trans.*, II, **71**, 28-40 (1975).
681. Brandt N.B., Tolmachev V.V. *Letters to ZhETF*, **19**, 7, 439-43 (1974).
682. Georgiev G.S. *et al. Vysokomol. soed.*, **14 A**, 1, 177-85 (1972).
683. Garina Ye.S. *et al. Vysokomol. soed.*, **18B**, 4, 287-89 (1976).
684. Kotin Ye.B., Gerasimov G.N., Abkin A.D. *DAN SSSR*, **211**, 3, 636-38 (1973).
685. Yenikolopov N.S. In: "Materials of the All-Union Symposium on Chemical Kinetics" (V.N. Kondratyev, ed.). Nauka, Moscow, 1976 (in Russian).
686. Fenrick H.W. *et al. J. Am. Chem. Soc.*, **85**, 23, 3731-32 (1963).
687. Stacey F.W., Sauer J.C., McKusick B.S. *J. Am. Chem. Soc.*, **81**, **4**, 987-92 (1959).
688. Shpolskii E.V., Bolotnikova T.N. *Pure and Appl. Chem.*, **37**, 1-2, 183-95 (1974).
689. Nurmukhametov R.N. *Usp. khim.*, **38**, 2, 351-75 (1969).
690. Sirota A.G., Nalivaiko E.I., Ryabikov E.P. *Khimiya vysokikh energii*, **8**, 3, 281-82 (1974).
691. Adadurov G.A. *et al. Khimiya vysokikh energii*, **7**, 6, 554-55 (1973).
692. Adadurov G.A. *et al. DAN SSSR*, **165**, 4, 851-54 (1965).
693. Babare L.V. *et al. DAN SSSR*, **184**, 5, 1120-23 (1969).
694. Kompaneyets A.S., Romanova V.I., Yampolsky P.A. *Letters to ZhETF*, **16**, 4, 259-62 (1972).
695. Borisov V.T., Dukhin A.I., Miroshnichenko G.I. *DAN SSSR*, **223**, 4, 893-95 (1975).
696. Dukhin A.I. *et al.* Abstract of a report at the 6th All-Union Conference on the Kinetics and Mechanism of Chemical Reactions in Solids, pp. 12-17, Minsk, 1975 (in Russian).
697. Borisov V.T. *et al. Izv. AN SSSR. Ser. met.*, 6, 104-09 (1971).
698. Anastasyuk N.V. *et al. Izv. AN SSSR Ser. neorg. mater.*, **10**, 7, 1307-10 (1974).
699. Osipov K.A. *DAN SSSR*, **215**, 6, 1407-09 (1974).
700. Fletcher N.H. *Rep. Prog. Phys.*, **34**, 913-1014 (1971).
701. Butyagin P.Yu. *Usp. khim.*, **40**, 11, 1935-59 (1971).
702. Jellinek H.H.G., Fok S.J. *Makromol. Chem.*, **104**, 18-26 (1967).
703. Trout G.J., Moore D.E., Hawke J.G., *J. Phys. Chem.*, **79**, 15, 1519-27 (1975).
704. Boldyrev V.V. *Kinetika i kataliz*, **13**, 6, 1411-21 (1972).
705. Boldyrev V.V. *et al. DAN SSSR*, **221**, 3, 634-37 (1975).
706. Hochstrasser R.M., King D.S. *J. Am. Chem. Soc.*, **97**, 16, 4760-62 (1975).
707. Rowland F.S. In: "Materials of the All-Union Symposium on Chemical Kinetics" (V.N. Kondratyev, ed.). Nauka, Moscow, 1976 (in Russian).

708. *Cosmochemistry*. In: "Topics in Current Chemistry (F. Boschke, ed.), v. 44, pp. 57-73. Springer Verlag, New York-Berlin, 1974.
709. Watson W.D., Salpeter E.E., *Astrophys. J.*, **174,** 321-32 (1972).
710. Galperin I.I., Daryusin A.T. *Zh. V. Kh. O. im. Mendeleyeva,* **9,** 2, 289-99 (1964).
711. Ugo R., ed. *Aspects of Homogeneous Catalysis. A Series of Advances,* v. 1. Carlo Manfredi, Editore-Milano, 1970.
712. Howard W.F., Andrews L. *J. Am. Chem. Soc.*, **96,** 26, 7864-68 (1974).
713. Randell J.E. Patent Application 33503/73. University of Salford, England.
714. Haselden G.G. In: "Materials of the 14th International Congress on Refrigeration". Moscow, 1975 (in Russian).
715. Hogan W.H., Klipping G., eds. *Low-Temperature Refrigeration of Microwave Systems*. Boston Technical Publishers, Inc., 1967.
716. Flink J., Hoyer H. *Nature*, **234,** 5329, 420, (1971).
717. Timmerhaus K.D., O'Sullivan W.J., Hammel E.F., eds. *Low-Temperature Physics* – LT13, v. 4. Electronic Properties, Instrumentation and Measurement. Plenum Press, New York-London, 1974.
718. Bajolle J.E., Naimpally A., Mason H.L. *Freezing Process Studies. Res. and Develop. Progress Report No. 658*, Gov. Print. Office, Washington (1971).
719. Shvartsev S.L. *Priroda*, 7, 67-73 (1975).
720. Weiser C.J. *Science*, **169,** 3952, 1269-78 (1970).
721. King C.J. *Freeze-Drying of Foods. CRS Monoscience Series*, 1971.
722. *Freeze-Drying of Foods and Biologicals. Food Processing Review*, 1, Noyes R, **1968.**
723. Lorentsen G. In: "Materials of the 14th International Congress on Refrigeration". Moscow, 1975 (in Russian).
724. Van Pelt V.G. In: "Materials of the 14th International Congress on Refrigeration", Moscow, 1975 (in Russian).
725. Harris K.J.C., ed. *Biological Applications of Freezing and Drying*. Academic Press, New York, 1954.
726. *Freeze-Drying of Biological Materials*. Intern. Institute of Refrigeration, Paris, 1973.
727. Pushkar N.S., ed. *Cryobiology and Cryomedicine*. Issue I, Naukova dumka, Kiev, 1975 (in Russian).
728. Vinograd-Frenkel F.R. In: "Materials of the 14th International Congress on Refrigeration", Moscow, 1975 (in Russian).
729. Gifford W.E. In: "Materials of the 14th International Congress on Refrigeration", Moscow, 1975 (in Russian).
730. Valeri K. R. In: "Materials of the 14th International Congress on Refrigeration". Moscow, 1975 (in Russian.)
731. Pribor D.B. *Cryobiology*, **11,** 60-71 (1974).
732. Pushkar N.S. *et al.* In: "Materials of the 14th International Congress on Refrigeration", Moscow, 1975 (in Russian).
733. Fedotenkov A.G. *et al.* In: "Materials of the 14th International Congress on Refrigeration", Moscow, 1975 (in Russian).
734. Konikova A.S. In: "Materials of the 14th International Congress on Refrigeration, Moscow, 1975 (in Russian).
735. Walton K.G., Kervina M., Fleisher S. *Bioenergetics*, **1,** 3-8 (1970).
736. Faranti J. *et al. Nature*, **249,** 5456, 452-53 (1974).
737. Wolfstenholme G.E.W., O'Connor M., eds. *The Frozen Cell*. Churchill, London, 1970.
738. Freed S., Sack R. *Anal. Biochem.*, **43,** 2, 492-508 (1971).
739. Kandel E.I., ed. *Cryosurgery*. Meditsina, Moscow, 1974 (in Russian).

INDEX

Activation
  by electric discharge, 17
  by explosion, 17
  by irradiation, 21
  by pyrolysis, 19
Activation energy, negative, 149
Addition
  at double bonds, 128, 155
Addition reactions, 128
Argon matrix, 25
Arrhenius equation, 13
Attack
  acid-assisted, 160
  base-assisted, 160
  direct, 160

Bimolecular reactions, 175
Biochemical reactions at low temperatures, 241
Biopolymers in frozen solutions, 253
Bombardment by electrons, 22
Bromination of olefins, 139

Cage effect, 61
Cage model, 177
Calorimeters, 49
  low-temperature, 51
Calorimetric methods, 49
Catalysis, displacement, 102
Chain explosions, 112
Chain hydrobromination, 118
Chain polymerization, 235
Chain reactions, 104
Chlorination
  nitrosyl, 140
  olefins, 138
Circular dichroism, 48
Cocondensation, 25, 90
  from molecular beams, 131
  techniques, 45
Cohalogenation, 151
Consecutive exposure, 73
Contact reactions, 27
Conversion of α-oxides, 150
Copolymerization, 98
Correlation time, 187
Cryogenic fluorination, 32
Cryogenic hydrogenation, 29
Cryogenic isolation, 18
  combustion products, 18
  pyrolytic products, 20
Cryogenic polymerization, 81
Cryogenic scrubbing, 270
Cryogenic systems, miniature, 276
Cryogenic temperatures, effects of, 14
Cryostats, 35
  continuous-flow, 42
  controllers for, 52
  for ESR work, 53
  glass, 37
    for IR spectroscopy, 49
  liquid-gas, 39
  multi-temperature, 40
  optical, 49
  refrigerator-based, 42
  rotating, 18
  thermoelectrically cooled, 42
  variable-temperature, 40
Crystal growth, 254

Dewar vessel, 36
Dielectric constant, 227
  liquid microphase, 228
  mixed solvents, 244
Differential thermal analysis, 50, 109, 116, 117
  setup for, 50
Diffraction methods, 52
Diffusion-recombination model, 70
Dihalides, 270
Diluents, 213, 219, 222
Dispersion of optical rotation, 48
Double-bond addition, 155
DTA, 50, 109, 116, 117
Dynamic statistical model, 56

Electron diffraction analysis, 24, 52
Electron exchange reaction, 183
Electron spin echo technique, 53
Electronmicroscopy, 52

- Enzyme activity, 243
  - at reduced temperatures, 245
  - in frozen solutions, 256
- Enzymes, irreversible inactivation, 246
  - membrane, 247
- Enzyme-substrate complexes, 254
- Enzymic catalysis, 260
- Enzymic hydrolysis, 256
- ESE technique, 53
- ESR, 52
  - spectra, 18
    - dipole-dipole broadening, 64
  - spectroscopy, 187
  - technique, 52
- Experimental techniques for low-temperature processes, 46
- Experiments on human hemoglobin, 261
- Explosion, thermal, 96, 111, 132
- Explosive chain reactions, 110
- Explosive polymerization, 86
- Explosive postpolymerization, 86

- Fluorination
  - hydrocarbons, 32
  - olefins, 32
- Fluorine-containing compounds, 26
- Free radicals, production, 22
- Free-volume concept, 100
- Freezing, effect on concurrent reactions, 224
- Frozen biopolymer solutions, 253
  - photochemical processes in, 253
  - stabilization of dynamic conformations, 255
- Frozen solutions
  - hydration of macromolecules in, 252
  - structure of, 186
  - phase state of, 193

- Gamma irradiation, 33, 263

- Halogenation of olefins, 135
  - fast, 136
  - in absence of solvents, 126
  - in cocondensates, 130
  - in nonpolar solvents, 139
  - in solvents, 138
  - mechanism of, 135
  - role of molecular complexes in, 143
- Halogen-olefin complexes, 145, 151
- Helium temperatures, uses of, 262
- Heterogeneous reactions, 27
- Homolysis, 142
- Hydration of macromolecules, 252
- Hydrobromination
  - low-temperature, 107
  - olefin halides, 116
  - olefins, 104-105
- Hydrohalogenation of olefins, 126
  - in cocondensates, 130
- Hydrolysis
  - enzymic, 256
  - in frozen solutions, 158
  - spontaneous, 159
- Hydroxyaminolysis
  - nonenzymic, 255
  - of amides, 161

- Inclusion compounds, 65
- Induction period, 110
- Infrared spectroscopy, 49
- *In-situ* experiments, 46
- Irradiation, gamma-rays, 22
- Isolated radicals, 59

- Kinetic models of chemical reactions in solid phase, 166
- Kinetics
  - bimolecular reactions in solid phase, 175
  - concurrent reactions, 231-232
  - halogenation of olefins, 143
  - hydrobromination of olefins, 107
  - nonisothermal, 25
  - radical accumulation, 56
  - radical loss, 58
  - radiophotoluminescence, 76
  - radiothermoluminescence, 76
  - reactions in frozen solutions, 154, 198
  - redox reactions in frozen solutions, 216
  - solid-phase initiated polymerization, 91
- Kirkwood equation, 230

- Liquefied gases, 36
  - natural, 271
- Liquid microphase, 190
  - composition, 195
  - dielectric constant, 228
  - in Menshutkin reaction, 215
  - total concentration, 215, 232
  - volume, 195
- Liquid-phase polimerization, 82
- Liquid refrigerants, 36
- Loss of radicals, 56, 166
  - effect of matrix structure, 172
- Loss of radiolyzed products, 166
  - isothermal, 168
- Low-temperature chemical processes, 45
- Low-temperature gamma radiolysis, 59

Low-temperature halogenation, 45
Low-temperature IR spectroscopy, 24, 49
Low-temperature polymerization, 81
Low-temperature reaction cells, 44
Low-temperature reactions
  mechanism of, 135
Low temperatures,
  applications in science and engineering, 262

Macroethers, cyclic, 152
Matrix isolation technique, 45, 262
Menshutkin reaction, 155, 210
  dependence on dielectric constant, 229
Mercury-lamp photolysis, 25
Micellar catalysis, 259
Michaelis constant, 257
Michaelis-Menten equation, 257
Michaelis scheme, 257
Microcalorimeters, 51
Microcooler, 42
Microinclusions, 190
Model
  for diffusion-controlled reactions, 175
  polychromatic kinetic, 180
Molecular complexes, 150
Molecular mobility, 60
Multiple bonds, 146

Negative temperature coefficient, 221
Nitration, 140
NMR, 52
Noninitiated spontaneous reactions, 15

Olefin reactivity, 28
Optical activity, 48
Organo-aqueous solvents, 242
Oxygen-containing compounds, 23
Ozone production, 22

Penetrating radiations, 22
Periodic exposure, 73
Peroxydase oxidation, 255
Phase inhomogeneity, 205
Photochemical chain hydrobromination, 124
Photochemical halogenation of olefins, 106
Photochemical hydrobromination, 112, 115
  fast, 110
  olefin halides, 116
  olefins, 105
Photochemical processes in frozen biopolymer solutions, 253
Photochemical reactions, 61
  in rigid glassy matrices, 22
Photochemistry of diluted solutions, 21
Photodimerization, 253
Photodissociation, 21
Photo-induced chemical reactions, 82
Photo-induced polymerization, 82
Photolysis, 22
Polanyi-Semenov relation, 107
Polymerization
  by cocondensation, 91
  during warm-up, 100
  induced, 93
  low-temperature, 263
  solid-phase, 95
Postpolymerization, 85, 235
Pre-exposure time, 111
Prequenching, 102
Proton transfer, 99

Quantum yield, 61
  effect of electron energy, 61
  hydrobromination, 122
  photochemical hydrobromination, 108
  photolysed products, 76
  photolysis of hydrogen peroxide, 61
  reactions in solid phase, 61
Quick freezing, 46

Radiation-induced chemical synthesis, 21
Radiation-induced polymerization, 82
Radical recombination, 56
Radical yield, 57
Radiolysis
  advantages, 22
  experiments, 57
  solid glassy matrices, 181
Radiophotoluminescence, 76, 236
Radiothermoluminescence, 76
Raman spectroscopy, 24, 49
Reaction rate in frozen solutions, 207
Reactions
  addition, 138
  chain, 104
  concurrent, 146
  displacement, 128
  disproportionation, 29
  enzyme-catalyzed, 255
  in cocondensates, 129
  in frozen solutions, 154, 199-204
  in layered samples, 126
  in multicomponent frozen systems, 186
  low-temperature, 135

Reactions
  Menshutkin, 155
  oxygen-fluorine, 23
  recombination, 30
  sequential, 146
  solvolysis, 157
  spontaneous, 126
Reactive species
  behaviour in solids, 239
  production of, 16
Reactivity
  proteins, 255
Recombination of immobilized radicals, 58
Redox reactions in frozen solutions, 216, 219
Refrigeration, 271
Re-hybridization, 167
Relaxation, structural, 167
Relaxation time, 169

Sensibilization, 74
Solid matrices, 21
Solid-phase polymerization, 48, 82
Solid-to-solid transitions, 267
Solute concentration,
  effect on reaction rate, 258
Solvents, 44
  effect on reaction rate, 221
Space chemistry, 268
Spatial distribution of radicals, 63
Spectroscopic investigations, 132
Spin-lattice relaxation time, 65
Sputtering, 139
Stepwise recombination, 58, 166, 172, 236
Stop-flow apparatus, 48
Structural-kinetic model, 205, 209
Supercooled liquid solutions, 198
Synthesis of H_2O_4, 23

Temperature perturbation spectroscopy, 247
Temperature-jump method, 48
Tesla-discharge species, 20
Thermal explosion, 96, 111, 132
Thermoelectric cooling, 42
Thermographic investigations, 132
Thiolactones, 160
Trapped electrons, 68
Trapped radiation defects, 33
Trapped radicals
  behaviour in solids, 67
Tunnel mechanism, 68, 180
Tunnel transfer, 68, 180, 181, 184
  in polymerization, 186

UV-irradiation, 33
UV-visible spectroscopy, 47

Vacuum-UV photolysis, 25

Warm-up experiments, 46

X-ray diffraction, 52